ADVANCES IN PHYSICS

A QUARTERLY SUPPLEMENT
of the
PHILOSOPHICAL MAGAZINE

VOLUME 3 APRIL 1954 NUMBER 10

PRICE per part 15*s.* 0*d.*
PRICE per annum £2 15*s.* 0*d.* post free

PRINTED AND PUBLISHED BY TAYLOR & FRANCIS LTD.
RED LION COURT, FLEET ST., LONDON E.C.4

Early Scientific Publications

DIARY OF ROBERT HOOKE, M.A., M.D., F.R.S.
1672-1680

Edited by **H. W. ROBINSON** and **W. ADAMS**
Recommended for publication by the Royal Society, London

25/-
net

"This vivid record of the scientific, artistic and social activities of a remarkable man during remarkable years has too long remained in obscurity."—Extract from foreword by Sir Frederick Gowland Hopkins, O.M., President of the Royal Society.

MATHEMATICAL WORK OF JOHN WALLIS, D.D., F.R.S.

By **J. F. SCOTT, Ph.D., B.A.**

12/6
net

"His work will be indispensable to those interested in the early history of The Royal Society. I commend to all students of the Seventeenth Century, whether scientific or humane, this learned and lucid book."—Extract from foreword by Prof. E. N. da C. Andrade, D.Sc., Ph.D., F.R.S.
Recommended for publication by University of London

CORRESPONDENCE AND PAPERS OF EDMOND HALLEY

Arranged and Edited by **EUGENE FAIRFIELD MACPIKE**

21/-
net

First published on behalf of The History of Science Society by Oxford University Press. Now re-issued by Taylor & Francis, Ltd.

MEMOIRS OF SIR ISAAC NEWTON'S LIFE

5/-
net

By **WILLIAM STUKELEY, M.D., F.R.S., 175**
From an Original Manuscript
Now in the possession of the Royal Society, London

HEVELIUS, FLAMSTEED AND HALLEY

12/6
net

Three Contemporary Astronomers and their Mutual Relations
By **EUGENE FAIRFIELD MACPIKE**
Published by arrangement with The History of Science Society

Established over 150 years

TAYLOR & FRANCIS, LTD.
RED LION COURT, FLEET ST., LONDON E.C.
PRINTERS & PUBLISHERS OF SCIENTIFIC BOOKS

CONTENTS

Theory of Ferroelectrics. By A. F. Devonshire, H. H. Wills Physical Laboratory, University of Bristol . . . 85

On the Theory of Liquid Helium. By I. Prigogine, Faculté des Sciences de l'Université de Bruxelles 131

The Transition Metals and their Alloys. By W. Hume-Rothery, F.R.S., The Inorganic Chemistry Laboratory, Oxford, and B. R. Coles, Department of Physics, Imperial College of Science and Technology, London, S.W.7 149

ADVANCES IN PHYSICS

A QUARTERLY SUPPLEMENT

of the

PHILOSOPHICAL MAGAZINE

VOLUME 3 APRIL 1954 NUMBER 10

Theory of Ferroelectrics

By A. F. DEVONSHIRE

H. H. Wills Physical Laboratory, Royal Fort, Bristol

CONTENTS

§1. INTRODUCTION.
- 1.1. Definition of a ferroelectric.
- 1.2. Classification of ferroelectrics.

§2. THERMODYNAMICS OF CRYSTALS.
- 2.1. Introduction.
- 2.2. Definition of physical constants.
- 2.3. Constants for Rochelle salt.
- 2.4. Adiabatic and isothermal conditions.
- 2.5. Free energy.
- 2.6. Adiabatic and isothermal constants for KH_2PO_4.
- 2.7. Electrostriction.
- 2.8. Relation of piezoelectric to electrostrictive constants.
- 2.9. Piezoelectric constants of the perovskites.

§3. THERMODYNAMICS OF THE TRANSITION.
- 3.1. Introduction.
- 3.2. Susceptibility near the transition point.
- 3.3. Effect of electric field on a transition.
- 3.4. Hysteresis.
- 3.5. Observed types of transition.
- 3.6. Entropy of spontaneous polarization.
- 3.7. Effect of clamping on the transition temperature.
- 3.8. Effect of stress on the transition temperature.
- 3.9. Transitions between two ferroelectric states.
- 3.10. Antiferroelectric transitions.
- 3.11. Dielectric constant at an antiferroelectric transition.
- 3.12. Effect of electric field on an antiferroelectric transition.

§4. ATOMIC MODELS.
- 4.1. Introduction.
- 4.2. Particular cases.
  - 4.2.1. Barium titanate.
  - 4.2.2. Potassium dihydrogen phosphate.
  - 4.2.3. Rochelle salt.
- 4.3. Types of atomic model.
- 4.4. Rotating dipoles with interaction.
- 4.5. Dipoles with two positions of equilibrium.
- 4.6. Oscillating ions.
- 4.7. Comparison of previous two models.
- 4.8. Further discussion of particular cases.
  - 4.8.1. Barium titanate.
  - 4.8.2. Potassium dihydrogen phosphate.
  - 4.8.3. Rochelle salt.
- 4.9. Antiferroelectrics.
- 4.10. Perovskites.

ACKNOWLEDGMENT.

REFERENCES.

§ 1. Introduction

1.1. *Definition of a Ferroelectric*

Ferroelectrics are a section of a much larger class of substances called pyroelectrics. A pyroelectric has the property that a single crystal with no surface charges is polar ; the polarity is normally masked by twinning or by surface charges and is only revealed by heating the crystal, hence the name. A ferroelectric has the additional property that the polarization can be reversed by applying a sufficiently large electric field ; in a strong alternating field it therefore shows hysteresis.

Pyroelectricity and hysteresis are the essential properties that define a ferroelectric, but it usually shows other special properties closely connected with these. If an electric field can reverse the polarization this is because a small relative shift of atoms in the crystal turns it into its electrical twin. If the atoms make half this shift then the crystal will be in a more symmetrical and non-polar state. It commonly happens that this half shift can be brought about by temperature change ; hence most ferroelectrics have a transition temperature above which they are normal and non-polar. Above the transition temperature the dielectric constant obeys a Curie–Weiss law

$$\epsilon = \frac{A}{T - T_c}, \qquad \ldots\ldots (1.1)$$

(where T_c is the critical temperature or just below it), similar to the susceptibility law for ferromagnets ; below the transition temperature it drops sharply, though it may still be very large ; dielectric constants of several hundred or even several thousand are in fact characteristic of ferroelectrics.

It can be shown that the Curie–Weiss law is to be expected on thermodynamic grounds whatever the atomic structure. Thermodynamics predicts other changes that should accompany the transition from the non-polar to the polar state. Thus the polarization will be accompanied by strains ; there will be strains proportional to the polarization if the non-polar crystal is piezoelectric, and in all cases there will be strains proportional to the square of the polarization. The anomaly of the dielectric constant will be accompanied by anomalies in some of the piezoelectric and elastic constants. There will be a discontinuity in specific heat at a second order transition, and a latent heat at a first order transition. Most of these predictions are verified in practice.

1.2. *Classification of Ferroelectrics*

Pyroelectrics are very numerous ; pyroelectricity is in fact mainly a matter of crystal symmetry, and of the 32 crystal classes 11 are normally pyroelectric. Very few pyroelectrics, however, possess the essential property of polar reversibility that makes them ferroelectric. The known ferroelectrics can conveniently be grouped into two classes : the first

class are orthorhombic (class D_2) or tetragonal (D_{2d}) when non-polar; they have only one possible polar axis and two possible directions of polarization, and hence form a fairly simple domain pattern when polar; they are piezoelectric even in the non-polar state. The second class have complete cubic symmetry (O_h); there are therefore always several equivalent directions of polarization, and hence a complicated domain pattern; they are of course not piezoelectric when non-polar.

Fig. 1

Dielectric constants as functions of temperature.

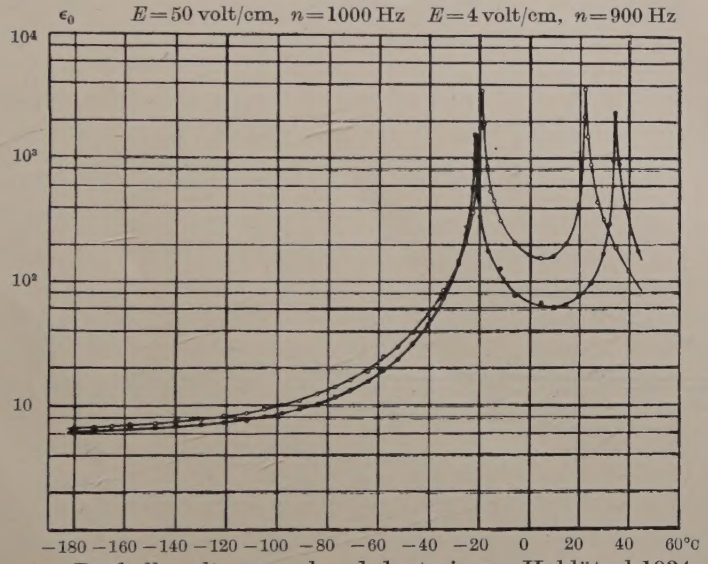

(*a*) Rochelle salt, normal and deuterium. Hablützel 1934.

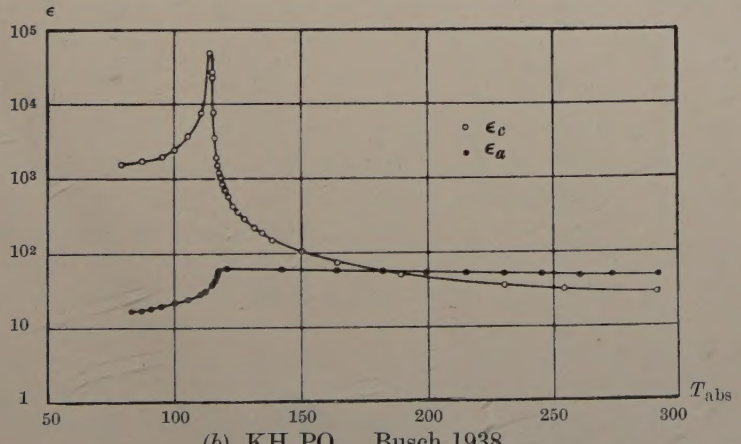

(*b*) KH_2PO_4. Busch 1938.

The first class can conveniently be divided into two subclasses. A typical member of the first subclass is Rochelle salt ($NaKC_4H_4O_6 \cdot 4H_2O$), the first known ferroelectric. Rochelle salt is unusual in having a lower

as well as an upper transition temperature, and it is polar only between those temperatures. The polarity is along the x-axis and is accompanied by a shear of 3 or 4′ in the yz plane. The saturation polarization and dielectric constant are shown in figs. 2 (a) and 1(a). Mixed crystals in

Fig. 1

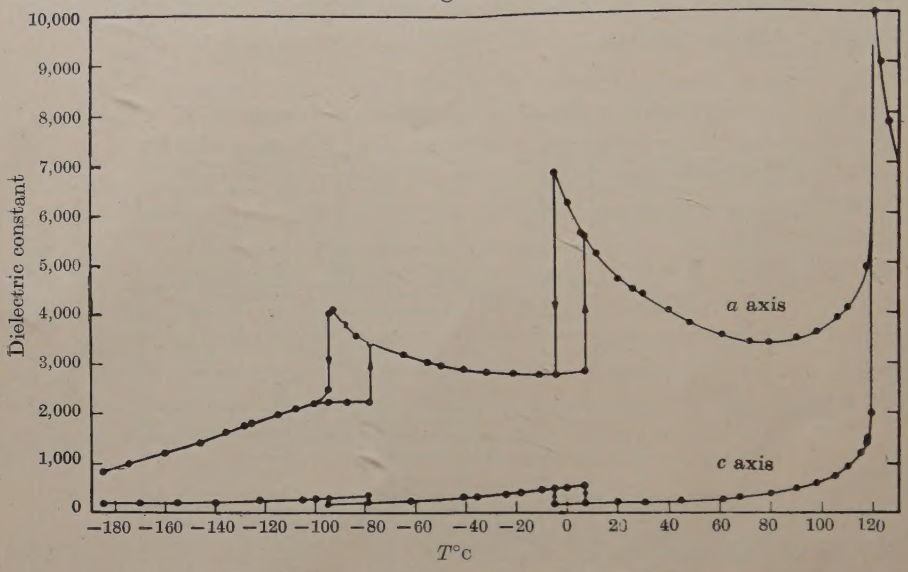

(c) $BaTiO_3$, single crystal. Merz 1949.

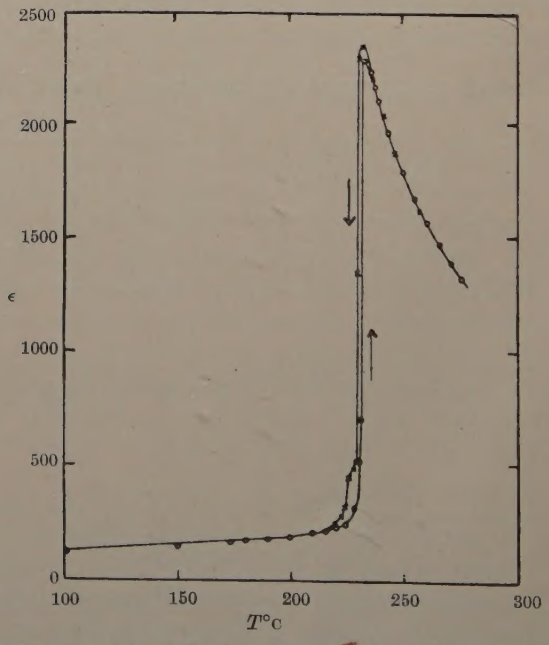

(d) $PbZrO_3$, ceramic. Shirane, Sawaguchi and Takeda 1951.

which some of the potassium in Rochelle salt is replaced by ammonium, rubidium, or thallium have similar properties (Cady 1946). Lithium ammonium tartrate and lithium tantalum tartrates have only upper transition temperatures at 106°K and 13°K respectively (Matthias and Hulm 1951, Merz 1951).

The second subclass consists of KH_2PO_4 and a number of chemically similar compounds such as KH_2AsO_4, RbH_2PO_4. These all have tetragonal symmetry; the polarization is along the axis of symmetry (z-axis) and is accompanied by a shear in the xy plane; and there is one transition temperature. The saturation polarization, dielectric constant, and strains are shown in figs. 2 (*b*), 1(*b*), 3 (*a*).

The second class of ferroelectrics belong to a group of substances called perovskites after one of its members ($CaTiO_3$). They all have the chemical formula ABO_3, where A is a di- or monovalent metal and B a tetra- or pentavalent one. In the state with complete cubic symmetry the A atoms are at the cube corners, the B atoms at the body-centres, and the O atoms at the face-centres. The axis of polarization may be parallel to a cube edge, a face diagonal, or a body diagonal. $BaTiO_3$, which has been more studied than any other perovskite, passes through all these forms in turn as the temperature is lowered. The polarizations are accompanied by the expected strains; polarization along a cube edge is accompanied by an extension in the direction of polarization and contractions perpendicular to it, reducing the symmetry to tetragonal (C_{4v}); similarly polarization along a face diagonal reduces the symmetry to orthorhombic (C_{2v}); polarization along a body diagonal reduces it to rhombohedral (C_{3v}). The strains are of course electrostrictive in character, that is second order in the polarization; nevertheless they are the same order of magnitude as the piezoelectric strains in ferroelectrics of the first class. In fig. 3 (*b*) we show the strains for $BaTiO_3$, and in fig. 2 (*c*) the saturation polarization. In fig. 1 (*c*) we show the dielectric constants of $BaTiO_3$; it will be seen that the dielectric constant across the direction of polarization is normally greater than that along it. Because of the difficulty of getting single crystals much of the dielectric work on perovskites has been done on ceramics. One difficulty is that a crystal that is single in the non-polar state may break up into a complicated domain pattern when polarized.

Some perovskites have a transition at which the dielectric constant behaves in the same way as at a ferroelectric transition, and yet below the transition temperature there is no hysteresis and no permanent polarization. A typical example of this is $PbZrO_3$ (Shirane, Sawaguchi and Takeda 1951). The transition is to a new non-polar state. Like the polar states this is a slight distortion of the cubic states; x-ray examination shows it to have orthorhombic symmetry (Sawaguchi, Maniwa and Hoshino 1951) but with a multiple unit cell, whereas the polar states have unit cells of about the same size as the cubic state. The similarity of the behaviour of the dielectric constant to that at a

Fig. 2
Saturation polarizations as functions of temperature.

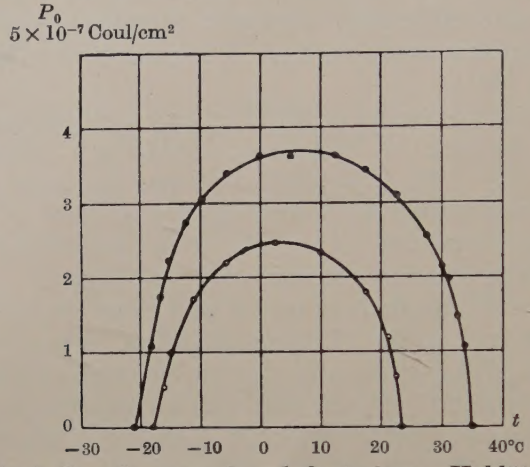

(*a*) Rochelle salt, normal and deuterium. Hablützel 1934.

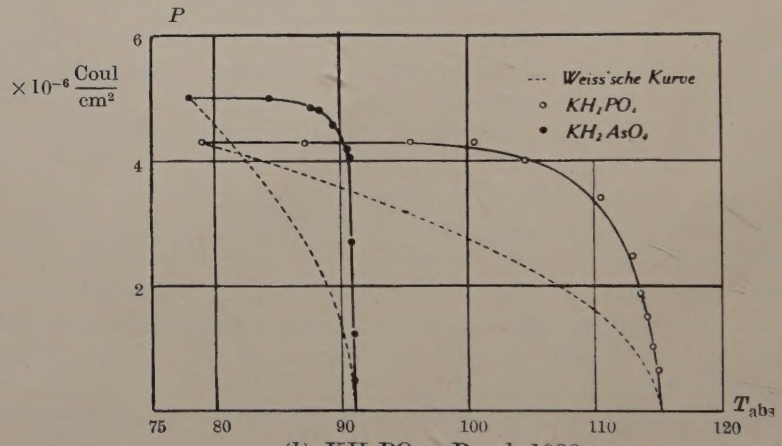

(*b*) KH_2PO_4. Busch 1938.

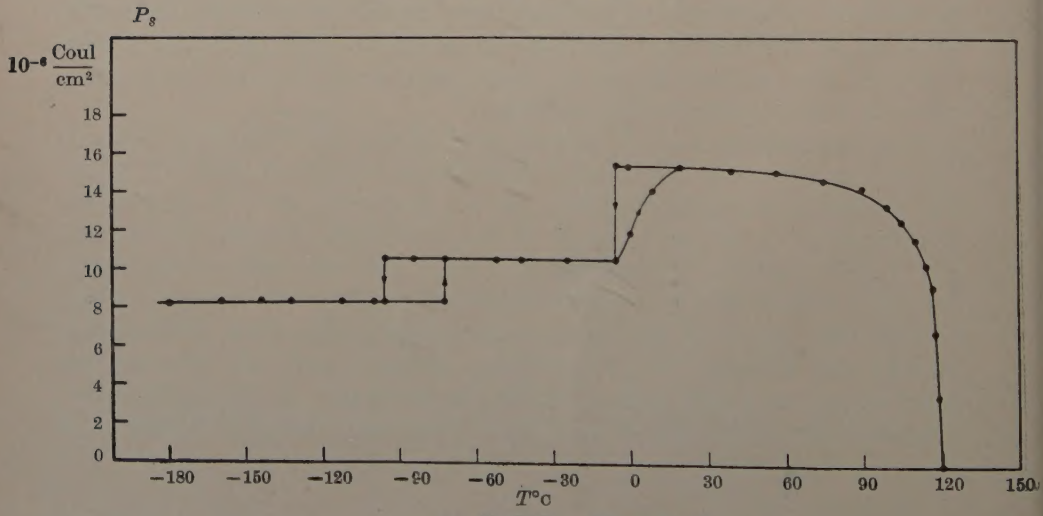

(*c*) $BaTiO_3$. Merz 1949.

Fig. 3
Spontaneous strains.

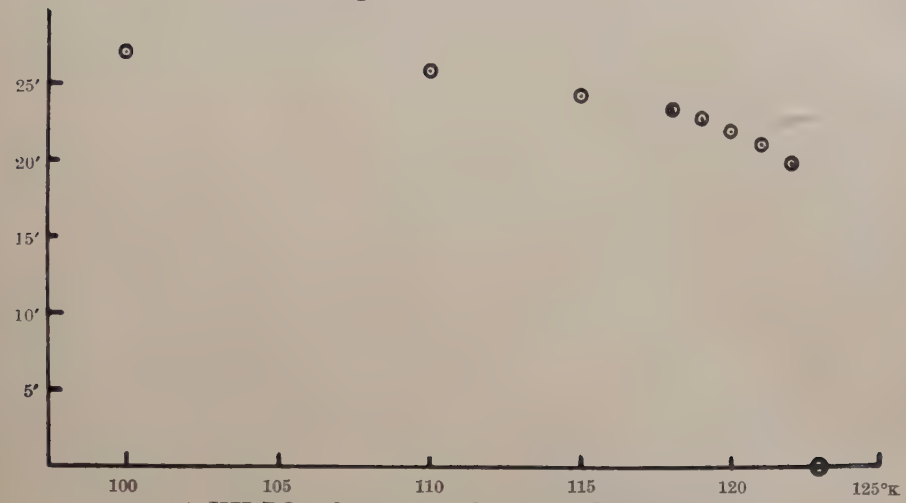

(*a*) KH_2PO_4, shear in *xy* plane. De Quervain 1944.

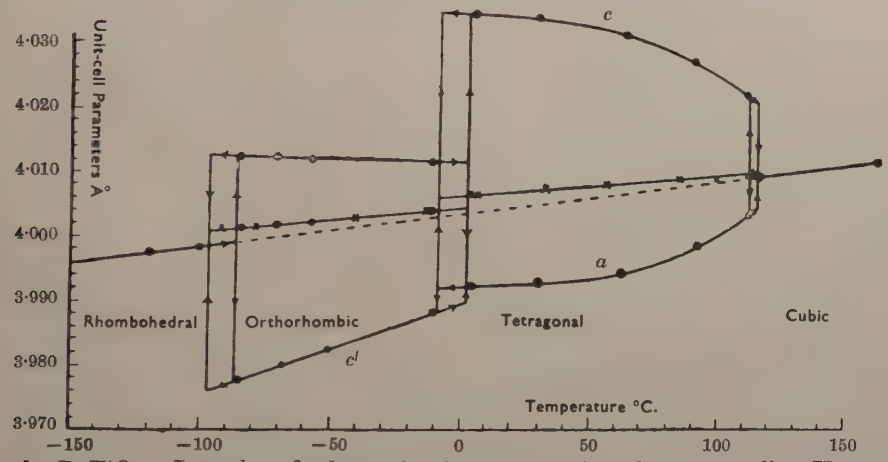

(*b*) $BaTiO_3$. Lengths of edges of cubic or pseudo-cubic unit cell. Kay and Vousden 1949.

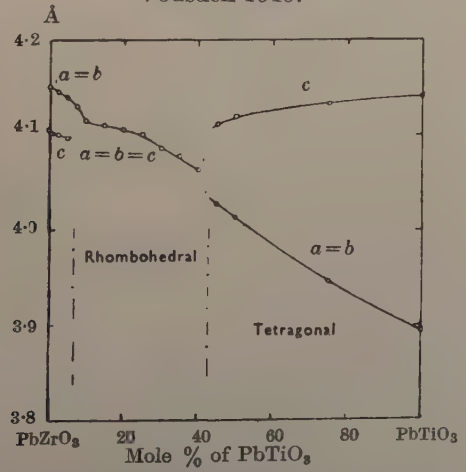

(*c*) Lattice-spacing of $Pb(Zr—Ti)O_3$ at room temperature as a function of composition. Shirane and Suzuki 1952.

ferroelectric transition (see fig. 1 (*d*)), is probably due to the fact that a polar state is very close in free energy to the non-polar one ; this is shown by the fact that the polar state can be induced by applying a very strong electric field or by slightly varying the composition (fig. 4 (*b*) and (*c*)).

Fig. 4

Phase diagrams.

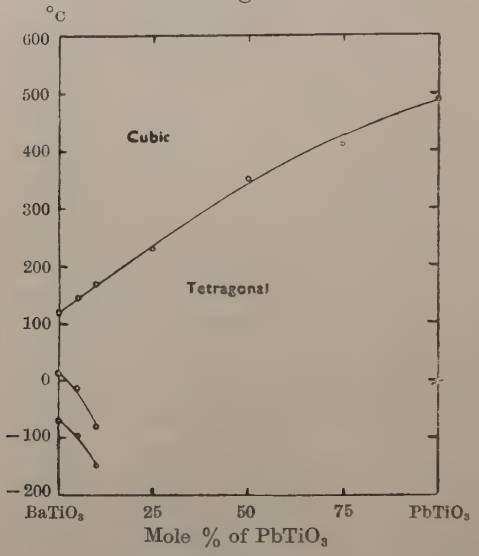

(*a*) (Ba—Pb)TiO_3. Shirane and Suzuki 1951.

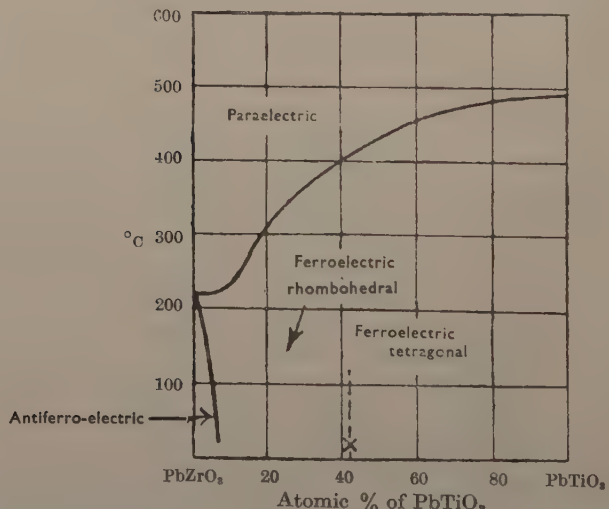

(*b*) Pb(Zr—Ti)O_3. Shirane, Suzuki and Takeda 1952, and Shirane and Suzuki 1952.*

* *Note added in proof.*—A second antiferroelectric phase has since been discovered (Sawaguchi 1953).

It has become customary to give the name antiferroelectric to the non-cubic, non-polar states. Some mixed perovskites pass through both antiferroelectric and ferroelectric states and a few typical phase-diagrams are shown in fig. 4.

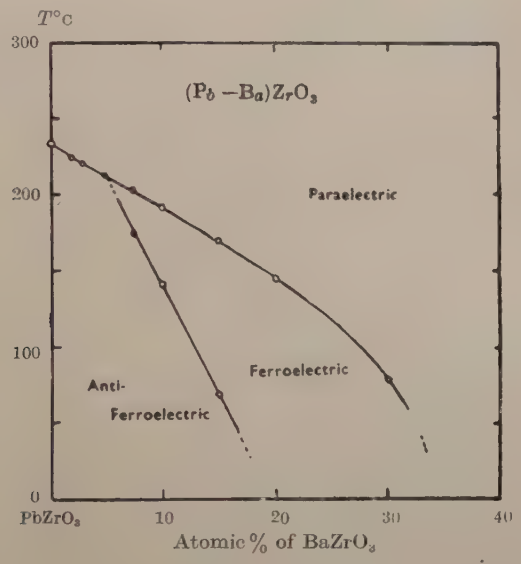

(*c*) (Pb—Ba)ZrO_3. Shirane 1951.

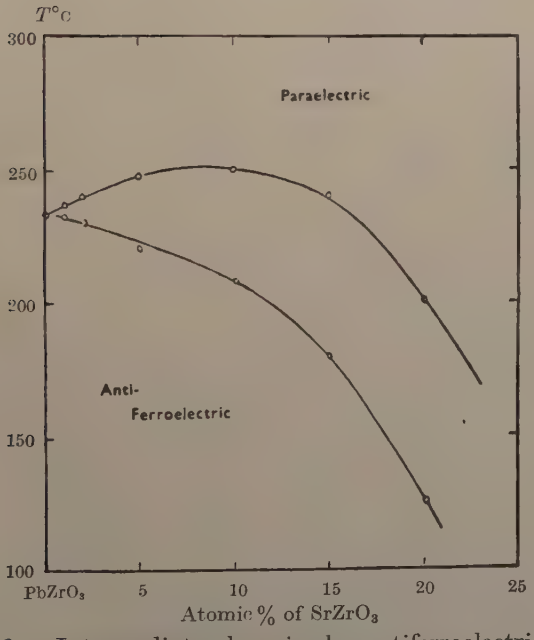

(*d*) (Pb—Sr)ZrO_3. Intermediate phase is also antiferroelectric. Shirane 1951.

In table 1 we list the forms found in various perovskites in order of increasing temperature. We see that at least six forms are present and that the order in which they appear with increasing temperature is always the same, namely : non-polar orthorhombic, non-polar tetragonal, polar rhombohedral, polar orthorhombic, polar tetragonal, cubic, though in any particular substance there are always gaps in the sequence. We shall consider the significance of this later.

Table 1

Substance	Crystal forms
$BaTiO_3$	Polar rhombohedral, polar orthorhombic, polar tetragonal, cubic.
$SrTiO_3$	Cubic.
$CaTiO_3$	Non-polar orthorhombic.
$PbTiO_3$	Polar tetragonal, cubic.
$PbZrO_3$	Non-polar orthorhombic, cubic.
$Pb(ZrTi)O_3$	Non-polar orthorhombic, polar rhombohedral, cubic.
$(PbBa)ZrO_3$	Non-polar orthorhombic, polar . . . , cubic.
$(PbSr)ZrO_3$	Non-polar orthorhombic, non-polar . . . , cubic.
$NaNbO_3$	Non-polar orthorhombic, non-polar tetragonal, cubic.
$KNbO_3$	Polar orthorhombic, polar tetragonal, cubic.

(In $NaNbO_3$ it has been assumed that a multiple unit cell implies a non-polar form.)

Ferroelectric behaviour has also been observed in $Cd_2Nb_2O_7$ and $Pb_2Nb_2O_7$ (Cook and Jaffe 1953) and also in WO_3 (Matthias 1949). In the latter substance a phase change has been observed (Ueda and Ichinokawa 1950). All these substances may be considered to be pseudo-perovskites with some lattice-sites vacant.

Ferroelectric behaviour has been observed in $LiTaO_3$ and $LiCbO_3$, which have an ilmenite structure (Matthias and Reimaker 1949).

§ 2. Thermodynamics of Crystals

2.1. *Introduction*

It is now desirable to spend some time defining the physical constants of a crystal and examining the relations between them. Although the results will be true for any crystal they are specially important for ferroelectrics. One reason for this is the high dielectric constant of most ferroelectrics. This means that certain pairs of constants, such as the elastic constants for constant polarization and constant field, which are indistinguishable for most substances, are quite different for ferroelectrics. Again because of the relations between the various constants, the existence of an anomaly in one, as in the dielectric constant at the transition temperature, means that anomalies exist in others, and it is important to show the connection between them.

2.2. *Definition of Physical Constants*

The elastic and piezoelectric constants, and the dielectric susceptibilities are defined by the equations :

$$\begin{cases} x_h = -s_{hi}^{E} X_i + d_{mh} E_m, & \ldots\ldots (2.1a) \\ P_m = -d_{mh} X_h + \eta_{km}^{X} E_k, & \ldots\ldots (2.1b) \end{cases}$$

$$\begin{cases} X_h = -c_{hi}^{P} x_i + a_{mk} P_m, & \ldots\ldots (2.1c) \\ E_m = -a_{mk} x_h + \chi_{km}^{x} P_k, & \ldots\ldots (2.1d) \end{cases}$$

$$\begin{cases} X_h = -c_{hi}^{E} x_i + e_{mh} E_m, & \ldots\ldots (2.1e) \\ P_m = e_{mh} x_h + \eta_{km}^{x} E_k, & \ldots\ldots (2.1f) \end{cases}$$

$$\begin{cases} x_h = -s_{hi}^{P} X_i + b_{mh} P_m, & \ldots\ldots (2.1g) \\ E_m = b_{mh} X_h + \chi_{km}^{X} P_k. & \ldots\ldots (2.1h) \end{cases}$$

X_h and x_h are the components of stress and strain respectively ; E_m and P_m are the components of electric field and polarization. The Voigt notation is used, so that the suffixes h and i take six values ; X_1, X_2 and X_3 are compressions and X_4, X_5, X_6 shear stresses ; x_1, x_2, x_3 are extensions, and x_4, x_5, x_6 shears. The suffixes k and m take, of course, only three values. The summation convention is used, that is, any suffix occurring twice in a product is to be summed. In a polar crystal the polarization is measured relative to its value for zero field and stress. We assume that relations between field, polarization etc. are linear, and for the present we assume that conditions are all isothermal (or all adiabatic).

We see that the equations define twelve sets of coefficients, but only three sets are independent since the coefficients occurring in any pair of equations can be found in terms of those occurring in any other pair ; the repetition of the coefficients a, b, d, e is a consequence of the existence of free energy, as we shall see later. The meaning of the coefficients is clear from the equations ; thus η^X is the dielectric susceptibility measured at constant stress, and η^x the same quantity measured at constant strain ; for non-piezoelectric substances these quantities are the same, and for most piezoelectrics the difference may be neglected, but for ferroelectrics the difference may be important.

It is quite easy to obtain relations between the coefficients. Thus if we substitute from (2.1b) in (2.1g) we have

$$x_h = -s_{hi}^{P} X_i - b_{mh} d_{mi} X_i + b_{mh} \eta_{km}^{X} E_k,$$

and comparing this with (2.1a) we see that

$$s_{hi}^{E} = s_{hi}^{P} + b_{mh} d_{mi}, \quad \ldots\ldots (2.2a)$$

$$d_{kh} = b_{mh} \eta_{km}^{X}. \quad \ldots\ldots (2.2b)$$

Any other relations we need can be obtained in a similar way.

2.3. *Constants for Rochelle Salt*

Since the elastic constants and susceptibilities are symmetrical the s_{hi}, c_{hi} will have 21 independent components, and χ_{km}, η_{km} will have six independent components ; the piezoelectric coefficients will in general have 18 independent components. In most crystal classes, however, the number of independent components will be much reduced by symmetry. Thus in the case of Rochelle salt above the transition temperature the crystal class is D_2, and each piezoelectric coefficient has only three components, e.g. d_{14}, d_{25}, d_{36} (Mason 1950) ; these connect shears in a plane with polarization or field perpendicular to the plane. If we now write down the components of eqns. (2.1) for $h=4$ and $m=1$, we find that

$$\begin{cases} x_4=-s_{44}{}^E X_4+d_{14}X_1, & (2.3a) \\ P_1=-d_{14}X_4+\eta_{11}{}^X E_1, & (2.3b) \end{cases}$$

$$\begin{cases} X_4=-c_{44}{}^P x_4+a_{14}P_1, & (2.3c) \\ E_1=-a_{14}x_4+\chi_{11}{}^x P_1, & (2.3d) \end{cases}$$

$$\begin{cases} X_4=-c_{44}{}^E x_4+e_{14}E_1, & (2.3e) \\ P_1=e_{14}x_4+\eta_{11}{}^x E_1, & (2.3f) \end{cases}$$

$$\begin{cases} x_4=-s_{44}{}^P X_4+b_{14}P_1, & (2.3g) \\ E_1=b_{14}X_4+\chi_{11}{}^X P_1. & (2.3h) \end{cases}$$

By comparing these equations it is quite easy to see that

$$\chi_{11}{}^X=1/\eta_{11}{}^X \text{ etc.}, \quad (2.4a)$$

$$c_{44}{}^P=1/s_{44}{}^P \text{ etc.}, \quad (2.4b)$$

$$b_{14}=a_{14}s_{44}{}^P, \quad (2.4c)$$

$$d_{14}=\eta_{11}{}^X b_{14}=\eta_{11}{}^X a_{14}s_{44}{}^P, \quad (2.4d)$$

$$s_{44}{}^E=s_{44}{}^P+b_{14}d_{14}=s_{44}{}^P(1+a_{14}d_{14}), \quad (2.4e)$$

$$\chi_{11}{}^x=\chi_{11}{}^X+a_{14}b_{14}=\chi_{11}{}^X(1+a_{14}d_{14}), \quad (2.4f)$$

$$\frac{\chi_{11}{}^X}{\chi_{11}{}^x}=\frac{s_{44}{}^P}{s_{44}{}^E}=\frac{\eta_{11}{}^x}{\eta_{11}{}^X}. \quad (2.4g)$$

In table 2 we have listed some measured physical constants and others calculated from them by eqns. (2.4).

We see that the directly measured values of the ' clamped ' dielectric stiffness coefficient $\chi_{11}{}^x$ agree very well with the values calculated from the ' free ' coefficient $\chi_{11}{}^X$. Another point of interest is that some coefficients, e.g. $\eta_{11}{}^X$, d_{14}, $s_{44}{}^E$, show a large anomaly at the transition temperature, whereas others, such as b_{14} or s_{44} are almost constant, although they are derived by calculation from the first set. This is very important, as we shall see later when we are considering what atomic model would account for the properties of Rochelle salt. For it is usually convenient to take as our independent variables the strain x and the polarization P. Then we see from (2.1) that the coefficients to be calculated directly from the model are c^P, a, and χ^x. From eqn. (2.4) and table 2 we see that $c_{44}{}^P$ and a_{14} are approximately

constant, while $\chi_{11}{}^x$ decreases steadily to a small value near the transition temperature. Since all the other coefficients can be derived from these our atomic model has only to account for the behaviour of $\chi_{11}{}^x$ and all the anomalies will be accounted for.

Table 2. Physical Constants of Rochelle Salt above Upper Transition Temperature

	Obs.		Calc.	Obs.	Obs.	Calc.	Obs.	Calc.
T (°C)	$\eta_{11}{}^X$	$\chi_{11}{}^X$	$\chi_{11}{}^x$	$\chi_{11}{}^x$	$d_{14}\times10^6$	$b_{14}\times10^7$	$s_{44}{}^E\times10^{12}$	$s_{44}{}^P\times10^{12}$
24·7	119	0·008	0·051	0·053	67·7	5·7	47·2	8·6
25·7	64·3	0·016	0·061	0·060	37·2	5·8	29·7	8·1
28·2	34·2	0·029	0·075	0·076	20·6	6·0	20·8	8·4
31·0	21·0	0·048	0·094	0·094	12·8	6·1	16·3	8·5
34·2	14·3	0·070	0·114	0·115	9·1	6·3	14·4	8·7
38·0	10·6	0·094	0·141	0·140	6·65	6·3	13·0	8·8
40·2	9·1	0·110	0·157	0·154	5·88	6·4	12·6	8·9
42·0	8·2	0·122	0·169	0·166	5·07	6·2	12·1	9·0
47·5	6·3	0·159	0·206	0·202	4·00	6·3	11·6	9·1

(Observed results from Mueller 1940, except those for $\chi_{11}{}^x$ which are from figure in paper by Mason 1947.)

2.4. *Adiabatic and Isothermal Conditions*

So far we have not specified whether the coefficients are to be measured under adiabatic or isothermal conditions, since this usually makes little difference to the value. There are, however, one or two cases where the difference cannot be neglected, so we must now consider this point. We may note here that static measurements will normally give isothermal coefficients and high frequency measurements will give adiabatic ones.

To get a complete picture we should have to replace eqns. (2.3) by more complicated ones connecting the variables E, X, S, and P, x, T. Each coefficient in the eqns. (2.3) would be duplicated (being measured at constant S or constant T), and new coefficients such as the thermal expansion coefficient and pyroelectric coefficients would be introduced. As before there will be relations between the different coefficients. We shall, however, content ourselves with working out a special case, that of KH_2PO_4, where the adiabatic and isothermal coefficients have been measured near the transition point and found to be markedly different.

Before considering this case, however, it is desirable to say something about the free energy.

2.5. *Free Energy*

If U is the internal energy of a body subject to external stresses and electric fields then we have

$$dU=T\,dS-X_i\,dx_i+E_m\,dP_m. \quad . \quad . \quad . \quad . \quad (2.5)^*$$

* In this expression P_m is sometimes replaced by $D_m/4\pi$. This means that the internal energy of the body is defined so as to include the energy of the field *in vacuo*.

We can define other potential functions in terms of the internal energy, entropy, etc., and it is convenient to introduce the following (Mason 1950):

Helmholtz free energy, $A=U-TS$, ... (2.6*a*)

Enthalpy, $H=U+X_i x_i-E_m P_m$, . . . (2.6*b*)

Elastic enthalpy, $H_1=U+X_i x_i$, ... (2.6*c*)

Electric enthalpy, $H_2=U-E_m P_m$, ... (2.6*d*)

Gibbs function, $G=H-TS$, ... (2.6*e*)

Elastic Gibbs function, $G_1=H-TS$, ... (2.6*f*)

Electric Gibbs function, $G_2=H_2-TS$. . . . . (2.6*g*)

From these definitions we can at once obtain the differential relations :

$$dA=-S\,dT-X_i\,dx_i+E_m\,dP_m, \quad . . . . . \quad (2.7a)$$

$$dH=T\,dS+x_i\,dX_i-P_m\,dE_m, \quad . . . . . \quad (2.7b)$$

$$dH_1=T\,dS+x_i\,dX_i+E_m\,dP_m, \quad . . . . . \quad (2.7c)$$

$$dH_2=T\,dS-X_i\,dx_i-P_m\,dE_m, \quad . . . . . \quad (2.7d)$$

$$dG=-S\,dT+x_i\,dX_i-P_m\,dE_m, \quad . . . . . \quad (2.7e)$$

$$dG_1=-S\,dT+x_i\,dX_i+E_m\,dP_m, \quad . . . . . \quad (2.7f)$$

$$dG_2=-S\,dT-X_i\,dx_i-P_m\,dE_m. \quad . . . . . \quad (2.7g)$$

From these equations we can at once deduce relations of the Maxwell type such as

$$\left(\frac{\partial X_i}{\partial P_m}\right)_{T,x_i}=-\left(\frac{\partial^2 A}{\partial x_i \partial P_m}\right)_T=-\left(\frac{\partial E_m}{\partial x_i}\right)_{T,P_m} \quad . . . . \quad (2.8)$$

It is the existence of relations such as this that explain why the coefficients a, b, c, d, occur twice in eqns. (2.1).

2.6. *Adiabatic and Isothermal Constants for* KH_2PO_4

Baumgartner (1950) has made an extensive series of measurements of the properties of KH_2PO_4 near the transition temperature. One set of measurements were those of susceptibility using an alternating field plus a constant biasing field ; these give the adiabatic susceptibility for zero stress as a function of temperature and field. Another set of measurements made ballistically give the polarization as a function of temperature and field ; from these by differentiation we can find the isothermal susceptibility as a function of temperature and polarization.

The applied field E is always along the tetragonal axis (which is also the axis of spontaneous polarization), and since this is a principal axis the resultant polarization P is also along this axis. The ballistic measurements show that E can be expressed in the form

$$E=\alpha(T-\Theta)P+\psi(P), \quad . . . . . \quad (2.9)$$

where Θ is the transition temperature. The isothermal reciprocal susceptibility is given by

$$\left(\frac{\partial E}{\partial P}\right)_T = \alpha(T-\Theta)+\psi'(P). \quad . \quad . \quad . \quad . \quad . \quad (2.10)$$

To find the adiabatic susceptibility we use the equation

$$\left(\frac{\partial E}{\partial P}\right)_S = \left(\frac{\partial E}{\partial P}\right)_T + \left(\frac{\partial E}{\partial T}\right)_P \left(\frac{\partial T}{\partial P}\right)_S ;$$

but from (2.7 *c*) we have

$$\left(\frac{\partial T}{\partial P}\right)_S = \left(\frac{\partial E}{\partial S}\right)_P = \left(\frac{\partial E}{\partial T}\right)_P \Big/ \left(\frac{\partial S}{\partial T}\right)_P ,$$

and hence

$$\begin{aligned}\left(\frac{\partial E}{\partial P}\right)_S &= \left(\frac{\partial E}{\partial P}\right)_T + \left(\frac{\partial E}{\partial T}\right)_P^2 \Big/ \left(\frac{\partial S}{\partial T}\right)_P \\ &= \left(\frac{\partial E}{\partial P}\right)_T + \alpha^2 P^2 T/C^P \\ &= \alpha(T-\Theta)+\psi'(P)+\alpha^2 P^2 T/C^P, \quad . \quad . \quad (2.11)\end{aligned}$$

where C^P is specific heat for constant polarization. The measurements of dielectric constant with alternating field already referred to give $(\partial E/\partial P)_S$ as a function of field and temperature, but by making use of the ballistic measurements we can find $(\partial E/\partial P)_S$ as a function of polarization and temperature, and the results can be expressed in the form

$$\left(\frac{\partial E}{\partial P}\right)_S = \beta(T-\Theta)+\xi(P). \quad . \quad . \quad . \quad . \quad . \quad (2.12)$$

If eqn. (2.12) is to agree with (2.11) we should have therefore

$$\left.\begin{aligned}\beta &= \alpha \\ \xi(P) &= \psi'(P)+\alpha^2 P^2 T/C^P.\end{aligned}\right\} \quad . \quad . \quad . \quad . \quad . \quad . \quad (2.13)$$

The ballistic measurements in fact give

$$\alpha = 0{\cdot}0033,$$

and the susceptibility measurements give

$$\beta = 0{\cdot}0038,$$

so that there is moderate agreement. The values of ξ and ψ' as functions of P are given in table 3. It will thus be seen that rather less than half

Table 3

P (microcoul/cm^2)	1·5	2·0	2·5	3·0
$\xi \times 10^3$	4·94	9·69	18·75	39·9
$\psi' \times 10^3$	0·76	2·71	7·28	16·5
$(\xi-\psi') \times 10^3$	4·18	6·98	11·47	23·4
$\alpha^2 P^2 T/C^P \times 10^3$	1·71	3·04	4·75	6·8

the difference between the susceptibility measurements made with an alternating field and those made ballistically is due to the difference between adiabatic and isothermal measurements. The susceptibility measured with alternating field is, however, further reduced for other reasons.

2.7. *Electrostriction*

When an electric field is applied to a piezoelectric crystal it produces strains proportional to the field ; but in all crystals, whether piezoelectric or not, it also produces strains proportional to the square of the field. This second order effect is called the electrostrictive effect. It is easier to study it in non-piezoelectric crystals, so we shall deal with it for these classes. Just as there are four types of piezoelectric constant—the a's, b's, d's and e's—all mutually related, so there are four types of electrostrictive constant. It will, however, be sufficient to define only two of them, those relating strain and stress to polarization ; they are defined by the equations

$$X_h = -c_{hi}^{P} x_i + q_{hkl} P_k P_l, \quad . \quad . \quad . \quad . \quad . \quad (2.14a)$$

$$x_i = -s_{ij}^{P} X_j + Q_{im\,n} P_m P_n. \quad . \quad . \quad . \quad . \quad (2.14b)$$

The electrostrictive constants are here written in the Voigt notation with three suffixes, but they are really fourth order tensors. The q's and Q's are simply related, a substitution from (2.14a) into (2.14b) shows that

$$\left.\begin{aligned} q_{hm\,n} &= c_{hi}^{P} Q_{im\,n}, \\ Q_{im\,n} &= s_{ih}^{P} q_{hm\,n}\,; \end{aligned}\right\} \quad . \quad . \quad . \quad . \quad (2.15)$$

they are, of course, symmetrical in the last two suffixes.

Just as the piezoelectric constants all have two physical interpretations so do the electrostrictive constants. For we have

$$2Q_{im\,n} = 2Q_{i\,nm} = \frac{\partial^2 x_i}{(\partial P_m \partial P_n)}\,; \quad . \quad . \quad . \quad . \quad . \quad (2.16)$$

but

$$\left(\frac{\partial x_i}{\partial P_m}\right)_X = \left(\frac{\partial E_m}{\partial X_i}\right)_P,$$

and hence

$$2Q_{im\,n} = \frac{\partial^2 E_m}{\partial X_i \partial P_n} = \frac{\partial \chi_{m\,n}^{x}}{\partial X_i}, \quad . \quad . \quad . \quad . \quad . \quad (2.17)$$

so that the electrostrictive constant is also a measure of the rate of variation of dielectric stiffness coefficient with stress. Similarly we can show that

$$2q_{im\,n} = -\frac{\partial^2 E_m}{\partial x_i \partial P_n} = -\frac{\partial \chi_{m\,n}^{x}}{\partial x}. \quad . \quad . \quad . \quad . \quad . \quad (2.18)$$

2.8. *Relation of Piezoelectric to Electrostrictive Constants*

From eqn. (2.14*b*) we have

$$\frac{\partial x_i}{\partial P_m} = 2Q_{im\,n}P_n. \quad . \quad . \quad . \quad . \quad . \quad . \quad . \quad . \quad (2.19)$$

Now the left-hand side defines the piezoelectric coefficient b_{mi}, so that a substance that normally has zero piezoelectric coefficients will have finite ones if it is given a polarization, e.g. by applying a biasing field. The piezoelectric coefficients will then be proportional to the polarization.

2.9. *Piezoelectric Constants of Perovskites*

Equation (2.19) is particularly useful when applied to the ferroelectric perovskites. As we have already mentioned these are not piezoelectric when in the cubic state. All the other forms can be considered as strained and polarized forms of the cubic state; the piezoelectric constants can then be calculated from (2.19) in terms of the saturation polarization and the electrostrictive constants of the cubic state.

Now in a crystal with complete cubic symmetry there are only three distinct, non-vanishing electrostrictive constants, namely

$$Q_{111}=Q_{222}=Q_{333},$$
$$Q_{122}=Q_{133}=\ldots,$$
$$Q_{423}=Q_{531}=Q_{612}=\ldots.$$

It is convenient to drop one suffix and write*

$$Q_{11}=Q_{111}=\ldots,$$
$$Q_{12}=Q_{122}=\ldots,$$
$$Q_{44}=2Q_{423}=\ldots.$$

These ferroelectrics are often prepared in ceramic form. If we consider the ferroelectric to be an isotropic substance then the number of independent constants is reduced to two; for it can be shown that

$$Q_{44}=2(Q_{11}-Q_{12}).$$

The Q's for the ceramic will not, of course, be the same as for the single crystal; however they are closely related and must be of similar magnitude.

We see from the previous paragraphs that there are three ways of determining the electrostrictive constants: by comparing the polarization —either spontaneous or induced—with the corresponding strain; by measuring the variation of dielectric stiffness coefficient with stress; and by measuring the piezoelectric coefficients of the spontaneously polarized substance. All three types of measurement have been made, but unfortunately they are not strictly comparable.

Shirane and Sato (1951) have made measurements of the effect of stress on the dielectric constant above the transition point of a ceramic

* The notation is now the same as that used by Devonshire (1951).

mixture of $BaTiO_3$ and $SrTiO_3$ (molar proportions 60/40). From the table at the end of their paper we can deduce that

$$Q_{11}=0{\cdot}82\times10^{-12} \text{ c.g.s. units},$$

$$Q_{12}=-0{\cdot}19\times10^{-12} \text{ c.g.s. units}.$$

Measurements of the piezoelectric constants of a $BaTiO_3$ ceramic below the transition temperature have been made by Mason, and from his results he deduced that

$$Q_{11}=3{\cdot}6\times10^{-12},$$

$$Q_{12}=-1{\cdot}35\times10^{-12}.$$

Again, from a comparison of the measurements of spontaneous polarization of a $BaTiO_3$ single crystal by Merz (1949 b) and x-ray measurements of the spontaneous strain by Kay and Vousden (1948), we find that

$$Q_{11}=2{\cdot}9\times10^{-12},$$

$$Q_{12}=-1{\cdot}1\times10^{-12},$$

$$Q_{44}=2{\cdot}7\times10^{-12}.$$

The agreement is perhaps as good as could be expected when we remember that the constants of a ceramic are necessarily ill-defined; for a given polarization may correspond to several different internal states since it may be produced by altering the polarization of each domain uniformly or by rotating some of them.

§ 3. Thermodynamics of the Transition

3.1. *Introduction*

The behaviour of a substance near its transition temperature can best be studied by examining its free energy. The appropriate free energy to use depends on the external conditions; if, as is usually the case, these are a fixed temperature, zero stress, and zero field, we may use indifferently the quantities A, G, G_1 and G_2, since these are then all equal.

The most convenient quantity to use is G_1, which is normally expressed as a function of temperature, stress and polarization. If we take the stress to be zero then we can expand G_1 in powers of the polarization, the coefficients being functions of temperature. For simplicity we shall first suppose that the polarization is along only one axis. We can discuss all the transitions in ferroelectrics of the first class on this basis, and the upper transitions in the perovskites, but not the lower transitions, since these involve a change in direction of polarization.

Expanding G_1 in this way we have

$$G_1-G_{10}=\tfrac{1}{2}\chi^X P^2+\tfrac{1}{4}\xi^X P^4+\tfrac{1}{6}\zeta^X P^6+\ldots, \quad . \quad . \quad . \quad (3.1)$$

where G_{10} is the free energy for zero polarization and the coefficients are functions of temperature. The field E is then given by

$$E=\frac{\partial G_1}{\partial P}=\chi^X P+\xi^X P^3+\zeta^X P^5+\ldots . \quad . \quad . \quad . \quad . \quad (3.2)$$

It is clear that G_1 will always have a stationary value for P zero and that this will be a minimum if χ^X is positive. If, however, χ^X is negative then G_1 will be a maximum for P zero and it will have at least one stationary value for a non-zero value of P. If, therefore, χ^X changes continuously from a positive to a negative value then the stable state of the system will change from one with P zero to one with P non-zero, that is, we have a ferroelectric transition. The nature of the transition will depend on the signs of the other coefficients. The simplest case occurs when all the coefficients except χ^X are positive. P is then continuous at the transition; indeed it is clear that for χ^X small and negative the value of P is given by

$$P^2=-\chi^X/\xi^X. \quad . \quad . \quad . \quad . \quad . \quad . \quad . \quad . \quad (3.3)$$

The form of the free energy curves and also the form of P as a function of χ^X are shown in figs. 5 (*a*) and (*b*). We shall show later that in this case we have a transition of the second order, that is one without latent heat, but with a discontinuity in specific heat. If, however, some of

Fig. 5

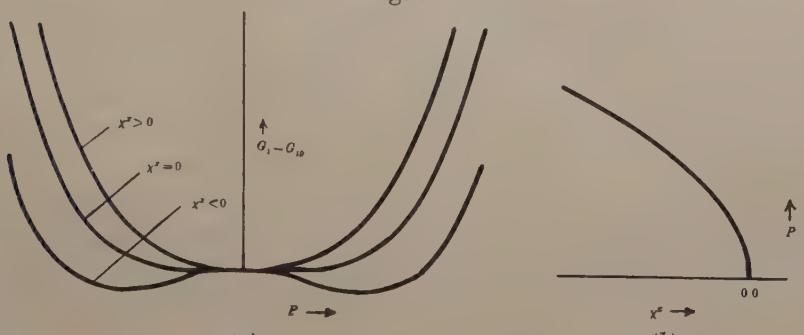

(*a*) (*b*)

(*a*) Second order transition. Free energy as a function of polarization at the transition temperature and at temperatures just above and just below.
(*b*) Spontaneous polarization as a function of temperature at a second order transition.

the other coefficients are negative then the free energy curves may take a more complicated form as shown in fig. 6 (*a*). It is then possible for a minimum for a non-zero value of P to co-exist with one for P zero; the transition will take place when the two minima are equal, and P will jump discontinuously from zero to a finite value; the transition is now a first order one with a latent heat. As an example of this we shall suppose that the free energy is given by the first three terms of (3.1), that ξ^X is negative and ζ^X is positive. Then

$$G_1-G_{10}=\tfrac{1}{2}\chi^X P^2+\tfrac{1}{4}\xi^X P^4+\tfrac{1}{6}\zeta^X P^6,$$
$$E=\chi^X P+\xi^X P^3+\zeta^X P^5.$$

For a stationary value of G_1, E is zero, and hence if P is not zero we have

$$\chi^X+\xi^X P^2+\zeta^X P^4=0.$$

At the transition this stationary value of G_1 is the same as the value at the origin, so that

$$\tfrac{1}{2}\chi^X P^2+\tfrac{1}{4}\xi^X P^4+\tfrac{1}{6}\zeta^X P^6=0,$$

and from these two equations we find that

$$P^2=(3/4)(-\xi^X/\zeta^X), \quad . \quad . \quad . \quad . \quad . \quad . \quad . \quad . \quad (3.4)$$

$$\chi^X=(3/16)(\xi^X)^2/\zeta^X, \quad . \quad . \quad . \quad . \quad . \quad . \quad . \quad . \quad (3.5)$$

thus showing that P changes discontinuously at the transition and that χ^X is positive.

Fig. 6

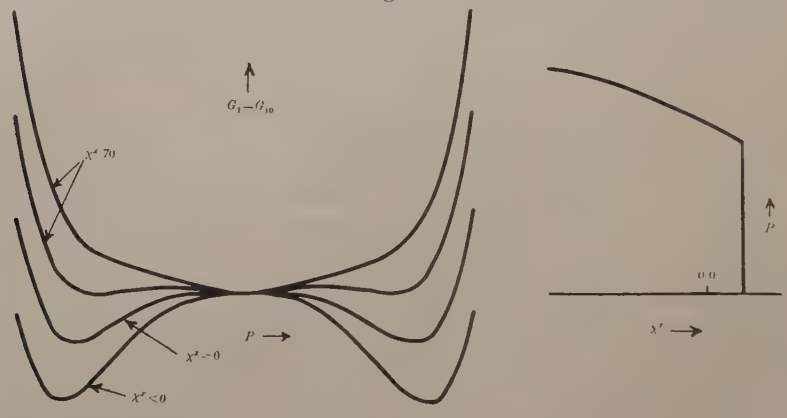

(*a*) (*b*)

(*a*) First-order transition. Free energy as a function of polarization at the transition temperature and at temperatures just above and just below.
(*b*) Polarization as a function of temperature at a first-order transition.

3.2. *Susceptibility near the Transition Point*

Above the transition point the dielectric stiffness coefficient is χ^X; below the transition point it is given by

$$\frac{\partial E}{\partial P}=\chi^X+3\xi^X P^2+5\zeta^X P^4+\ldots, \quad . \quad . \quad . \quad . \quad . \quad (3.6)$$

where P is given by

$$0=E=\chi^X+\xi^X P^2+\zeta^X P^4+\ldots.$$

Near a second-order transition where P is given by (3.3) we have

$$\frac{\partial E}{\partial P}=-2\chi^X, \quad . \quad . \quad . \quad . \quad . \quad . \quad . \quad . \quad (3.7)$$

and since χ^X is zero at the transition the dielectric stiffness coefficient has the form shown in fig. 7 (*a*), so that the dielectric constant is infinite

at the transition. Near a first-order transition the dielectric stiffness coefficient has the form shown in fig. 7 (*b*), and therefore the dielectric constant is finite but discontinuous.

Fig. 7

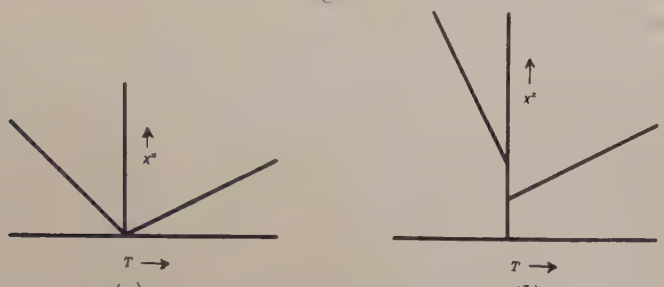

(*a*) (*b*)

Dielectric stiffness coefficient as a function of temperature.
(*a*) Near a second-order transition.
(*b*) Near a first-order transition.

3.3. *Effect of Electric Field on a Transition*

If we have a second-order transition then the effect of an electric field is to blur the transition so that the plot of P against temperature no longer has discontinuities (fig. 8 (*a*)). This we can see easily by examining eqn. (3.2). If all the coefficients on the right-hand side are positive except χ^X it is easy to see that for E positive there is only one positive solution for P, and, that for fixed E, P is a continuous function of χ^X and therefore of temperature.

Fig. 8

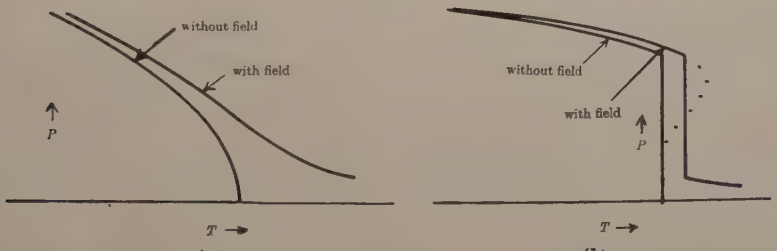

(*a*) (*b*)

Polarization as a function of temperature with and without a biasing field.
(*a*) Near a second-order transition.
(*b*) Near a first-order transition.

A first-order transition, however, will remain a first-order transition in the presence of a field—if it is not too large—and normally the temperature of the transition will be raised. We can best see this by examining fig. 6 (*a*) ; for the condition for a transition is that G, that is $G_1 - EP$, shall have the same value for two different values of P ; and, since E is equal to the slope of G_1 when plotted against P, this will

happen when two points of the curve have a common tangent whose slope is E. It is clear from the diagram that as E increases the value of χ^X at the transition increases also. Thus in general the transition temperature will increase with field.

3.4. *Hysteresis*

It is clear that when the substance is spontaneously polarized we shall have hysteresis. For there are two states of minimum (and equal) free energy with equal and opposite values of the polarization; so that to

Fig. 9

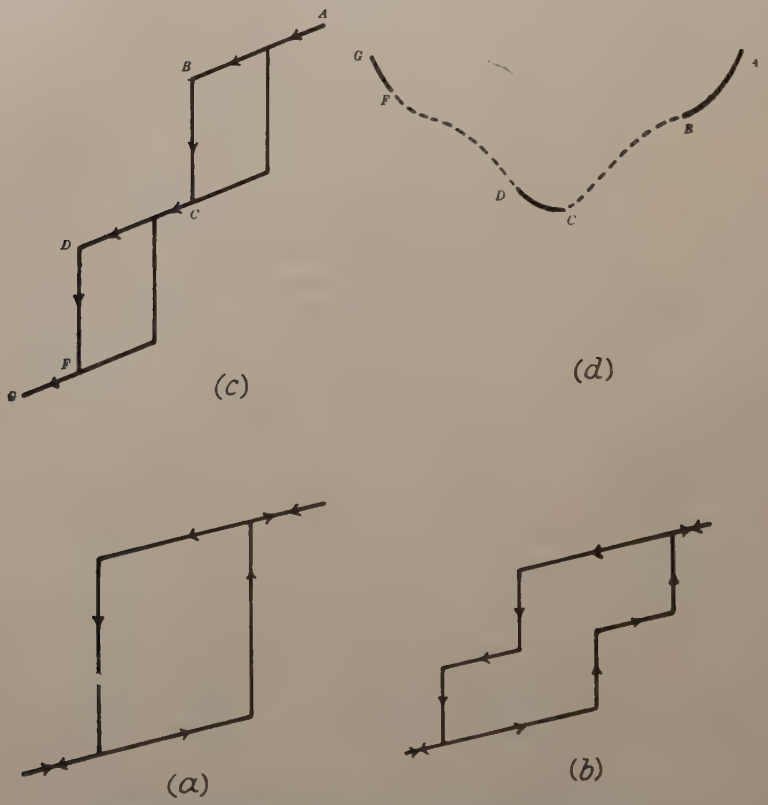

Ideal hysteresis loops near a first-order transition.

(*a*) Just below the transition temperature.
(*b*) Just above the transition temperature.
(*c*) Slightly higher temperature than (*b*).
(*d*) Free energy as a function of polarization at same temperature as for (*c*). The lettering in the two figures corresponds.

reverse the polarization and go from one state to the other it will be necessary to apply a coercive field. In fig. 9 (*a*) we have plotted an ideal hysteresis loop: this is the plot of polarization against field that

we should obtain if the polarization reversed completely at a precise value of the field ; in practice, of course, the loop will have its corners rounded off, as for various reasons the reversal will take place over a range of field strength.

A special type of hysteresis loop should occur just above the normal transition temperature for substances that have a first-order transition. If we use a field large enough to cause a transition at the working temperature then as the field diminishes we shall reach a point where the polarization will change discontinuously to a lower value, and we get a double hysteresis loop as shown in figs. 9 (*b*) or (*c*). Figure 9 (*d*) shows the change in free energy corresponding to 9 (*c*). The lettering in the two figures corresponds. Loops of this kind have been observed by Merz (1953) for $BaTiO_3$ just above the transition temperature.

3.5. *Observed Types of Transition*

In practice it is not always easy to decide whether a particular transition is first or second order. A first order transition is usually spread over a degree or two, different parts of the body making the transition at slightly different temperatures. This spread may be due to impurities, internal strains, or crystal defects, to all of which the transition temperature is sensitive. The result is that the observed polarization never changes discontinuously with temperature, and for the same reason we never have a latent heat, but only a peak in the specific heat. The difficulty may be partly got over by making x-ray measurements of the spontaneous strains : these will have a discontinuity for a first-order transition, and not for a second-order transition. As the x-ray measurements do not give mean strains over the whole crystal, but show if different parts have different strains, it is easier to detect discontinuities in the strains than in the polarization.

The three ferroelectrics that have been studied most are Rochelle salt, potassium dihydrogen phosphate, and barium titanate ; so we shall now consider these in turn.

For Rochelle salt the plot of polarization against temperature in fig. 2 (*a*) suggests a second-order transition, as there is no evidence of discontinuity. The plot of dielectric stiffness coefficient against temperature also supports the view that both transitions are second-order. Deuterium Rochelle salt certainly has the same type of transition as the normal salt.

In the case of KH_2PO_4 it is very difficult to decide whether the transition is first or second-order. The plot of polarization against temperature shown in fig. 2 (*b*) might indicate either a blurred first-order transition or a very sharp second-order one. The x-ray measurements of strain shown in fig. 3 (*a*) suggest a first-order transition. However the measurements of dielectric constant and field that we have already described (Baumgartner 1950) indicate that the coefficients in eqn. (3.1) are all positive (except χ^X) ; this implies a second-order transition.

These measurements, however, confirm that the transition, though second-order, is very sharp. There are fewer measurements on the analogues of KH_2PO_4 such as KD_2PO_4, KH_2ASO_4 etc., but these also probably have very sharp second-order transitions.

In the case of $BaTiO_3$, also, the measurements of saturation polarization are inconclusive. However x-ray measurements of spontaneous strain, fig. 3 (*b*), strongly suggest that the transition is a first order one. This is supported by the dielectric measurements of Kanzig and Maikoff (1951), and also by the hysteresis measurements of Merz already referred to (Merz 1953) ; the types of hysteresis loop found by Merz could only occur near a first-order transition.

3.6. *Entropy of Spontaneous Polarization*

The entropy is given by

$$S=-\left(\frac{\partial G_1}{\partial T}\right)_{X,P},$$

and hence from (3.1) we have

$$S=S_0-\tfrac{1}{2}P^2\frac{\partial \chi^X}{\partial T}-\tfrac{1}{4}P^4\frac{\partial \xi^X}{\partial T}-\ldots,$$

where S_0 is the entropy for zero polarization. It is clear from this equation that if P changes discontinuously so does S ; hence in a first order transition we should have latent heat. Similarly in a second-order transition, where the slope of P^2 changes discontinuously, we should have a discontinuity in the specific heat.

If we assume that the first term in the expansion is the most important we have approximately

$$S-S_0=-\tfrac{1}{2}P^2\frac{\partial \chi^X}{\partial T}, \quad . \quad . \quad . \quad . \quad . \quad . \quad . \quad . \quad (3.7a)$$

and since all the terms in the equation are known it is possible to check it. The results of the comparison are shown in table 4.

Table 4. Entropies of Polarization, Directly Observed, and Calculated from eqn. (3.7*a*)

Substance	KH_2ASO_4	KH_2PO_4	KD_2PO_4	$BaTiO_3$
Spontaneous polarization (micro/coul/cm^2)	5·0*	4·95*	4·83†	20·0‡
$\partial\chi^X/\partial T$ (deg.$^{-1}$)	0·0033*	0·0028*	0·0026†	0·000075‡
Entropy calculated (cals/mole/deg.)	0·56	0·43	0·39	0·12
Entropy observed (cals/mole/deg.)	0·87†	0·47†	0·47†	0·12§

* Busch 1938.
† Bantle 1942.
‡ Merz 1953.
§ Kanzig and Maikoff 1951.

3.7. *Effect of Clamping on the Transition Temperature*

Since the spontaneous polarization is accompanied by spontaneous strain it is clear that if we could prevent the spontaneous strain by clamping the crystal we should affect the transition and possibly alter the transition temperature. We cannot do this in practice because the substance normally becomes polarized in domains ; thus each domain can have its own spontaneous strain although the total strain of the whole block is kept at zero. Nevertheless the subject is very important when we consider atomic models. For from a model we usually deduce directly the behaviour of a substance at constant strain, whereas observations usually give the behaviour at constant stress ; thus we must know how to relate the two.

The transition of the clamped crystal can be discussed in the same way as the transition of the free crystal ; the only difference is that we must use the potential function A instead of the function G_1. Now we have

$$A-A_0=\tfrac{1}{2}\chi^x P^2+\tfrac{1}{4}\xi^x P^4+\ldots, \quad . \quad . \quad . \quad . \quad . \quad (3.8)$$

which may be compared with eqn. (3.1).

In Rochelle salt and KH_2PO_4 the transition is a second-order one, and the transition temperature for the free crystal is given by the vanishing of χ^X ; for the clamped crystal it is given by the vanishing of χ^x. Now the relation of these two quantities is given by eqns. (2.4), and from these we can deduce the effect of clamping on the transition temperature. Since χ^x is always greater than χ^X the effect of clamping is to reduce the range of the self-polarized state, and Mueller has shown that for Rochelle salt it would be just sufficient to reduce the range to zero. For KH_2PO_4 the effect of clamping would be to reduce the temperature by about 3·5°–4° (Mason 1946, Baumgartner 1951).

It should be emphasized that when we measure the clamped dielectric constant by using a very high frequency field we affect only the induced polarization and *not* the spontaneous polarization ; hence the transition temperature is unaltered. This point is illustrated in fig. 10.

The perovskites are not piezoelectric in the non-polar state, and hence χ^x is equal to χ^X ; however the transition is a first-order one, and so the transition temperature will be altered by changes in the coefficients of P^4 and higher powers of P.

The difference between ξ^x and ξ^X can be expressed in terms of the electrostrictive and elastic constants. This has been done by Devonshire (1951), who found that for $BaTiO_3$, although ξ^X is negative, ξ^x is positive. Since the coefficients of higher powers of P are probably positive also this means that the transition of the ' clamped ' crystal will be second-order although that of the free crystal is first-order. This point will be very important when we consider atomic models for $BaTiO_3$.

3.8. *Effect of Stress on the Transition Temperature*

If we have a material (such as Rochelle salt or KH_2PO_4) that is piezoelectric above the transition temperature, and apply a stress that

would cause a strain similar to the spontaneous strain, then this will also cause a polarization similar to the spontaneous polarization : thus the effect is the same as applying an electric field.

For any other type of stress (or for a non-piezoelectric substance) the effect on the transition temperature is due to the effect on the coefficients in the expression for the free energy. The effect on the dielectric stiffness

Fig. 10

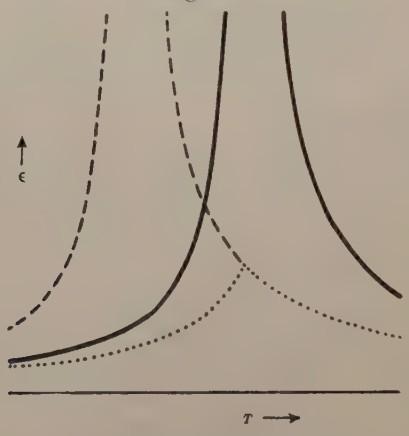

Dielectric constant near a second-order transition. (The substance is supposed to be polar *above* the transition temperature.)
Full curve : ' free ' dielectric constant.
Dotted curve : ' clamped ' dielectric constant with ' free ' spontaneous polarization.
Dashed curve : ' clamped ' dielectric constant with ' clamped ' spontaneous polarization.

coefficient χ is given in terms of the electrostrictive constants Q by eqn. (2.17). Now if the transition is a second-order one the transition temperature is given by the vanishing of χ^X. Hence the rate of variation of temperature with stress is given by

$$\left(\frac{\partial T}{\partial X_i}\right)_\chi = \frac{\partial \chi_{11}}{\partial X_i} \Big/ \frac{\partial \chi_{11}}{\partial T} = Q_{i11} \Big/ \frac{\partial \chi_{11}}{\partial T}, \quad . \quad . \quad . \quad . \quad (3.9)$$

if the axis of spontaneous polarization is the x-axis. If the stress is a hydrostatic pressure this becomes

$$\frac{\partial T}{\partial p} = -(Q_{i11}+Q_{211}+Q_{311}) \Big/ \frac{\partial \chi_{11}}{\partial T}. \quad . \quad . \quad . \quad . \quad (3.10)$$

For a cubic crystal, as in the perovskites, this becomes

$$\frac{\partial T}{\partial p} = -(Q_{11}+2Q_{12}) \Big/ \frac{\partial \chi_{11}}{\partial T}, \quad . \quad . \quad . \quad . \quad . \quad (3.11)$$

in the notation of (2.9). For a first-order transition the variation of the higher-order terms with temperature and pressure also affects the answer, so eqn. (3.11) is no longer accurate : it may or may not be a

good approximation. We can test this in the case of $BaTiO_3$ since all the quantities are known. The rate of variation of the upper transition temperature with pressure has been found by Merz (1950) to be $5{\cdot}7\times10^{-9}$ degree cm^2/dyne. The other quantities have been given in table 4 and at the end of § 2, and using those values we find that the right-hand side of (3.11) becomes 9×10^{-9}; the difference of the two values is perhaps within the errors of measurement, so we cannot certainly tell whether the effect of temperature on higher order terms is important or not.

We can also find the rate of change of transition temperature with stress in terms of the entropy or specific heat change at the transition. Let us consider a first-order transition, and let us denote the polarized and unpolarized phases by suffixes a and b. Then since the Gibbs free energy G is always equal in the two phases at the transition we have

$$0=dG_a-dG_b=-(S_a-S_b)\,dT+(x_{ia}-x_{ib})\,dX_i-(P_{ma}-P_{mb})\,dE_m, \quad . \quad (3.12)$$

from (2.7*e*) where T is the transition temperature corresponding to the stress X_i and the field E_m. If we assume that the field is constant, and all the stress-components constant except one, then we have

$$\frac{\partial T}{\partial X_i}=\frac{x_{ia}-x_{ib}}{S_a-S_b}. \quad . \quad . \quad . \quad . \quad . \quad . \quad . \quad . \quad (3.13)$$

If the stress is a hydrostatic pressure this becomes

$$\frac{\partial T}{\partial p}=\frac{\Delta v}{S_a-S_b}, \quad . \quad . \quad . \quad . \quad . \quad . \quad . \quad . \quad (3.14)$$

which is the well-known Clausius–Clapeyron equation. Similarly by keeping the stresses constant we can show that

$$\frac{\partial T}{\partial E_m}=-\frac{P_{ma}-P_{mb}}{S_a-S_b}, \quad . \quad . \quad . \quad . \quad . \quad . \quad . \quad (3.15)$$

which gives the rate of change of transition temperature with field.

In the second-order transition the entropy of the two phases is the same, and by applying the same reasoning as above with S replacing G we can show that

$$\frac{\partial T}{\partial X_i}=\frac{T(\alpha_{ia}-\alpha_{ib})}{C_a^{\,X}-C_b^{\,X}}, \quad . \quad . \quad . \quad . \quad . \quad . \quad . \quad (3.16)$$

where α is the thermal expansion coefficient and C^X the specific heat at constant stress.

Equation (3.14) can be readily tested for $BaTiO_3$. The value of $\partial T/\partial p$ has been given by Merz (1950), and the fractional change in volume at the transition has been found by Kay and Vousden (1949) to be about 5×10^{-4}, so that we can deduce that the entropy of transition should be about 0·08 cals/mole/deg. The value given in table 4 is 0·12, but this includes a contribution from the increase in polarization taking place below the transition, so that there is fair agreement.

3.9. *Transitions between Two Ferroelectric States*

As we stated in the introduction barium titanate passes through three distinct ferroelectric states as the temperature is lowered ; it is successively polarized along an edge, a face diagonal, and a body diagonal. We can specify the state of the crystal in terms of the x, y and z-components of polarization. At the first transition polarization sets in along one axis, at the second transition an equal polarization sets in along a second axis, at the third transition it sets in along the third axis also. Because of the cubic symmetry the three axes are equivalent ; hence if displacements in the three directions were independent polarization would set in along the three axes at the same temperature ; since it does not a spontaneous polarization along one axis must tend to inhibit spontaneous polarization in the directions at right angles. It is easy to see one reason why this should happen ; a polarization in the x-direction will cause a contraction of the unit cell in the y- and z-directions, and this will tend to prevent polarization in these directions. Mathematically this interaction between polarizations can be expressed by putting cross-terms in the expression for the free energy. Thus we have

$$\begin{aligned} G_1-G_{10}=&\tfrac{1}{2}\chi^X(P_x^2+P_y^2+P_z^2)+\tfrac{1}{4}\xi^X(P_x^4+P_y^4+P_z^4)\\ &+\tfrac{1}{6}\zeta^X(P_x^6+P_y^6+P_z^6)+\ldots\\ &+\tfrac{1}{2}\lambda(P_y^2P_z^2+P_z^2P_x^2+P_x^2P_y^2)+\ldots, \end{aligned} \tag{3.17}$$

where the term in λ corresponds to an interaction between the polarizations ; if λ is positive this means that polarization along one axis tends to inhibit polarization along an axis at right angles. If we choose suitable constant values for all the coefficients except χ^x (which is assumed to decrease steadily with the temperature) then the system will pass successively through the polarization states observed in $BaTiO_3$ (Devonshire 1949).

The dielectric stiffness coefficient in, say, the x-direction is given by

$$\begin{aligned} \frac{\partial^2 G_1}{\partial P_x^2}=&\chi^X+3\xi^XP_x^2+5\zeta^XP_x^4+\ldots\\ &+\lambda(P_y^2+P_z^2)+\ldots. \end{aligned} \tag{3.18}$$

In the cubic region it is, of course, just χ^X ; in the tetragonal region, if the spontaneous polarity is along the z-axis, it becomes

$$\chi^X+\lambda P_z^2.$$

The dielectric stiffness coefficient at right angles to the direction of spontaneous polarization will therefore increase discontinuously at the transition ; but at lower temperatures the increase in P_z will be counter balanced by the decrease in χ^X so that it will remain small over a wide temperature range, that is the dielectric constant will remain large, as observed.

3.10. *Antiferroelectric Transitions*

We said in § 1 that some substances undergo transitions to new non-polar states, which we called antiferroelectric states. There is no definition that distinguishes these precisely from other non-polar states, but in practice we apply the term to a state that is a *small* distortion of a more symmetrical state ; the new unit cell is also normally a multiple of the old. Normally, too, the dielectric constant is large at the transition, but this may be in part accidental and due to the fact that transitions with this feature are easier to detect.

The thermodynamic theory of antiferroelectrics was first considered by Kittel (1951). He assumed that the substance contains two equivalent lattices, each of which can be polarized, and that there is an interaction between them. Then if we denote by P_a and P_b the polarizations of the two lattices the free energy can be expanded in the form

$$G_1-G_{10}=f(P_a^2+P_b^2)+gP_aP_b+h(P_a^4+P_b^4)+\ldots . \quad (3.19)$$

From the symmetry of the expression it is clear that there are some stationary values of G_1 for which

$$P_a=\pm P_b.$$

If P_a is equal to $-P_b$ then the net polarization is zero and we have an antiferroelectric displacement. Whether the antiferroelectric displacement does or does not give a lower free energy than the ferroelectric ones depends on the values of the coefficients, and in particular on the value of g.

It is convenient to transform eqn. (3.19) by putting

$$\left.\begin{aligned} P&=P_a+P_b,\\ p&=P_a-P_b,\end{aligned}\right\} \quad . . . . . \quad (3.20)$$

so that P is now the total polarization and p a measure of the antiferroelectric displacement. The free energy can now be expressed in the form

$$\begin{aligned} G_1-G_{10}=&\tfrac{1}{2}\chi^X P^2+\tfrac{1}{4}\xi^X P^4+\tfrac{1}{6}\zeta^X P^6+\ldots\\ &+\tfrac{1}{2}\chi'^X p^2+\tfrac{1}{4}\xi'^X p^4+\tfrac{1}{6}\zeta'^X p^6+\ldots\\ &+\tfrac{1}{2}\lambda p^2P^2+\ldots , \quad . . . . . \quad (3.21)\end{aligned}$$

where the coefficients are, of course, related to those in (3.19). Although (3.21) is mathematically equivalent to (3.19) it can be applied to a wider range of physical models, since p can be any type of antiferroelectric displacement ; it might, for example, be a displacement in a plane at right angles to P, and the form of the equation would still be the same.

Now there will be an antiferroelectric state if G_1 has a minimum for a finite value of p. Normally the coefficient χ'^X decreases as the temperature decreases and the antiferroelectric state is stable at low temperatures. Whether the antiferroelectric transition or the ferroelectric transition

takes place first depends on the relative values of the coefficients. It is possible in principle to have both a ferroelectric and an antiferroelectric displacement, but if the cross-terms in (3.21) (such as $\frac{1}{2}\lambda p^2P^2$) are positive and sufficiently large, then the presence of one kind of displacement will prevent the formation of the other ; this appears to be the case in practice.

3.11. *Dielectric Constant at an Antiferroelectric Transition*

From (3.21) the dielectric stiffness coefficient for zero polarization is given by

$$\frac{\partial^2 G_1}{\partial P^2} = \chi^X + \lambda p^2 + \ldots, \qquad \ldots\ldots \quad (3.22)$$

and hence will be discontinuous at a first order antiferroelectric transition. Moreover if λ is positive the dielectric stiffness coefficient will increase, that is the dielectric constant will decrease, in the antiferroelectric state. This decrease is observed for $PbZrO_3$ and its solid solutions (fig. 1(*d*)), and also for ammonium periodate and silver periodate (Baertschi 1945). The numerical change in the dielectric stiffness coefficient is quite small for $PbZrO_3$, about 0·035, but because of the small value of χ^X the proportionate change is very large. If, however, the dielectric constant had had a normal value of, say, 10, so that χ^X was about 1·3, then the discontinuity would hardly have been noticed. This may be the reason why antiferroelectric transitions in the perovskites are apparently associated with large dielectric constants, though there seems no theoretical reason why they should be. It is simply that the discontinuities are much larger in this case and so the transition is easy to observe.

3.12. *Effect of Electric Field on an Antiferroelectric Transition*

Equation (3.15) which gives the rate of increase of transition temperature with field, is true for any type of transition, so that we still have

$$\frac{\partial T}{\partial E} = \frac{P_b - P_a}{S_a - S_b}, \qquad \ldots\ldots\ldots \quad (3.15)$$

but in the case of an antiferroelectric transition the polarization is induced by the field. Since the dielectric constant is smaller in the antiferroelectric state the polarization will also be smaller and hence the transition temperature will decrease with the field, as is observed for $PbZrO_3$. At a ferroelectric transition the transition temperature is increased by an applied field so that this effect can be used to differentiate between the two types of transition.

§ 4. Atomic Models

4.1. *Introduction*

In the previous sections we have been concerned exclusively with the macroscopic properties of ferroelectrics ; in this section we shall discuss the relation of these properties to the atomic structure.

Since all the equilibrium properties of a substance can be deduced if we know one of the free energies (G, G_1, G_2 or A) as a function of the appropriate variables, it is convenient to start by deducing the free energy from the experimental observations as far as we can ; this free energy will then collect in a single formula a number of experimental results, and since the free energy of an atomic model can in principle always be calculated by the methods of statistical mechanics, we can check the accuracy of the model. Of course, the free energy tells us nothing about the dynamic properties of the substance, such as the dielectric loss at a given frequency ; these must be calculated directly from the model. The most convenient variables to use in constructing the free energy from an atomic model are the linear dimensions, temperature, and either polarization or field, so that the free energy we construct is either A (if polarization is the variable) or G_2 (if field is the variable) ; these are the free energies therefore that we must deduce from experiment.

If we make a direct comparison between theory and experiment we must take care that we are comparing the same things. Thus a direct calculation of susceptibility from an atomic model usually gives the isothermal susceptibility at constant strain, but measurements usually give the adiabatic susceptibility at constant stress ; hence before comparing theory and observation it is necessary to find the relation between these two quantities. Similarly the transition temperature most readily calculated from a model is the transition temperature of the clamped crystal, whereas the transition temperature normally measured is that of the free crystal.

4.2. *Particular Cases*

4.2.1. *Barium Titanate*

The points in the preceding section will be made clearer if we consider a particular substance : $BaTiO_3$. We shall consider conditions only in the tetragonal and cubic region and therefore assume that the only polarization is along a fixed axis. Then from a knowledge of the dielectric susceptibility above the transition temperature and a knowledge of the spontaneous polarization below we can deduce that

$$G_1-G_{10}=\tfrac{1}{2}\beta^X(T-\Theta)P^2+\Psi^X(P), \quad . \ . \ . \ . \quad (4.1)$$

where the free energy is measured at zero stress and Ψ^X includes only terms of order P^4 and higher. All the quantities in this expression can be determined ; for the dielectric stiffness coefficient at zero polarization is given by

$$\frac{\partial^2 G_1}{\partial P^2}=\beta(T-\Theta).$$

This is known above the transition temperature, so that we can determine β and Θ, and we assume that the expression can be extrapolated below the transition temperature. Again for zero field we have

$$0=\frac{\partial G_1}{\partial P}=\beta^X(T-\Theta)P+\Psi^X(P),$$

and hence

$$\beta(\Theta-T)P=\Psi^X(P). \quad . \quad . \quad . \quad . \quad . \quad . \quad (4.2)$$

The solution of this equation gives us the spontaneous polarization. If we know the spontaneous polarization as a function of temperature —which we do for $BaTiO_3$—then we can determine $\Psi^X(P)$.

Now at zero stress the free energies A and G_1 are equal, so that (4.1) also gives the variation of A with polarization at zero stress. What, however, we need to know is how A varies with polarization under conditions of constant strain. We must therefore distinguish between the direct dependence of free energy on polarization and the indirect dependence via the strain produced by polarization ; similarly, we must distinguish between the direct effect of temperature on free energy and the indirect effect arising from the thermal expansion.

The derivation of the expression for A in terms of polarization and strain is a straight forward matter of thermodynamics, and we shall not discuss the details here. The final result we obtain is that the dependence of A upon polarization at constant strain is of the same form as (4.1) and is given by

$$A-A_0=\tfrac{1}{2}\beta^x(T-\Theta)P^2+\Psi^x(P). \quad . \quad . \quad . \quad . \quad (4.3)$$

The quantity β^x is greater than β^X (about twice the value) and the function $\Psi^x(P)$ is markedly different in form from $\Psi^X(P)$. Whereas the coefficient of P^4 in the expansion of Ψ^X is negative, the coefficient of P^4 in the expansion of Ψ^x is positive. This means, as shown in the last section, that although the transition at constant stress is a first-order transition, the transition at constant strain would be a second-order transition (if it were possible to observe it). This result is clearly very important ; for it means that in constructing our atomic model we must make it give a second-order transition under conditions of constant strain ; the observed first-order transition is due to the interaction of strain and polarization that takes place when the stress is kept constant.

4.2.2. *Potassium Dihydrogen Phosphate*

Similar considerations apply to this substance. The transition at constant stress is, as we saw in § 3, probably a very sharp second-order one ; calculations indicate that the transition at constant strain will be a much less sharp one.

One feature that must be explained is the large difference in transition temperature (90°) between the normal and the deuterium salt. This suggests that motion of the hydrogen atoms plays a large part in the transition and that quantum considerations are important.

4.2.3. *Rochelle Salt*

The most striking feature of Rochelle salt is that it has two transition temperatures and is polarized only between them ; both transitions are second-order. At a second-order transition as we have already pointed

out in § 3 the quantity χ^X (defined by (3.1)) vanishes. Hence for Rochelle salt this quantity must be positive at high temperatures, decrease as the temperature decreases, become negative, and then increase and become positive again. It is this unusual behaviour of χ^X that any atomic model must explain. Now for Rochelle salt we are exceptionally fortunate as we know χ^X as a function of both temperature and pressure from the susceptibility measurements of Bancroft (1938). The contours of constant χ^X are plotted on a pressure–temperature diagram in fig. 11. The diagram shows that the temperature range of the spontaneously polarized state increases as we increase the pressure. Moreover we can get two transitions by varying the *pressure* while keeping the temperature constant (provided it is high enough). On the diagram we have plotted the lines of constant volume and we see that we shall still get two transitions if we vary the temperature at constant volume instead of constant pressure. Strictly speaking, of course, if we are examining the behaviour

Fig. 11

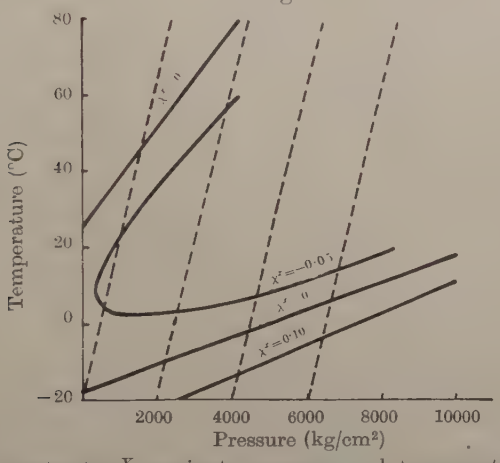

Contours of constant χ^X against pressure and temperature for Rochelle salt. The dotted lines are lines of constant volume. Bancroft 1938.

at constant volume we ought to use χ^x (defined by (3.8)) instead of χ^X, but as the difference of the two quantities is almost constant and small (table 2), this will make little difference; the zero contour of χ^x corresponds approximately to that of $\chi^X = -0{\cdot}04$, so that the temperature range of the polar state is somewhat reduced. Our atomic model therefore must give two transitions either as we vary the temperature at constant volume or as we vary the volume at constant temperature.

4.3. *Types of Atomic Model*

The polarization of a body can conveniently be considered as built up from a number of small dipoles of atomic dimensions; these may be dipolar groups of atoms, polarized atoms, or pseudo-dipoles formed by the movement of a charged ion from its normal position. These dipoles

may be of fixed magnitude, the variation of polarization then being due to a change in their relative orientation, a random orientation giving of course zero total polarization ; alternatively the dipoles may be of fixed parallel orientation and the variation in total polarization due to a change in their magnitude, the dipoles disappearing completely when the polarization vanishes.

Since most ferroelectrics are spontaneously polarized at low temperatures and not at high there is presumably a balance between the forces that tend to produce an ordered array of dipoles, and thermal motion, which tends to destroy this ordered array. Now the forces that tend to order the dipoles are of two kinds : first there is always the electrostatic force between the dipoles, which is a long-range force and may depend on the shape of the body ; second there may be short range forces that are not of dipolar origin, but still tend to produce a dipolar array. It should be noted that either type of force can produce an ordered array of dipoles that are not parallel but arranged in such a way that the net polarization is zero, that is to say an antiferroelectric state.

The electrostatic interaction of the dipoles can be calculated fairly easily. It was shown by Lorentz that the electrostatic energy of a random arrangement of parallel dipoles in an uninsulated body is $-(2\pi/3)P^2$ per unit volume, where P is the polarization. If the body is insulated the energy is dependent on the external shape ; its minimum value is $-(2\pi/3)P^2$, and this value is attained for thin plates or needles polarized parallel to their length ; this value is also attained if the body is polarized in domains forming closed rings of polarization. The energy of a regular array of parallel dipoles in which each dipole has surroundings of cubic symmetry is the same as that of a random array ;* the energy of other regular arrays is different but of the same order of magnitude. The energies of some regular antiparallel arrays of dipoles (with net polarization zero) have been worked out by Sauer (1940) ; he found that the energy might be greater or less than that of a parallel array of the same dipoles according to the particular arrangement.

Now if we examine the expression for the available energy A when expanded in powers of P^2 (eqn. (3.8)), we find that the coefficient of P^2 is $\frac{1}{2}\chi^x$, which vanishes at or near the transition temperature and is normally a linearly increasing function of T. Moreover its magnitude over a fairly wide range of temperature is less than one. Hence the contribution of the electrostatic energy is clearly very important and cannot be neglected ; also there must be positive contributions to the free energy that will cancel the electrostatic contribution at the transition point and explain the temperature variation of χ^x. In the case of dipoles of variable magnitude a positive energy is usually required to create the dipole, but this is not dependent on temperature, and the

* It is not sufficient that the crystal as a whole has cubic symmetry ; in the perovskites the crystal has complete cubic symmetry, but the surroundings of the individual oxygen atoms have not cubic symmetry.

source of the temperature dependent term must be the entropy ; the variation of entropy with polarization is due to the variation of vibration frequency with polarization and is normally small ; even its sign cannot be certainly predicted, but usually the entropy decreases with increasing polarization. In the case of dipoles of fixed magnitude but variable orientation the entropy supplies both the positive contribution to the free energy and the variation with temperature ; the entropy here arises from the arrangement of the dipoles, and clearly decreases as the polarization increases and the arrangement becomes less random. In the latter case we shall get a much more rapid variation of χ^x with temperature than in the former.

It is interesting to compare ferromagnetism with ferroelectricity. In a ferromagnetic material the dipoles are of fixed magnitude and variable orientation, and the interaction is almost entirely a local one due to the coupling between spins of neighbouring atoms ; in contrast to the ferroelectric case the magnetostatic interaction between the dipoles is negligible.

We shall now consider some types of model in more detail.

4.4. *Rotating Dipoles with Interaction*

This is one of the simpler types of model. It is not likely to be a very good one for ferroelectrics since it is unlikely that the dipole or pseudo-dipoles in a solid can rotate freely. It has, however, been much discussed, and it shows very well certain features which are also important in other models ; hence it is worth devoting some time to it.

In its simplest form, as in the Weiss theory of ferromagnetism, we assume that there are a number of similar dipoles of fixed magnitude and capable of rotating freely ; there is a field on each dipole of magnitude $E+\lambda P$, where E is the external field and P is the mean polarization ; the term in λP is supposed to come from the electrostatic (or magnetostatic) field of the dipoles. This model gives a second-order transition and reproduces roughly the ordinary features of ferromagnetism, though in order to obtain the correct transition temperature it is necessary to make λ about a thousand times larger than if the term λP were really due to magnetostatic forces.

A similar model has been applied to the dielectric theory of polar liquids, usually with the refinement that the dipoles are embedded in a dielectric medium which represents the contribution of the electronic polarizibility. In this case assumption of the Lorentz value for the internal field predicts a fairly high transition temperature ; in fact it predicts that many liquids should become spontaneously polarized at room temperatures, which is untrue.

This simple theory has been criticized by Onsager (1936). He has pointed out that assumption of the Lorentz field implies that the orientation of the dipoles round a given dipole is independent of the orientation of

that dipole, which is certainly not true. In his theory he assumes that the orientation of dipoles round a particular dipole is the same as if it is permanently fixed in the particular orientation it has at that moment. It is usually stated that Onsager's theory does not give a self-polarized state at all, but it has been shown by Pirenne (1949 a) that this is not so. It is true that on Onsager's theory the non-polar state is always stable, that is it corresponds to a minimum of the free energy ; but the free energy may also have a minimum for a finite value of the polarization, and at sufficiently low temperatures this will be the lower minimum of the two. It can be shown that the transition is now a first-order one and that the transition temperature is much reduced ; this removes the experimental difficulty mentioned in the last paragraph as the predicted temperatures are now outside the liquid range.

Like the simple theory, however, Onsager's theory is clearly inaccurate ; the simple theory neglects the coupling between the movements of neighbouring dipoles, but Onsager's theory exaggerates it. Certainly the simple theory is wrong in assuming that the orientation of the dipoles round a given dipole is independent of its orientation, but Onsager's theory is also wrong in assuming that they have time to attain their equilibrium values corresponding to its orientation : the true state of affairs must be intermediate. More accurate theories have been put forward by Kirkwood and Fröhlich,* but the conditions for transition to a self-polar state do not seem to have been investigated. Since both the simple theory and the Onsager theory give a transition it is almost certain that a correct theory would give a transition also, and one of intermediate character, but whether it would be first- or second-order we cannot say.

4.5. *Dipoles with Two Positions of Equilibrium*

We shall now consider a substance containing a number of similar dipoles, each of which has two positions of equilibrium (with the dipole pointing in opposite directions). To increase the generality we shall suppose that the substance also has electronic polarizability. Apart from the electrostatic interaction we assume that each dipole has the same energy in its two positions. Thus the dipoles might be formed by ions that have two similar equilibrium positions. In the next section we shall consider a model in which the ions oscillate about an equilibrium position, and then compare the behaviour of the two models.

Let us suppose that there are N dipoles per unit volume each of moment μ, and that a fraction $\frac{1}{2}(1+x)$ of them are pointing in the positive direction, so that the dipole polarization P_d is $N\mu x$. We shall assume that the electronic polarization is P_e, and that the energy can be written in the form

$$-\tfrac{1}{2}\gamma_{dd}P_d^2-\gamma_{de}P_dP_e+\tfrac{1}{2}\gamma_{ee}P_e^2. \quad . \quad . \quad . \quad . \quad (4.4)$$

* For a full account, see *Theory of Dielectrics* by H. Fröhlich, Clarendon Press, Oxford, 1949.

Here the first term gives the mutual electrostatic interaction energy of the dipoles and the second term the electrostatic interaction between the dipoles and the electronic polarization; these terms are, of course, negative. The third term is the difference between the mutual electrostatic energy of the electronic polarization and the work required to produce the electronic shifts; it will normally be positive. The entropy of the system is proportional to the logarithm of the number of arrangements of the dipoles, and is given by

$$\begin{aligned} S&=k\log\left\{\frac{N!}{\frac{1}{2}N(1+x)!\,\frac{1}{2}N(1-x)!}\right\}\\ &=k[N\log N-\tfrac{1}{2}N(1+x)\log\{\tfrac{1}{2}N(1+x)\}-\tfrac{1}{2}N(1-x)\log\{\tfrac{1}{2}N(1-x)\}]\\ &=\tfrac{1}{2}kN[-(1+x)\log(1+x)-(1-x)\log(1-x)+2\log 2], \quad . \ . \ . \quad (4.5) \end{aligned}$$

so that the available energy A is given by

$$\begin{aligned} A=&-\tfrac{1}{2}\gamma_{dd}P_d^2-\gamma_{de}P_dP_e+\tfrac{1}{2}\gamma_{ee}P_e^2\\ &+\tfrac{1}{2}kNT\{(1+x)\log(1+x)+(1-x)\log(1-x)-2\log 2\}, \ . \ . \quad (4.6) \end{aligned}$$

where

$$P_d=N\mu x. \quad . \ . \ . \ . \ . \ . \ . \ . \quad (4.7)$$

Now the total polarization P is given by

$$P=P_e+P_d, \quad . \ . \ . \ . \ . \ . \ . \ . \quad (4.8)$$

and the two components of polarization P_e and P_d will adjust themselves to make A a minimum subject to this equation. The condition for this is that

$$\left(\frac{\partial A}{\partial P_e}\right)_{P_d}=\left(\frac{\partial A}{\partial P_d}\right)_{P_e}=\frac{\partial A}{\partial P}=E.$$

Hence

$$\left.\begin{aligned} E&=\gamma_{ee}P_e-\gamma_{de}P_d,\\ E&=-\gamma_{dd}P_d-\gamma_{de}P_e+\tfrac{1}{2}\frac{kT}{\mu}\left\{\log\frac{N\mu+P_d}{N\mu-P_d}\right\}, \end{aligned}\right\} \ . \ . \quad (4.9)$$

using (4.7).

From eqns. (4.9) and (4.8) we can deduce the relation between E and P. If we take E to be zero then the equations give us the spontaneous polarization. In this case we have

$$\left.\begin{aligned} \gamma_{ee}P_e&=\gamma_{de}P_d,\\ \gamma_{ee}P&=(\gamma_{de}+\gamma_{ee})P_d, \end{aligned}\right\} \ . \ . \ . \ . \ . \ . \quad (4.10)$$

$$P_d\frac{\gamma_{dd}\gamma_{ee}+\gamma_{de}^2}{\gamma_{ee}}=\frac{kT}{2\mu}\log\frac{N\mu+P_d}{N\mu-P_d},$$

so that

$$\frac{P_d}{N\mu}=\tanh\frac{\mu P_d}{kT}\frac{\gamma_{dd}\gamma_{ee}+\gamma_{de}^2}{\gamma_{ee}},$$

and hence

$$\frac{P}{P_0}=\tanh\frac{P}{P_0}\frac{T_0}{T}, \ . \ . \ . \ . \ . \ . \ . \quad (4.11)$$

where

$$\left.\begin{aligned} P_0 &= N\mu(\gamma_{de}+\gamma_{ee})/\gamma_{ee}, \\ T_0 &= \frac{N\mu^2}{k}\frac{\gamma_{dd}\gamma_{ee}+\gamma_{de}^2}{\gamma_{ee}} = \frac{P_0^2}{Nk}\frac{(\gamma_{dd}\gamma_{ee}+\gamma_{de}^2)}{(\gamma_{ee}+\gamma_{de})^2}\gamma_{ee}. \end{aligned}\right\} \quad . \quad . \quad .(4.12)$$

P_0 is clearly the maximum value of the saturation polarization (which will be attained at zero temperature), and T_0 is clearly the transition temperature. For it is easy to see that above that temperature the only value of P which satisfies eqn. (4.11) is zero, and below that temperature there is a non-zero solution, which is the saturation polarization. The saturation polarization as a function of temperature is shown in fig. 12.

Fig. 12

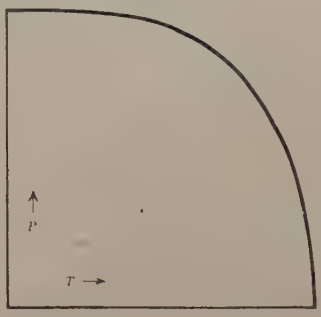

Saturation polarization as a function of temperature for dipoles with two possible orientations.

We can obtain the susceptibility for small fields above the transition temperature from (4.9) by assuming that $P_d/N\mu$ is small. The equation then becomes

$$E=\gamma_{ee}P_e-\gamma_{de}P_d=-\gamma_{dd}P_d-\gamma_{de}P_e+\frac{kT}{N\mu^2}P_d, \quad . \quad . \quad (4.13)$$

so that

$$\left.\begin{aligned} E &= \frac{\gamma_{ee}(kT/N\mu^2)-\gamma_{de}^2-\gamma_{ee}\gamma_{dd}}{\gamma_{ee}+2\gamma_{de}-\gamma_{dd}+(kT/N\mu^2)}P \\ &= \frac{Nk}{P_0^2}\frac{(T-T_0)}{\{1+(T-T_0)Nk/\gamma_{ee}P_0^2\}}P, \end{aligned}\right\} \quad . \quad . \quad .(4.14)$$

which for $T-T_0$ small can be written

$$E=\frac{Nk}{P_0^2}(T-T_0)P, \quad . \quad . \quad . \quad . \quad . \quad . \quad (4.15)$$

and thus gives the Curie law for susceptibility.

In deriving the formulae for saturation polarization and susceptibility we have implicitly assumed that there is no correlation between the positions of neighbouring dipoles. This derivation is therefore open to the kind of criticisms made in the section on rotating dipoles, and the true formulae would give rather lower transition temperatures and rather sharper transitions.

We see from (4.15) that in this model the susceptibility immediately above the transition point is known in terms of the maximum polarization, and this gives us one means of testing whether the model is a good one for any particular substance. Again (4.9) gives us a relation between the transition temperature and the maximum polarization if we can determine the γ's. Now γ_{ee} can be found experimentally since it gives the electronic polarizability and therefore the dielectric constant at high frequencies (such that of visible light); we have, in fact, the relation

$$n^2-1=4\pi/\gamma_{ee}, \quad . \quad . \quad . \quad . \quad . \quad . \quad . \quad . \quad . \quad (4.16)$$

where n is the refractive index. The quantities γ_{dd} and γ_{de} will depend on the particular atomic structure but will be of the order of $4\pi/3$. If, however, we take γ_{de} smaller than we should if the polarization were uniform this will partly allow for the correlation. For the electronic polarization has a high relaxation frequency, and therefore will be instantaneously adjusted to the positions of the dipoles. Thus even at zero polarization there will be some interaction between the dipoles and the electronic polarization, since each dipole will produce an electronic polarization in its immediate neighbourhood even if the total adds up to zero. Thus the change in interaction energy when the dipoles are fully or partly aligned will be relatively small. If we neglect it altogether then γ_{de} becomes zero and eqns. (4.12) and (4.15) become

$$\left.\begin{aligned} P_0&=N\mu, \\ T_0&=\gamma_{dd}P_0^2/Nk, \\ E&=\{\gamma_{dd}(T-T_0)/T_0\}P. \end{aligned}\right\} \quad . \quad . \quad . \quad (4.17)$$

4.6. *Oscillating Ions*

We shall assume that there are N oscillating ions per unit volume, and that each ion produces an electric moment qz when it is displaced a distance z from its normal equilibrium position (this may include a contribution from the electronic polarization of the surrounding medium). For simplicity we shall assume that all the ions are similar and that the oscillation takes place in one dimension only. Then, if we do not take into account the electrostatic energy, the energy of an ion relative to its equilibrium energy can be expressed in the form az^2+bz^4, neglecting terms of order z^6 or higher. Then in the absence of electrostatic interaction each ion would oscillate about its equilibrium position; but, if the electrostatic interaction is large enough, then we shall get a lowering of energy if the ions all move in the same direction so that they form a set of parallel pseudo-dipoles.

Now the electrostatic interaction energy of two pseudo-dipoles can be expressed as $q^2\lambda_{nm}z_nz_m$, where z_n and z_m are the displacements of the dipoles and λ_{nm} depends on their relative position. Thus the total electrostatic energy per unit volume is

$$\sum_{n,m} q^2\lambda_{nm}z_nz_m,$$

where the summation is over all pairs of dipoles. If we denote by $\bar{z}$ the mean displacement of the ions then we can write the above expression as

$$\sum_{n,m} q^2\lambda_{nm}\{\bar{z}^2+\bar{z}(z_m-\bar{z})+\bar{z}(z_n-\bar{z})+(z_m-\bar{z})(z_n-\bar{z})\}$$
$$=\tfrac{1}{2}N\lambda q^2\bar{z}^2+\sum_m q^2\lambda\bar{z}(z_m-\bar{z})+\sum_{n,m} q^2\lambda_{nm}(z_m-\bar{z})(z_n-\bar{z}), \quad . \quad . \quad . \quad (4.18)$$

where

$$\lambda=\sum_n \lambda_{nm},$$

and λ is of course independent of m if we exclude surface ions. The last term in the expansion depends on the product of displacements from the mean, and we shall neglect it. The total energy of the system (in the absence of a field) is now

$$\tfrac{1}{2}N\lambda q^2\bar{z}^2+\sum_m\{az_m^2+bz_m^4+q^2\lambda\bar{z}(z_m-\bar{z})\}$$
$$=\sum_m\{az_m^2+bz_m^4+q^2\lambda\bar{z}z_m-\tfrac{1}{2}q^2\lambda\bar{z}^2\}. \quad . \quad . \quad . \quad (4.19)$$

In the presence of a field E we must add terms $-Eqz_m$. Since the energy is now expressed as a sum of the energies of the individual ions, therefore the partition function of the system will be a product of the partition functions of the individual ions. The partition function for a single ion is

$$f=\left(\frac{2\pi mkT}{h^2}\right)^{1/2}\int_{-\infty}^{\infty}\exp\{-(az^2+bz^4-E'qz-\tfrac{1}{2}q^2\lambda\bar{z}^2)/kT\}\,dz,$$

where

$$E'=E-q\lambda\bar{z}.$$

If we put

$$z=y+E'q/2a,$$

this equation becomes

$$f=\left(\frac{2\pi mkT}{h^2}\right)^{1/2}\int_{-\infty}^{\infty}\exp\left\{\left(\tfrac{1}{2}q^2\lambda\bar{z}^2+\frac{q^2E'^2}{4a}-ay^2-b\left(y+\frac{E'q}{2a}\right)^4\right)\Big/kT\right\}dy,$$
$$. \quad . \quad . \quad . \quad . \quad (4.20)$$

and if we assume b is small so that terms in b^2 can be neglected, then we have

$$f=\left(\frac{2\pi mkT}{h^2}\right)^{1/2}\exp\left\{\frac{q^2\lambda\bar{z}^2}{2kT}+\frac{q^2E'^2}{4akT}\right\}$$
$$\times\int_{-\infty}^{\infty}\left\{1-\frac{b}{kT}\left(y+\frac{E'q}{2a}\right)^4\right\}\exp\left(-\frac{ay^2}{kT}\right)dy$$
$$=\left(\frac{2\pi mkT}{h^2}\right)^{1/2}\left(\frac{\pi kT}{a}\right)^{1/2}\exp\left\{\frac{q^2\lambda\bar{z}^2}{2kT}+\frac{q^2E'^2}{4akT}\right\}$$
$$\times\left\{1-\tfrac{3}{4}\frac{bkT}{a^2}-\tfrac{3}{4}\frac{bq^2E'^2}{a^2}-\frac{bq^4E'^4}{16a^4kT}\right\} \quad . \quad . \quad . \quad . \quad . \quad (4.21)$$

Since the partition function is calculated under conditions of constant field, volume and temperature, the free energy we derive from it is the electric Gibb's function G_2 (see § 2.6). This is given by the equation

$$G_2 = -NkT \log f$$

$$= -NkT\tfrac{1}{2} \log \left\{ \left(\frac{2\pi mkT}{h^2} \right) \left(\frac{\pi kT}{a} \right) \right\}$$

$$-N\left\{ \frac{q^2\lambda\bar{z}^2}{2} + \frac{q^2E'^2}{4a} - \tfrac{3}{4}\frac{bk^2T^2}{a^2} - \tfrac{3}{4}\frac{bq^2E'^2kT}{a^3} - \frac{bq^4E'^4}{16a^4} \right\}, \quad . \quad . \quad . \quad (4.22)$$

and the polarization P is given by

$$P = -\frac{\partial G_2}{\partial E} = N\left\{ \frac{q^2E'}{2a} - \tfrac{3}{2}\frac{bq^2E'kT}{a^3} - \frac{bq^4E'^3}{4a^4} \right\}. \quad . \quad . \quad . \quad . \quad (4.23)$$

But P is clearly $NQ\bar{z}$, and hence

$$E' = E - \lambda P/N.$$

Now the constant λ is negative and inversely proportional to the distance apart of the dipoles and therefore directly proportional to N, the number of dipoles per unit volume. Hence it is convenient to put λ equal to $-\gamma N$, since γ will then be a pure number (γ will be $4\pi/3$ for a simple cubic array). We then have

$$P = N\left\{ \frac{q^2}{2a}(E+\gamma P) - \tfrac{3}{2}\frac{bq^2kT}{a^3}(E+\gamma P) - \frac{bq^4}{4a^4}(E+\gamma P)^3 \right\},$$

and since b is small this becomes approximately

$$P = \frac{Nq^2}{2a}(E+\gamma P) - \frac{3bkT}{a^2}P - \frac{2b}{aN^2q^2}P^3,$$

and hence

$$E = P\left\{ -\gamma + \frac{2a}{Nq^2} + \frac{6bkT}{aNq^2} \right\} + P^3\frac{4b}{N^3q^4}, \quad . \quad . \quad . \quad (4.24)$$

which we can write as

$$E = P\frac{6bk}{aNq^2}(T - T_0) + P^3\frac{4b}{N^3q^4}, \quad . \quad . \quad . \quad . \quad (4.25)$$

where

$$kT_0 = \frac{aNq^2}{6b}\left(\gamma - \frac{2a}{Nq^2} \right) = \frac{aNq^2\gamma}{6b} - \frac{a^2}{3b}. \quad . \quad . \quad . \quad (4.26)$$

It is clear from (4.25) that we have a second-order transition at temperature T_0, and that below this temperature the spontaneous polarization is given by

$$P^2 = \tfrac{3}{2}\frac{kN^2q^2}{a}(T - T_0). \quad . \quad . \quad . \quad . \quad . \quad . \quad (4.27)$$

The reciprocal susceptibility for small fields above the transition temperature is given by

$$\chi = \frac{\partial E}{\partial P} = \frac{6bk}{aNq^2}(T - T_0). \quad . \quad . \quad . \quad . \quad . \quad (4.28)$$

From (4.24) we see that the variation of susceptibility with temperature, and hence the existence of a transition, depends on the anharmonic term bz^4 in the energy of an ion. If b is small the variation of χ with temperature will be small, but the transition temperature T_0 may have any value since γ may be nearly equal to $2a/Nq^2$.

4.7. *Comparison of Previous Two Models*

The dipole with fixed magnitude is practically equivalent to an ion moving in the type of field shown in fig. 13 (*b*). In the last section we discussed the motion of an ion in the type of field shown in fig. 13 (*a*). It is clear that we can have any intermediate type of field, such as that shown in fig. 13 (*c*), so that the two models we have discussed are simply extreme cases of a more general type. One difference between these two extreme cases that we have not already mentioned is that in the first model there will be a relaxation time corresponding to the time it takes an ion to jump from one potential well to another.

Fig. 13

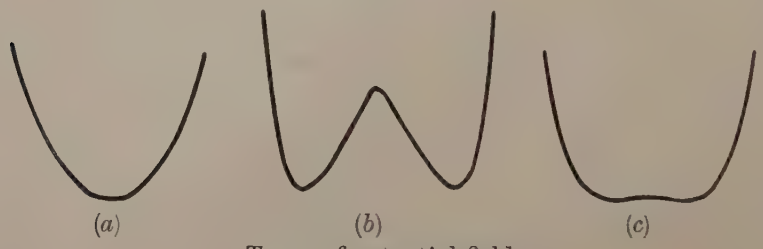

Types of potential field.

We are now in a position to continue the discussion of particular substances that we started at the beginning of the section.

4.8. *Further Discussion of Particular Cases*

4.8.1. *Barium Titanate*

The properties of $BaTiO_3$ have been discussed by different authors in terms of both types of model. The atomic structure would rather suggest the oscillating ion type and the experimental results confirm this. The main evidence is from the rate of variation of reciprocal susceptibility (table 4) ; this is very small for $BaTiO_3$, far smaller than would be given by an equation of type (4.17) ; on the other hand it could be accounted for quite well by an equation of type (4.28) since the anharmonic coefficient b may be quite small.

The model as we described it was only a one-dimensional one, and could only account for one transition. It is, however, easy to modify it to account for the three transitions. We suppose that the oscillating ions are the oxygen ions, and that the direction of movement is along the line joining the oxygen to the neighbouring Ti ions. Then one-third

of the oxygens will be vibrating in the x-direction, one-third in the y-direction, and one-third in the z-direction. If the vibrations in the three directions are quite independent, then spontaneous polarization will set in along each direction at the same temperature, and the substance will go directly to the rhombohedral form. However, the interaction between strain and polarization will cause a spontaneous polarization in one direction to inhibit spontaneous polarization in the directions at right angles. For a polarization along the z-direction will cause an extension in that direction and a contraction in the x- and y-directions; these contractions will check the onset of spontaneous polarization in these directions. Thus if the interaction has a suitable value spontaneous polarization will set in along one, two, and three axial directions as the temperature is lowered; that is the substance will pass successively through the tetragonal, orthorhombic, and rhombohedral phases. X-ray examination of the tetragonal structure by Evans (1953) indeed suggests that the movement of the oxygen ions as described plays an important part in the polarization, though, of course, there are other ionic movements as well. These are all taken into account in a paper by Slater (1949), who has discussed the problem in some detail.

4.8.2. *Potassium Dihydrogen Phosphate*

The crystal structure of this substance is more in agreement with a two-position dipole model. According to Weiss (1930) the phosphorus and oxygen atoms are arranged in tetrahedral groups; the hydrogen atoms are presumed to lie between the oxygen atoms of two neighbouring groups, and as the distance apart of these is rather more than twice an O–H bond it seems plausible that the H-atoms may have two equilibrium positions. The rate of variation of reciprocal susceptibility is also a good deal larger than in $BaTiO_3$ (table 4), but is still rather small for the two-position model; in fact it seems probable that the potential field is one of intermediate type. The formulae we have given are also inconsistent with the fact that KH_2PO_4 and KD_2PO_4 have very different transition temperatures (120°K and 210°K) although the spontaneous polarizations are not much different. This is due, however, not to the incorrectness of the model but to the failure of classical mechanics under these conditions. Pirenne (1949 b) has applied quantum theory to the motion of a hydrogen atom in an intermediate type of field and has obtained reasonably satisfactory results.

An earlier theory by Slater (1941) tried to account for the behaviour of the phosphates on the assumption of a local, non-electrostatic, interaction between the dipoles, but it gave much too sharp a transition. Moreover, the electrostatic interactions can certainly not be neglected even if there are local interactions as well.

The other ferroelectric phosphates and arsenates have similar properties to KH_2PO_4 and KD_2PO_4 and the same type of theory will, no doubt, explain the behaviour of all of them.

4.8.3. *Rochelle Salt*

It is clear that neither of the two models we have discussed can explain the behaviour of Rochelle salt, since they give only an upper transition temperature, whereas Rochelle salt has both an upper and lower transition temperature. Now the crystal structure of Rochelle salt has been determined by Beevers and Hughes (1941). The x-ray analysis does not show the positions of the hydrogen atoms, which must be guessed, but it seems likely that one atom per molecule lies between two oxygen atoms, whose distance apart is such that the hydrogen atoms may have two positions of equilibrium as in KH_2PO_4. There is, however, an important difference from KH_2PO_4; the two oxygen atoms are attached to different groups, so that the hydrogen atoms move in unsymmetrical fields and the dipoles they form have different energies according to the direction in which they are parting; there are four molecules per unit cell, and two of the dipoles have minimum energy when pointing in one direction, and the other two have minimum energy when pointing in the opposite direction.

Mason (1950) has discussed the theory of Rochelle salt in terms of a model based on this structure. He assumed that there were two similar sets of asymmetric dipoles, as above. Then it is clear that, if the energy difference between the two positions of a dipole is greater than twice the interaction energy per dipole of the dipoles when set parallel, the anti-parallel position will have the lowest energy and will therefore be stable at low temperatures. Mason was able to show that, under certain conditions, the substance will become spontaneously polarized over a higher range of temperatures. He found it necessary, however, to assume that the dipole moment itself varies with temperature owing to the thermal expansion. Against this we may argue that we still get two transition temperatures if we keep the volume constant instead of the pressure as we pointed out earlier. This objection is not conclusive, however, as even if the volume is kept constant it is still possible for some strain to take place. Whether it would be possible to have two transition temperatures if the dipole moment is constant is not certain.

4.9. *Antiferroelectrics*

Models for an antiferroelectric transition can be constructed in the same way as for a ferroelectric one. The only difference is that the state of minimum energy is one in which the dipoles are arranged in an anti-parallel array, and our variable is no longer the fraction of dipoles pointing in a given direction, but the fraction pointing in the 'right' direction. Just as in the ferroelectric case the model can either be one of fixed magnitude dipoles or of oscillating ions or of intermediate type.

4.10. *Perovskites*

We have already discussed in some detail one of the perovskites, $BaTiO_3$, but if we consider the perovskites as a whole we find that there

are some problems which do not appear in the special case of $BaTiO_3$. These are as follows :

(1) The existence of both antiferroelectric and ferroelectric substances with the same basic structure.

(2) The existence of both antiferroelectric and ferroelectric phases in a given substance at different temperatures, and the reason why the antiferroelectric phase appears to be always the low-temperature one.

The first problem is fairly easy to explain. It has been shown by Sauer (1940) that if we have a set of dipoles in a crystal they may have minimum energy when either parallel or antiparallel according to the particular arrangement. A simple cubic array has its minimum energy when antiparallel, and a body-centred or face-centred array when parallel. Now in its distorted form a perovskite must be considered as having pseudo-dipoles at the cube corners, body-centres, and face-centres, and it is clearly possible for this array to have its minimum when either parallel or anti-parallel according to the relative magnitude of the dipoles. Takagi (1952) has discussed a model composed of rotating dipoles at the cube corners and polarizable ions at the body centres and has shown that this may give either a ferroelectric or an antiferroelectric transition according to the magnitudes assumed.

The second problem is more difficult. No simple model which gives a temperature transition from an antiferroelectric to a ferroelectric state has been suggested. It may be that the problem is essentially complex and no plausible simple model is possible. Since the antiferroelectric state, when it exists, is stable at low temperatures it presumably has smaller entropy than the ferroelectric ones ; in terms of the oscillation type of model this means that the average vibration frequencies are greater in the antiferroelectric state, so that a suitable model should explain this. Alternatively the transition may not be directly due to the temperature change but due to the thermal expansion, that is the antiferroelectric state is stable at low volumes rather than low temperatures.

An alternative method of approach, which we have not had time to consider here, is to think of the transition as associated with a change of the type of chemical binding rather than a change in the dipole structure. This has been done by Megaw (1952 and 1954).

Acknowledgment

The author wishes to thank the Electrical Research Association for financial assistance in aid of this work, and for permitting its publication.

References

Baertschi, P., 1945, *Helv. Phys. Acta*, **18.**
Bancroft, D., 1938, *Phys. Rev.*, **53,** 587.
Bantle, W., 1942, *Helv. Phys. Acta*, **15,** 373.
Baumgartner, H., 1950, *Helv. Phys. Acta*, **23,** 651 ; 1951, *Ibid.*, **24,** 326.
Beevers, L. A., and Hughes, W., 1941, *Proc. Roy. Soc.* A, **177,** 251.

Busch, G., 1938, *Helv. Phys. Acta*, **11,** 269.
Cady, W. G., 1946, *Piezoelectricity* (New York : McGraw-Hill).
Cooke, W. R., and Jaffe, H., 1953, *Phys. Rev.*, **89,** 1297.
De Quervain, M., 1944, *Helv. Phys. Acta*, **17,** 509.
Devonshire, A. F., 1949, *Phil. Mag.*, **40,** 1040 ; 1951, *Ibid.*, **42,** 1065.
Evans, H. T., Jr., 1953, *Technical Report*, Laboratory for Insulation Research, M.I.T.
Fröhlich, H., 1949, *Theory of Dielectrics* (Oxford : Clarendon Press).
Hablützel, J., 1934, *Helv. Phys. Acta*, **12,** 488.
Känzig, W., and Maikoff, N., 1951, *Helv. Phys. Acta*, **24,** 343.
Kay, H. F., and Vousden, P., 1949, *Phil. Mag.*, **40,** 1019.
Kittel, C., 1951, *Phys. Rev.*, **82,** 729.
Mason, W. P., 1946, *Phys. Rev.*, **69,** 173 ; 1947, *Ibid.*, **72,** 854 ; 1950, *Piezoelectric Crystals* (New York : van Nostrand).
Matthias, B., 1949, *Phys. Rev.*, **76,** 430.
Matthias, B., and Hulm, J. K., 1951, *Phys. Rev.*, **82,** 108.
Matthias, B., and Remeika, J., 1949, *Phys. Rev.*, **76,** 1886.
Megaw, H. E., 1952, *Acta Cryst.*, **5,** 739 ; 1954, *Ibid.*, **7,** 187.
Merz, W. J., 1949 a, *Phys. Rev.*, **75,** 687 ; 1949 b, *Ibid.*, **76,** 1221 ; 1950, *Ibid.*, **78,** 52 ; 1951, *Ibid.*, **82,** 562 ; 1953, *Ibid.*, **91,** 513.
Mueller, H., 1940, *Phys. Rev.*, **57,** 829.
Onsager, L., 1936, *J. Amer. Chem. Soc.*, **58,** 1486.
Pirenne, J., 1949 a, *Helv. Phys. Acta*, **22,** 479 ; 1949 b, *Physica*, **15,** 1019.
Sauer, J. A., 1940, *Phys. Rev.*, **57,** 142.
Sawaguchi, E., 1953, *J. Phys. Soc. Japan*, **8,** 615.
Sawaguchi, E., Maniwa, H., and Hoshino, S., 1951, *Phys. Rev.*, **83,** 1078.
Shirane, G., 1951, *Phys. Rev.*, **86,** 219.
Shirane, G., and Sato, K., 1951, *J. Phys. Soc. Japan*, **6,** 20.
Shirane, G., Sawaguchi, E., and Takeda, A., 1951, *Phys. Rev.*, **84,** 476.
Shirane, G., and Suzuki, K., 1951, *J. Phys. Soc. Japan*, **6,** 274 ; 1952, *Ibid.*, **7,** 333.
Shirane, G., Suzuki, K., and Takeda, A., 1952, *J. Phys. Soc. Japan*, **7,** 12.
Slater, J. C., 1941, *J. Chem. Phys.*, **9,** 16 ; 1949, *Phys. Rev.*, **78,** 748.
Takagi, Y., 1952, *Phys. Rev.*, **85,** 315.
Ueda, R., and Ichinokawa, T., 1950, *Phys. Rev.*, **80,** 1106 ; **81,** 563.
Weiss, P., 1930, *Z. Kristallogr.*, **74,** 306.

On the Theory of Liquid Helium

By I. Prigogine
Faculté des Sciences de l'Université de Bruxelles

§ 1. Introduction

The purpose of this paper is to give an account of the recent theory of liquid helium which the author and his co-workers have put forward (Prigogine and Philippot 1952, 1953 a, b, c, and Prigogine, Bingen and Jeener 1954, Prigogine and Bellemans 1954).

At the present time there exists no rigorous theory of liquid helium, and considering the fact that there does not even exist a satisfactory statistical model for classical liquids, it seems unlikely that such a theory will be developed in the near future. The characteristic feature of helium is that the so-called ' reduced ' de Broglie length (de Boer 1948)

$$\Lambda^*=h/\sigma\sqrt{(m\epsilon)} \quad . \quad . \quad . \quad . \quad . \quad . \quad . \quad . \quad (1.1)$$

where σ, ϵ are the characteristic parameters in the ' 6–12 ' interaction law $[\epsilon(r)=4\epsilon\{(\sigma/r)^{12}-(\sigma/r)^6\}]$, is very large. The quantity Λ^* is 2·64 for ^{4}He and 3·04 for ^{3}He, which may be compared with 0·591 for Ne and 1·73 for H_2. Therefore the wave character of the molecules plays an important role even on a macroscopic scale.

At absolute zero the quantum kinetic energy no longer appears as a small correction to the lattice energy, but the two are of the same order of magnitude ; this is what prevents helium from being solid at zero pressure. The usual approach to such a situation is to start with a perfect Bose–Einstein gas (London 1954) and to take account of the interactions by some minor refinements as for instance by a self-consistent field (cf. the excellent review article by Dingle 1952). The recent interesting considerations by Feynman (1953) correspond also to this conception. The advantage of such a procedure is clear : the differences in behaviour of liquid helium of masses three and four, and specially the absence of a λ-point for the former, immediately result from the difference in statistics. But other problems remain unsolved. The molar volume of liquid helium decreases with increasing temperature below the λ-point. This behaviour is completely unexpected for such simple molecules, only water showing the same anomaly, and is not explained by the ' gas ' models.

Another striking feature of liquid helium is the occurrence of strong positive deviations from Raoults law for mixtures of ^{3}He and ^{4}He (Daunt 1952). Daunt and Heer (1951) suggested considering these deviations as due to the difference in statistics. It is certainly remarkable that their model gives correct orders of magnitude for a temperature of about 1°K. On the other hand it predicts negative

deviations from Raoult's law at sufficiently low temperatures. No indication of such a reversal exists. Also a solution of ^{4}He and ^{6}He ought to show two separate λ-points !

On the other hand liquid helium has many properties in common with ordinary condensed phases, such as the validity of the T^3 law for the specific heat at sufficiently low temperatures for ^{4}He, the validity of Curie's law down to low temperatures for the spin–spin interaction for ^{3}He.

For all these reasons it appeared interesting to develop a quite different approach starting from the behaviour of ordinary condensed systems.

Fröhlich's (1937) ingenious suggestion for the interpretation of the λ-point as an order–disorder process belongs to this type of theory. This approach however does not include the role of statistics and thus the difference in the behaviour of ^{3}He and ^{4}He. We may mention also that de Boer (1953) has quite recently developed a model which has many points in common with our theory.

§ 2. Density Fluctuations in Classical Liquids

Before going into details about our theory it may be useful to visualize the physical model which is used. Let us first consider the case of a classical liquid. Near the melting point the density remains very high (the reduced volume $v^*=v/\sigma^3=1{\cdot}15$). The molecules nearly touch each other and so there remains a high local order around each molecule, the number of nearest neighbours being about the same as for a solid. No important density fluctuations on a molecular scale are possible for such a compressed medium. The situation undergoes a radical change near the critical temperature. The volume is then increased by a factor of the order 3. Then there appear, both in the liquid phase and in the vapour phase, an important excess specific heat (cf. the beautiful measurements of Strijland (1953) for CO_2). This sharp increase of entropy may be described as due to the formation of ' clusters ' or of ' holes ' in the liquid. Such clusters or holes are density fluctuations on a molecular scale. In other words the distance between nearest neighbours now fluctuates widely around its mean value.

This disordering process may be formulated more quantitatively using a cell model for the liquid state. Let us subdivide the geometrical volume of the liquid V into ν cells each of value ϕ, then

$$V=Nv=\nu\phi. \qquad (2.1)$$

Let us also call α_i the number of cells containing i particles. The usual approximation introduced in the cell model are to treat interactions of particles belonging to different cells in an approximate way (' mean field ') and to neglect the correlations between different cells. The

configurational partition function is then (Van Hove 1949, Janssens and Prigogine 1950, Pople 1951)

$$Q=\sum_{\{\alpha_i\}}\frac{\nu!}{\pi_i\alpha_i!}\prod_i\Psi^{\alpha_i}(i\,;\,\phi)\exp\left(-\frac{E_0}{kT}\right) \quad . \quad . \quad . \quad . \quad (2.2)$$

with

$$\Sigma\alpha_i=\nu,\ \Sigma i\alpha_i=N \quad . \quad . \quad . \quad . \quad . \quad . \quad (2.3)$$

where $\Psi(i\,;\,\phi)$ is the configurational partition function for a group of i molecules located in a cell of volume ϕ. This takes into account the exact interaction between the molecules of this group in i molecules and the mean field due to molecules belonging to other cells ; E_0 is generally introduced to take account of the choice of the zero of the energy.

This formula is not directly useful for numerical calculations as the evaluation of $\Psi(i\,;\,\phi)$ for i greater than 2 presents great difficulties. But different particular cases may be considered. If we take

$$\nu=N\ ;\ \alpha_1=N\ ;\ \alpha_i=0\ (i=0,\,2,\,3,\,\ldots.) \quad . \quad . \quad . \quad . \quad (2.4)$$

so that only the mean distribution of particles (that is one particle per cell) is considered, we obtain the well-known model of Lennard-Jones and Devonshire (1937, 1938). Another approximation is to take account of doubly occupied cells (Janssens and Prigogine 1950, Pople 1951)

$$\nu=N\ ;\ \alpha_0,\,\alpha_1,\,\alpha_2\neq0\ (\alpha_0=\alpha_2)\ ;\ \alpha_i=0(i>2). \quad . \quad . \quad . \quad (2.5)$$

Then the configurational free energy may be put into the form (Janssens and Prigogine 1950)

$$-\frac{F_{\text{conf}}}{kT}=-\frac{E_0}{kT}+\ln\Psi(1\,;\,v)+\ln\left[1+2\frac{\Psi^{1/2}(2\,;\,v)}{\Psi(1\,;\,v)}\right]. \quad . \quad (2.6)$$

From this formula we may deduce all other thermodynamic quantities like the configurational entropy or specific heat. All these properties may be split up into two parts ; the first corresponding to the mean distribution (1 particle per cell) the other due to multiple cell occupation or density fluctuations. For the particular model under consideration we have for the excess entropy and the excess specific heat at constant volume

$$\frac{S_e}{Nk}=\ln\left[1+2\frac{\Psi^{1/2}(2\,;\,v)}{\Psi(1\,;\,v)}\right]+T\frac{\partial}{\partial T}\ln\left[1+2\frac{\Psi^{1/2}(2\,;\,v)}{\Psi(1\,;\,v)}\right] \quad . \quad . \quad . \quad (2.7)$$

$$\frac{C_{v,e}}{NkT}=2\frac{\partial}{\partial T}\ln\left[1+2\frac{\Psi^{1/2}(2\,;\,v)}{\Psi(1\,;\,v)}\right]+T\frac{\partial^2}{\partial T^2}\ln\left[1+2\frac{\Psi^{1/2}(2\,;\,v)}{\Psi(1\,;\,v)}\right]. \quad . \quad (2.8)$$

For a clearer understanding of these effects let us consider the case of a perfect gas. There we have

$$\Psi(1\,;\,v)=v\ ;\ \Psi(2\,;\,v)=\tfrac{1}{2}v^2. \quad . \quad . \quad . \quad . \quad . \quad (2.9)$$

The ordinary cell model (2.5) would give

$$-F_{\text{conf}}/NkT=\ln v. \quad . \quad . \quad . \quad . \quad . \quad . \quad (2.10)$$

The model (2.6) with doubly occupied cells

$$-F_{\text{conf}}/NkT=\ln v+0{\cdot}9. \quad . \quad . \quad . \quad . \quad . \quad (2.11)$$

Also taking account of triply-occupied cells we may find similarly

$$-F_{\text{conf}}/NkT = \ln v + 0{\cdot}99. \quad . \quad . \quad . \quad . \quad . \quad . \quad (2.12)$$

The exact result is, of course

$$-F_{\text{conf}}/NkT = \ln v + 1. \quad . \quad . \quad . \quad . \quad . \quad . \quad (2.13)$$

So we see that the density fluctuations are closely related to the entropy of the system. One can say that density fluctuations are the mechanism by which appears the so-called *communal entropy* of the system (Janssens and Prigogine 1950, Pople 1951).

Other approximations may be used, for instance,

$$v > N,\ \alpha_0,\ \alpha_1 \neq 0,\ \alpha_i = 0\ i \geqslant 2 \quad . \quad . \quad . \quad . \quad . \quad (2.14)$$

this corresponds to the 'hole' model of liquids (or 'lattice gas' approximation).

All these descriptions are very crude and can hardly be used for a really quantitative treatment of liquids, but they permit us to understand at least qualitatively the origin of the high excess specific heat in the critical region. We may also note that this excess specific heat has nothing to do with condensation or vaporization. It appears also for the same density above the critical temperature.

§ 3. Physical Model for Liquid Helium

Let us now consider the situation for liquid helium at 0°K. A fundamental role is now played by the quantum kinetic energy. Compression of the molecules increases this kinetic energy, but expansion decreases the attractive part of the potential. So some mean distance between the particles must correspond to the minimum of the total energy. As result of the quantum kinetic energy we have more or less a regular structure in which each atom tends to remain separate from the others.

It is a remarkable fact that the thermodynamic properties at absolute zero seem to be largely independent of statistics. Indeed we shall see in §§ 4 and 6 that the change in the energy, volume and compressibility at 0°K when ^{4}He and ^{3}He are compared may be understood from the change of the zero point energy without introducing any effects depending on statistics. Another pointer in the same direction is that, when reduced thermodynamic properties (like reduced volume) are plotted on a graph against de Boer's parameter Λ^* (1.1), the properties of ^{3}He lie on the same smooth curve with the properties of A, Ne, D_2, H_2 and ^{4}He. This is even true for many properties at temperatures different from 0°K, like the reduced critical temperature and reduced critical pressure. This fact permitted de Boer and Lunbeck (1949) to predict the values of these parameters for ^{3}He before they had been measured.

This shows that the thermodynamic properties at 0°K of helium may be calculated from a model in which particles are localized in small cells

around some mean positions. Of course this does not mean that exchanges of position do not occur. On the contrary such exchanges are fundamental for the understanding of the hydrodynamic properties and flow processes. There, statistics must play a dominant role, ^{4}He being a ' superfluid ' and ^{3}He not. In a certain sense the situation is the same as for ordinary liquids for which the cell model permits us to calculate the orders of magnitude of thermodynamic properties but not the transport processes, unless we introduce some supplementary hypotheses.

Let us now consider what happens when we raise the temperature. First of all phonons are formed.* But the mere existence of the λ-point shows that other excitation processes must occur. In order to have some idea of their nature we must keep in mind the following facts :

The spacing between the molecules at 0°K is abnormally high, so that it would be easy to introduce some molecules ' between ' others without any overlapping of the electronic atmospheres. From the point of view of the volume, we may say that helium at 0°K is already in the same condition as is a classical liquid at the critical temperature.

Secondly, the anomaly in the density of liquid helium below the λ-point shows that part of the thermal energy is used to *decrease* the intermolecular distances. Such decrease may proceed either in a homogeneous way preserving the more or less regular disposition of particles or as local increases of density, that is as density fluctuations. We may, however, immediately observe that the second way strongly increases the entropy and so will correspond to a lower free energy. A homogeneous contraction would correspond to an increase of energy without compensation by entropic effects and therefore seems impossible.

Finally, we may consider the relation between such density fluctuations and delocalization of particles, that is exchange effects. In principle both effects may occur separately. In a linear chain of hard spheres we may have density fluctuations, but the order of the particles is always preserved and no statistics dependent effects can arise. The difference in the behaviour between ^{4}He and ^{3}He shows however that here the two effects must be closely connected. At the same time that density fluctuations occur for ^{4}He we must also have some partial delocalization of the molecules.

Summarizing all these physical considerations we may put forward the following model for liquid helium. At 0°K we have a more or less regular distribution of particles. Each particle is localized in a small region of space for a sufficiently long period of time (as compared with the inverse of the zero point frequency) in order to make the effects of statistics on thermodynamic properties negligible. Now thermal agitation has the double effect of introducing density fluctuations and also exchange effects by delocalizing the particles. Both effects may occur

---

* The signification of phonons in media which remain strongly anharmonic even at 0°K, would deserve a more detailed study.

together in the formation of 'clusters', that is small regions of abnormal density in the interior of which particles exchange places. The energy of formation of such clusters may be roughly estimated (cf. § 8) and it is shown that it is really much higher for Fermi particles than for Bose particles due to the difference in the exchange effects. Therefore for helium 3 such a process may occur only in the neighbourhood of the critical region. On the contrary, for helium 4 it may occur at a much lower temperature.

Such an interpretation of the λ-point has some analogy with the interpretation of the transition point of symmetrical chemical compounds like CCl_4, at which roughly speaking, free rotation occurs. The entropy of melting compared with that of $SnCl_4$, which does not show such a transition point, is considerably lowered. The sum of the entropies of transition and of melting remains however about the same.

In our interpretation of the λ-point of liquid ^{4}He we also have a splitting up of two processes (density fluctuations and vaporization) which generally occur together.

§ 4. The Ground State

Even if we consider according to § 3 the molecules at 0° K as localized, the problem of the evaluation of the main thermodynamic properties such as energy, equation of state and compressibility remains a very difficult one. Indeed, we have here an extreme case of an assembly of anharmonic oscillators. This is the reason why we shall use here a 'one particle' model like Einstein's model for the specific heat.

The use of such a model for the evaluation of the properties of the ground state is not unreasonable, because the main contribution to the zero point energy comes from high frequencies, that is from the motion of a particle with respect to its first neighbours.

Let us consider a very simple example, a chain of hard spheres. This is indeed a limiting case of anharmonic oscillators. The zero point energy may be calculated exactly (Nagamiya 1940) and is found to be

$$E_0 = N h^2 / 24 m (l - \sigma)^2, \qquad (4.1)$$

where m is the mass of the particles, l the mean distance ($= L/N$), N the number of particles and σ their diameter.

Now let us consider a cell model. Here, each particle is allowed to move freely along some characteristic length l_c and the zero point energy will become

$$E_0 = N h^2 / 8 m l_c^2. \qquad (4.2)$$

The question is now to specify the value of this 'free length'. If we take simply the mean geometrical length l and subtract the diameter, we obtain

$$l_c = l - \sigma. \qquad (4.3)$$

This gives a zero point energy too high by a factor of 3. On the contrary if we assign to each particle the total distance between it and its two

first neighbours and subtract from this total length the two diameters, we have

$$l_f = 2(l-\sigma). \quad \ldots\ldots\ldots \quad (4.4)$$

The second choice (4.4) gives a much better agreement with (4.1). We may say that the price that we have to pay for using a one-particle model is that we have to use a zero point energy which corresponds to a free volume or effective volume which is much greater than the mean geometrical volume accessible to each particle.

In the three-dimensional case we no longer can fix the free volume by comparison with the exact formula (because this is not known) but we have to fix it from the experimental data. We may think that in this case it will become comparatively even larger than in the one-dimensional case because the number of low frequencies is higher for purely geometrical reasons.

Fig. 1

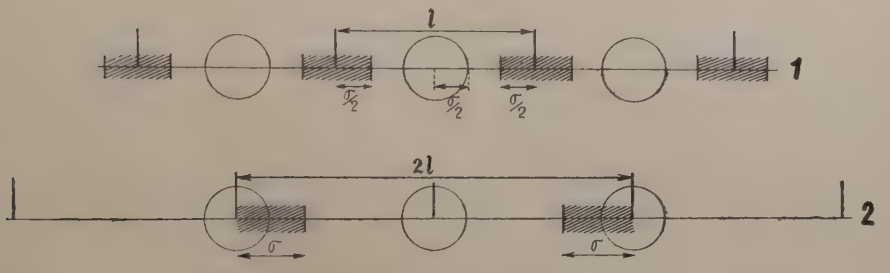

Different definitions of the free volume.
1. Formula (4.3).
2. Formula (4.4).

Let us now come back to the case of liquid helium. In the one-particle model the energy is the sum of the potential (lattice) energy and of the zero point energy corresponding to the motion of a particle in its cell. Due to the large distances between the particles, the curvature of the intermolecular potential is small and it seems sufficient in this rough approximation to consider a free translation of the particle in its cell. This corresponds (for a cubic cell) to a zero point energy (cf. (4.2))

$$E_0 = N3h^2/8mv_f^{2/3}, \quad \ldots\ldots\ldots \quad (4.5)$$

where v_f is the free volume per particle. Let us write

$$v_f^{2/3} = \gamma(a-\sigma)^2 \quad \ldots\ldots\ldots \quad (4.6)$$

where a is the mean distance between first neighbours ($a \sim 4$ Å if we suppose a face-centred cubic lattice, $\sigma \sim 2{\cdot}5$ Å) and fix γ from the experimental data. From what we have seen for the one-dimensional example, we may expect

$$\gamma \geqslant 8^{2/3} = 4. \quad \ldots\ldots\ldots \quad (4.7)$$

In fact we found a satisfactory agreement with this order of magnitude (cf. figs. 2 and 3). In the subsequent calculations we have taken

$$\gamma = 4{\cdot}5. \quad . \quad . \quad . \quad . \quad . \quad . \quad . \quad . \quad . \quad (4.8)$$

The effective or free volume is thus

$$v_f \sim 8 \times 3{\cdot}4 \sim 27 \text{ cubic Angstrom.} \quad . \quad . \quad . \quad (4.9)$$

This corresponds to a point in a cube of length 3A or to a point in a sphere of radius $\sim 1{\cdot}7$A (which is of the order of $a-\sigma$).

Fig. 2

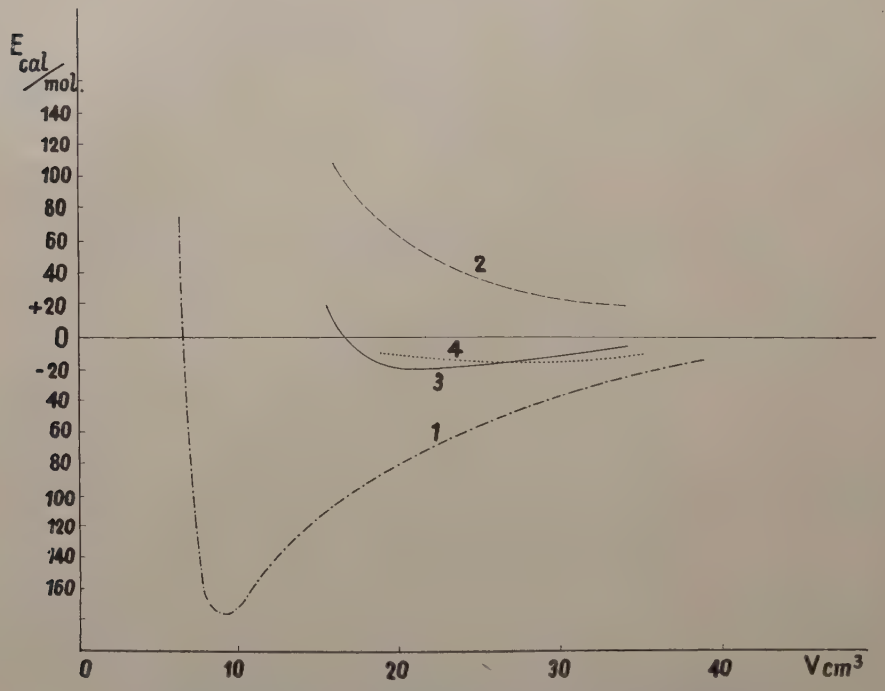

1. Lattice energy for a 6–12 law and cubic face centred lattice.
2. Zero-point energy (4·5)–(4·8).
3. Total energy (4·5)–(4·7).
4. Experimental energy (cf. (4·10)).

In fig. 2 we have drawn the lattice energy, the zero point energy (4.5)–(4.6) with (4.8) and the total energy. We also have drawn the experimental total energy (small letters are always relative to quantities per mole or per particle),

$$e = e_{\min} + \tfrac{1}{2} \frac{\partial^2 e}{\partial v^2} (v - v^0)^2, \quad . \quad . \quad . \quad . \quad . \quad . \quad . \quad (4.10)$$

using the experimental value for the compressibility

$$\kappa = \left(v \frac{\partial^2 e}{\partial v^2} \right)^{-1} \sim 0{\cdot}34 \text{ cm}^3/\text{cal}. \quad . \quad . \quad . \quad . \quad . \quad (4.11)$$

We obtain using (4.6), the following values:

	Experiment	Calc. with $\gamma=4$	Calc. with $\gamma=4{\cdot}5$
v	27 (cm^3/mole)	24·5	22·4
e	14 (cal/mole)	8	18
Curvature $(\partial^2 e/\partial v^2)$	0·11 (cal/cm^6)	0·14	0·19

All these properties have the right order of magnitude. If we take the same formulae (4.5) and (4.6) with the same value (Prigogine *et al.* 1953, 1954) of γ for ^{3}He we may predict its properties at 0°K. The result is

Fig. 3

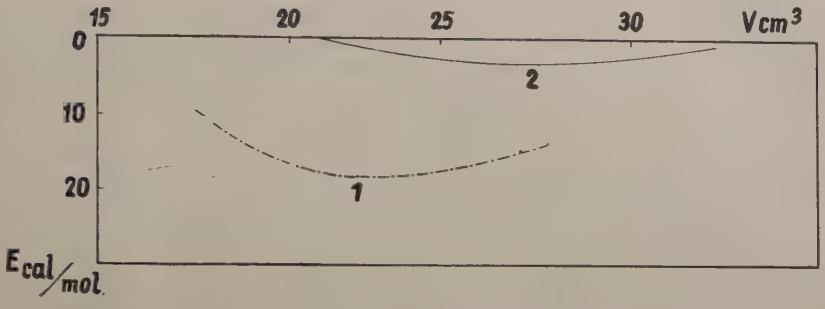

Comparison between ^{4}He and ^{3}He using (4.5) and (4.6) with $\gamma=4{\cdot}5$.

indicated in fig. 3. The shift in the properties due to the difference in mass is correctly obtained. We find the following values:

	Experiment	Calc. ($\gamma=4{\cdot}5$)
Δv	10 (cm^3/mole)	5
e	10 (cal/mole)	14·5
κ	— (cal/cm^6)	0·09

Here, Δv is the volume difference between ^{3}He and ^{4}He. So it seems that the one-particle model is really sufficient to understand the orders of magnitude of the main thermodynamic properties. Let us now pass directly to the case of mixtures of ^{4}He and ^{3}He.

§ 5. The Ground State for Mixtures of ^{4}He and ^{3}He

The total energy for a mixture of ^{3}He and ^{4}He at 0°K may be written in the form

$$E=N_3e_3+N_4e_4$$
$$=N_3(\epsilon_3+u)+N_4(\epsilon_4+u) \quad . \quad . \quad . \quad . \quad . \quad . \quad . \quad (5.1)$$

where ϵ_3 and ϵ_4 are the zero point energies of ^{3}He and ^{4}He and u the potential energy (per particle). We shall assume that the zero point energies depend only on the effective volume per particle and on the *mass of the particle in the cell* (cf. § 6).

The equation of state at zero pressure is

$$p=-\frac{\partial}{\partial V}[N_3(\epsilon_3+u)+N_4(\epsilon_4+u)]=0. \quad . \ . \ . \quad (5.2)$$

It is quite easy to deduce from (5.1) and (5.2) expressions for the excess volume and the excess energy, that is for the change of the volume and for the change of the energy by mixing the pure isotopes.

Let us call v the volume per molecule in the mixture ; v_3^0, v_4^0 for the pure isotopes. Neglecting terms of a higher order than the second in differences of volume, we may write for the energies of the isotopes

$$\left.\begin{aligned} e_3&=e_3^0+\tfrac{1}{2}\chi_3(v-v_3^0)^2 \\ e_4&=e_4^0+\tfrac{1}{2}\chi_4(v-v_4^0)^2 \end{aligned}\right\} \chi_3,\ \chi_4>0. \quad . \ . \ . \ . \ . \quad (5.3)$$

Here e_3^0, e_4^0 are the energies (per particle) of the pure isotopes and χ_3, χ_4, the corresponding curvatures. With increasing zero point energy, the minimum of e versus v becomes more and more flat. So we have

$$\chi_3<\chi_4. \quad . \ . \ . \ . \ . \ . \ . \ . \ . \quad (5.4)$$

If we write

$$\chi_4=\chi_3(1+\lambda) \quad . \ . \ . \ . \ . \ . \ . \ . \ . \quad (5.5)$$

χ may be estimated from fig. 2 and fig. 3 and is found to be of the order 10^{-1}.

It is immediately clear from these relations that the excess energy is positive. Indeed (5.1) and (5.3) give

$$E=N_3e_3^0+N_4e_4^0+\tfrac{1}{2}N_3\chi_3(v-v_3^0)^2+\tfrac{1}{2}N_4\chi_4(v-v_4^0). \quad . \ . \quad (5.6)$$

So we have for the energy of mixing

$$\Delta E=\tfrac{1}{2}N_3\chi_3(v-v_3^0)^2+\tfrac{1}{2}N_4\chi_4(v-v_4^0)^2>0. \quad . \ . \ . \quad (5.7)$$

The ground state for the mixture is higher than that for the pure isotopes. There is thus a separation of phases at 0°K. This in turn gives positive deviations from the laws of perfect solutions at sufficiently low temperatures.

The explicit equation of state of the mixture is obtained by putting (5.6) into (5.2). We get, if x_3, x_4 are mole fractions, so that $x_3+x_4=1$,

$$v=\frac{x_3\chi_3v_3^0+x_4\chi_4v_4^0}{x_3\chi_3+x_4\chi_4}. \quad . \ . \ . \ . \ . \ . \quad (5.8)$$

This gives for the excess volume per particle,

$$\Delta v=v-x_3v_3^0-x_4v_4^0\simeq\left(1-\frac{\chi_4}{\chi_3}\right)(v_3^0-v_4^0)x_3x_4<0 \quad . \ . \quad (5.9)$$

and for the excess energy per particle

$$\Delta e=\tfrac{1}{2}(v_3^0-v_4^0)\chi_4x_3x_4>0. \quad . \ . \ . \ . \ . \quad (5.10)$$

This is of the order of magnitude of 1 cal/mole for $x_3=x_4=0{\cdot}5$ (Prigogine and Philippot 1953 b, Prigogine and Bellemans 1954). Such a difference of energy between the solution and the pure isotopes is of the correct order of magnitude. It is quite clear that this model gives too large an isotopic effect, because fluctuations in the free volume due to

differences in mass have been neglected. Also correlations between cell occupations will reduce the value of the excess energy. On the other hand it is noteworthy that the existence of positive deviations from Raoult's law has been obtained without any assumption about the form of the zero point energy.

Another interesting effect is the predicted contraction upon mixing (5.9). It seems difficult to measure this small effect directly.

§ 6. Some General Considerations on Isotopic Mixtures

The considerations of § 5 are clearly not restricted to mixtures of ^{4}He and ^{3}He. The influence of differences in the masses of molecules on the thermodynamic properties of mixtures is a very general and interesting problem, which is beyond the scope of this paper. We shall here present only some brief comments (for more details, see Prigogine, Bingen and Jeener 1954, Prigogine and Bellemans 1954).

This problem may be considered, using two different approaches. The first consists in studying the properties of a regular lattice. If we consider as an example an equimolecular mixture of two isotopes A and B. we may compare the energy levels of the ordered state ABABAB . . . . with those of the pure compounds AAA . . . ., BBB . . . . In the first case we have a frequency spectrum containing one 'acoustical' branch and one 'optical' branch and in the other, two acoustical branches (one for each isotope). The energy of the ground state is simply proportional to the area of the frequency spectrum in the first Brillouin-zone.

This area depends on the distribution of the masses over the system. We may immediately infer that differences in mass will give rise to purely quantum transitions at sufficient low temperatures. The relative distribution of the isotopes will be completely random at high temperatures and will become ordered at low temperatures in such a way that the energy of the system is as small as possible. Such isotopic transitions are quantum mechanical analogues of classical order–disorder phenomena, but have a certain number of characteristics of their own.

The frequency spectrum of an isotopic mixture and hence the zero-point energy will depend on the complete specification of the positions of the masses. In this sense the perturbations introduced by the difference in masses are analogeous to the effect of long-range forces, and it would generally be difficult to calculate this effect exactly. But it is possible to calculate easily the *mean perturbation* for a given number of couples of first neighbours AA, AB, BB.

Let us call

$$m_A=(1+\mu_A)\bar{m},\ m_B=(1+\mu_B)\bar{m} \quad . \quad . \quad . \quad . \quad . \quad (6.1)$$

where m_A, m_B are the masses of the isotopes and $\bar{m}$ the mean mass

$$\bar{m}=x_A m_A+x_B m_B. \quad . \quad . \quad . \quad . \quad . \quad . \quad . \quad (6.2)$$

The quantities μ_A, μ_B represent the deviation from the mean mass (with $x_A\mu_A+x_B\mu_B=0$). The kinetic energy of the system is

$$T=\tfrac{1}{2}\Sigma_i m_i\dot{y}_i^2=\tfrac{1}{2}\bar{m}\Sigma_i(1+\mu_i)\dot{y}_i^2$$
$$=T_0+\tfrac{1}{2}\bar{m}\Sigma_i\mu_i\dot{y}_i^2 \quad . \quad . \quad . \quad . \quad . \quad . \quad . \quad . \quad . \quad (6.3)$$

where μ_i is μ_A or μ_B according to whether the site i is occupied by A or B.

It is easy to show that the first order perturbation (that is of the order $\mu_A-\mu_B$) is zero and that the *mean value* of the second order perturbation of the frequencies is determined by the second moments

$$\overline{\mu_n\mu_{n+l}} \quad . \quad . \quad . \quad . \quad . \quad . \quad . \quad . \quad . \quad (6.4)$$

These second moments may easily be calculated when the numbers of first neighbours are given. As the result of this method it may be shown that the energy of a random distribution of isotopes is higher than that of the pure isotopes. We therefore always have phase separation at sufficiently low temperatures. This result is not altered when one takes account of the effects of anharmonicity.

The second approach consists in the application of a quantum cell model to solutions of isotopes. Here again it is easy to show that one has to expect positive deviations from Raoult's law. As an example we may mention that this method predicts an excess free energy of mixing of 2·5 cal. per mole for an equimolecular mixture of H_2 and D_2. This is in good agreement with the experimental value which is of the order of 2 cal. per mole (Hoge and Arnold 1951).

This shows again that the thermodynamic properties of mixtures of ^{3}He and ^{4}He, and especially the positive excess free energy of mixing, is not exceptional.

§ 7. Excitations in Liquid Helium

After the discussion of the ground state of liquid helium in the preceding paragraphs we shall now go into a more detailed discussion of the excited states of liquid helium. According to the qualitative considerations of § 3 we have to discuss the possibility of density fluctuations and exchange effects. Let us consider a molecule moving in its free volume (or effective volume), which we shall suppose to be of cubic form. The zero point energy which we shall call $\epsilon_0^{(1)}$ is then ($l_1\simeq 3$ Å, cf. § 4)

$$\epsilon_0^{(1)}=\frac{3h^2}{8ml_1^2}\simeq 26\times 10^{-16}\text{ ergs.} \quad . \quad . \quad . \quad . \quad . \quad (7.1)$$

The simplest way of considering a density fluctuation is to take a group of two molecules which share the same free volume. If we call l_2 the length of the cube corresponding to this common free volume, we shall have for the zero point energy of this group

$$2\times\frac{3h^2}{8ml_2^2}\text{ in the Bose–Einstein case (+),} \quad . \quad . \quad . \quad (7.2)$$

$$\frac{3h^2}{8ml_2^2}+\frac{6h^2}{8ml_2^2}\text{ in the Fermi–Dirac case (−).} \quad . \quad . \quad (7.3)$$

The Fermi–Dirac case refers to particles without spin. Also taking account of some change Δu in the Van der Waals energy we have for the excitation energy per particle, in the Bose–Einstein case

$$\Delta_+ = \frac{3h^2}{8ml_2^2} - \frac{3h^2}{8ml_1^2} - \Delta u \quad . \quad . \quad . \quad . \quad . \quad . \quad (7.4)$$

and in the Fermi–Dirac case

$$\Delta_- = \frac{9}{2}\frac{h^2}{8ml_2^2} - \frac{3h^2}{8ml_1^2} - \Delta u \quad . \quad . \quad . \quad . \quad . \quad (7.5)$$

and so for the difference in the excitation energies

$$\Delta_- - \Delta_+ = \tfrac{1}{2}\frac{3h^2}{8ml_2^2}. \quad . \quad . \quad . \quad . \quad . \quad . \quad (7.6)$$

Now we have to discuss the following questions :

(*a*) Is the excitation energy Δ_+ sufficiently low to cause density fluctuations in the liquid state of ^{4}He ?

(*b*) Is the difference $\Delta_- - \Delta_+$ sufficiently large to rule out density fluctuations for the corresponding Fermi particles (without spin) ?

This second question may be answered immediately. Even if the free volume for the group of two particles would be the same as for a simple particle, we would have (cf. (7.1))

$$\Delta_- - \Delta_+ \simeq 13 \times 10^{-16} \text{ ergs}. \quad . \quad . \quad . \quad . \quad . \quad . \quad (7.7)$$

This is a lower limit. Indeed l_2 is smaller than l_1 because we have to subtract the mutually excluded volume of the two spheres. The value obtained in this manner is rather large. Indeed, the appearance of fluctuations and so the position of the λ-point is determined by the value of (cf. §8)

$$\exp(-\Delta/kT). \quad . \quad . \quad . \quad . \quad . \quad . \quad . \quad (7.8)$$

This expression has an inflexion point at

$$T \sim \Delta/2k, \quad . \quad . \quad . \quad . \quad . \quad . \quad . \quad . \quad (7.9)$$

which gives the approximate position of the λ-point. Even if Δ_+ were of the right order of magnitude (e.g. $\Delta_+ \simeq 6 \times 10^{-16}$ ergs) we should have $\Delta_- = 6 + 13 \simeq 20 \times 10^{-16}$ ergs, which is far too great to give an appreciable contribution in the liquid phase. So these fluctuations may appear in the Fermi case only in the neighbourhood of the critical point, as for a classical liquid. The Fermi statistics maintain the liquid in a much more ordered state than do the Bose statistics.

We come now to the evaluation of Δ_+. It is nearly impossible to perform such an evaluation exactly. We may write (7.4) in the form (cf. also (7.1))

$$\Delta_+ \simeq -2\frac{(l_2 - l_1)}{l_1}\frac{3h^2}{8ml_1^2} - \Delta u = -2{\cdot}26\frac{\Delta l}{l_1} - \Delta u. \quad . \quad . \quad (7.10)$$

We have to estimate Δl and Δu. If we suppose that the neighbours of the group of two particles under consideration remain at the same mean positions as before, we may roughly estimate Δl to have an order of magnitude of 0·5 A. We have already seen that the free volume for a single particle is a cube with side of 3 A. Thus the molecules of diameter 2·5 A move in a cube with side of $\sim$5·5 A. We have to subtract from the corresponding value the excluded volume, that is $\frac{4}{3}\pi(2{\cdot}5)^3$ A^3. We so obtain a cube with side 4·7 A from which we have to subtract the diameter 2·5 A to obtain finally the free volume. This gives a cube with side 2·2 A or $\Delta l = 0{\cdot}8$ A. But we have clearly overestimated the effect of the excluded volume, which is counted twice (once for each molecule). If we subtract each time half of the excluded volume we obtain $\Delta l = 0{\cdot}5$ A.

In reality even this should be an overestimation of the effect of the zero point energy because the higher zero point pressure of the group of two molecules will compress the neighbours a little.

The difference Δu may also be estimated. If we admit that the only effect is to increase slightly the attractive part of the Van der Waals forces because the two particles are now on the average at a smaller distance, we obtain $\Delta u = 3 \times 10^{-16}$ ergs. This is again a lower limit because the increase of local density will increase the interactions with neighbouring cells (cf. § 8).

Using these estimates we have for the order of magnitude

$$\Delta_+ \simeq 10 \times 10^{-16} \text{ ergs} \quad . \quad . \quad . \quad . \quad . \quad . \quad (7.11)$$

which would correspond to a λ-point of about 3°K.

So the excitation energy Δ_+ has really the correct order of magnitude.

Before we consider other effects we may observe that exchange effects are automatically included in this description of density fluctuations. The two molecules of these groups are not localized with respect to each other. This accounts for the whole difference between the Bose–Einstein and the Fermi–Dirac case.

Let us now consider briefly how the other striking properties of liquid ^{4}He fit into this description.

First the volume anomaly. Each time a density fluctuation appears a ' hole ' is formed. But this hole interfers with the Van der Waals interactions and is submitted to the zero point pressure of neighbouring particles. So it is not stable and will collapse. In this way a contraction results. However, we have to take account of a second effect which will lower this contraction. A certain number of cells are now doubly occupied. The *mean* zero point pressure, *averaged over all cells*, increases and as a consequence, the mean volume per cell increases. Therefore we have two competing processes. However, it is clear that the second process is a ' second order ' consequence of the density fluctuations and so the first process should be dominating. This is in agreement with rough numerical estimates (Prigogine and Philippot 1953). Now let us

consider the specific heat associated with the λ-point and especially its singularity. The entropy associated with the λ-point appears here as due to a order–disorder process which depends on the type of statistics. Its order of magnitude is correct (about k per particle). But how can we explain the cooperative character of the transitions? The excitation energy depends in this model primarily on the dimensions of the cell. Now we have just seen that the zero point pressure averaged over all cells increases with the fluctuations and also with the mean volume per cell. This in turn decreases the excitation energy and introduces quite directly a cooperative character of the transition. Again the numerical estimates appear to give reasonable results.

We may add a final remark to this section, concerning the influence of nuclear spin. We have been able to introduce a sufficient difference in the excitation energy between Bose particles and Fermi particles without spins using groups of two molecules only. But such a group is not sufficient to introduce the difference between Bose particles and Fermi particles with spin, like real molecules of ^{3}He. Indeed, in this case it would be possible to put both particles in the ground state with opposite spins. This difficulty comes from our consideration of a two-body problem instead of the real N-body problem. So it would be necessary to introduce at least groups of three delocalized molecules. This is quite possible in principle but makes the calculation much more difficult (Prigogine and Philippot 1952). The qualitative conclusions of our model are however not altered.

§ 8. Cell Models for Excitations

We shall now consider very briefly how we may deduce the thermodynamic properties of liquid helium from the considerations of the preceding sections. If we are interested only in the excess properties introduced by the density fluctuations and neglect the contribution of the phonons, we may use the cell model developed for classical liquids in § 2. We may directly use formula (2.2), but it gives now the partition function including the kinetic energy. Also the $\Psi(i\,;\,\phi)$ is now the partition function for i molecules in a volume ϕ. We must then specify a particular cell model (cf. (2.4), (2.5), (2.14)). The simplest cell model which permits us to introduce statistics-dependent density fluctuations is (2.5). This takes account of doubly-occupied cells but introduces an equal number of holes.

We may then use directly (2.7) and (2.8) for the excess entropy and excess specific heat. We have here, neglecting excited one-particle or two-particle states (cf. (7.1), (7.2), (7.4))

$$\Psi(i\,;\,v)=\exp\left\{-\frac{1}{kT}\frac{3h^2}{8ml_1^{\,2}}\right\}, \quad . \quad . \quad . \quad . \quad . \quad (8.1)$$

$$\Psi(2\,;\,v)=\exp\left\{-\frac{2}{kT}\left(\frac{3h^2}{8ml_2^{\,2}}-\Delta u\right)\right\}. \quad . \quad . \quad (8.2)$$

E_0 in (2.2) refers to the 'lattice' energy corresponding to all particles being in the centre of their cells. Using an excitation energy Δ_+ equal to $5{\cdot}5\times10^{-16}$ ergs we obtain the results indicated in fig. 4. The total excess entropy is $R\ln 3\simeq 1{\cdot}1\ R$, which is of the correct order of magnitude.

Fig. 4

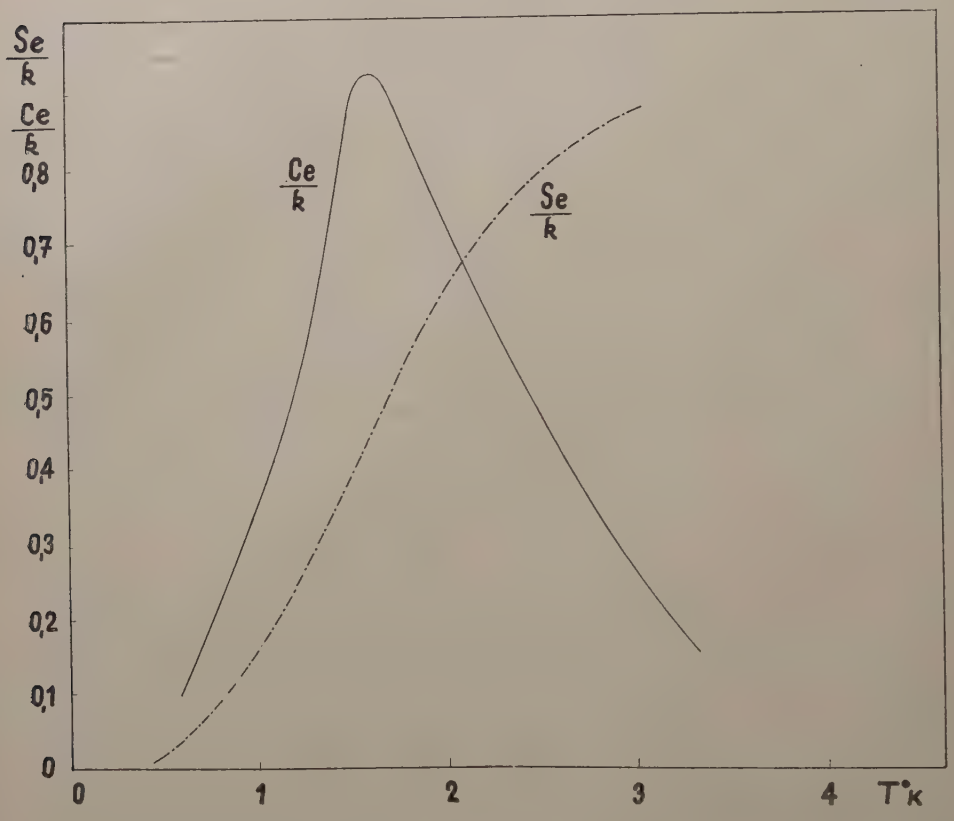

Excess entropy and excess specific heat in the cell model (2.5).

This model, which is extremely simple, does not permit us however to discuss the equation of state and the cooperative character of the transition. The volume simply remains constant, the doubly-occupied cells being compensated by holes. This is the reason why we have performed calculations with a slightly different model (Prigogine and Philippot 1953) in which the number of holes is not supposed to be equal to that of doubly-occupied cells. In this model we take two independent variables (instead of one) for instance, the total number of cells (that is for a given total volume the size per cell) and the number of doubly-occupied cells. Both parameters are fixed by minimum conditions of the free energy. As expected, the number of holes remains much smaller

than the number of doubly-occupied cells, but on the other hand the mean volume per cell increases. This gives the two effects indicated in the preceding section.

We shall not give the details of the calculations which are very elementary. We must mention however that they introduce a certain number of quantities like the volume dependence of the change in Van der Waals interactions when we have fluctuations, which can only be estimated very roughly.

One can only say that the orders of magnitude required to give the experimental effects are consistent with the physical picture which is used.

After the completion of this manuscript the author has seen two very interesting papers which are closely related to the theory we have developed here. The first is a note by Sommers, Keller and Dash (1953) on the heat of mixing of ^{3}He and ^{4}He in which these authors show that the deviation from Raoult law in these solutions is really due to the heat of mixing. This is in complete agreement with our theory, which considers that the excess free energy is due to an excess energy related to the differences in the zero point energy.

The second note we wish to mention briefly is a paper by Dyson (1953) on the dynamics of a disordered linear chain. This paper has many points in common with the method we briefly mentioned in § 6 to treat the ground state of mixture of isotopes. In both methods the mass of a particle is considered as a random variable and the *mean* effects of the frequency distribution are calculated. On the other hand Dyson was able to give exact but only implicit formulae for the mean frequency distribution, while we have used a perturbation approach which seems sufficient for our purpose.

I wish to express my appreciation for the interesting discussions I had during this work with my co-workers, Messrs. Philippot, Bingen. Jeener, Bellemans and Dr. Mazur.

References

Chwoles-Englert, A., 1952, *J. Chem. Phys.*, **20,** 125.
Daunt, J. G., 1952, *Advances in Physics*, **1,** 209.
Daunt, J. G., and Heer, C. V., 1951, *Phys. Rev.*, **81,** 447.
Dingle, R. B., 1952, *Advances in Physics*, **1,** 111.
de Boer, J., 1948, *Physica*, **14,** 139; 1953, *Proceedings International Conference on Theoretical Physics, Tokio.*
de Boer, J., and Lumbeck, R. J., 1949, *Proceedings International Conference on Physics of Very Low Temperatures* (M.I.T.), p. 38.
Dyson, F. J., 1953, *Phys. Rev.*, **92,** 1331.
Feynman, R., 1953, *Phys. Rev.*, **91,** 1291, 1301.
Fröhlich, H., 1937, *Physica*, **4,** 639.
Hoge, H. J., and Arnold, R. D., 1951, *N.B. Standards, J. of Research*, **47,** 63.
Janssens, P., and Prigogine, I., 1950, *Physica*, **16,** 895.
Lennard-Jones, J. E., and Devonshire, A. F., 1937, *Proc. Roy. Soc.* A, **165,** 53; 1938, *Ibid.*, **166,** 1.

London, F., 1953, *Superfluids*, Vol. 2 (New York: John Wiley) (to be published in 1954).
Nagamiya, T., 1940, *Proc. Phys.-Math. Soc., Japan*, **22,** 705.
Pople, J. A., 1951, *Phil. Mag.*, **41,** 459.
Prigogine, I., and Bellemans, A., 1954, *Physica*, **20** (in the press).
Prigogine, I., Bingen, R., and Jeener, J., 1954, *Physica*, **20** (in the press).
Prigogine, I., and Philippot, J., 1952, *Physica*, **18,** 729; 1953 a, *Ibid.*, **19,** 227; 1953 b, *Ibid.*, **19,** 235; 1953 c, *Ibid.*, **19,** 508.
Sommers, H. S., Keller, W. E., and Dash, J. G., 1953, *Phys. Rev.*, **92,** 1345.
Strijland, J. C., 1953, *Thesis*, Amsterdam.
Van Hove, L., 1949, *Physica*, **15,** 951.

The Transition Metals and their Alloys

By W. Hume-Rothery, F.R.S.
The Inorganic Chemistry Laboratory, Oxford
and
B. R. Coles
Department of Physics, Imperial College of Science and Technology, London, S.W.7

CONTENTS

§ 1. Introduction.

§ 2. Some Physical Properties.
- 2.1 Crystal type.
- 2.2 Interatomic distances.
- 2.3 Compressibility.
- 2.4 Coefficients of thermal expansion.
- 2.5 Heats of sublimation.
- 2.6 Melting points.
- 2.7 Magnetic properties.
- 2.8 Summary.

§ 3. The Atomic and Co-valent Radii of the Transition Elements.

§ 4. The Electron Theory of the Transition Metals.
- 4.1 General.
- 4.2 Bloch functions.
  - 4.2.1 The nearly-free electron approximation.
  - 4.2.2 The tight-binding approximation.
  - 4.2.3 The cellular method.
- 4.3 Heitler–London–Heisenberg functions.
- 4.4 Comparison of the methods.
- 4.5 Band models and magnetism.
- 4.6 The origin of the Weiss molecular field.
- 4.7 Band models : cohesion and band widths.
- 4.8 Electrical properties.
- 4.9 Developments of the Pauling hypothesis.

§ 5. Alloys of the Transition Metals.
- 5.1 Solid solutions in transition metals.
- 5.2 Alloys of intermediate composition.
- 5.3 Dilute solid solutions of transition metals in other metals.
- 5.4 Theoretical models for alloys.
  - 5.4.1 The collective electron model.
  - 5.4.2 The localized wave-function model.

§ 6. Alloys of Aluminium with the Transition Metals.
- 6.1 Introductory.
- 6.2 The equilibrium diagrams.
  - 6.2.1 Aluminium–Titanium and Aluminium–Vanadium.
  - 6.2.2 Aluminium–Chromium and Aluminium–Manganese.
  - 6.2.3 Aluminium–Iron.
  - 6.2.4 Aluminium–Cobalt and Aluminium–Nickel.
  - 6.2.5 Aluminium–Copper.
- 6.3 Melting point relations.
- 6.4 Crystal structures and interatomic distances.
- 6.5 Ternary alloys of transition metals with aluminium.
- 6.6 Theoretical discussion.

§ 7. Physical Properties as a Source of Information on Electronic Structures.
- 7.1 Properties of interest.
- 7.2 Band widths and x-ray spectroscopy.
- 7.3 The density of states : specific heats and paramagnetic susceptibilities.
  - 7.3.1 Electrical properties.
- 7.4 Ferromagnetic moments and d-band holes.
- 7.5 Paramagnetic measurements.
  - 7.5.1 Metals and alloys of the second and third transition groups.
  - 7.5.2 Paramagnetic moments in dilute alloys.
- 7.6 Atomic moments from neutron diffraction.
- 7.7 Ferromagnetic alloys of manganese.

Appendices A and B.
References.

§1. Introduction

The transition metals occupy places in the Periodic Table of the Elements where groups of 8 electrons, which acquire a provisional stability in the atoms of the inert gases, expand into groups of 18 electrons by the building up of an $(nd)^{10}$ sub-group. In each Long Period this process begins in Group III A. In the First Long Period the transition process results in the building up of the $(3s)^2(3p)^6(3d)^{10}$ group of 18 electrons. This is the maximum number ($2n^2=18$) of electrons which can occupy the 3-quantum shell, and no further expansion is possible. In the Second Long Period, the transition process builds up a group of 18 4-quantum electrons, and since the 4-quantum shell can contain a maximum of $2\times4^2=32$ electrons, a further expansion can take place by the building up of the $(4f)^{14}$ sub-group. This occurs in the series of elements known as the *rare-earths* or *lanthanons* which lie between lanthanum and hafnium in the Periodic Table. As a result of this, the transition process in the Third Long Period begins in the normal way at lanthanum in Group III A, and is then broken by the building up of the $(4f)^{14}$ sub-group, and resumed at hafnium.

In the Fourth Long Period the transition process is again broken into by the building up of the (5f) sub-group, and it is known that this process occurs in the elements from actinium onwards, although the exact electronic configurations of the free atoms are not yet established conclusively. In the present report we shall not deal with the lanthanons or the actinons.

We may consider first the free atoms of the transition metals. Expressed in terms of the energies of the different electron levels, the transition process means that in potassium the electronic energy levels are in the order $(4s)<(3d)<(4p)$, whereas on reaching copper for which the transition process is complete, the order is $(3d)<(4s)<(4p)$. Increasing atomic number in the elements of the First Long Period thus means a general lowering of the (3d) level relative to the (4s) level, although it is not possible to define the relative positions of the two levels exactly.* In the Second Long Period a similar change takes place in the relative positions of the (4d) and (5s) levels. In the Fourth Long Period, the lanthanons represent the stage at which the (4f) level is moving rapidly down through the (5d) and (6s) levels, whilst the positions of these two levels relative to one another varies in the normal way with increasing atomic number.

In the First Long Period the transition process takes place in such a way that, in the ground state, each atom has two electrons in the (4s) level, except for chromium where the outer electron configuration is $(3d)^5(4s)^1$. This exception is due to the fact that an increased stability is associated with an exactly half filled sub-group, as reflected in the great stability of the Mn^{2+} and Fe^{3+} compounds in which the $(3d)^5$ grouping persists ; the

* The spectral terms will show whether a configuration such as $(3d)^8(4s)^2$ has a higher or lower energy than a configuration $(3d)^9(4s)^1$, but one cannot specify the exact value of any one level. The concept of a general raising or lowering of one level relative to another is of course often quite justifiable.

condition of maximum multiplicity is satisfied, and all 5 electrons have the same spin. In the Second Long Period, the electronic configurations of the ground states of Yt and Zr are analogous to those of Sc and Ti, but from niobium onwards the ground states have only one electron in the (5s) level. This means that, when compared with the (3d) and (4s) levels of the First Long Period, the (4d) levels in the Second Long Period are in general relatively lower compared with the (5s) level. This is reflected in the fact that the $(4d)^{10}$ completely filled sub-group is more stable than the $(3d)^{10}$ sub-group in the preceding Period. Thus palladium has the ground state $(4d)^{10}(5s)^0$, whilst for nickel the ground state is $(3d)^8(4s)^2$; and silver with ground state $(4d)^{10}(5s)^1$ is predominantly univalent, whilst copper gives rise to stable divalent compounds in which one electron is removed from the $(3d)^{10}$ sub-group. The difference between the elements of the First and Second Long Periods is reflected in the optical and magnetic properties of the solid metals, as well as in their specific heats at low temperatures, and in their behaviour in alloys. The increased stability of the $(4d)^{10}$ sub-group is accompanied by a less marked stability of the exactly half-filled $(4d)^5$ sub-group.

In the Third Long Period, the transition process, both before and after the intervention of the Rare Earths, takes place so that the ground states of the atoms contain two electrons in the (6s) levels, and the behaviour thus resembles that in the First Long Period, except that the added stability of the half-filled $(5d)^5$ sub-group is less pronounced, and for tungsten the ground state is $(5d)^4(6s)^2$, in contrast to the ground state $(3d)^5(4s)^1$ of chromium. Gold gives rise to stable trivalent compounds in which two electrons are removed from the $(5d)^{10}$ sub-group, and this grouping is less stable than the $(3d)^{10}$ sub-group, and very much less stable than the $(4d)^{10}$ sub-group. These relative stabilities of the $(nd)^{10}$ sub-groups are reflected in the spectroscopy of the ions; their ionization potentials are Cu^+ 20·2 v, Ag^+ 21·37 v and Au^+ 20·35 v, and the energies of their first excited states (d^9s) are Cu^+ 2·7 v, Ag^+ 4·8 v, Au^+ 1·86 v.

The transition elements exert variable valencies in chemical compounds, and in Groups VI, VII and VIII A, B, C, there is a general tendency towards higher valencies in the later Periods. Thus the predominant valencies of iron, cobalt, and nickel are 3 and 2 with increasing stability of the lower valency on passing from Fe→Co→Ni. In the Third Long Period, osmium exhibits an array of high valencies, and there is a marked decrease in the predominant valency on passing from Os→Ir→Pt, the chief valencies of the last element being 4 and 2. The tendency to favour higher valencies with increasing number of the Period is reflected in the physical properties of the elements, and is of great importance in understanding their alloys.

If we imagine the free atoms of a transition element to be compressed until they form a solid metal, the general effect is that, at the interatomic distances found in metallic crystals, the energy levels of the ns, np, and (n−1)d states of the free atoms have broadened into overlapping bands. The electrons are thus in hybrid (spd) states, the proportions of the three

components varying with the position in the Period. Thus in potassium, the one outer electron* per atom may be regarded as in a nearly pure s state. In calcium the approximate methods of Manning and Krutter (1937) indicate a slight overlap of 4s and 3d states, and on proceeding to scandium and titanium the proportions of the d function increase, but the exact condition is not yet understood. According to Pauling (1938), all the transition elements involve (spd) bonding in the metallic crystals, although other investigators (e.g. Mott and Jones 1936), have assumed that only s and d functions need be considered for the elements of Group VIII. The existence of undoubted (spd) bonding in chemical compounds of the transition elements (involving approximately the same atomic radii as those in metallic crystals) makes it probable that Pauling's view is correct. If we regard the sharp energy levels of the free atoms as giving rise to hybrid electron bands in the solid metals, the passage along one of the Long Periods, e.g. Ti→V→Cr→Mn . . . results in an increase in the admixture of d-function in the lower energy portion of the band and a decrease in the higher energy portion. When Group II B is reached (Zn, Cd, Hg) the electrons in states derived from d functions have become almost purely atomic, and the cohesion is the result of electrons in states derived from s and p functions.

The overlapping of electron bands referred to above creates difficulty in defining exactly what is meant by a transition metal in the solid state. In the free atoms we can distinguish clearly between those with empty or partly filled d levels. In the solid metals, the overlapping of the ns and (n—1)d bands may begin in Group II A, but few people would call calcium a transition metal. If we deal with the Second Long Period, it is probably correct to say that in the earlier members Rb → Sr → Yt → Zr → Nb, we have elements in which all of the outer electrons are bonding electrons which hold together the Rb^{+}, Sr^{2+}, Yt^{3+} . . . . ions. As will be appreciated from the next section there is a critical stage in the region of Group VI, and it is probable that here some or all of the d-wave functions become much more associated with individual atoms, and from this point of view it may be said that the transition process begins at about Group VI or VII in the Second and Third Long Periods ; in the First Long Period (see p. 171) the critical stage may be at Group V. The theory of these metals is a matter of controversy, and we shall therefore describe first some of the physical properties with which a successful theory must deal.

§2. Some Physical Properties

In crystals of the transition metals, the atoms are held together by the shared electrons, whose interactions are discussed in §4. Although central forces are not present, it is often convenient to regard the atoms as held together by attractive forces, and to use expressions such as

* For convenience we use the term ' outer electrons ' to describe the s and d electrons outside the inert gas shell.

' strength of bonding ', ' atomic cohesion ', etc. The definition of these is not always made clear, and confusion often exists between what are really measurements of different quantities. We may on the one hand measure the work required to produce a small displacement of the atoms from the equilibrium distance. The compressibility of a metal is a measure of the ease with which the atoms can be squeezed together under hydrostatic pressure, and since the process is reversible a low compressibility means that it is difficult to pull the atoms apart, and is thus an indication of strong bonding, in the usual sense of the term. A low coefficient of expansion means a strong resistance to increasing amplitude of thermal vibration, and thus also indicates strong bonding. We may expect increase in the strength of bonding to be accompanied by a decrease in the atomic distance provided that other changes do not intervene ; such changes may be an increase in the quantum number of the electrons concerned, or the building up of a new group of electrons. It will be noted that the above quantities refer to the solid phase alone. In a general way a high melting point indicates strong bonding in the solid, but as the melting point is by definition the temperature at which the solid and liquid phases are in equilibrium, it is not so suitable a property because, if some factor lowers the free energy of the liquid phase, the melting point may fall, even though the bonding forces in the solid are strong.

The latent heat of sublimation, or cohesive (or binding) energy, is the measure of the work required to remove an atom from the solid to the gaseous state, and is a definite physical quantity of great interest. High binding energies are generally accompanied by low compressibilities but the binding energy bears no simple relation to the work required to produce a small displacement of the atoms from their equilibrium positions in the solid. Different energy states of the atoms may cross one another in going from the solid to the free atom, but the compressibility is a characteristic only of that state which has lowest energy in the solid.

In the succeeding sections we shall consider some of the physical properties of interest in attempting to understand the nature of the transition metals.

2.1. *Crystal Type*

In the transition metals, polymorphism is common, but all the elements of all the Long Periods crystallize in one or more of the three typical metallic structures (f.c. cube, b.c. cube, c.p. hexagonal). The data are summarized in fig. 1, from which it will be seen that abnormal complicated structures are found only in Groups VI A and VII A (α Mn, β Mn, β W, α U, β U). These Groups appear to occupy a critical position in the Periodic Table, and that this effect is electronic in origin is suggested by the fact that the structure of βU is of the σ type which is found in alloys such as V–Ni, Cr–Co, Cr–Fe, Cr–Mn in which (except for Cr–Mn) one element lies to the left and the other to the right of Group VII.

Fig. 1

K ○	Ca ○ ⟨⎯⟩ □	Sc □ * ⟨⎯⟩	Ti ○ ⟨⎯⟩	V ○	Cr ○	Mn δ ○ γ □ β Complex α Complex	Fe δ ○ γ □ α ○	Co β □ α ⟨⎯⟩	Ni □	Cu □
Rb ○	Sr ○ ⟨⎯⟩ □	Y ⟨⎯⟩	Zr ○ ⟨⎯⟩	Nb ○	Mo ○	Tc ⟨⎯⟩	Ru ⟨⎯⟩	Rh □	Pd □	Ag □
Cs ○	Ba ○	La β □ α ⟨⎯⟩	Hf ○ ? † ⟨⎯⟩	Ta ○	W α ○ β Complex	Re ⟨⎯⟩	Os ⟨⎯⟩	Ir □	Pt □	Au □
			Th □	Pa B.c. tetragonal	U γ ○ β Complex α Complex					

The crystal structures of the transition metals.

○=B.c. Cube ; □=F.c. Cube ; ⟨⎯⟩=C.p. Hex. In all cases, the allotropic forms are shown in the order of the temperature ranges in which they are stable, the form stable at the highest temperature being at the top.

* It is not known which allotrope is stable at the higher temperature.

† Hf is known to undergo a transformation, and work on alloys suggests that the high-temperature form is body-centred cubic,

When an element crystallizes in the b.c. cubic as well as some other structure, the b.c. cubic modification is the one stable at the highest temperature (Ti, Zr, Mn, Fe). Iron is unique in having a body-centred cubic structure at both high and low temperatures, with a face-centred cubic structure stable over an intermediate range. This is thought to be due to the contribution of an electronic specific heat term (see Seitz 1940).

It will be noted that the axial ratios of the close-packed hexagonal metals are always less than that ($c/a=\sqrt{(8/3)}=1{\cdot}633$) corresponding to

Fig. 2

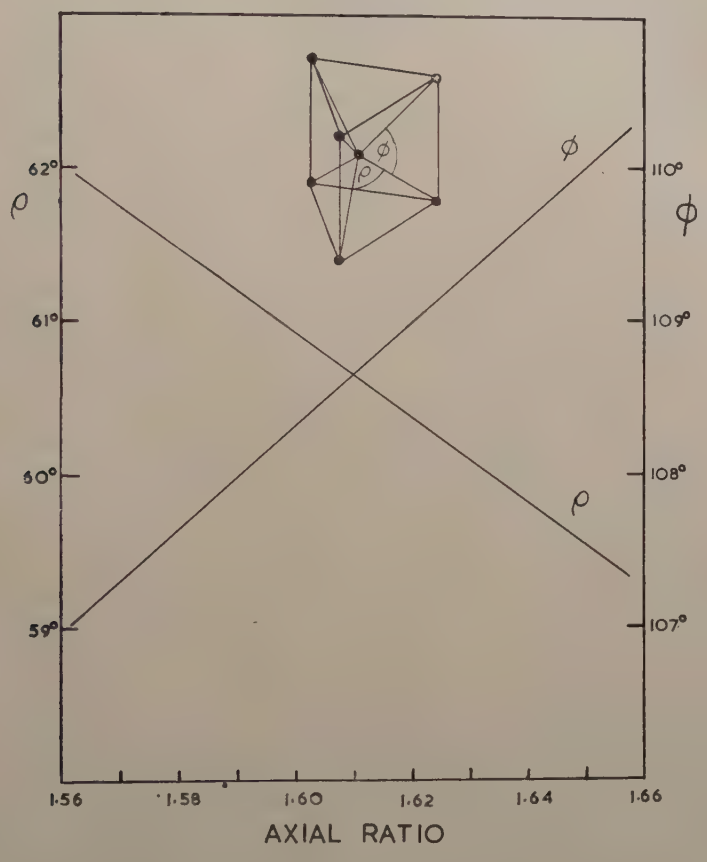

close-packed spheres. For cobalt ($c/a=1{\cdot}623$) the difference is not very great, but for titanium (1·587) and zirconium (1·592) in Group IV A, and for ruthenium (1·582) and osmium (1·579) in Group VIII A, the difference is appreciable, and the closest distances of approach (d_1) to a given atom are not those of its neighbours in the basal plane, but are to the six neighbours, three in the plane above and three in that below, which occupy the corners of a trigonal prism. Figure 2 shows the effect of this variation on the bond angles, ϕ and ρ.

2.2. *Interatomic Distances*

Other things being equal we may expect a small interatomic distance to indicate strong bonding. We may use the term *atomic diameter* to denote the closest distance of approach of the atoms in the crystals of the elements. In the First, Second, and Third Long Periods there is a progressive fall in the atomic diameter* on passing from Group I to Group VI, after which an abrupt change occurs, and the details for the Periods are not the same. In the First Long Period, the abnormal structures of α-Mn and β-Mn contain a few distances of approach† smaller than those in chromium, although the average distance of an atom from its close neighbours is greater, and in the normal structures of γ-Mn and δ-Mn the atomic diameters (*ca.* 2·6 kx) are greater than those

Fig. 3. Atomic Diameters

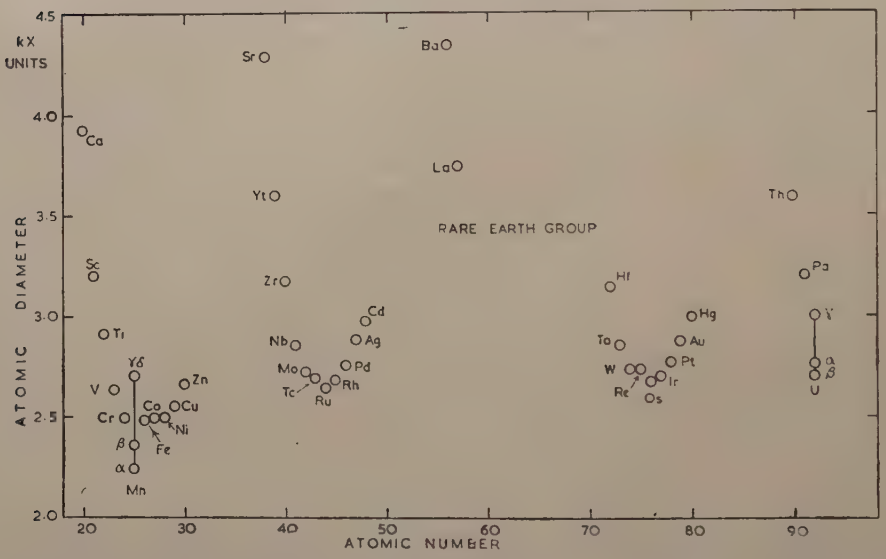

for the preceding element chromium (2·5 kx), and for the following elements iron, cobalt, and nickel, all of which have nearly the same atomic diameter (2·5 kx) (see fig. 3). In the *Second Long Period* the atomic diameters continue to diminish slightly on passing from Mo (2·72 kx) → Tc (2·71 kx) → Ru (2·64 kx) and then show a distinct increase on passing to Rh (2·68 kx) → Pd (2·75 kx), and in the *Third Long Period* there is again a minimum in Group VIII A W (2·74 kx) → Re (2·73 kx) → Os (2·67 kx) → Ir (2·71 kx) → Pt (2·77 kx). The atomic diameters of the elements at the end of the Second and Third Transition Series thus follow different principles from those in the First.

* This statement applies also if attempts are made to correct the atomic diameters to refer to a standard co-ordination number 12.

† In α Mn and β Mn the closest distances of approach are 2·24 kx and 2·38 kx respectively.

2.3. *Compressibility*

A low value of the compressibility means that it is difficult to squeeze the atoms closer together, and since the process is reversible a low compressibility means that it is difficult to pull them apart, and hence indicates strong bonding. In the First, Second, and Third Long Periods there is a rapid fall in compressibility on passing from Group I → Group V.* In the Second and Third Long Periods, the compressibilities continue to diminish and reach minimum values at ruthenium and iridium respectively. In the First Long Period the compressibility of α-manganese is anomalous, as is to be expected from its abnormal crystal structure, but otherwise there is little change on passing from V → Cr → Fe → Co → Ni, and the minimum value is reached at the end of the transition series. This characteristic of the First Long Period is illustrated in fig. 4 which shows clearly how the compressibilities of chromium and iron are much higher than would be expected from the values for corresponding elements in the later Periods.

Fig. 4. Compressibilities

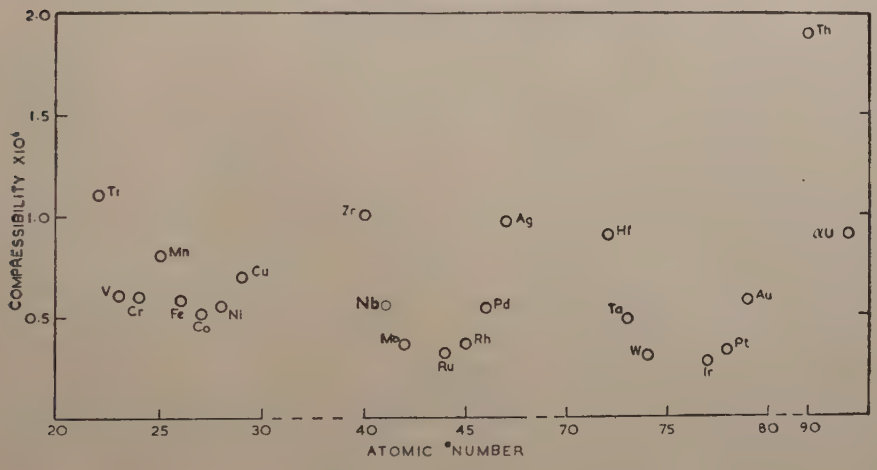

2.4. *Coefficients of Thermal Expansion*

A low coefficient of expansion means a strong resistance to increasing amplitude of thermal vibration, and is thus an indication of strong bonding. In so far as they have been determined, the coefficients of expansion of the transition metals follow the same general sequence as the compressibilities, although minor differences exist (see fig. 5). Unfortunately the data are not too well established.

A point of considerable theoretical interest is that, in the close-packed hexagonal metals, zirconium, ruthenium and osmium, the coefficients of expansion in the direction of the hexagonal axes are greater than those in the perpendicular directions, in spite of the fact that the axial ratio is less than that for close-packed spheres. These coefficients of expansion† have

* The data for vanadium refer to very impure metal.

† The data for zirconium are by Skinner and Johnston (1953).

been determined by the careful x-ray work of Owen and Roberts (1937), and they show that the coefficient of expansion in the direction of closest approach is greater than that in the direction of the somewhat larger distances of approach in the basal planes.

Table 1. Coefficients of Thermal Expansion at 50°C $\times 10^6$

Metal	Axial ratio	$\alpha_{\parallel}$	$\alpha_{\perp}$
Zr*	1·592	10·8	5·5
Ru	1·5835	8·8	5·9
Os	1·5790	5·8	4·0

* Mean values between 298° and 1143°K.

Fig. 5. Coefficients of Expansion

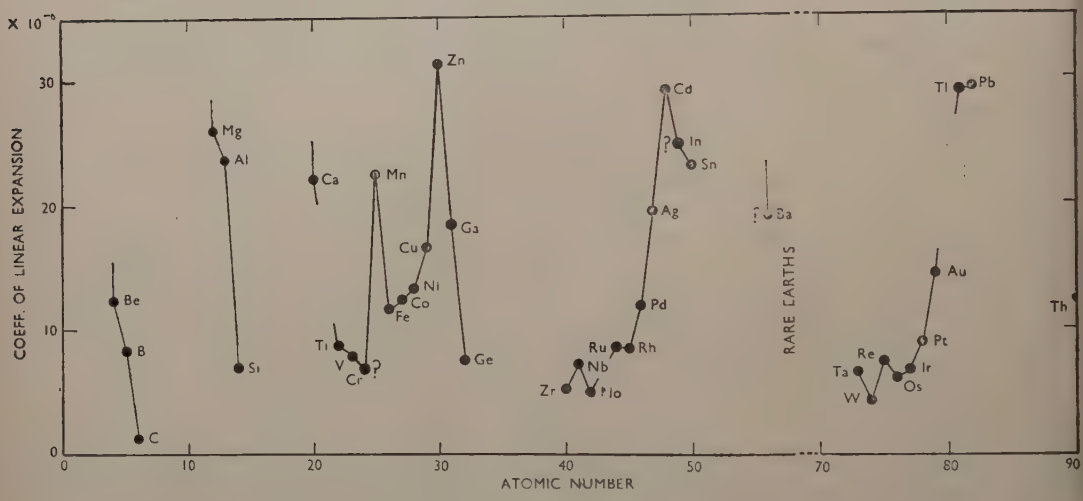

2.5. *Heats of Sublimation*

The heat of sublimation of a metal is a definite physical constant expressing the difference in energy of the solid and gaseous states. In a general way it is a measure of the strength of atomic bonding in the solid, but it should not be used uncritically for this purpose. The values observed depend on the particular atomic states in the different vapour phases, and the results for different elements are not necessarily strictly comparable. Apart from this, as explained in the introduction to this section, the heat of sublimation is not a direct indication of the character of the bonding between atoms at equilibrium in the solid.

Recent values for the heats of sublimation of all the elements of the First Transition Series are available, mainly from the work of Johnston and his co-workers (Johnston *et al.* 1950, 1951, 1952, 1953), who have also

made determinations for some other elements. Further values are given in the earlier critical surveys of Kelley (1935, 1946), but as these are drawn from many sources the accuracy is very variable, and the originals should be consulted.

The data from these sources are summarized in fig. 6 and are of great interest. In the Second and Third Long Periods the values rise continually on passing from Group I A to Group VI A. In the First Long Period, the maximum is at vanadium, and there is then a fall on passing to chromium and manganese, with a recovery to iron, cobalt and nickel, for which the values are nearly equal. The value for platinum shows stronger bonding than that for nickel, in agreement with the data of figs. 4 and 5. The

Fig. 6

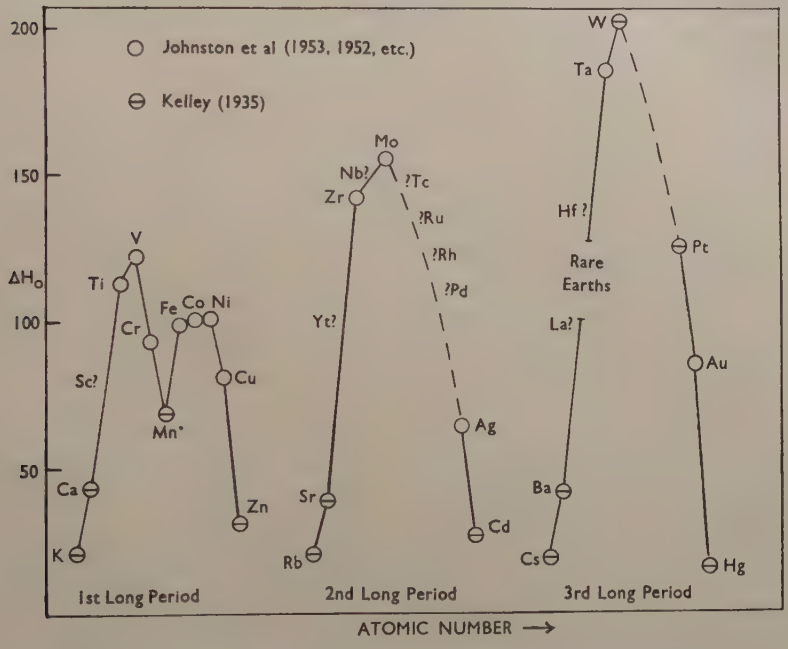

Heats of Sublimation at 0°K (ΔH_0). K cals. per g mol.

*The differences between the values for the different forms of manganese are very small.

relatively high values for copper and gold suggest that the d electrons are still contributing to the cohesion in the solids, and if it is assumed that zinc, cadmium, and mercury are divalent metals, the relative positions of the points for (Ni, Cu, Zn), (Ag, Cd), and (Pt, Au, Hg) suggest that the d shell contribution is relatively less in silver, in agreement with conclusions from figs. 4 and 5.

2.6. *Melting Points*

In a general way strong bonding is accompanied by high melting point, but the property is not always satisfactory because, by definition, the

melting point is the temperature at which solid and liquid phases are in equilibrium, and consequently involves the free energies of both phases (see p. 153).

Fig. 7. Melting Points

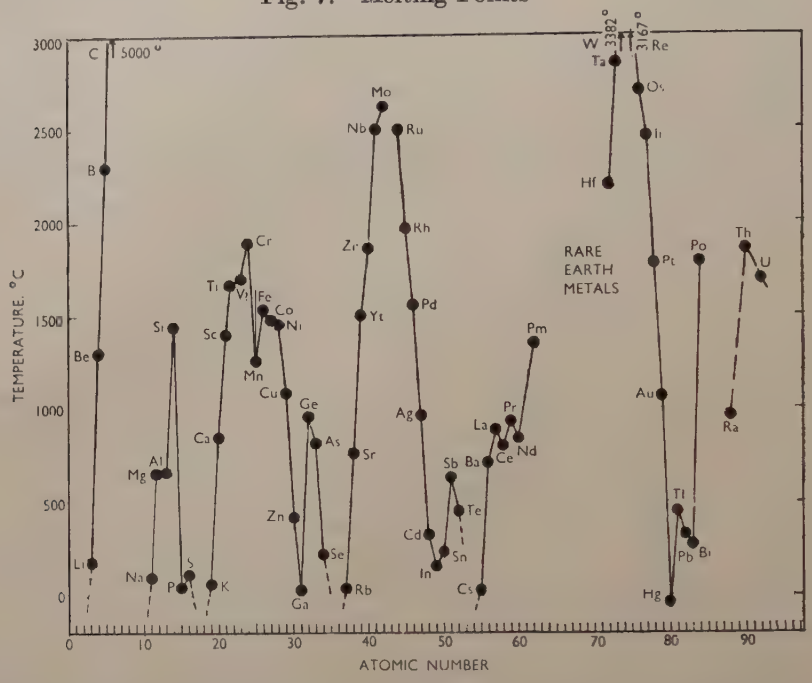

In the Second and Third Long Periods the melting points rise to high maxima in Group VI (Mo and W), and on passing through Groups VII and VIII, the melting points fall rapidly. In the First Long Period, the behaviour is quite different. The melting points rise rapidly on passing from K→Ca→Sc→Ti (1660°C). The value for vanadium is uncertain whilst that for chromium (1860°C) is only 200°C higher than that for titanium, whereas the difference between the melting points of zirconium and molybdenum, and of hafnium and tungsten are of the order 800°C and 1200°C respectively. On passing from chromium (1860°C) to manganese (1245°C) there is a marked fall in melting point, and then a rise to iron (1534°C), cobalt (1493°C), and nickel (1453°C). The difference between the melting points of iron and nickel is thus only about 80°C, and may be contrasted with a difference of about 900°C between the melting points of osmium and platinum. The difference between the melting points of chromium and nickel (207°C) is less than $\frac{1}{8}$ of that between the values for tungsten and platinum.

2.7. *Magnetic Properties*

The First Long Period is characterized by the appearance of ferromagnetism in iron, nickel, and cobalt. Manganese itself is not ferromagnetic, but ferromagnetism is shown by manganese nitride, and by

alloys of the Heusler type (Cu_2MnAl, Cu_2MnSn, Cu_2MnIn), as well as in compounds with arsenic, antimony, and bismuth. In all of these the distances between the manganese atoms are greater than in the element. Some compounds of chromium are also ferromagnetic.

Ferromagnetism is not shown in the transition metals of the later Periods, although, among the Rare Earths, gadolinium and dysprosium are ferromagnetic at low temperatures, and many of the Rare Earth metals are strongly paramagnetic. The majority of the transition metals are weakly paramagnetic (mass susceptibilities of the order 0 to 2×10^{-6}), although chromium ($\chi=3\times10^{-6}$) and manganese ($\chi=11\times10^{-6}$) are more strongly paramagnetic.

In the ferromagnetic elements, the saturation moments at the absolute zero enable the number of unpaired electron spins to be determined, and the numerical values in Bohr magnetons per atom (μ_B) are :

Fe $2{\cdot}2\,\mu_B$

Co $1{\cdot}71\,\mu_B$

Ni $0{\cdot}6\,\mu_B$

The maximum saturation moment for alloys of this group of elements is $2{\cdot}44\,\mu_B$ in an iron–cobalt alloy containing 35 atomic per cent of cobalt. These non-integral values mean that the crystal structures are not arrays of atoms, each in the same electronic state, and the theoretical interpretation of this is discussed later. We may note here that methods of neutron diffraction have disproved the suggestion that ferromagnetic iron involves the long range order of interpenetrating lattices of magnetic and non-magnetic atoms.

There is a marked difference between the ferromagnetism of iron on the one hand, and of cobalt and nickel on the other. When elements are dissolved in α-iron to form substitutional solid solutions, the saturation moment is generally reduced by $2{\cdot}22\,\mu_B$ for each atomic substitution. Exceptions are shown by the elements immediately adjacent to iron in the Periodic Table (Mn, Co, Ni) which increase the saturation moment when dissolved in iron, but apart from these, the general effect of the formation of a solid solution is as though the ferromagnetic lattice of iron were being diluted by non-magnetic atoms. In contrast to this, when elements of well-defined valency (e.g. Cu, Zn, Al) are dissolved in nickel, the saturation moment is reduced by $v\,\mu_B$ per atomic substitution, where v is the valency of the solute. The behaviour of solid solutions in cobalt resembles that for nickel, although the data are not so well established. The saturation moments of nickel and cobalt are raised by the solution of some adjacent elements, as in the case of the iron alloys referred to above, and in systems such as Fe–Co and Fe–Ni each metal raises the saturation moment of the other. These effects have been dealt with in detail in the review by Stoner (1947).

As explained later, some theories suggest that certain of the transition metals are antiferromagnetics, and in particular that the body-centred

cubic metals of Groups V A and VI A involve antiferromagnetic superlattices of the caesium chloride type with the corners and centres of the unit cubes occupied by atoms of opposite spin. The methods of neutron diffraction used by Shull *et al.* (1951, 1953) have produced entirely negative results for vanadium. For chromium at low temperatures a weak superlattice line was observed. The results may be taken to disprove any suggestion that, at room or high temperatures the structures of these elements are stabilized by long-range antiferromagnetic order involving high spins. It has been pointed out that the negative experimental results do not necessarily disprove the existence of moments on individual atoms, because they could be reconciled with the presence of short-range order, or might be the result of resonance between different configurations.

2.8. *Summary*

Omitting the complications introduced by the Rare Earths and the Actinides, the physical properties described above lead to the following conclusions :—

(*a*) In all of the first three Long Periods there is an increase in the strength of the bonding in the solid metals on passing from Group I A to Group IV A.

(*b*) In the First Long Period the strength of bonding shows comparatively little increase after Groups IV A (titanium) and V A (vanadium). The atomic diameter continues to decrease on passing to Group VI A (chromium), but there is relatively little difference between the compressibilities, or coefficients of expansion of vanadium and chromium. On passing to manganese there is a clear decrease in the strength of bonding, followed by an increase on passing to iron, cobalt and nickel, for which the values in figs. 2–6 are very similar. On proceeding to copper in Group I B there is a weakening in the strength of the bonding as indicated by all the physical properties, but when compared with zinc, the bonding in copper is so very much stronger that we may reasonably conclude that the 3d electrons are in some way contributing to the cohesion in copper.

(*c*) In contrast to this behaviour of the elements in the First Long Period, the later Periods show bonding which continues to increase in strength on passing from Group IV A→VI A. The different physical properties are not in complete agreement as to where the maximum strength of bonding occurs. Thus the compressibilities and interatomic distances show minimum values at the beginning of Group VIII, whilst the coefficients of expansion and melting points indicate a weakening of the cohesion after Group VI A.

(*d*) The physical properties suggest that after Group IV A, the strength of the cohesion in any one Group increases rapidly on passing from the First→Second→Third Long Period. This change is in the opposite direction from the normal effect of increasing atomic number in elements of well-defined valency ; thus in Groups I A, II A and II B the strength of bonding decreases with increasing atomic number.

(*e*) The physical properties suggest that on passing through Group VIII, the decrease in bonding is more pronounced in the later Periods. On passing from Ru→Rh→Pd there is a considerable increase in atomic diameter, coefficient of expansion and compressibility, and a marked fall in melting point ; all these changes are much greater than those in the sequence Fe→Co→Ni.

(*f*) The changes in physical properties on passing from Pd→Ag indicate a much greater weakening in the bonding than in the corresponding changes from Ni→Cu or Pt→Au.

(*g*) Considered empirically, there is a clear correspondence between the effects described in (*b*), (*c*), (*d*), (*e*) and (*f*) above, and the predominant valencies in the chemistry of the elements of Groups VI A→I B. It is well known that in these Groups, the predominant valencies in the members of any one Group increase with increasing atomic number, and this runs parallel to the effects in (*d*) above. On passing through Group VIII, the chief valencies of iron, cobalt and nickel are 3 and 2 and there is a slight increase in the preponderance of the divalent state on passing from Fe→Co→Ni. In contrast to this, osmium exhibits many high valencies, and there is a relatively rapid decrease in the predominant valency on passing from Os→Ir→Pt. This effect is clearly parallel to that described in (*e*) above. In Group I B, silver is almost exclusively univalent, whilst copper and gold also show valencies of 2 and 3 respectively, in which electrons are removed from the d shell, and this effect is parallel to that in (*f*) above which suggests clearly that in silver the d electrons of the ion are contributing relatively less to the cohesion than in copper of gold.

§ 3. The Atomic and Co-valent Radii of the Transition Elements

Although acute differences of opinion exist about the details and the mathematical treatment, there is general agreement that the cohesive forces in metals and alloys are closely related to those in co-valent bonds.

We may define the *atomic radius* as one half of the closest distance of approach of the atoms in the crystal of the face-centred and body-centred cubic metals. For the close-packed hexagonal metals whose axial ratio is usually slightly less than that (1·633) for close-packed spheres, we take the atomic radius to be $\frac{1}{4}(d_1+d_2)$, where d_1 and d_2 are the two close distances of approach. This procedure* is arbitrary, but can at the worst introduce an error of about 0·015 kx for the atomic radii.

Table 2 shows the atomic radii for the transition elements to two places of decimals in kx units—to this degree of accuracy these are the same as Angstrom units. For many purposes it is desirable to reduce the atomic radii to refer to the same co-ordination number, and the co-ordination No. 12 is usually taken as standard. For the b.c. cube it seems preferable

* With two sets of neighbours, any definition is to some extent arbitrary.

Table 2 (*a*)

Element	A.R.	A.R. C.N. 12	Pauling single bond radius	Empirical co-valent radius	Univalent ionic radius
Sc	1·60 □	1·60	1·44	—	1·06 (3+)
Ti	1·46 △	1·46	1·32	1·36 ⊙ IV	0·96 (4+)
V	1·31 ⊡	1·35	1·22	1·3 ?	0·88 (5+)
Cr	1·25 ⊡	1·28	1·17*	1·3 ?	0·81 (6+)
Mn	1·35 ⊡	1·35	1·17*	1·2–1·3 ?	—
Fe	1·24 ⊡	1·28	1·16*	1·20 ⊙ IV	1·3 ? (−2)
Co	1·25 □ △	1·25	1·16*	1·22 ⊙ III 1·32 ⊙ II	1·2 ? (−1)
Ni	1·24 □	1·24	1·15*	1·22 ⊙ IV 1·30 ⊙ III 1·39 ⊙ II 1·42 ● II	1·05 ? (0)
Cu	1·275 □	1·275	1·17*	1·35 ● I	0·96 (1+)

□ F.c. Cube. △ C.p. Hex. ⊡ B.c. Cube.

⊙ Octahedral radii, ● Tetrahedral radii; the Roman numerals giving the valency state.

For the ionic radii, the numbers in brackets give the charge on the ion. Thus Co (−1) means the ion with the $(3d)^{10}$ group.

* These values involve the high valencies of the Pauling scheme, and are in our opinion doubtful.

Table 2 (*b*)

Element	A.R.	A.R. C.N. 12	Pauling single bond radius	Empirical co-valent radius	Univalent ionic radius
Y	1·81 △	1·81	1·62	—	1·20 (3+)
Zr	1·60 △	1·60	1·45	1·48 IV	1·09 (4+)
Nb	1·43 ⊡	1·47	1·34	—	1·00 (5+)
Mo	1·36 ⊡	1·40	1·29	—	0·93 (6+)
Tc	1·35(5) △	1·36	1·27	—	—
Ru	1·34 △	1·34	1·24	1·33 ⊙ II	—
Rh	1·34 □	1·34	1·25*	1·32 ⊙ III	1·6 ? (−1)
Pd	1·37 □	1·37	1·28*	1·31 ⊙ IV	1·4 ? (0)
Ag	1·44 □	1·44	1·34*	1·53 ● I	1·26 (1+)

□ F.c. Cube. △ C.p. Hex. ⊡ B.c. Cube.

⊙ Octahedral radii, ● Tetrahedral radii; the Roman numerals giving the valency state.

For the ionic radii, the numbers in brackets give the charge on the ion. Thus Rh (−1) means the ion with the $(4d)^{10}$ group.

* These figures involve the high valencies of the Pauling scheme, and are in our opinion doubtful, especially for Pd and Ag.

Table 2 (*c*)

Element	A.R.	A.R. C.N. 12	Pauling single bond radius	Empirical co-valent radius	Univalent ionic radius
La	1·87 □	1·87	1·69	—	1·49 (3+)
Hf	1·58 △	1·58	1·44	—	—
Ta	1·43 ⊡	1·47	1·34	—	—
W	1·37 ⊡	1·41	1·30	—	—
Re	1·37 △	1·37	1·28	—	—
Os	1·37(5) △	1·37	1·25(5)	1·33 ⊙ II	1·8 ? (2−)
Ir	1·35 □	1·35	1·26*	1·32 ⊙ III	1·6 ? (1−)
Pt	1·38 □	1·38	1·29*	1·31 ⊙ IV	1·5 ? (0)
Au	1·44 □	1·44	1·34*	1·50 ●	1·37 (1+)
				1·40 ⊙ IV	

□ F.c. Cube. △ C.p. Hex. ⊡ B.c. Cube.
⊙ Octahedral radii, ● Tetrahedral radii; the Roman numerals giving the valency state.
For the ionic radii, the numbers in brackets give the charge on the ion. Thus Ir (−1) means the ion with the $(5d)^{10}$ group.
* These figures involve the high valencies of the Pauling scheme, and are in our opinion doubtful, especially for Pt and Au.

Notes to tables 2 (*a*), (*b*) *and* (*c*).—In these tables the first column gives the symbol for the element, and the second column the atomic radius as defined by the closest distance of approach in the crystals of the body-centred cubic and face-centred cubic metals. For the close-packed-hexagonal metals the atomic radius is assumed to be equal to $\frac{1}{4}(d_1+d_2)$, where d_1 and d_2 are the two close distances of approach. The third column shows the atomic radius for co-ordination No. 12, and this is obtained by using the Goldschmidt factor of 3% contraction on passing from [12] → [8]. The fourth column shows the Pauling single-bond radius and the figures are taken from the original paper (*J. Amer. Chem. Soc.*, 1947, **69**, 542). The * symbols indicate the elements for which, in our opinion, the high valencies assumed make the values doubtful. The fifth column shows the empirical octahedral d^2sp^3 and tetrahedral sp^3 radii taken from Pauling's book, *The Nature of the Co-Valent Bond*. The final column gives the univalent ionic radius of Pauling (see *The Nature of the Chemical Bond*, p. 326). These values are a rough indication of the relative sizes of the ions concerned, but their nature must be clearly understood. The univalent ionic radius of, say, calcium does not mean the radius of a Ca^+ ion, but is that of a Ca^{2+} ion on the assumption that this is present in a crystal where the interionic forces are those between univalent ions. The values given by Pauling for sequences such as $Ge^{4+} \rightarrow Ga^{3+} \rightarrow Zn^{2+} \rightarrow Cu^{1+}$ have been extrapolated to give approximate values for the preceding elements, e.g. Ni^0, Co^-, Fe^{2-}.

to use the empirical correction factor of Goldschmidt, who regarded the co-ordination No. as 8, and deduced

$$[12] \rightarrow [8] = 3\% \text{ contraction.}$$

For the atomic radii of 1·25 kx (Fe) and 1·8 kx (Th) the contractions are 0·038 and 0·054 kx respectively. According to the Pauling equation

(see p. 168) this contraction is a constant equal to 0·053 kx, if the co-ordination number of the b.c. cube is taken to be 8, and is a variable if varying degrees of bonding to second closest neighbours are considered. As shown below, the Pauling equation may be erroneous for metals, and we think that the Goldschmidt correction term is to be preferred (see p. 238). Table 2 also contains values for the Single Bond Radii of Pauling, the empirical co-valent radii for some elements, and some of the univalent ionic radii of Pauling.

The atomic radii show the same variation as the atomic diameters described in § 2, except that for the close-packed hexagonal structures, the definition of atomic radius as $\frac{1}{4}(d_1+d_2)$ results in the minimum values occurring in Group VIII B (rhodium and iridium) in the Second and Third Long Periods, whereas if the atomic diameter is defined as the closest distance of approach of the atoms, the minimum values are in Group VIII A (ruthenium and osmium).

The empirical co-valent radii show little change on passing through Group VIII, and the differences between the values for Ti and Fe, and for Zr and Ru are comparatively small, so that in general the empirical co-valent radii do not vary greatly on passing through the transition metals of any one Long Period. The Pauling single bond radii show a slightly greater increase and are uniformly smaller than the empirical co-valent radii.

The univalent ionic radii for the elements at the beginning of a Long Period show a rapid shrinkage on passing through a sequence such as $K \rightarrow Ca^{2+} \rightarrow Sc^{3+} \rightarrow Ti^{4+}$, indicating that the electron cloud of the outer group of 8 electrons contracts rapidly with increasing atomic number. At the end of the Transition Series the values given by Pauling for a sequence such as $Cu^{+} \rightarrow Zn^{2+} \rightarrow Ga^{3+} \rightarrow Ge^{4+}$ enable us to obtain a rough indication of the univalent ionic radii of the $(nd)^{10}$ ions of the preceding elements (e.g. Ni^{0}, Co^{-1}, Fe^{-2}), and these are of interest in connection with theories of alloys which assume negative valencies for these elements.

In the accepted theory of a co-valent diatomic molecule A—A, the wave-function is of the form

$$a\psi_{A-A}+b\psi_{A^+A^-}+b\psi_{A^-A^+}. \quad \ldots\ldots (1)$$

The last two terms represent the resonance contribution of the ionized states, and this is generally small (e.g. 5% of the bond energy for the H_2 molecule). In a symmetrical single bond of this type, each atom contributes one electron, and these are shared equally between the two atoms, giving what Pauling calls a normal co-valent bond, although such bonds are not purely co-valent because they contain contributions from the ionized states. In an actual co-valent bond between two unlike atoms A and B, there is again resonance with the ionized forms, and the wave-function is of the general type

$$a\psi_{A-B}+c\psi_{A^+B^-}+d\psi_{A^-B^+} \quad \ldots\ldots\ldots (2)$$

where the ratios c/a and d/a are in general different from b/a in (1), one ratio being larger and the other smaller. Experimentally it is found that the energy of an actual A—B co-valent bond is greater than the arithmetical mean of the normal A—A and B—B co-valent bonds. The increase, Δ, in bond energy is particularly marked when one element is, in the chemical sense, very electro-negative compared with the other, and this has been taken to mean that actual co-valent bonds A—B involve a greater proportion of the ionized states than the normal bonds, and all actual co-valent bonds are of a partly ionic nature. Pauling (1932) showed that the values of $\sqrt{\Delta}$ were approximately additive, and he drew up tables in which the elements were assigned values such that their differences were approximately equal to the square roots of the Δ values in electron volts. These values were called *electronegativities*, but it is important to realize that these are really terms relating to bond energies, and are not based on any measured electrical or electrochemical properties of the atoms concerned.*

In the general case of a co-valent bond between atoms of two different elements, the bond is not symmetrical, and the electron cloud is associated more with one atom than with the other; to a rough approximation this effect will be greater, the greater the difference between the Pauling electronegativity values for the two elements concerned. Provided that resonance is possible† between the co-valent A—B, and ionic $A^+ B^-$ or $A^- B^+$ structures, there may from this point of view be bonds ranging from the almost purely ionic to the purely co-valent type according to the relative values of the coefficient in eqn. (2).

The idea that interatomic distances or bond lengths could be interpreted in terms of co-valent radii was advanced first for the compounds of carbon for which the single bond radius deduced from the crystal structure of the diamond agreed with the C—C distances in many compounds. The double bond C=C co-valent radius was determined experimentally, and, the triple bond C≡C radius was deduced from the spectrum of acetylene. By a variety of methods, some accurate, and others empirical or less certain, tables of single, double, and triple bond co-valent radii were drawn up by Pauling (1940), and to these were added tables for single bond (sp^3) tetrahedral, and (d^2sp^3) octahedral radii for many elements. These tables were of great importance in the development of the subject, and although later work has shown that some values or assumptions were erroneous, the outstanding value of the preliminary schemes must always be acknowledged.

Experiment showed that co-valent single bond interatomic distances were not exactly additive, and could not be accounted for by one set of co-valent radii. Schomaker and Stevenson (1941) suggested an empirical equation according to which the actual bond length was less than the sum

* It is unfortunate that the electronegativity values are sometimes tabulated or referred to as though they were electrochemical constants.

† This requires several conditions, of which the most important is that the two structures have the same number of unpaired electron spins.

of the co-valent radii by an amount proportional to the difference in electronegativities of the two elements forming the bond. This has been discussed by Wells (1950) who shows that, when the data are considered as a whole, a correction term of this kind introduces more errors than it removes,* although there is no doubt that bond shortening occurs when one element (e.g. F or Cl) is relatively very electronegative.

The alternative explanation of the divergences from a simple additive law was based on multiple bond character. From the known values for the C—C, C=C, and C≡C radii, a curve was drawn connecting the covalent radii with the bond numbers or bond orders, on the assumption that these were 1, 2, and 3 respectively. Later work has led to the conclusion that many bonds whose orders were thought to be integral, are really of non-integral bond order, and this throws doubt on the finer details of much of the early argument. Omitting this point, it was clear that in some carbon compounds, the interatomic C to C distances corresponded to non-integral bond numbers, and this was interpreted in terms of the resonance theory of co-valent bonds, according to which the observed interatomic distance is the sum of the co-valent radii for the bond order concerned (e.g. 3/2 for C to C in the benzene ring) less a correction term due to the resonance between the different structures.

The concept of non-integral bond orders was then introduced into the theory of metals by Pauling (1938, 1947, 1949) according to whom in a crystal of, say, potassium (b.c. cube), each atom contributes one electron which resonates between the 8 positions of the closest neighbours.† According to Pauling the effect of bond order and resonance can be combined in a single equation of the form

$$R(1)-R(n)=0{\cdot}300 \log n. \quad . \quad . \quad . \quad . \quad . \quad . \quad . \quad (3)$$

Here $R(1)$ is the co-valent radius of a normal single co-valent bond, $R(n)$ is the radius in a structure where v single bonds resonate among N positions, and $n=v/N$. This equation was then used by Pauling (1947) to calculate the single bond radii of all the metallic atoms in terms of his well-known valency schemes.‡ The use of a single equation requires justification, for it is by no means clear that a given change in n will produce the same effect in metals of widely different character. Unfortunately, discussion of this point involves the complicated story of the development of the theory of co-valent bond lengths, and for clarity this is dealt with in Appendix A. From this we conclude that the equation is valid for C, Si, and Ge in Group IV, but is less convincing for adjacent Groups, whilst its extension to metals is by analogy only,

* The problem is complicated by the fact that resonance occurs in some cases but not in others.

† In more elaborate discussions the possibility of bonding to the six second closest neighbours is also considered.

‡ See § 4.9.

and has no real justification. The single bond radii calculated by Pauling thus involve two distinct assumptions :—

(*a*) *The Validity of Equation* (3).—It is improbable that the correction for the effects of bond order will be independent of the size and nature of the atom, and as shown in Appendix A much of the supposed evidence for this is illusory. The logarithmic relation is based on the experimental values for the C—C, C=C, and C≡C bond lengths, and will therefore involve contributions of the ionized states to these bonds, but these are not necessarily the same as those in metals. In so far as the Pauling single-bond radii are calculated from interatomic distances in the crystals of the metals, they will involve the contributions of the ionized states in the individual metals, but these contributions may well differ from one metal to another, and are almost certainly different in alloys.

(*b*) *The Correct Choice of Valency for the Metal.*—As explained in § 4.4 the exact meaning of the term 'valency' of a transition metal is not always clear. In the Pauling sense it is used to denote the number of electrons regarded as present in bonding (spd) orbitals, and in his 1947 paper Pauling assumed a constant valency of 5·78 for all the elements of Groups VI A, VII A, and VIII A, B, and C.* If the true valency of iron, cobalt, or nickel were 2 or 3, the calculated single-bond radii would be reduced by 0·14 kx and 0·085 kx respectively. Until the valencies of the transition elements are established securely, the calculated single bond radii are not significant to the three places of decimals to which they are sometimes discussed.

For these and the other reasons given in Appendix A, we think that great caution is necessary before the Pauling single-bond radii, or related quantities calculated by means of eqn. (3), are used to a degree of refinement greater than 0·1 kx, or at the best 0·05 kx, in the interpretation of alloy structures. In table 2 we summarize the Pauling single-bond radii, which we have rounded off to 0·01 kx, and in order to show the magnitudes involved, fig. 8 shows the value of ΔR, where

$$\Delta R = R(1) - R(n) = 0{\cdot}300 \log n$$

is the difference between the length of a single bond, and of one in a structure where v single bonds resonate among N positions, and $n = v/N$. It must be emphasized that figure refers really to compounds of carbon.

In using the co-valent or single-bond radii of table 1 for the interpretation of alloy structures the following points should be noted :—

(1) As pointed out by Pauling (1940)† the effects of increasing positive and negative charges on an atom are, respectively to decrease and increase the co-valent radii ; thus the values for the octahedral Ni^{III} and Ni^{II} radii are 1·30 and 1·39 kx respectively.

---

* In the 1949 paper, the valency was changed to 6 for some of these elements.

† This point was elaborated in the 1949 paper (*loc. cit.*) but we do not discuss the details because they involve the disputed Valency Schemes.

(2) According to Pauling (1945) " the interatomic distance between the atoms of opposite electric charge is not appreciably affected by the charges, since the radius of one atom is increased, and that of the other atom is decreased by the charge effect ". As shown in Appendix B, when the correct radii are used, the example which was given by Pauling really contradicts his conclusion, but there is some evidence that the effect of opposite charge is variable, and at present it is not understood. In the theory of alloys there has been a tendency to assume that interatomic distances are shortened by the building up of opposite charges, and this is probably true, although the magnitude of the effect may vary greatly.

(3) In complicated alloy structures, direct resonance may be possible between alternative structures, and may produce a shortening of the interatomic distance.

Fig. 8

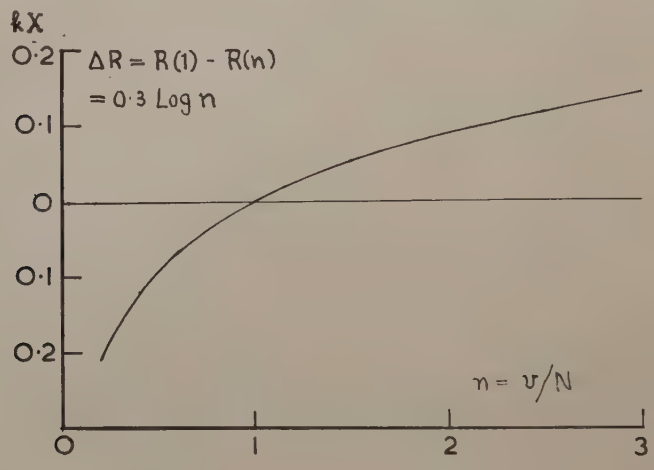

(4) In the early work (Pauling 1940) it was thought that the co-valent radii were the same for d^2sp^3 as for dsp^2 bonds, but in later papers Pauling (1947, 1949) concluded that the co-valent radius decreases with increasing proportion of the d function, and this is probably true at any rate up to about 50% of the d function.

From the above survey we must reluctantly conclude that it is seldom justifiable to consider co-valent radii to more than one place of decimals in kx units. The lack of a theoretical justification for such radii throws doubt on attempts to use them to deduce electron configuration in alloys, and in particular the use of one simple equation for a wide range of substances is open to criticism. There are of course many cases in which the study or comparison of interatomic distances in crystals may be justifiably carried out to the full limits of the accuracy of the data, but attempts to interpret these in detail in terms of electronegativities, fractional bond orders, resonance corrections, etc., are at present usually little but speculation.

§4. The Electron Theory of the Transition Metals

4.1. *General*

The general qualitative picture of electron configuration in the transition metals is quite clear. In the alkali metals (K, Rb, Cs), the electron bands derived from the ns and np levels of the free atoms overlap, and the one outer electron per atom is in a nearly pure s state. For convenience we shall use the term outer electron to describe all the electrons outside the rare gas configurations. On passing to the alkaline earth metals the d bands derived from the (n−1)d levels of the free atoms have probably dropped to such an extent that they overlap the ns band (cf., the work of Manning and Krutter on calcium, p. 152). Further passage from Group II A→III A→IV A . . . results in a continuation of this general process, and the outer electrons are properly described by hybrid spd functions.* the proportion of the d function in the lower energy range of the hybrid band increasing with the number of the Group. There is general agreement that up to the stage at which the breaks in the sequences of properties occur (§2.8), all of the outer electrons are involved in the cohesion. After this stage, two different and conflicting methods of approach have been used. In the *collective electron theories*, all of the outer electrons are regarded as being in energy bands of the whole crystal, and so contributing to the cohesion in the elements of Groups VI A, VII A, and VIII A, B, and C, and the breaks in the sequences of physical properties are regarded as due to a marked increase in the repulsive characteristics of the wave-functions. In the *Pauling hypotheses*, the breaks in the sequences of physical properties are assumed to result from the entry of some of the outer electrons into atomic or non-bonding d-orbitals, these being distinct from the remaining d orbitals which are regarded as forming hybrid spd bonding orbitals whose resonance gives rise to the metallic bond. Finally on passing from Group I B→II B . . . , the d portion of the functions rapidly becomes purely atomic in nature.

The mathematical difficulties have prevented these simple considerations from being expressed in any real quantitative form, and there is as yet no satisfactory theory of the transition metals as a whole. As the two main lines of approach involve different types of wave-function, it is convenient to summarize the main characteristics of these.

4.2. *Bloch Functions*

In the collective electron theories use is made of Bloch functions, in which the function for each electron extends through the whole crystal, and is of the general form

$$\psi = e^{i\mathbf{k}\cdot\mathbf{r}}\,\phi_k(\mathbf{r}).$$

ϕ_k depends on **k**, the wave number, and has the 3-fold periodicity of the lattice. The term ' collective electron theory ' is in some ways misleading,

* For abbreviation we use the expression ' spd function ' to describe the functions derived from the ns, np and (n−1)d states of the atoms.

because the functions are one electron functions, in which the electrons are considered singly, and in treating any one electron, the remainder are regarded as smoothed out, so that the field which they produce has the periodicity of the lattice. The Bloch functions imply that in the three normal metallic structures, all the atoms of a pure metal are in the same state, and have the same spin,* and the functions are equivalent to the L.C.A.O. (Linear Combination of Atomic Orbitals) functions of molecular theory.

Bloch functions, or at least the more simple types, do not take into account the correlation of positions of electrons. Consequently they become increasingly unsatisfactory as the volume per electron becomes smaller. If they are corrected to take this into account, the functions are no longer Bloch functions, but correspond with the configuration interactions of molecular theory.

In the development of the collective electron theory, three main lines of approach may be noted.

4.2.1. *The Nearly Free-Electron Approximation*

In this approximation, $\phi_k(\mathbf{r})$ is assumed to be nearly constant, so that the deviation from a simple free electron theory is small. In practice, this means that the behaviour of an electron when near to an atom is ignored, and the crystal structures are used to deduce Brillouin Zones, for which the magnitudes of the energy gaps are assumed to agree with some observed physical property. The method is justifiable for univalent metals, and in particular for the alkali metals, but it is seldom valid for electron : atom ratios greater than 1·8, whilst its extension to structures with 5 or 6 electrons per atom is quite unjustified.

4.2.2. *The Tight-Binding Approximation*

This expression is unfortunate, because it does not mean that the atoms are tightly bound, but rather that they are so far apart that the wave function resembles that of the free atom. The difference between this and the free electron approximation is that there may now be a considerable variation in potential near to an atom, and the wave function can be built up from atomic functions. Correlation of position of electrons is partly taken into account provided that a determinantal wave-function is used, and not a simple product. In molecular theory, the tight binding approximation can be used even when electrons are bi-centric, as in the H_2 molecule, and it is this kind of agreement which provides the justification for the use of the approximation for calculations such as those of Fletcher and Wohlfarth (1951), and of Fletcher (1952) for nickel. In these methods the potential field round each atom has to be assumed or calculated, and for this purpose use is generally made of the Hartree methods of self-consistent fields. Thus the work of Fletcher on nickel is based on a Hartree field for the Cu^+ ion.

* We are here omitting the possibility of antiferromagnetic arrangements in the pure metals.

4.2.3. *The Cellular Method*

In this method each atom is regarded as surrounded by a polyhedron of such a shape that the different polyhedra fit together and fill the whole space of the crystal. The potential within the polyhedron is regarded as spherically symmetrical (ion core field), and the Schrödinger equation is solved for an electron in this field, subject to the continuity of ψ and its normal derivative at the boundary. In the cellular method it is again necessary to assume or calculate the atomic field. Use is generally made of the Hartree methods, and some of the numerical results are very sensitive to the exact field used. Thus in the work of Howarth (1953) on copper, calculations were made both for the original Hartree (1933, 1934) field for the Cu^+ ion as used by Krutter (1935), and also for the more accurate Hartree–Fock potential of Hartree and Hartree (1936) which includes the effect of exchange between the ion-core electrons ; the difference between these two fields affected the energy gap in the [002] direction by a factor of 7. In principle the cellular method is the best, but in practice with more than one electron per atom, there are great difficulties in obtaining a self-consistent field, and in spite of much highly skilled work, it is seldom that detailed comparison between calculated and observed results is justified.

4.3. *Heitler–London–Heisenberg Functions*

It is these functions which underlie the Pauling hypotheses, and for abbreviation we shall refer to them as H.L.H. functions. In these the wave function for each electron is localized round an individual atom or pair of atoms, but exchange of electrons occurs, so that the electrons move freely through the lattice as with Bloch functions. The electrons are considered two by two in pairs of opposite spin, and the correlation of the electrons in a pair is considered. There is also a partial correlation throughout the crystal, because in considering any one pair of electrons, the other electrons are in different regions. The method resembles the valence-bond theory of molecular structure.

The H.L.H. functions may be regarded as derived from atoms in different states, or with different spins. But since resonance is assumed to occur, and we cannot look within the resonance process, the atoms in the three normal metallic structures are usually regarded as being in the same state, as in the Bloch theory. There is thus no real difference here between the two pictures, but the advantage of the valence bond method is that the metallic structure may be connected with the known valencies of the atoms concerned. In abnormal structures such as that of α-manganese, the atoms are regarded as being in different states, and in principle there is no reason why superlattices of different states should not exist in the more normal metals.

In developments based on H.L.H. functions, there is nothing corresponding to the free-electron, tight-binding, or cellular methods of the Bloch theory, and the H.L.H. function for a crystal cannot be

calculated, even in approximate form. It can be shown that the use of H.L.H. functions will lead to an insulator if only neutral atoms are considered, and for insulators, the methods based on Bloch functions and H.L.H. functions would lead to the same result if carried through completely. In order that conductivity should occur, it is necessary to introduce ionized states, and the electrons and ions must be widely separated on the atomic scale. There is a difference of opinion as to whether both types of function may be used for conductors. According to Mott (1949, 1952), the separation of the electron and ion necessary to produce conductivity would result in an increase in energy, and so the process would not occur. Others consider that this increase in energy might be counterbalanced by a loss in energy resulting from resonance of configurations in which the ion and electron were not widely separated. For the moment it seems better to accept the possibility that both approaches may be used in qualitative discussions.

4.4. *Comparison of the Methods*

The Bloch-collective electron theory is the better approach, if by ' theory ' we mean the calculation of physical properties from fundamental principles, with the minimum number of assumptions, and without introducing numerical constants deliberately chosen to fit the facts. Unfortunately, for the transition metals, the assumptions are generally so crude and approximate that the calculated results can seldom be compared critically with facts. In these circumstances the H.L.H.–Pauling approach, with its intuitive seizing on valency as a characteristic of an atom may often be the better way of trying to interpret, understand, and generalize the facts, but those who adopt this approach must not claim to have produced a theory of transition metals, when they have, in fact, made an array of assumptions, including numerical values, deliberately chosen to agree with the numerical values of the physical properties they are trying to understand.

It is to be noted that the two methods of approach may lead to confusion as to what is meant by the term ' valency ' in a solid metal. As explained later, the collective electron theories lead to the conclusion that the electrical conductivity of transition metals is due to a relatively small number of electrons whose wave-functions include a high proportion of s-type functions. Some writers consider that the term ' valency ' should be used to describe the number (per atom) of these electrons. In this case the ' valency ' may be very much smaller than the number of electrons per atom taking part in the cohesion. In the H.L.H.–Pauling approach, the term ' valency ' is used to describe the number of bonding electrons per atom, a concept which is obviously related to the chemist's use of the word. In view of the fact that ' valency ' is a chemical concept, this latter procedure seems preferable. In this case it must be recognized that for some metals, the term valency may have no exact meaning if the collective electron theory is used. In solid nickel, for

example, Wohlfarth (private communication) regards all ten outer electrons per atom as taking part in the cohesion, but few people would say that the valency of nickel was here equal to 10. On the other hand, even in the collective electron theories, useful correlation with valencies may be expected. For the valencies of an element are an indication of the numbers of electrons per atom which may be perturbed sufficiently to take part in the various types of molecular cohesion, and it is not unreasonable to expect the predominant valencies to be related to the cohesion in a metallic crystal which is itself a gigantic molecule. Thus as explained in § 2 the predominant valencies of the elements in the different Transition series show a remarkable parallelism to the sequences of physical properties. This suggests that even though, in the collective electron theories, the ' valency ' in the solid crystal cannot be exactly defined, because all the outer electrons take part in the cohesion, the degree to which they do so take part is related to the predominant valencies of chemistry. Provided the limitations are recognized, discussion in terms of valencies may lead to generalizations, and may for some purposes be the most helpful approach until the electron theory has reached a more precise stage, although this view is not accepted by some physicists.

In so far as the concept of valency is justified in crystals of transition metals and their alloys, the valency of a transition metal is generally not a constant number which can be applied to all alloys. The non-integral valencies of the Pauling hypothesis result from resonance between different valency states, and in an alloy the proportions of the states may be quite different from those in a pure metal. As shown later (§ 5) a study of some alloy equilibrium diagrams makes it almost certain that the valency of a transition metal may change with composition in a given alloy system.

4.5. *Band Models and Magnetism*

Although the outer electrons in crystals of transition elements are in hybrid spd states, the collective electron theories have usually ignored the p part of the function, and considered it justifiable to consider separate s and d bands. This is a justifiable approximation for the elements of Group VIII C, but becomes increasingly invalid on passing back to the earlier Groups. The first suggestion that the d-electrons should be treated on a collective band basis was made by Stoner (1933) who pointed out that this led to a reasonable interpretation of the non-integral values of the saturation moments when expressed in Bohr magnetons per atom. Stoner also suggested that the width of the d-band decreased on passing from titanium to iron, and this is now accepted as a general characteristic of the effect of increasing atomic number on the width of the d-band in each Transition series.

Mott (1935), and later Mott and Jones (1936) developed the d band treatment, and introduced the concept of overlapping s and d bands, which can contain up to two and ten electrons per atom respectively.

Many considerations indicated that the d bands are relatively high and narrow compared with the s bands, and the general band form for a metal such as nickel in the paramagnetic state is as shown in fig. 9. This model was used (Mott 1936 a, b), for the discussion of electronic specific heats, paramagnetic susceptibilities, and electrical resistances ; and idealized band forms were assumed in which the s band was parabolic (fig. 9), whilst the head of the d band was parabolic in the reverse direction, and was thus of the form $N(E) \propto (E_0 - E)^{1/2}$.

Fig. 9

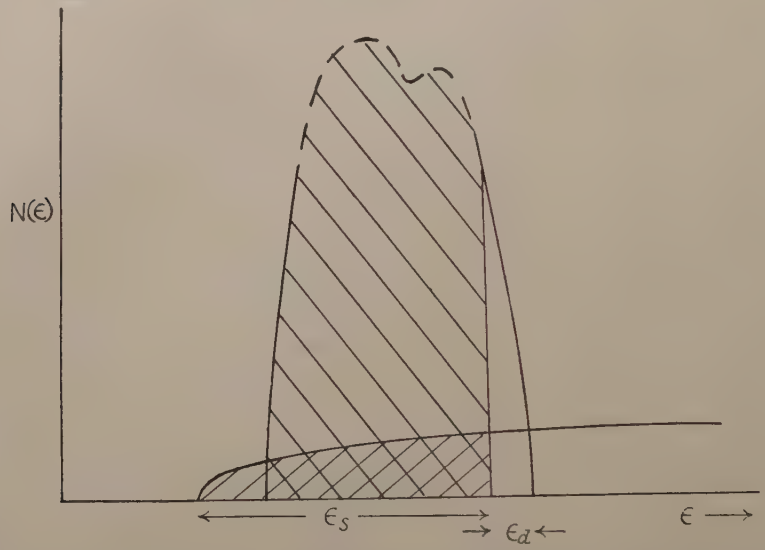

Overlapping d-band and s-band model. (Shading indicates occupied states.) Number of occupied s-band states $= n_s$; number of unoccupied d-band states $= n_d$; relative magnetization (ζ) and degeneracy temperature (T_0) are defined by $\zeta = q_f/n_{0d}$ and $kT_0 = \epsilon_{0d}$, where q_f is the observed intensity of magnetization in Bohr magnetons per atom, k is Boltzmann's constant, and zero suffixes refer to 0°K.

The d-band containing 10 electrons per atom may be regarded as divided into two halves, containing 5 electron states of + and − spins respectively. In the paramagnetic state the two halves are occupied up to the same limit, and the early theory assumed that in the ferromagnetic state, the ferromagnetic interaction forces were such that a lowering of energy resulted from one half-band being completely filled, whilst the other contained unoccupied states or holes, so that there was a preponderance of positive spins equal to the number of holes per atom in the partly filled half-band; the number of these holes was identified with the saturation moment in Bohr Magnetons.* Since nickel, cobalt, and iron contain 10, 9, and 8 outer electrons respectively, and since the observed saturation

* That is to say, it was assumed that d levels in the solid metal, as in the free atoms, followed a maximum multiplicity rule.

moments are 2·2, 1·7, and 0·6 μ_B, the numbers of d electrons were assumed to be 7·8, 8·3, and 9·4, and the numbers of s electrons were 0·2, 0·7, and 0·6 respectively. It is now generally agreed that whilst the values 0·6 d holes and 0·6 s electrons per atom are approximately correct at the absolute zero for nickel, the ferromagnetic interaction forces in iron are insufficient completely to fill one half of the d-band, and that for this metal there are holes in both halves of the d band. From a survey of the magnetic properties of alloys Coles (1950) concludes that in iron the approximate distribution is 0·9 s electrons per atom, and 7·1 d electrons of which 4·65 are of + and 2·45 of — spin.

In all the early work the ferromagnetic interaction forces were regarded as arising from exchange forces between the d electrons of adjacent atoms. In ordinary co-valent bonds, the exchange integral is negative, and the lowest energy is found when the two electrons have opposite spins. It was postulated that in ferromagnetic metals, the exchange integral might be positive, the conditions for this being (*a*) an incomplete shell of electrons whose charge density remains high in the outer parts of the atom (in practice d or f electrons), and (*b*) a critical distance between the atoms, such that the overlap is neither too great nor too small. By accepting the assumption of ferromagnetic interaction forces of this kind, Stoner (1938, 1939, 1947) and Wohlfarth (1949 a) developed a collective electron theory of ferromagnetism in terms of a two-band assumption. This work showed that for ferromagnetism to occur, the exchange integral must not only be positive, but must exceed a critical limit. With parabolic bands the theory gives ferromagnetism with $\zeta_0 < 1$ for some values of the exchange interaction energy. On raising the temperature, there is increasing d→s excitation, and the number of holes in the d band becomes greater than at the absolute zero. This work has led to much valuable generalization and interpretation of magnetic data, but as this has already been extensively reviewed (Stoner 1947, 1951), we shall not deal with it here. Wohlfarth (1949 a, b) has used a collective electron treatment as a basis for deriving information about the electronic structures of actual metals and alloys from their magnetic properties, and has considered (Wohlfarth 1951) how such interpretations would be modified by the assumption of other band shapes.

4.6. *The Origin of the Weiss Molecular Field*

The above theories of ferromagnetism depend on the assumption that ferromagnetic interaction forces of some kind produce the Weiss molecular field which aligns the spins with a lowering of energy, and in spite of their success they are unsatisfactory in that the real origin of the Weiss molecular field remains obscure. Heisenberg (1928) gave the first quantum mechanical interpretation when he identified it with the exchange interaction of the Heitler–London treatment of molecules. The assumption of a positive exchange integral is in a sense arbitrary, and has not been justified by explicit calculation. Heisenberg type exchange

integrals for d-electrons have been calculated by Wohlfarth (1949 c) who considered only the radial part of the wave-function and obtained a negative integral. Kaplan (1952) who used a more complete wave-function obtained a positive value, although this calculation has been criticized by van Vleck (1953) on the grounds that appropriate interatomic distances were not used. It is to be noted that the exchange process is between different quantum states, and not necessarily between different positions in space. In the original Heisenberg theory of Heitler–London exchange between the d shells of adjacent atoms, the process could be regarded as an exchange of electrons between two neighbouring atoms. In collective electron theories where each electron is described by a Bloch function extending over the whole crystal with the periodicity of the lattice, exchange between different states may still occur, but cannot be visualized.

Slater (1936) concluded that the internal field which aligns the spins is of intra-atomic origin, and involves exchange between electrons on the same atom, and a similar conclusion has been reached on different grounds by van Vleck (1953). This approach has been criticized by Wohlfarth (1949 d) on the grounds that it is incompatible with the essentially co-operative nature of ferromagnetism, and this author claims that Slater obtained his results only because of certain approximations in the cellular method employed. Stoner (*loc. cit.*) and Wohlfarth (1949 a, b, 1953) have used an exchange interaction of an interatomic type in a phenomenological way. Slater (1953) has recently discussed the form that should be taken by a complete quantum-mechanical calculation, using orthogonalized wave-functions, in which all interactions and correlations are present from the start. He objects to Wohlfarth's approach on the grounds that it introduces exchange interaction and correlation as a final effect separating a magnetized from an unmagnetized state, instead of making complete and independent calculations for each of the two states. Unfortunately the difficulties of such calculations are prohibitive.

The problem of exchange interaction has been discussed in many publications and useful references will be found in Volume 25 of the *Reviews of Modern Physics*. The uncertainty regarding the exchange integral has led to alternative suggestions regarding the cause of ferromagnetism. In particular Zener (1951 a, b, c, 1952) has concluded that the exchange integral between d shells of adjacent atoms is always negative, and that the ferromagnetic interaction forces arise from a spin coupling between the conduction electrons and the d electrons, the conduction electrons serving to carry the spin from one atom to the next. Unfortunately, this work has included many developments which are generally regarded as unacceptable, but the underlying ideas that the exchange integral is always negative, and that coupling between conduction and core electrons is responsible for ferromagnetism are favoured by some physicists, and need quantitative development. In its original form the Zener theory postulated that the assumed negative

sign of the exchange integral produced an antiferromagnetic alignment of opposite spins, and that in the body-centred cubic metals of Groups VA and VI A, atoms with large opposite spins formed superlattices of the caesium-chloride type each element having only one conduction electron per atom. When this was disproved by neutron diffraction methods, it was suggested that resonance occurred between the two possible configurations, but the data on diffuse neutron scattering make it improbable that large spins are present.

In a recent paper Pauling (1953) has advanced views in which both s and d electrons are concerned in producing the ferromagnetic interaction forces, but the quantitative results depend on the assumption that no fewer than 6 electrons per atom can be treated as constituting a free electron gas, and this is generally regarded as highly improbable.

4.7. *Band Models: Cohesion and Band Widths*

In the early band models of Mott and Jones (1936), the cohesion in the transition metals of Group VIII was regarded as due mainly to the s electrons, but there was difficulty in reconciling the strong cohesion with the small numbers of electrons (Fe 0·2, Co 0·7, Ni 0·6 per atom) assumed. Mott and Jones suggested that the atoms could be regarded as existing in different states, and that although continual interchange occurred, an atom existed in a given state for a time sufficient for forces of a quasi-ionic nature to be set up, which added to the cohesion. This view was later withdrawn by Mott (1953), one of whose arguments was that the process assumed would lead to the formation of superlattices in systems such as copper–nickel, where they have not been observed. It is perhaps significant that superlattices are formed in the systems Fe–Co and Fe–Ni, although the atomic diameters and general chemical properties of the metals are so similar that superlattice formation would not be expected. It is possible, therefore, that the original view of Mott and Jones is correct in such alloys. For pure metals, so far as they have been examined, the experiments on neutron diffraction suggest that if atoms do exist in different states, the life of these cannot be greater than about 10^{-13} sec. There is, however, much need for more work of this kind.

In his later paper, Mott (1953) suggests that whilst the main cohesion is due to the s electrons, additional attraction is produced by van der Waals forces between the d electrons of the cores, as is probably the case in copper (see Appendix C).

From the point of view of the more complete collective electron theories, all of the d electrons should be regarded as contributing to the cohesion, and much interest attaches to the various attempts to calculate the width of the d-bands. Unfortunately this work is very difficult, and the results obtained by different methods are not in agreement. For copper the early work of Krütter (1935), based on the cellular method, indicated a width of 5·5 ev for the 3d band, but the much more accurate work of Howarth

(1953)* reduced this to 3·4 ev. The cellular method has not been used for nickel, but a band width of 2·7 ev was obtained by Fletcher (1952), and by Fletcher and Wohlfarth (1951) who used the tight binding approximation. The band obtained is shown in fig. 10. It is almost certain that the width of the d band increases with decreasing atomic number, and the above numerical values must therefore be accepted with caution. The tight-binding approximation by its nature tends to give too narrow a band width, but the discrepancies between the above results for copper and nickel are probably due also to the ionic fields assumed. For iron, Manning (1943), and Manning and Greene (1943) used approximate cellular methods to calculate bands for both body-centred and face-centred cubic iron (see figs. 11 (*a*) and 11 (*b*)) and the results showed a total band width of about 11 ev, of which about 7·5 ev covered the occupied states. The change in band width in passing from copper to iron is in the direction expected.

Fig. 10

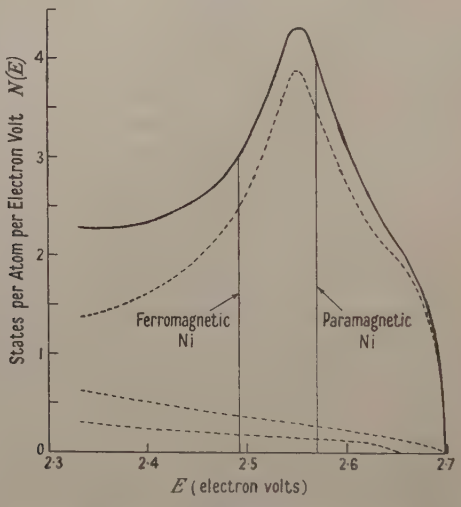

Density of states curve for nickel. E, electronic energy in ev, measured from zero at the bottom of the band; $N(E)$, density of states, such that the total area under the (complete) curve corresponds to 5 states of either spin. Fermi limits as shown; the ferromagnetic limit is for one half of the band only, the other is completely filled.

– – – – – – – – Constituent $N(E)$ curves.

For elements of the earlier Groups calculations of the type made by Krütter for copper have been made for tungsten by Manning and Chodorow (1939). It was assumed that the newly-filled (4f) shell is comparatively little affected by the solid binding, and curves for the densities of states were calculated for five d-bands, and one predominantly s–p band. In view of the numerical discrepancies referred to above between the band widths obtained for copper and nickel, the exact numerical

* In this work accurate solutions for the ion-core fields used were made available by means of an electronic computer.

Fig. 11

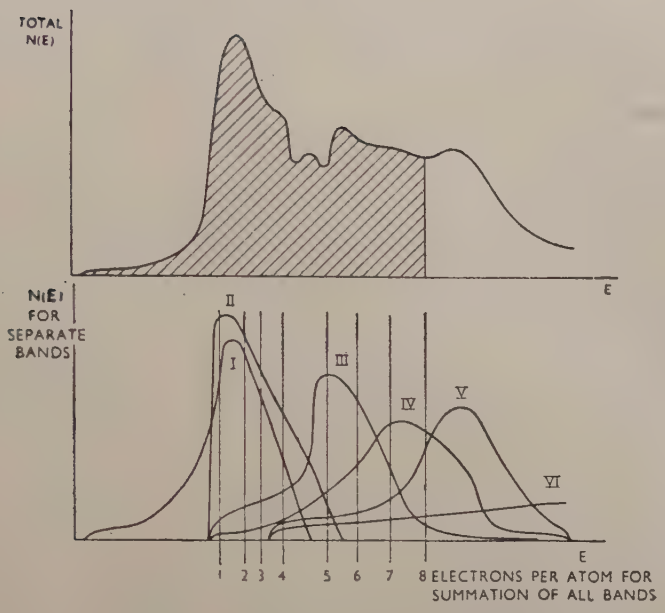

(*a*) $N(E)$ curves for body-centred cubic iron.

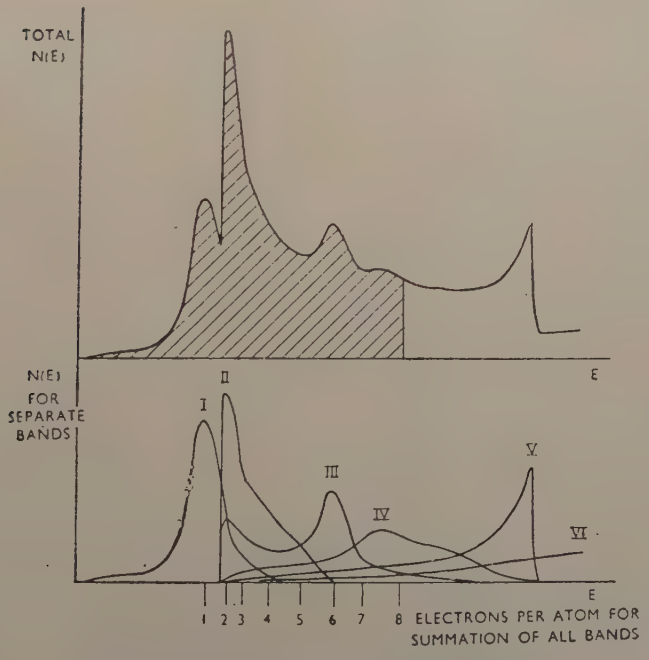

(*b*) $N(E)$ curves for face-centred cubic iron.

values for tungsten are of doubtful value, but the work was interesting in showing that the bands obtained by this kind of calculation were such that all of the d electrons could be accommodated in the low energy region of a broad d band, giving rise to a large cohesive energy in agreement with observation.

4.8. *Electrical Properties*

In the early two-band theories, it was suggested that the main current carriers in the later Transition Groups are electrons in the s bands, and this is supported by the negative Hall coefficients of cobalt, nickel, palladium, and platinum. This picture cannot be used for the elements of the earlier Groups, and even for rhodium and ruthenium the Hall coefficients are positive (Gehloff and Justi 1949), and suggest that conduction by the movement of d-band holes is important. The high electrical resistances are regarded as due to s→d transitions which are not possible in other metals, but for which there is a high probability if the d-band N(E) curve is high at the Fermi surface of a transition metal.

Discussion of the implications of a two band model for the electrical properties of metals has taken place (see Wilson 1953, Sondheimer and Wilson 1947). Sondheimer (1948) has derived the values of the mobilities of s-electrons and d-holes implied by the Hall effect data for palladium. Data on this effect for iron, cobalt, nickel and some of their alloys have been assembled by Pugh and his co-workers (Pugh and Foner 1953, Pugh and Schindler 1953, Pugh and Rostoker 1953), the assumption being made that in fields greater than that required to produce saturation a coefficient can be derived which has the same significance as that for non-ferromagnetics. In nickel–cobalt and nickel–copper alloys the results are in reasonable agreement with those calculated on the assumption that the current carriers are free electrons equal in number to the accepted number of s-band electrons. The values for pure nickel agree less well ; the agreement can be improved by the assumption of a contribution to conduction by the d-band holes of the sort suggested for palladium, but it is difficult to see why such a contribution should not be even more important in cobalt and in nickel–cobalt alloys. In iron, as in ruthenium and rhodium (Gehloff and Justi 1949), the coefficient is positive.

4.9. *Developments of the Pauling Hypothesis*

The Pauling hypothesis has already been extensively reviewed and criticized (Raynor 1949, Hume-Rothery 1949, 1952), and we shall deal here only with some of its developments. The original assumption that the breaks in the sequence of physical properties are due to the entry of d electrons into atomic or non-bonding orbitals is entirely reasonable, and attempts to interpret facts or to deduce electronic structures from this viewpoint are fully justified, and should not be condemned because they cannot be expressed in precise mathematical form.

The original Pauling hypothesis (Pauling 1938) assumes that metallic cohesion is the result of resonating co-valent bonds in which the number of

electrons is too small for an atom to form normal co-valent bonds to all of its close neighbours. This assumed resemblance between co-valent and metallic bonding is supported by various empirical relations* between interatomic distances in crystals and molecules. The first Pauling scheme (Pauling 1938) assumed that on passing from Group I A→V A, the number of bonding electrons per atom was equal to the Group number, and that from Group VI A→VIII C, the number of bonding electrons remained constant at 5·78 per atom, the remaining electrons entering atomic orbitals, whose number was assumed to be 2·44 per atom in order to agree with the known saturation moments of iron, cobalt and nickel, and the maximum moment of $2{\cdot}44\,\mu_B$ in iron–cobalt alloys. According to Pauling (1949) " the non-integral valencies shown by the transition elements are to be interpreted as averages, corresponding to resonance of each atom among two or more electronic structures with integral valencies ". This concept has been objected to on the grounds that it is physically meaningless, but if the idea of resonance is accepted and it is granted that one must not look within the resonance process, it may be useful to think of a non-integral number of valency (i.e. bonding) electrons in the crystal of the element. In this case the non-integral valency is a characteristic of the particular crystal, and, in general, is not a characteristic of the atom which can be carried over from one structure to another. Unfortunately this point has not been appreciated by some writers.

In Pauling's (1947) paper, the Pauling scheme was extended so as to include valencies of 5·44, 4·44 . . . for copper, zinc . . . . The position of copper, silver and gold is discussed in Appendix C, but there is now almost general agreement that a valency of 4·44 for zinc is incorrect and we shall not consider these later elements. The 1947 paper also included methods for calculating single bond radii, but as shown in § 3 these are of doubtful validity. Pauling (1949) later claimed that resonance with ionic states was necessary to obtain the desired bonding strength, and it was emphasized that the existence of an unoccupied or ' metallic ' orbital was essential ; this metallic orbital probably corresponds to the unoccupied levels necessary for conductivity in the Bloch theory. Finally in Pauling (1953), the picture was slightly modified, in that dependence on states with integral numbers of electrons per atom in the d orbitals was emphasized in a semi-quantitative discussion of ferromagnetism (see § 4.6).

For the elements of Groups I A–IV A in the First Long Period, and for those of Groups I A–VI A in the Second and Third Long Periods (excluding the Rare Earths), the Pauling valencies are undoubtedly equal to the number of bonding electrons per atom, and there is little difference between the Pauling concepts and those of the collective electron theories. For the elements of Groups V–VIII C in the First Long Period, and from Groups VII–VIII C in the later Periods, the

* Some of these are summarized in *The Structure of Metals and Alloys* by W. Hume-Rothery and G. V. Raynor, 1954.

constant valency of 5·78 of the Pauling scheme is not in agreement with the physical properties of figs. 3 to 7. This was pointed out by Hume-Rothery, Irving and Williams (1951), who emphasized the correspondence between the physical properties and predominant valencies of the elements concerned, and suggested that the relatively low cohesion in the elements from chromium to nickel as compared with that in the later sequences molybdenum to palladium, and tungsten to platinum, suggested that higher valencies were exerted in the later Periods. These authors also pointed out that if an atom with n valency electrons had N neighbours in a crystal, the stabilization by resonance might be expected to reach a maximum for $n=N/2$, and that in this way the existence of the breaks in the sequences of physical properties might be understood, since $N=12$ for the close-packed structures, and somewhere between 8 and 14 for the body-centred cubic structure, according to whether the second closest neighbours are included. The introduction of ionized states was also shown to lead to a limit to the number of bonding electrons, and these considerations give some understanding of why the breaks in the sequences of physical properties occur. If the views of Hume-Rothery, Irving and Williams are accepted, the valencies of Fe, Co and Ni in the elementary state are between 3 and 2, with a gradual decrease with increasing atomic number, whilst manganese has a lower valency in agreement with the known stability of the divalent compounds. Chromium has a higher valency than manganese, although a lower valency than molybdenum or tungsten (see pp. 156–160). For vanadium the data are not yet known for pure metal. In the later Periods, Hume-Rothery, Irving and Williams agreed with Pauling that the valency continues to rise as far as Group VI, but then considered that there was a fall which was increasingly steep on passing from the Second to the Third Long Period. It has been objected that this interpretation gives undue weight to the melting point data. The compressibilities* and interatomic distances suggest that there is little difference in valency on passing from Mo→Tc→Ru, or from W→Re→Os, but all the properties suggest that there is a much more rapid fall in valency on passing from Ru→Rh→Pd, and from Os→Ir→Pt, than in the corresponding change from Fe→Co→Ni.

§ 5. Alloys of the Transition Metals

In the absence of a satisfactory theory of the pure transition metals, it is only natural that there is at present no real quantitative theory of their alloys, and it is possible to see only the first signs of general qualitative principles. Some of these are described most clearly from the viewpoint of the collective electron (C.E.) theory, and others in terms of hypotheses of the Pauling type. In view of the differences of opinion about the valencies to be used in the latter, we shall refer to it as the R.V.B. (resonating valence bond) approach.

* For Tc and Re, only interatomic distances are available.

5.1. *Solid Solutions in Transition Metals*

Solid solutions in transition metals are subject to the size-factor principle first advanced for alloys of silver and copper (Hume-Rothery, Mabbott and Channell-Evans 1934), and if the atomic diameters of solvent and solute differ by more than about 15%, the solid solution is usually restricted to a few atomic per cent. This has been tested for iron alloys by Andrews (1952), for nickel alloys by Coles and Hume-Rothery (1951), and Pearson and Hume-Rothery (1951), for titanium alloys by Hume-Rothery (unpublished) and for chromium alloys by Sully, 1954. It should again be emphasized that the size-factor principle is a negative one, in the sense that an unfavourable size-factor restricts the extent of a solid solution, whilst a favourable size-factor merely permits the formation of a wide solid solution if other factors are also favourable. It is not justifiable to suggest that a wide solid solution will necessarily be formed if the size-factors are favourable; the formation of a wide range of primary solid solution is also prevented by a large electrochemical factor, and in alloys with electronegative elements (e.g. phosphorus, selenium) stable compounds are formed at the expense of the primary solid solution. It is not, however, possible to express this in quantitative terms, owing to an uncertainty as to which valency state of the transition metal is concerned. The effect of the relative valency of solvent and solute is considered in § 5.2 below.

The effects of unfavourable size-factor and electrochemical factor in preventing the formation of a solid solution in a transition metal are as described above. The atomic diameters of § 2.2 imply that in any one Period, the size-factors are very favourable for alloys of metals in Groups VI A, VII A, VIII A, B, and C with one another, and are still favourable for alloys of these groups with the corresponding element of Group V A, but on going back to Group IV A the zone of unfavourable size-factor is approached for Groups VI–VIII. For Groups IV A–VIII the atomic diameters of the elements of a given Group are so nearly the same for the Second and Third Long Periods that the same relations apply for alloys of these Periods with one another. The atomic diameters of the corresponding elements of the First Long Period are systematically smaller, but the values are such that any combination of metals of Groups VI A–VIII is within the favourable zone, although on passing to Group I B, the atomic diameters of silver and gold place them on the borderline of the favourable zone for the elements with the smallest atomic diameters (Cr, Fe, Co, Ni, Cu) in the First Long Period. These size-factors relations are reflected strikingly in the equilibrium diagrams of many of the binary systems.

It is a general principle that solid solutions in the close-packed hexagonal modifications of transition metals are much more restricted than those in the face-centred cubic or body-centred cubic forms. That this effect is electronic in origin is suggested by the fact that in the system Ti–Zr there are continuous solid solutions in both α (c.p. hexagonal) and β (b.c. cubic) modifications, although the size-factor is

here less favourable than in the systems Ti–Nb and Ti–Ta where there are continuous solid solutions between β-titanium and the body-centred cubic niobium or tantalum, but only slight solid solutions of these metals in α-titanium. The data are summarized in table 3 which shows that in every case (except Ti–Zr) the solubility is greater in β-titanium.

Table 3. Titanium Alloys

Solute and Group	Maximum solubility (atomic per cent)	
	α Ti (c.p. hex.)	β Ti (b.c. cube)
Al III A	38	49
Si IV A	0·8	5
Zr IV A	100	100
Sn IV B	10	12
V V	3 at 600°c	100
Nb V	2 at 600°c	100
Ta V	? 4 at 600°c	100
Cr VI	<0·5	100 at high temperatures
Mo VI	0·8 at 600°c	100
W VI	0·2	21
Mn VII	0·4	30
Fe VIII	<0·5	23
Co VIII	<1·0	10 ?
Ni VIII	<0·1	12
Cu I B	*ca.* 2	14
Ag I B	*ca.* 7	25 ?
Au I B	?	<25

Table 3 also shows that for elements in the same Period, there is a progressive diminution in solubility* on passing from V (100%)→Cr (100% at high temperatures only)→Mn (30%)→Fe (23%)→Co (*ca.* 10%). The change on passing from V→Cr may be ascribed to a less favourable size-factor since chromium is only just on the borderline, whilst vanadium is within the favourable zone. The further diminution on passing from Cr→Mn→Fe→Co† cannot be ascribed to size-factor effects, and there is a clear resemblance to the general diminution in solubility in copper with increasing separation in the Periodic Table of the solvent and solute in the series Cu–Zn, Cu–Ga, Cu–Ge, Cu–As.

* All compositions quoted are in atomic percentages.

† The data for cobalt are inaccurate and it is not possible to say whether there is really an increase on passing to nickel whose solubility in β-titanium is 12 atomic per cent.

With nickel as solvent a similar effect is shown on passing back along the Periodic Table, the values of the maximum solubility in this metal being Co (100%)→Fe (100% at high temperatures, superlattices at low temperatures)→Mn (100% at high temperatures, intermediate phases at low temperatures)→Cr (48%)→V (44%)→Ti (11%). The slight diminution on passing from Cr→V, and the much larger fall on passing to titanium can be ascribed to size-factor effects, but the remaining differences cannot be explained in this way. In the alloys of copper and silver with elements of well-defined valency, considerable generalization of the liquidus, solidus, and solid solubility data has been obtained (see Hume-Rothery and Raynor 1954) in terms of size-factor and valency, and for alloys of the transition metals with one another, there is a general tendency for the parts of the equilibrium diagrams which concern the primary solid solutions to be controlled by the size-factor, and the difference between the numbers of the Groups to which the solvent and solute belong, although precise numerical relations have not yet been discovered.

It is of interest to see whether the abnormalities in the sequence of physical properties of the elements occurring at manganese in the First Long Period are reflected in their behaviour in solid solutions. Figure 12 (*a*) which is due to Pearson (1951) shows the lattice spacing/composition curves for solid solutions of Ti, V, Cr, Mn, Fe, Co, and Cu in nickel. The lattice expansion at a given atomic percentage of solute diminishes rapidly on passing from Ti→V→Cr in agreement with the order expected from the atomic diameters, and the increasing atomic number. On passing to manganese there is a marked lattice expansion which becomes less pronounced on passing from Mn→Fe→Co, with a slight increase in expansion on passing to copper. The lattice spacing/composition curves for solid solutions in α-iron (Sutton and Hume-Rothery, unpublished), show an analogous effect ; the slopes of the curves diminish rapidly on passing from Ti→V→Cr, and again on passing from Mn→Co, but the curves for solid solutions of chromium and manganese in α-iron are nearly the same. For the solid solutions in nickel, the liquidus and solidus curves fall less and less steeply on passing from Ti→V→Cr, as would be expected from the size-factors and the relative positions of solvent and solute in the Periodic Table. On passing to manganese, the liquidus and solidus curves of the Ni-rich solid solution fall unexpectedly steeply, and then in the systems Ni–Fe, and Ni–Co there is a marked recovery. These results are summarised in figs. 12 (*b*) and 12 (*c*) which are due to Pearson, and when taken together with the lattice spacing data referred to above, they suggest that the abnormal behaviour of manganese in the sequences of physical properties (§ 2) is a real characteristic which is carried over into some alloys.

Figures 12 (*b*) and 12 (*c*) include also the liquidus and solidus curves for the solid solution of zinc and copper in nickel, and it will be seen that there is a close resemblance between the curves for manganese and zinc. This is

suggestive in view of the known stability of divalent manganous compounds involving the exactly half-filled $(3d)^5$ sub-group, and as shown below, there are other suggestions that in some composition ranges of the system Ni–Mn, the manganese is divalent.

Fig. 12

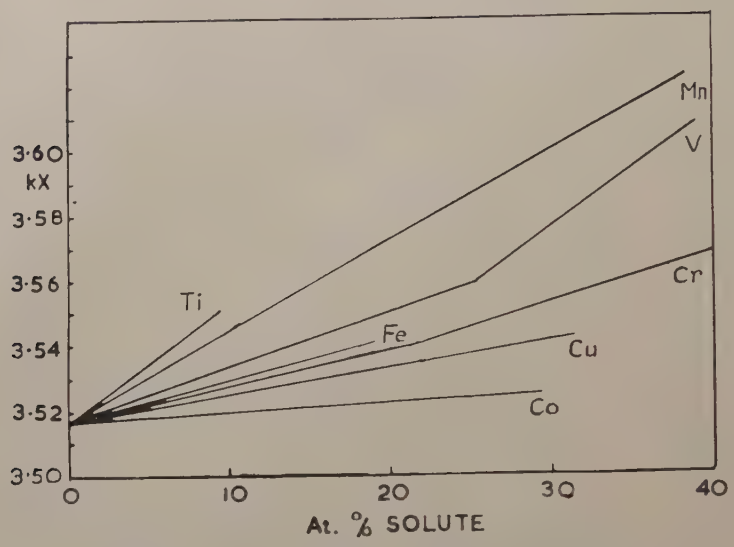

(*a*) Lattice spacing curves for nickel solid solutions.

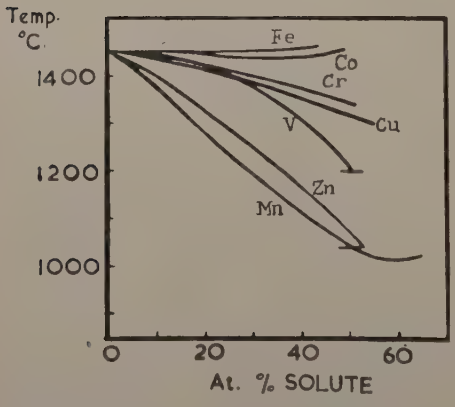

(*b*) Liquidus curves for nickel alloys.

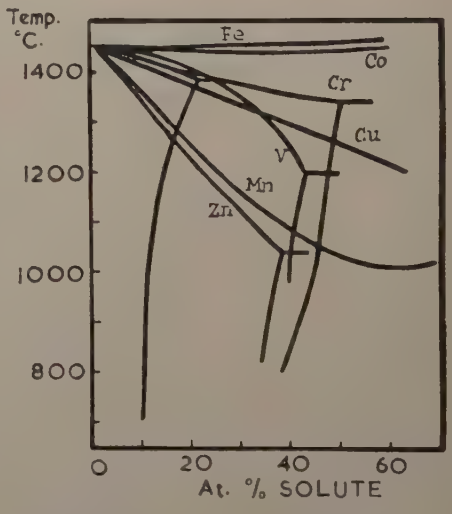

(*c*) Solidus curves for Ni alloys.

The concept of a stable $(3d)^5$ half-filled sub-group may also explain the curious effects found in alloys with copper. In the system Cu–Ni, there is a continuous solid solution which is readily understood from either the C.E. or the R.V.B. view points. In the systems Cu–Co and Cu–Fe the

solid solutions on both sides of the equilibrium diagrams are restricted (<10 atomic per cent), but a continuous solid solution is formed between γ-Mn and copper, and the latter element is appreciably soluble in δ-Mn. In contrast to this, copper and chromium are immiscible in both liquid and solid states. If manganese is divalent, and involves the exactly half-filled $(3d)^5$ sub-group, its bonding electrons will occupy (sp) hybrid orbitals, and we can understand why these mix readily with electrons of the same type in copper. Although the ground state of the free atom of chromium is $(3d)^5(4s)^1$, there are no stable univalent compounds of chromium, and as the size factors are all favourable the equilibrium diagrams suggest that the electrons in copper and chromium are in states which do not mix easily. There is much evidence for manganese acting as though it were a divalent element in some alloys, but this is not always the case, and there is direct evidence for the existence of univalent manganese in other alloys. The most conclusive example is found in the ferromagnetic alloys of the Heusler type (Bradley and Rodgers 1936), Cu_2MnAl, and Cu_2MnIn, where the saturation moment is $4\mu_B$ and indicates a $(3d)^6$ grouping with four electrons of unpaired spin (Coles, Hume-Rothery and Myers 1949). With the remaining manganese electron, the three electrons from each atom of aluminium or indium, and one electron from each atom of copper give an electron : atom ratio of 3 : 2 in agreement with the body-centred cubic structure—the structure is ordered. A study of the Mn-rich manganese–zinc equilibrium diagram by Coles (1950) strongly suggests that manganese is here univalent also.

5.2. *Alloys of Intermediate Composition*

Under this heading we shall include binary alloys lying outside the limits of a random solid solution, and within the composition range 25–75 atomic per cent of one constituent. In general, solid solution alloys of transition metals with one another tend to form superlattices to an extent which is much greater than would be expected from differences in atomic diameters or electrochemical characteristics. Thus superlattices are formed in systems such as Fe–Co and Fe–Ni where the atomic diameters and electrochemical characteristics are very similar. As explained previously (p. 179), the early ideas of Mott and Jones may provide an explanation of this. Alternatively, since these elements contain 1, 2 or 3 electrons fewer than the numbers required to form spherically symmetrical $(3d)^{10}$ electron clouds, it is conceivable that an ordered structure is taken up so that the ' bumps ' in the electron clouds of one kind of atom fit into the hollows in the electron clouds of the other kind. Although superlattices are formed in systems such as Fe–Co where the atomic diameters and chemical valencies are very similar, the general tendency for the ordered structures to become more stable as the size-factors increase is still found. Figure 13 shows the general types of equilibrium diagram in the systems Ni–Co, Ni–Fe, Ni–Mn, Ni–Cr, Ni–V, Ni–Ti. In the first four of these, the size factors are very favourable, and

the superlattices Ni_3Fe, Ni_3Mn and Ni_3Cr undergo disordering on heating to relatively low temperatures. In the system Ni–V the atomic diameters are 2·5 kx and 2·62 kx respectively, and the Ni_3V superlattice persists up to 1045°C and has a structure of the Al_3Ti type (fig. 14). In the system Ni–Ti, the Ni_3Ti phase with the DO 24 type of structure lies outside the limits of the face-centred cubic solid solution, and fig. 13 shows clearly how the increasing size-factor, and increasing difference between the positions of solvent and solute in the Periodic Table, unstable superlattices become more stable, and finally pass into intermetallic compounds.

Fig. 13

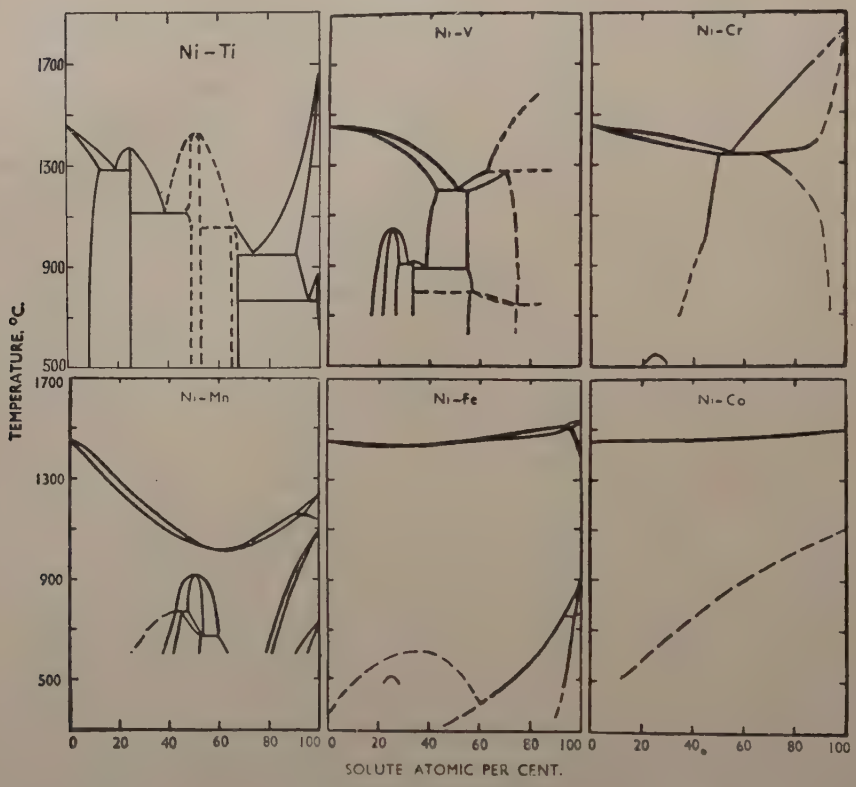

The Ni–Ti, Ni–V, Ni–Cr, Ni–Mn, Ni–Fe, and Ni–Co equilibrium diagrams (schematic).

The system nickel–vanadium is of interest in that apart from the usual tendency to form a superlattice at the compositions A_3B (Ni_3V denoted θ in fig. 15), a second type of ordered structure (δ) is formed at the composition Ni_2V. This structure is shown in fig. 16, and the system is remarkable for the way in which the random solid solution which extends to more than 40 atomic per cent at high temperatures, takes up different ordered arrangements at low temperatures. In fig. 15 the phase in the region 55–70 atomic per cent vanadium is denoted σ, and has the same general

Fig. 14

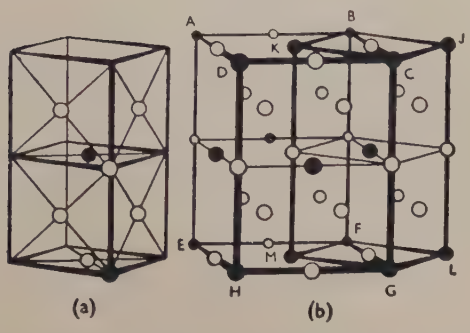

The $\theta(Ni_3V)$ Phase. (*a*) The unit cell; (*b*) the relationship of the 8-atom unit cell to the cell containing 16 atoms in terms of which Al_3Ti types of structure are generally described.

Fig. 15

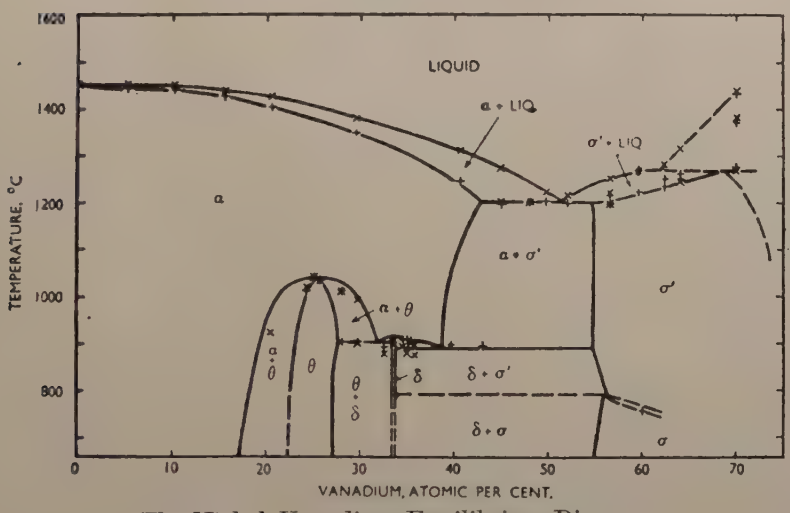

The Nickel–Vanadium Equilibrium Diagram.

Fig. 16

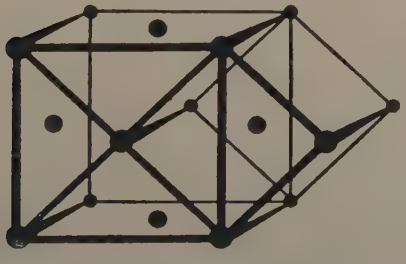

The $\delta(Ni_2V)$ Phase, showing the relationship of the f.c. monoclinic and b.c. orthorhombic unit cells.

type of structure as the equiatomic σ phase in the system Fe–Cr. This latter phase was at first thought to be of a superlattice type, but when it was discovered that phases with similar structures appeared in the system Cr–Mn in the region 75–80 atomic per cent manganese, and at a composition including NiV_2 in the system Ni–V, it was considered more likely to be an electron compound, and this interpretation was confirmed by the fact that the same structure is formed by β-uranium. The electronic structure of the σ-phases is not, however, understood. Attempts have been made by Sully (Sully and Heal 1948, Sully 1951) to interpret them on the assumption that the electrons from one kind of atom fill the holes in the ' atomic orbitals ' of the Pauling hypothesis. This interpretation appears to us improbable because (*a*) some σ-phases are ferromagnetic at low temperatures, and (*b*) as explained in § 4.9, the Pauling non-integral valencies and holes are not constants which can be carried over from one structure to another. Examination shows that other valency schemes will generalize the composition limits of the σ-phases as well as that based on the Pauling scheme, and for the present the structure is not understood.

In alloys of transition metals with elements such as zinc, aluminium, gallium, etc., phases are sometimes found whose structures are the same as some of the well-known ' electron compounds ' in copper and silver alloys. The best known examples of these are the well-known γ-brass structures which occur at compositions such as Ni_5Zn_{21}, Fe_5Zn_{21}, Mn_5Zn_{21}, in which the characteristic electron : atom ratio of 21 : 13 is obtained if a zero valency to the transition metal is ascribed. No great emphasis should be placed on a supposed exact zero valency of the transition metal in these compounds, because they are often of widely variable composition. Apart from this, the detailed examination of the γ-brass type of structure in the systems copper–aluminium (Bradley, Goldschmidt and Lipson 1938) and copper–gallium (Betterton and Hume-Rothery 1951, Hume-Rothery, Betterton and Reynolds 1951) has shown that, beyond a certain stage, increasing percentage of the element of higher valency results in the formation of a defect structure, in which atoms drop out of the lattice in such a way as to preserve a constant number of electrons per unit cell, the latter quantity being the real characteristic of Brillouin zone theory.* Until accurate measurements have been made of the lattice spacings and densities of these phases, it is not possible to be certain of the valencies of the transition metals. For the moment one can only say that, using the normal valencies (Zn, Cd 2 ; Al, Ga 3) the transition metal acts as though it exerted a low valency in phases such as Ni_5Zn_{21}. Attempts have been made to interpret these phases in terms of the Pauling valencies, but as shown by Betterton, Reynolds and Hume-Rothery (1951) these do not give such a good generalization as the normal valencies, and as emphasized in § 4.9 there is no reason to expect the non-integral valencies of any R.V.B. hypothesis to be constant in different structures.

* The empirical discovery of the electron concentration rules was possible only because most structures do not involve many lattice vacancies.

In copper, silver and gold alloys it is well known that body-centred cubic phases tend to occur at an electron concentration of 1·5, and this has been explained by the theory of Jones (1937). In some alloys with transition metals, body-centred cubic phases occur at compositions which correspond to an electron concentration of 1·5 if the transition metal exerts a zero-valency (e.g. NiAl, CoAl). It may be objected that the body-centred cubic phase can be formed for reasons quite different from those of electron concentration.* but the work of Bradley and Taylor (1937), and of Lipson and Taylor (1939) on defect lattices in NiAl is in such good agreement with the requirements of Brillouin zone theory (assuming zero valency for nickel) that it is highly probable that the number of valency electrons per unit cell is the controlling factor. In the system nickel–zinc, the body-centred cubic phase does not occur at the composition ($NiZn_3$) required by zero-valent nickel, but is found at the equiatomic composition NiZn. Coles and Hume-Rothery (1951) interpret this as indicating the existence of univalent nickel in the range of composition concerned, and there is indeed a close agreement between the forms of the Cu–Zn and Ni–Zn equilibrium diagrams in the equiatomic region. These investigators found that in the system Ni–Mn the body-centred cubic phase existed at high temperatures in the equiatomic region, so that manganese here behaved in the same way as zinc which is presumably divalent. The assumption of valencies merely to produce an electron concentration of 1·5 for body-centred cubic phases is admittedly not conclusive, but in so far as it is valid there is much evidence that nickel acts as a univalent element over a certain range of composition. On the other hand, although the solubility limit in the Ni-rich α-solid solution of the system Ni–Zn is what would be expected for univalent nickel and divalent zinc, the corresponding solubilities in the α-solid solutions of the systems Ni–Ga and Ni–Ge are not at the values expected for valencies of Ni 1, Ga 3, Ge 4. In so far as the assignment of valencies is valid in this type of alloy, it seems quite certain that the valency of nickel may vary from about zero in Ni_5Zn_{21}, to unity in NiZn, and then possibly to a higher value in nickel-rich alloys. It is probable that this behaviour is quite general, and that the valency of a transition metal may vary, not only from one system to another, but with the composition in any one system.

5.3. *Dilute Solid Solutions of Transition Metals in Other Metals*

With the exception of the alloys of Mn or Ni with copper, solid solutions of transition metals in other metals are generally limited. Some investigations have been carried out, however, on the effects of small amounts of transition elements on the $\alpha/\alpha+\beta$ and $\beta/\alpha+\beta$ boundaries in copper–zinc and copper–aluminium alloys (Hume-Rothery 1948, Hume-Rothery and Haworth 1952). The positions of these boundaries are controlled mainly

* Thus the alkali metals and barium are body-centred cubic.

by the condition that a constant valency-electron/atom ratio be maintained, so that from their behaviour in ternary alloys the electron contribution of the third element may be deduced. The effective valencies derived on this basis are shown in table 4. In the alloys with zinc, the apparent valencies of Ni, Co, and Fe are almost the same as the numbers of 4s electrons per atom in the crystals of these elements. Almost the same values are given by Fe and Co in the alloys with aluminium, but nickel behaves anomalously. In both zinc and aluminium alloys, manganese acts as though its valency were slightly less than 2.

Table 4

Valency	Cu–Zn		Cu–Al	
	$\alpha/\alpha+\beta$	$\alpha+\beta/\beta$	$\alpha/\alpha+\beta$	$\alpha+\beta/\beta$
Mn	1·83	1·83	1·91	1·93
Fe	1·0	1·0	1·1	0·9
Co	0·8	0·8	0·9	—
Ni	0·61	0·61	1·75	0·02

5.4. *Theoretical Models for Alloys*

In theoretical discussions of the alloys of normal metals a collective electron (C.E.) model is used. Thus the band structure of the γ-copper–zinc phase is regarded as common to all the atoms of the crystal, each type of atom contributing to this band a number of electrons equal to its conventional valency. In a similar way discussions of dilute solid solutions in magnesium (Jones 1949, 1950) assume that the band structure is essentially that of pure magnesium (modified only by the slight changes due to variations in the relative lattice dimensions), and that changes in concentration change only the extent to which this is occupied by electrons.

In discussing very dilute solid solutions of arsenic in germanium, however, it has been assumed (Mott 1951) that the extra electron provided by an arsenic atom enters a state described by a localized wave function based on this atom and not one in the conduction band. Friedel (1952 a, b) has suggested a related localized wave function (LWF) model for dilute solid solutions of zinc, gallium, etc., in copper, but this seems less successful than the collective band model (Jones 1937) in describing the behaviour of these alloys.

Resonating valence bond (RVB) models of the type discussed in § 4.9 have been applied only to the magnetic properties of transition metal alloys.

5.4.1. *The Collective Electron Model*

The C.E. model (applied to separate d- and s-bands) has been used by Wohlfarth in a number of papers (1948, 1949 a, b) in which the magnetic

properties of nickel alloys are discussed. Satisfactory agreement with experiment is obtained for nickel–cobalt alloys and nickel-rich nickel–copper alloys, 3d- and 4s-bands common to both types of atom in the alloy and of the character of those in pure nickel being assumed. It is to be noted that in each of these alloy systems the component metals are nearest neighbours in the Periodic Table. In the discussion of nickel–palladium alloys, bands of the same type were assumed to be formed by the 3d and 4s functions of the nickel atoms with 4d and 5s functions respectively of the palladium atoms.

Since both nickel and palladium have about 0·6 unoccupied d-band states a C.E. model would lead one to expect filled d-bands, and therefore diamagnetism, when the concentration of the Group I B metal exceeded about 60% in nickel–copper and palladium–silver alloys. It has been pointed out (Coles 1952) that such behaviour is in fact shown by the palladium–silver alloys, but that there is strong evidence for the existence of unoccupied 3d states in the copper-rich copper–nickel alloys. (Such evidence is by no means restricted to the magnetic properties, being supplied also by all the physical data available for these alloys.)

In the solid state both nickel and palladium may be represented as $(n-1)d^{9\cdot4}\,ns^{0\cdot6}$; but the free atom of nickel has the ground state $3d^84s^2$, whereas that of palladium is $4d^{10}$. This difference has been made the basis of an explanation of the behaviour of the above alloys suggested by Hume-Rothery (1952). Increasing freedom of the nickel atom leads to an increase in the number of unoccupied d-states per atom, while an opposite effect obtains for palladium; and since, in these alloy systems, the transition metal is entering a lattice of larger spacing and smaller ionic volume than its own, palladium can be expected to show a $4d^{10}$ configuration while nickel will tend towards the configuration $3d^84s^2$. On these grounds it might be expected that platinum (ground state $5d^86s^2$) would behave, in alloys, more like nickel than like palladium. Attention has been directed on p. 193 to the way in which the tendency of nickel to behave as univalent results in the appearance of a body-centred cubic β phase at the equi-atomic composition, and at higher temperatures, in the system nickel–zinc: this phase has been shown by Schramm (1938) to be markedly paramagnetic. In the closely related system palladium–cadmium a similar phase is found at about 60% cadmium (Nowotny, Stempfl and Bittner 1951); this seems, in general agreement with the above suggestion, to imply a smaller valency for palladium than for nickel in this type of alloy, although not a zero-valency. The palladium–zinc system (Koster and Zwicker 1951) is more complicated, with body-centred structures occurring on either side of a PdZn phase with the CuAu structure*; but only the solid solution of zinc in palladium is paramagnetic (Nowotny, Bauer and Stempfl 1950, 1951). Body-centred cubic phases are not found in the platinum–zinc and platinum–cadmium

* Similar structures are shown by NiZn (low temperatures), PdCd, PtCd, PtZn, PdHg, and PtHg.

systems, but a phase with the NiAs structure occurring in the latter at about 66% cadmium shows marked paramagnetism (Nowotny, Bauer, Stempfl and Bittner 1951). In the alloys of nickel, palladium and platinum with cadmium and zinc diamagnetic γ phases are found at compositions M_5Zn_{21} and M_5Cd_{21}, so that in all these the Group VIII C element would seem to be in a d^{10} state.

5.4.2. *The Localized Wave-Function Model*

In the above discussion of the breakdown of the C.E. picture in copper-rich nickel–copper alloys an L.W.F. picture for the d-electrons of the dissolved nickel atoms is implicit. For dilute solid solutions of transition metals in non-transition metals Jones (1953) has explicitly postulated that the d-electrons of the solute atoms are in localized states about their respective atoms, although there exists a conduction band, common to all atoms of the crystal, which may contain electrons contributed by the solute atoms. (In the terminology of the RVB models this conduction band is composed of (sp) hybrid states, as distinct from (spd) hybrids.) The number of electrons contributed to the conduction band by a solute transition metal atom will be the difference between the number of electrons in its localized d-states and the total number of its outer electrons. Jones showed that the former number should depend on the value of the Fermi energy in the conduction band, and suggested that this dependence provided an explanation of the valencies derived for transition metals in dilute solid solution (see §5.3) by Hume-Rothery and Haworth. On any simple L.W.F. picture these should be integral; but Jones pointed out that there are configurations of closely similar energy for nickel, a mixture of which might account for its apparently fractional valency. (The suggestion that non-suppressible ordering might modify the situation in some alloys arose from a misunderstanding of the experimental methods.)

It seems probable that an L.W.F. model should be appropriate even for dilute solid solutions of one transition metal in another, if they are not close neighbours in the Periodic Table, and a number of properties (some of which have already been discussed) seem to suggest that this is especially likely when the component metals of the alloy lie on opposite sides of the break observed in the properties of the elements. Thus an L.W.F. model has been suggested (Coles 1951) as a suitable basis for the discussion of the effects of small amounts of iron, cobalt, or nickel on titanium shown by the results of McQuillan (1951).

No theoretical models have yet been put forward for alloy phases where a transition metal is present to the extent of, say, 20–50% in alloys with a dissimilar metal. Interactions between the d-electrons of the transition metal atoms must certainly take place, but theory gives no indication of whether a d-band, which is a property of these randomly arranged atoms only, can be said to exist. A large linear term in the specific heat of copper–nickel alloys of this type* seems to point to the presence of

* See p. 229 for a discussion of the behaviour of the specific heat of the nickel-rich alloys.

such interactions, and of some type of band for the d-states of the nickel atoms only. Ferromagnetic interactions are shown clearly in gold–iron alloys containing as little as 6% of iron (Kaufmann, Pan and Clark 1945), but one would expect an L.W.F. treatment to be more appropriate than a collective band treatment for such alloys. Materials of this type might usefully be discussed in terms of R.V.B. models, but the application of these to alloys has been limited mainly to the discussion of ferromagnetic moments in terms of a variation of the number of electrons in a fixed number of atomic d-orbitals. Alloy formation in aluminium-transition metal systems has also been discussed in terms of these models, and this topic is considered fully in the section that follows.

§6. Alloys of Aluminium with the Transition Metals

6.1. *Introductory*

Aluminium alloys with many transition metals, and in most systems intermediate phases are formed which give rise to complicated equilibrium diagrams. These phases have aroused great interest because some of them occur in industrial alloys, and their intensive study has led to results of importance in the general development of alloy theory. In the present section we describe some of the phases found in alloys of aluminium with the elements Ti—V—Cr—Mn—Fe—Co—Ni—Cu. Previous reviews on some aspects of this subject have already been published (Raynor 1949), but some of these involve an interpretation which appears to us to be improbable or incorrect, and the following survey is therefore submitted. As the theoretical interpretation is a matter of acute controversy, we have as far as possible separated the facts from their interpretation.

6.2. *The Equilibrium Diagrams*

Figures 17 (*a*) to 17 (*e*) show the equilibrium diagrams of the alloys of aluminium with the above series of elements, and the following points may be noted :—

6.2.1. *Aluminium–Titanium and Aluminium–Vanadium*

The aluminium-rich phases are of the same composition Al_3Ti, Al_3V, and crystal structure (p. 191). The complete equilibrium diagram of the system Al–V is not known, and is much needed. The system Al–Ti is remarkable for the wide solid solutions* of aluminium in both α-Ti (c.p. hex) and β-Ti (b.c. cube), and in the intermediate γ-phase, and it is one of the few systems in which the formation of a substitutional solid solution raises the temperature of the $\alpha \rightleftarrows \beta$ transformation. The diagram suggests that the two kinds of atom resemble one another more

* Many metals of appropriate atomic diameter are soluble in β-Ti, but very few in the c.p. hexagonal Ti.

Fig. 17

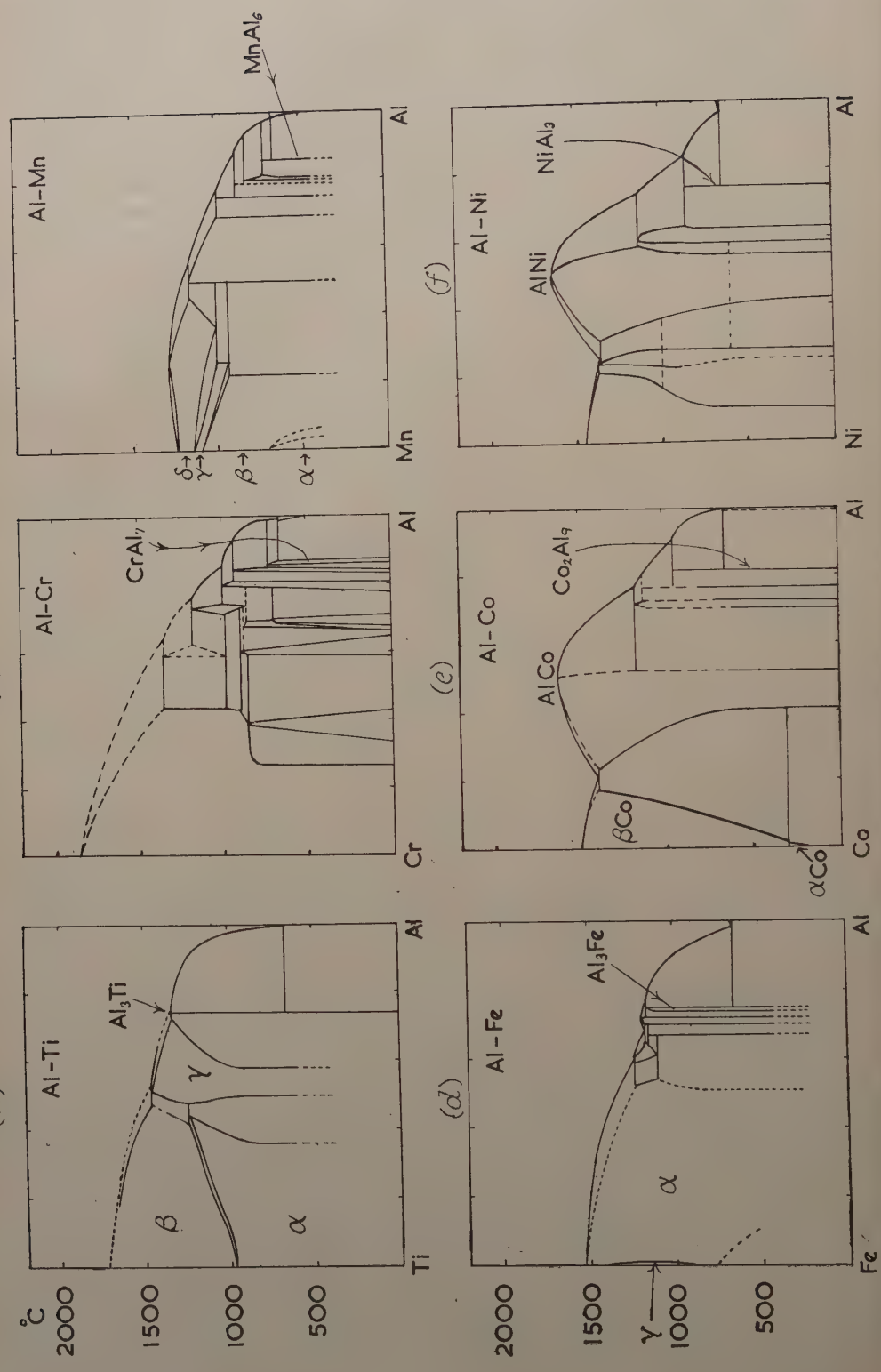
(a)
Al-Ti
Al3Ti
β
γ
α
Ti
Al
°C
2000
1500
1000
500
(b)
Al-Cr
CrAl7
Cr
Al
(c)
Al-Mn
MnAl6
δ→
γ→
β→
α→
Mn
Al
(d)
Al-Fe
Al3Fe
α
γ
Fe
Al
(e)
Al-Co
Co2Al9
AlCo
βCo
αCo
Co
Al
(f)
Al-Ni
NiAl3
AlNi
Ni
Al

than would be expected, and it is possible that this is due to a continuation of the well-known diagonal principle

Li Be
↘ ↘
Na Mg Al
. . .
Ti.

6.2.2. *Aluminium–Chromium and Aluminium–Manganese*

These equilibrium diagrams resemble one another in that, on the aluminium-rich sides, there are numerous intermediate phases formed by peritectic reactions, whilst the phases with the highest proportion of aluminium are Al_7Cr and Al_6Mn, in contrast to those of the type Al_3X in the vanadium and titanium alloys. Aluminium is freely soluble in chromium and δ-manganese, the maximum solubility being of the same order (45 atomic per cent) in each of these body-centred cubic solvents. It is also soluble in γ- and β-manganese, but almost insoluble in α-manganese. In each system the solubility of the transition metal in aluminium is small.

6.2.3. *Aluminium–Iron*

On passing from (Al–Mn)→(Al–Fe) the aluminium-rich compound reverts to the composition Al_3X of the alloys* with titanium and vanadium. The solubility of iron in aluminium is very small, but aluminium is freely soluble in body-centred cubic α-iron, and the solid solutions give rise to the well-known Fe_3Al and FeAl types of superlattice (Bradley and Jay 1932). As explained on p. 161 the saturation moment of iron is reduced by 2·22 μ_B for each atom of aluminium entering into solid solution. The equilibrium diagram of the iron-rich alloys is of the closed γ-loop type, and the maximum solubility of aluminium in γ-iron is only 2 atomic per cent.

6.2.4. *Aluminium–Cobalt and Aluminium–Nickel*

The equilibrium diagrams of these two systems resemble each other in many respects. The solubilities of both cobalt and nickel in aluminium are very small. Aluminium is almost insoluble in close-packed hexagonal α-cobalt, but is freely soluble in the face-centred cubic β-cobalt, and also in nickel. As stated on p. 161 the saturation moment of nickel is reduced by 3 μ_B for each atomic substitution of aluminium, and the behaviour in cobalt is similar, so that in each case the holes in the d-band are filled by valency electrons from aluminium. Each system contains a body-centred cubic phase whose freezing point rises to a high maximum at the equiatomic composition. On the aluminium-rich side, the system

* According to Bradley and Taylor (1938) the phase Al_3Fe decomposes at low temperatures into Fe_2Al_7 and Fe_2Al_5, but Dr. W. H. Taylor informs us that this has not been confirmed by recent work at the Cavendish Laboratory and at Birmingham.

Al–Ni has phases based on the composition Al_3Ni_2 and Al_3Ni, so that considered empirically the phases in this system contain 3 atoms of aluminium with 1, 2, and 3 atoms of nickel respectively. The system aluminium–cobalt contains phases based on the composition Al_5Co_2, $Al_{10}Co_3$, and Al_9Co_2, so that when the equiatomic phase is included, there are phases containing 10 atoms of aluminium with 4, 6, and 10 atoms of cobalt.

6.2.5. *Aluminium–Copper*

On the copper-rich side, this system shows the well known α, β, and 'γ'-phases whose general relations are well understood in terms of electron theory. On the aluminium-rich side, the maximum solubility of copper in aluminium is 2·5 atomic per cent at the eutectic temperature. The first intermetallic phase is based on the composition $CuAl_2$, although the exact whole number atomic ratio lies slightly to the copper-rich side of the homogeneous region. This is the only phase considered in the present section.

From the above survey it will be seen that in these alloys, the intermediate phases with the highest proportion of aluminium are based on the compositions :

$$Al_2Cu–Al_3Ni–Al_{4\cdot5}Co–Al_3Fe–Al_6Mn–Al_7Cr–Al_3V–Al_3Ti.$$

Considered empirically there is a clear suggestion of a sequence 2, 3 . . .6, 7 for the number of aluminium atoms associated with one atom of the transition metals from copper to manganese, except for a slight irregularity in the region of Co–Fe. This tendency was first pointed out by G. V. Raynor (1949), and it may be expressed empirically by saying that (except for iron) the number of atoms of aluminium associated with one atom of a transition metal is equal to the number of steps in the Periodic Table from the metal concerned to Group III B.

6.3. *Melting Point Relations*

When an intermetallic compound melts without decomposition, its melting point is an indication of the ability of the structure to resist thermal vibration, and is usually a rough measure of the strength of the interatomic bonding. When an intermetallic compound melts with a peritectic decomposition, the temperature of the peritectic horizontal involves equilibrium between one liquid and two solid phases, and is no indication of the strength of the interatomic bonding of the melting phase. Thus in fig. 18 the compound X melts with decomposition at the peritectic temperature t_1 to form liquid of composition B, and solid of composition Y. The equilibrium (Liquid B+Solid Y$\rightleftharpoons$Solid X) involves the free energies of both solid X and solid Y as well as that of the liquid phase. In fig. 18 AB is the portion of the liquidus that of the liquid phase. In fig. 18 AB is the portion of the liquidus involving equilibrium with solid X, and if the composition B of the liquid

at the peritectic horizontal is not too far from X, we may extrapolate the liquidus AB until it reaches the composition X at the temperature t_2. The temperature t_2 may be regarded as that at which X would melt without change of composition, if it were not for the intervention of the phase Y. For convenience we shall call such temperatures the E.C. (extrapolated congruent) melting points, and in so far as melting points may be used as a rough measure of interatomic bonding, we suggest that it is E.C. rather than the peritectic temperatures which should be used ; this procedure is

Fig. 18

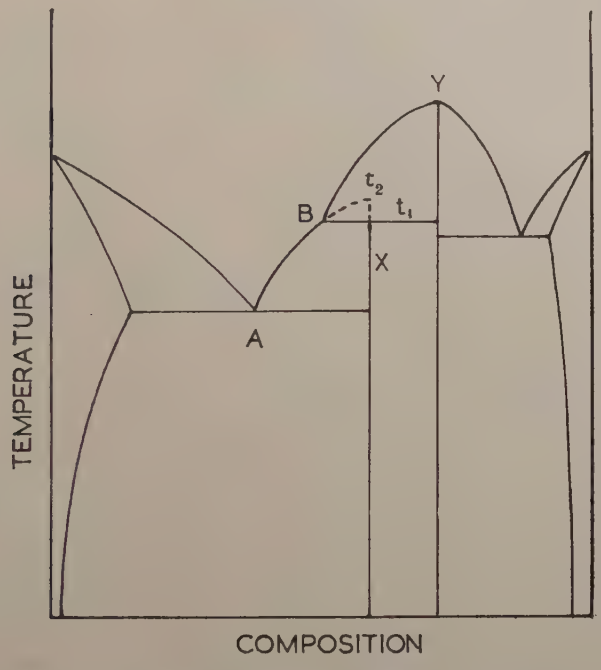

Extrapolated congruent melting point for a compound melting with peritectic decomposition.

admittedly an approximation, and the extrapolated values should not be compared too closely.

In fig. 19 we show the melting points of the intermediate phases which melt without change of composition, together with the peritectic and E.C. melting point temperatures where peritectic horizontals are involved. The following points may now be noted.

(*a*) In the nickel alloys the E.C. melting point of $NiAl_3$ is very slightly above the straight line joining the melting points of the pure metals. With increasing nickel content, there is a rapid rise in the melting points, and the E.C. points for $NiAl_3$, Ni_2Al_3, and NiAl* lie on a straight line rising markedly above that joining the points for the pure metals.

* NiAl melts without change of composition.

Fig. 19

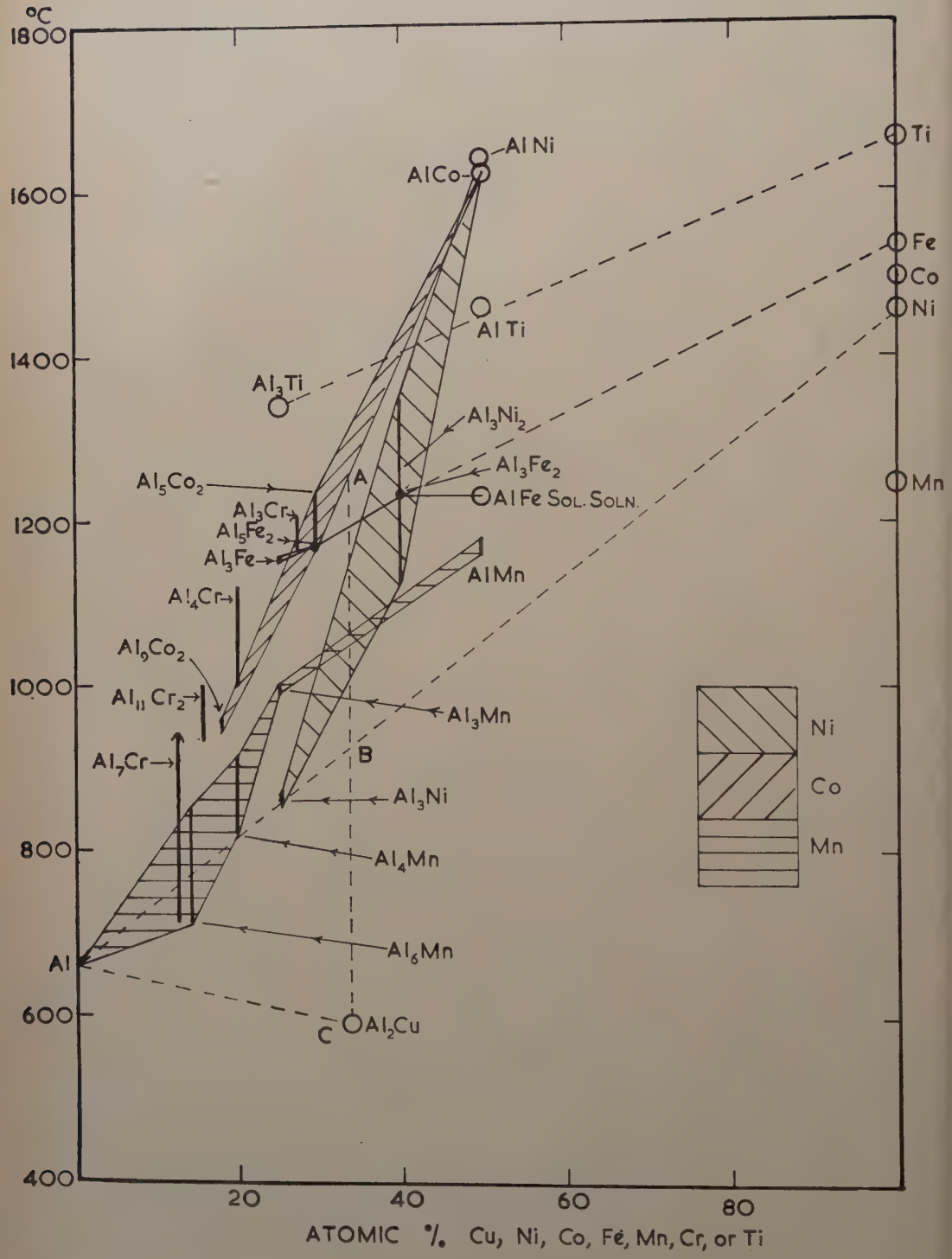
°C
1800
1600
1400
1200
1000
800
600
400
Al Ni
Al Co
Al Ti
Al₃Ti
Al₃Ni₂
Al₃Fe₂
Al Fe Sol. Soln.
Al₅Co₂
Al₃Cr
Al₅Fe₂
Al₃Fe
Al₄Cr
Al₉Co₂
Al₁₁Cr₂
Al₇Cr
Al Mn
Al₃Mn
Al₃Ni
Al₄Mn
Al₆Mn
Al₂Cu
A
B
C
Al
Ti
Fe
Co
Ni
Mn
Ni
Co
Mn
20
40
60
80
ATOMIC % Cu, Ni, Co, Fe, Mn, Cr, or Ti

(*b*) The melting points of NiAl and CoAl are very nearly the same, but the E.C. melting points (and also the peritectic temperatures) for the aluminium-rich cobalt phases are systematically higher than those for the nickel phases. The points for Co_2Al_9, Co_2Al_5, and CoAl are an almost linear function of the composition, and the straight line passes almost through the melting point of aluminium.

(*c*) The points for $FeAl_3$ and Fe_2Al_5 are very near to those for cobalt alloys of similar compositions, but the points for FeAl is almost 400°c lower than those for CoAl and NiAl.

(*d*) The E.C. melting points for $MnAl_6$, $MnAl_4$, and $MnAl_3$ are below those for cobalt alloys of similar composition, and the MnAl point is about 100°c below that for FeAl. The points for the chromium phases are above those for cobalt, whilst that for $TiAl_3$ is even higher. The manganese points are thus lower than would be expected from those for alloys with adjacent elements.

(*e*) The point for $CuAl_2$ lies below the straight line joining the points for Al and $NiAl_3$, and this difference (denoted BC in fig. 19) is equal to the length AB where A is the point corresponding to a hypothetical $CoAl_2$ in the cobalt series. The point for $NiAl_3$ is thus almost exactly half way between what would be expected from the values for the cobalt alloys and for $CuAl_2$.

The significance of these relations is discussed later.

6.4. *Crystal Structures and Interatomic Distances*

(*a*) $CuAl_2$.—The crystal structure of $CuAl_2$ is shown in fig. 20. The structure is tetragonal, space group D_{4h}^{18}, with cell constants $a=6{\cdot}05$ (2), $c=4{\cdot}87$ (8), $c/a=0{\cdot}806$. Homogeneous alloys always contain excess of aluminium above the ideal composition $CuAl_2$, but it is not known whether this is due to copper atoms dropping out from the lattice, or to substitutional or interstitial solution of excess atoms of aluminium.

The structure of fig. 20 is such that the copper atoms form vertical chains, the length of the Cu—Cu bond being 2·44 kx, which is distinctly less than the distance in metallic copper (2·55 kx), and this is the real characteristic of the structure. Each copper atom has 8 aluminium neighbours at 2·59 kx, these being arranged in two squares set at an angle of 45° to one

Fig. 19. The melting points of the aluminium-transition metal phases are plotted against the compositions in atomic percentages. In cases where the phase melts with decomposition at a peritectic horizontal, the phase is represented by a thick vertical line, of which the lower end represents the peritectic temperature, and the upper end gives the extrapolated congruent (E.C.) melting point (see p. 201). The E.C. melting points are often only approximate. The points for the systems Al–Ni, Al–Co and Al–Mn are enclosed in shaded regions for easy distinction; these regions give a rough indication of the variation of melting point with composition in the systems concerned, but they are of course *not* actual curves from the equilibrium diagrams. The oblique dotted lines show how certain points extrapolate approximately linearly to the values for the transition metals concerned. The vertical dotted line is referred to in (*e*) above.

another. This distance is less than would be expected from the atomic radii of aluminium, and copper (1·43+1·27=2·70 kx), but is approximately that expected for a structure in which Brillouin zone overlaps are not concerned,* since in this case the atomic radius of aluminium is 1·35 kx, and the expected Cu–Al distance is 1·35+1·27=2·63 kx.

The aluminium atoms are arranged in pairs with an Al–Al bond length of 2·71 kx, the normal length expected in the absence of Brillouin zone overlap effects. Each aluminium atom has also two Al neighbours (Al IV) at 2·90 kx, and four Al neighbours (Al V) at 3·09 kx arranged above one another in planes above and below, whilst in its own plane there are four Al neighbours (Al VI) at 3·22 kx.

Fig. 20

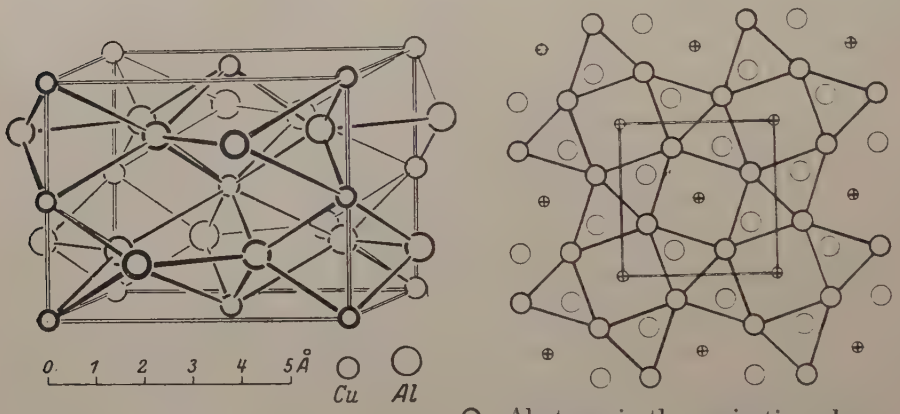

○ Al atoms in the projection plane.
⊕ Cu atoms C/4 above and below the projection plane.
○ Al atoms C/2 above and below the projection plane.

The $CuAl_2$ type of structure is formed in several other binary metallic systems including Nu_2Au, Pb_2Au, Pb_2Pd, Pb_2Rh, Ge_2Fe, Sn_2Fe, Sn_2Co, Ni_2B, Fe_2B. According to Wallbaum (1935) these are all characterized by a constant value of the parameter which determines the position of the B atoms in the cell of the AB_2 compound. This appears most improbable, and a more detailed determination of the crystal structures is desirable. The theoretical significance of these structures is dealt with later.

(*b*) $NiAl_3$.—The structure is orthorhombic (Bradley and Taylor 1937 b), space group C_{2h}^{16}, with cell constants $a=6·5982$, $b=7·3515$, $c=4·8021$ kx. Each nickel atom has 8 close neighbours at distances between 2·42 and 2·52 kx, and a ninth at 2·72 kx. The sum of the normal atomic radii is 1·43+1·25=2·68 kx, whilst if the value for aluminium is taken to be 1·35 kx in the absence of Brillouin zone effects, the sum is 2·60 kx. The interatomic distances thus involve a distinct contraction. Figure 21 shows the arrangement of the aluminium atoms round each nickel atom;

* See Hume-Rothery and Raynor (1940).

the structure contains layers of aluminium atoms, and also distorted hexagonal rings with alternate neighbours of nickel and aluminium. The aluminium atoms are divided into two structural types, in each of which the atom has two close nickel neighbours (2·42–2·46 kx), and one nickel neighbour at a greater distance (2·52 or 2·72 kx). Each aluminium atom has six aluminium neighbours at distances varying from 2·72–2·87 kx ; these distances are the normal values to be expected for varying degrees of Brillouin zone overlap. The average Ni–Al distance is 2·46 kx, and according to Bradley and Taylor (1937) the same average value is found for the eight Ni–Al close distances of approach in Ni_2Al_3, whilst in the caesium chloride structure of Ni–Al the Ni–Al distance is 2·49 kx.

Fig. 21

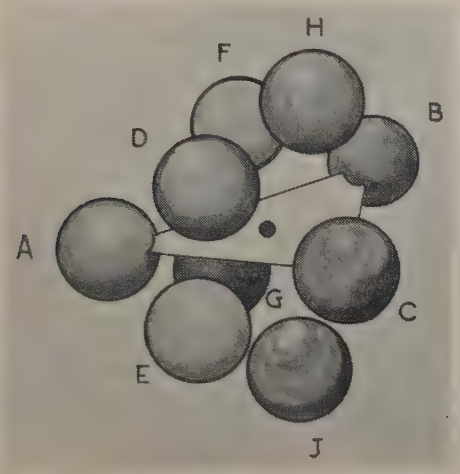

To illustrate the arrangement of aluminium atoms round a nickel atom in $NiAl_3$. The atoms A, B, C, are in a horizontal plane containing the nickel atom ●. The atoms D, F, and H are vertically over E, G, and J respectively.

(*c*) Co_2Al_9.—This crystal structure has been studied in detail by Douglas (1950). The structure is monoclinic, space group $P2_1/a$, and the cell constants are $a=8{\cdot}5392$, $b=6{\cdot}277$, $c=6{\cdot}2005$ kx, $\beta=94{\cdot}760°$. As shown in fig. 22 the structure contains well-defined crumpled* layers of aluminium atoms, between which the cobalt atoms lie so that each has nine aluminium neighbours. The arrangement round a cobalt atom is illustrated in fig. 23, from which it will be seen that six of the aluminium neighbours form almost (but not necessarily exactly) a trigonal prism,† whilst the remaining three lie in a plane half way between the top and bottom of the prism. The Al–Co distances vary between 2·37 and 2·53 kx, and are thus appreciably shorter than would be expected from the sum of the atomic radii (1·43+1·25=2·68 kx), and are also shorter

* We use the expression crumpled to denote that the atoms are not exactly in one plane.

† The symmetry does not require an exact trigonal prism.

Fig. 22

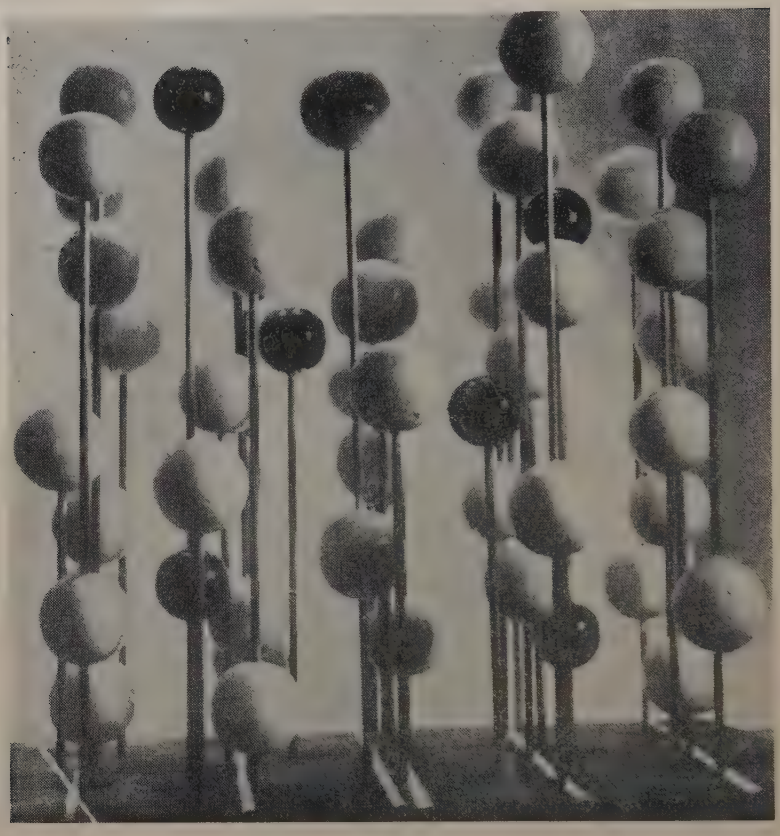

Fig. 23

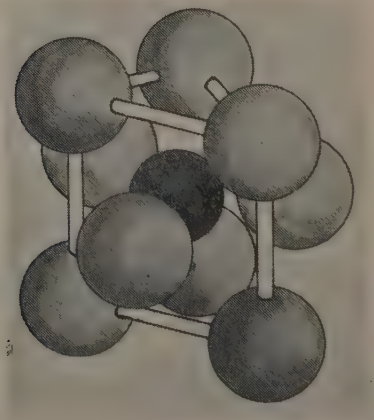

Co_2Al_9. Idealized structure to show arrangement of Al atoms round a Co atom. Each Co atom has 9 Al neighbours. Of these 6 may be regarded as occupying the corners of a trigonal prism (but see footnote on p. 205). The other 3 go round the prism roughly as shown.

than those expected on the assumption that aluminium has the atomic radius 1·35 kx corresponding to an absence of Brillouin zone overlap. This is in contrast to the Cu–Al distances in $CuAl_2$, but resembles the shortening of the Ni–Al distances in $NiAl_3$. In Co_2Al_9 each aluminium atom has two cobalt neighbours, and the aluminium atoms are divided into five structural types, of which three have seven close Al neighbours, and the others eight and ten respectively. The Al–Al distances vary from 2·70–2·94 kx, so that the characteristic value 2·70 kx again appears, whilst the general range of values is much the same as in $NiAl_3$.

In the work of Douglas, electron counts were made in order to estimate the numbers of electrons associated with the atoms, and it was estimated that the cobalt atoms contained about 29 electrons, i.e. 2 more than the atomic number (27), whilst the values for the aluminium atoms varied

Fig. 24

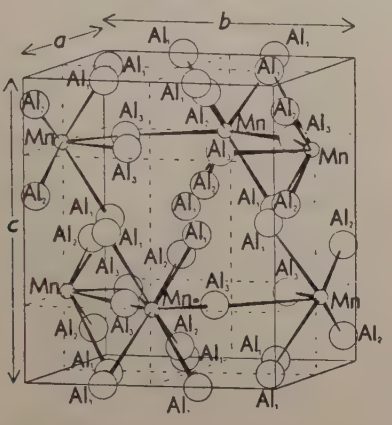

Distribution of atoms in the unit cell of $MnAl_6$. The bonds between the manganese atoms and their aluminium neighbours are shown.

between 11·6 and 12·9 as compared with an atomic number of 13. These values depend on the assumption that the electron density falls to zero between the atoms, and as pointed out by Douglas, a uniform distribution of 2·5 electrons per atom throughout the cell would reduce the number of electrons per cobalt peak from 29 to 27. The results of the electron counts are thus not yet conclusive, although they may be regarded as disproving the suggestion of Pauling (1951) that the aluminium atoms have absorbed electrons from the cobalt.

(*d*) $MnAl_6$.—The crystal structure of this compound has been studied in detail by Nicol (1953), and is orthorhombic, space group D_{2h}^{17}, with cell constants $a=6{\cdot}4847$ kx, $b=7{\cdot}5366$ kx, $c=8{\cdot}8524$ kx (all $\pm 0{\cdot}0005$). The distribution of atoms in the unit cell is shown in fig. 24, and as can be seen from fig. 25 the structure contains closely-packed slightly puckered layers of aluminium atoms parallel to the (101) planes. Each manganese atom has ten aluminium neighbours of which two, denoted Al_2 in fig. 24, are at 2·43 kx, and the remaining eight are at distances

from 2·54–2·64 kx. The bond length 2·43 kx is undoubtedly shorter than would be expected from the normal values, although it is larger than the closest Co–Al distance of approach in Co_2Al_9.

The aluminium atoms divide themselves into three structural types Al_1, Al_2, and Al_3, and the general environment of a manganese atom is shown in fig. 26. Each aluminium atom has 11 close neighbours, but whereas for the Al_1 and Al_3 atoms these consist of (2 Mn + 9 Al), the neighbours of an Al_2 atom are (1 Mn + 10 Al). The Al_2 atoms have the closest distances of approach both to Mn atoms (2·43 kx) and to each other, the length of the Al_2–Al_2 bond being 2·57 kx, which is slightly greater than that for a normal co-valent bond (2·53 kx). The Al_2 atoms form chains through the structure, the arrangement in these chains being as shown in fig. 27. The remaining Al–Al distances in the structure vary from 2·54–2·89 kx.

Fig. 25

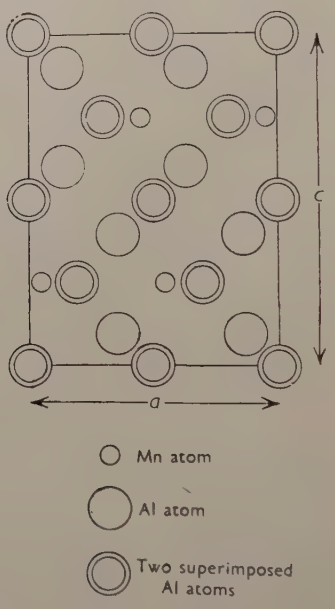

Projection of $MnAl_6$ structure down *b*-axis.

Electron counts were made for this structure and suggested that the electron peaks for the Mn atoms were associated with 27–28 electrons, and those for the Al atoms with from 10·7–11·8 electrons. The background intensity was allowed for, and the results show that there is no transference of electrons from the manganese to the aluminium atoms, but the accuracy and justification of these methods is at present under discussion.

(*e*) V Al_3 *and* Ti Al_3.—The $TiAl_3$ type of structure has already been shown in fig. 14 in connection with the Ni_3V (θ) phase of the NiV system.

Fig. 26

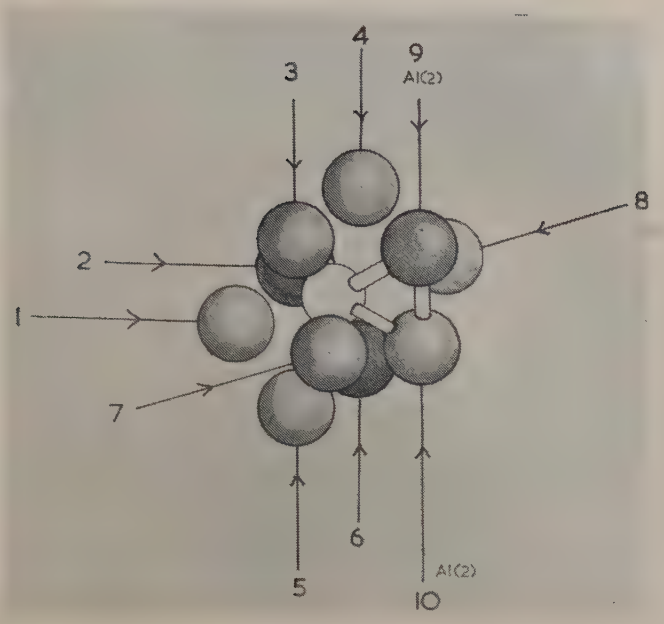

$MnAl_6$. To illustrate the arrangement of aluminium atoms around each manganese atom.

Atoms 3, 4, 5, and 6 are approximately at the corners of a vertical square with the manganese atom at its centre. Atoms 1, 2, 7, and 8 nearly form a corresponding horizontal square, but atoms 7 and 8 are displaced outwards to admit the pair of Al(2) atoms 9 and 10.

Fig. 27

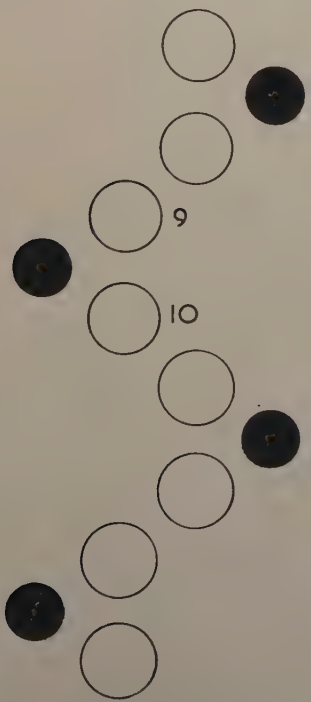

$MnAl_6$. To illutrate chains of Al(2) atoms through the structure. The Al atoms numbered 9 and 10 are those numbered 9 and 10 in fig. 26.

In $TiAl_3$, each Ti atom has 12 Al-neighbours, of which 4 are at 2·71 kx, and 8 at 2·88 kx. These may be compared with the value of (1·43+1·47=2·90 kx) expected from the normal atomic radii, whilst in the absence of effects due to Brillouin zone overlaps the values would be (1·35+1·47=2·82 kx).

6.5. *Ternary Alloys of Transition Metals with Aluminium*

The ternary alloys of aluminium with transition metals have aroused great interest because of their relation to the more complex industrial alloys in which small amounts of various transition metals are very often present. Much valuable work has been carried out by G. V. Raynor and his collaborators, who have devised elegant methods for the electrolytic extraction of single crystals of intermediate phases from ingots cooled under suitable conditions. Unfortunately the understanding of this work is difficult, and in the present section, only a few points will be dealt with. It is much to be hoped that further work of this type will make possible a clear interpretation of the data available.

The structure of the phase Co_2Al_9 has been described on p. 206. It was shown by Bradley and Taylor (1938) that in the ternary system Fe–Ni–Al a phase with the same structure occurred at the composition $FeNiAl_9$, so that one atom of iron and one of nickel appeared to be equivalent to two atoms of the intervening element cobalt. Raynor and Pfeil (1946) show that in the system Al–Co–Ni, the cobalt in Co_2Al_9 can be replaced by nickel, the substitution taking place atom by atom so that the aluminium content remains unchanged. In the system Al–Co–Fe the work of Raynor and Waldron (1948) shows that a similar substitution of iron for cobalt can take place in Co_2Al_9. These investigators and also Raynor and Pfeil (1946) suggest that the system Al–Fe–Ni can be regarded as built up from the two systems Al–Co–Fe and Al–Co–Ni on the principle that (2Co=Fe+Ni). This correspondence is shown in fig. 28, in which (*b*) shows the 600°c isothermal of the system Fe–Al–Ni drawn in the form of the usual equilateral triangle, whilst fig. 28 (*a*) shows the 600°c isothermals of the systems Al–Co–Fe and Al–Co–Ni in the form of triangles with angles of 90°, 60°, and 30° respectively. In fig. 28 (*a*) the point E represents the binary compound Co_2Al_9, whilst the heavy line EF parallel to BD indicates an atom for atom substitution of nickel for cobalt until about 2/3 of the latter is replaced. The heavy line EG indicates similar substitution of iron for cobalt until 1/3 of the latter is replaced. In fig. 28 (*b*) the point H represents the composition $FeNiAl_9$ and the heavy line HJ indicates an atom for atom substitution of nickel for iron, the point J lying in almost the same position as the point F in fig. 28 (*a*). The heavy line HK indicates an atom for atom substitution of iron for nickel in $FeNiAl_9$, but this proceeds only to about one half the extent expected from fig. 28 (*a*). The general correspondence between the two halves of fig. 28 is, however, striking. The same figure shows that in $FeAl_3$ the iron may be replaced atom for atom by cobalt or nickel, the extent to which this replacement

continues being roughly twice as great for cobalt as for nickel. In contrast to this, the phase Al_3Ni dissolves only a little cobalt by atom for atom substitution, whilst in the system Al–Ni–Fe the solution of iron in Al_3Ni takes place so that three atoms of nickel are replaced by two of iron, and one of aluminium.*

Fig. 28

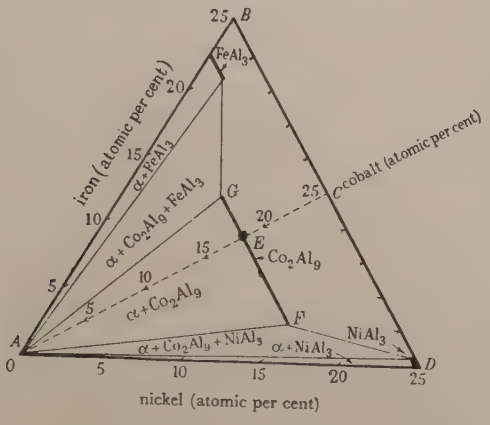

(*a*)

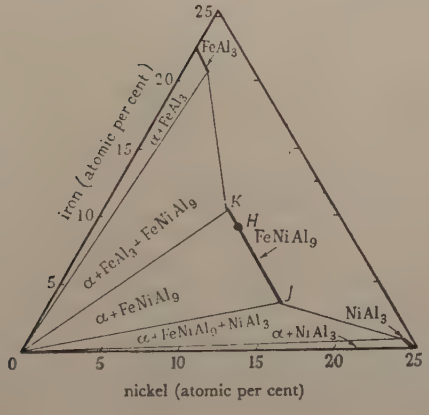

(*b*)

The above analogies would lead us to expect the ternary system Al–Fe–Ni to contain a phase $FeNiAl_5$ isomorphous with Co_2Al_5. This has not been found so far, but according to Bradley and Taylor (1938)† alloys of composition near to Fe_3NiAl_{10} have a structure similar to

* This can be seen clearly from fig. 15 (*a*) of Raynor and Pfeil's paper, *J. Inst. Met.*, 1946/7, **73**, 387.

† The diagrams of fig. 28 refer to very slowly cooled alloys, and not to conditions of true equilibrium, but the general form is probably correct.

Co_2Al_5, so that here the fundamental ratio (2 Transition : 5 Al atoms) is maintained, although the principle of (2Co=Fe+Ni) no longer holds. With higher percentages of iron and nickel there is a continuous range of body-centred cubic solid solutions extending from AlNi to AlFe, and according to the diagram of Bradley and Taylor (1938), the phase boundaries of this on the aluminium-rich side, although showing slight changes of direction at the points where equilibrium with different phases are involved, run roughly parallel to the Ni–Fe side of the triangular diagram, so that a general tendency to maintain a constant ratio of (Transition : Al atoms) persists, and the experimental work suggests strongly that one of the main characteristics of the systems Al–Co–Fe, Al–Co–Ni, and Al–Fe–Ni is the formation of phases whose composition limits correspond to constant ratios of (Transition : Al) atoms.

The work of Raynor and his collaborators has shown that somewhat similar principles underlie some of the ternary alloys of aluminium, manganese, and a third element. In the systems Al–Mn–Cu and Al–Mn–Ni (Raynor 1944), the compound $MnAl_6$ dissolves little or no copper or nickel. In the system Al–Mn–Co, the compound $MnAl_6$ dissolves a small amount of cobalt* but the compositions by analysis do not indicate a direct replacement of manganese by cobalt, atom for atom. In contrast to this, the data for the system Al–Mn–Fe show that manganese in $MnAl_6$ may be replaced by iron up to a maximum of 50% ; the replacement is by simple atom for atom substitution, and the composition of the phase remains at a constant atomic percentage of aluminium. In the system Al–Mn–Cr (Raynor and Little 1945) practically no chromium dissolves in $MnAl_6$, so that, as far as this phase is concerned, only iron is able to replace manganese readily. The work of Raynor and Wakeman (1947) shows, however, that in the system Al–Mn–Zn, a little zinc does dissolve in $MnAl_6$, the limiting solubility being of the order $Zn_{0\cdot03}Mn_{0\cdot96}Al_6$. The theoretical significance of this reversal of behaviour on passing from copper to zinc is referred to later.

Although in the system Al–Mn–Cr, there is practically no solubility of chromium in $MnAl_6$, there is wide solubility of manganese in both $CrAl_7$ and Cr_2Al_{11}, and there are several other suggestions that in this class of alloy a given transition atom is replaced more readily by one of slightly higher atomic number than by one of lower atomic number.† The behaviour of Cr_2Al_{11} and $CrAl_7$ is shown in fig. 29, and is extremely interesting. The structures of these two compounds are unknown but are very similar,‡ and the results in fig. 29 show that the solution of manganese in $CrAl_7$ does not take place atom for atom.§ The same

* The analysed composition of the extracted crystals was Mn 24·45%, and Co 1·7% by weight.

† Cf. the solubility of Fe and Ni in Co_2Al_9 as shown in fig. 28.

‡ Powder x-ray diffraction films of the two phases are almost indistinguishable.

§ Roughly three atoms of manganese replace two of chromium and one of aluminium, but this is not exact.

figure shows how manganese replaces chromium in Cr_2Al_{11}, and again the substitution is not atom for atom.* If the two straight lines in fig. 29 are extrapolated they meet at 0% of chromium, suggesting that the two phases would become identical if all the chromium were replaced by manganese.

Fig. 29

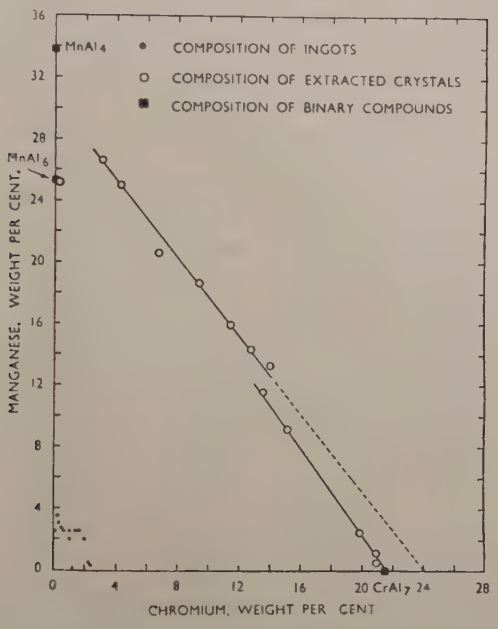

Compositions of primary crystals extracted from slowly cooled ingots.

The work of Raynor and Wakeman (1947) referred to above suggests that in $MnAl_6$ manganese is replaced more readily by zinc than by copper. This tendency is shown in a much more striking way by the compound $MnAl_4$ which dissolves zinc by simple atom for atom substitution up to a limit of about 2·6 atomic per cent. On exceeding this proportion of zinc, the crystal structure changes to that of a genuine ternary phase denoted T(AlZnMn) in which the atomic proportion of aluminium is still maintained at 80%. This phase includes the composition Mn_4ZnAl_{20} (i.e. (Mn, Zn)Al_4) and as shown in fig. 30 variation of composition by simple atom for atom substitution is possible over a certain range. In the system Al–Mn–Cu, there is a genuine ternary phase T(AlCuMn) with the same structure. This includes the composition ($Mn_3Cu_2Al_{20}$) on the 80 atomic per cent aluminium line (see fig. 30), but manganese and copper do not replace each other atom for atom, and manganese behaves as though its characteristics were between those of

* The diagram is in weight percentages but as manganese and chromium are adjacent elements in the Periodic Table, an atom for atom replacement would give lines at almost 45° to the axes.

copper and aluminium*—the significance of this is discussed later. On passing to the system Al–Mn–Ni, there is again a ternary compound with 80 atomic per cent of aluminium, the composition being almost fixed at $Ni_4Mn_{11}Al_{60}$. If all these compounds are referred to a constant number of aluminium atoms, their composition may be expressed

$$Mn_{12}Zn_3Al_{60},$$
$$Mn_9Cu_6Al_{60},$$
$$Mn_{11}Ni_4Al_{60}.$$

Fig. 30

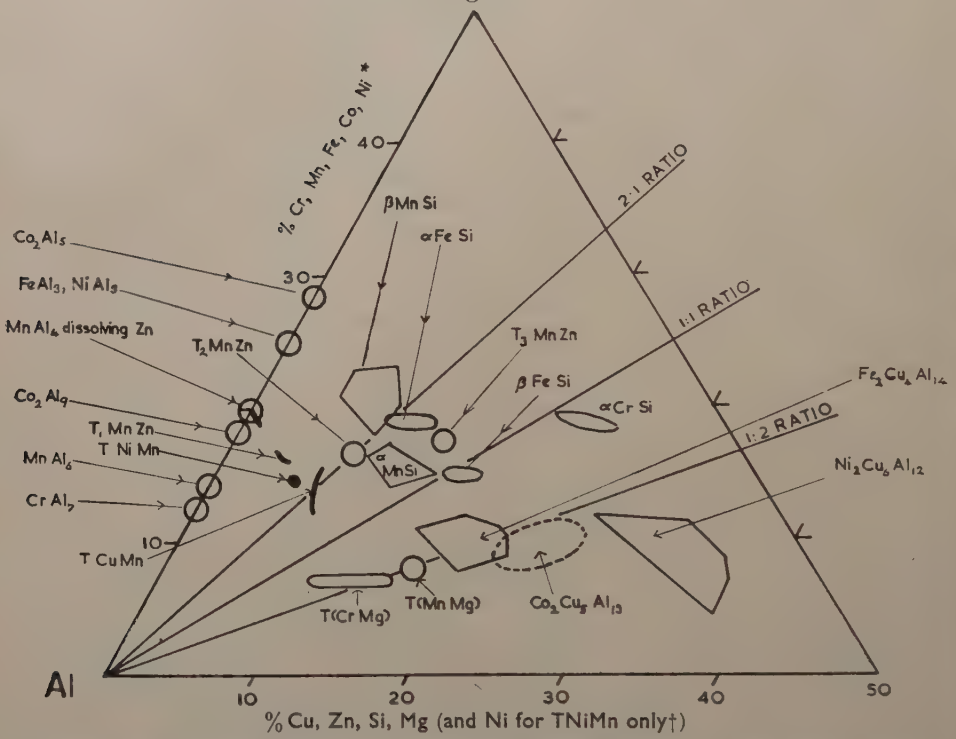

Binary and ternary aluminium-transition metal phases. In addition to the phases shown, Co_2Al_9 is able to dissolve appreciable amounts of silicon; up to approximately 4·5 atomic per cent, silicon replaces cobalt atom for atom but above this limit, atom for atom replacement ceases so that the arrangement $(CoSi)_2Al_9$ is no longer preserved, and the limits of the phase are not known.

† For the phase TNiMn the nickel content is shown along the bottom of the diagram and *not* along the left-hand side.

The composition of T(AlMnNi) is thus out of sequence as compared with the Zn- and Cu-T phases, and the significance of this is discussed later. These three phases have the same general type of structure, and

* If manganese and copper were equivalent the composition of the phase would lie along the line at 80 atomic per cent aluminium, whereas if manganese and aluminium were equivalent, the variation in composition would maintain a constant proportion of copper. The actual slope of the curve in fig. 30 is between these two effects.

according to Robinson (1952 a, c) their diffraction patterns may be indexed as belonging to orthorhombic cells whose dimensions are obviously related (see table 5).

Table 5

	a_0	b_0	c_0
T AlMnNi	23·8	12·5	7·55
T AlMnCu	24·2	12·5	7·72
T AlMnZn	25·1	24·8	30·3

In the ternary systems Al–Cu–Fe, Al–Cu–Co, and Al–Cu–Ni, genuine ternary phases are formed whose compositions are variable, but are regarded as based on $FeCu_2Al_7$, $Co_2Cu_5Al_{13}$, and $NiCu_3Al_6$, and of these the first two have been shown to be isomorphous (Raynor, private communication) but the last is not isomorphous with the other two (Brown, private communication). These compositions have the characteristic that if we use the term 'outer electrons' to denote electrons outside the argon shell of Fe, Co, Ni, together with the valency electrons of Cu and Al, then they correspond to a constant ratio of outer electrons to atoms, as may be seen by writing the formulae :

$$Fe_2Cu_4Al_{14},$$
$$Co_2Cu_5Al_{13},$$
$$Ni_2Cu_6Al_{12}.$$

On passing from $Fe_2Cu_4 \rightarrow Co_2Cu_5 \rightarrow Ni_2Cu_6$, the number of outer electrons increases by 3 at each step, and this is counterbalanced by the removal of one aluminium atom. This is irrespective of any assumption about the valency of the transition metal, but any scheme in which the valencies increase in unit steps on passing from Fe → Co → Ni will produce constant electron : atom ratios for the above formulae. In view of the wide range of composition of these phases, this may be without significance, and the general trend of compositions shown in fig. 30 suggests that the phases tend to occur at roughly 10 atomic per cent of the transition metal.

Interesting relations have been traced between ternary compounds of aluminium, silicon, and one transition metal (Pratt and Raynor 1951). The ternary compounds αAlMnSi and one form* of αAlFeSi have the compositions shown in fig. 30 and are probably isomorphous, because they form the end members of a continuous series of solid solutions in the quaternary system Al–Fe–Mn–Si. According to Robinson (1952 b), αAlMnSi is cubic with $a = 12{\cdot}644$ kx, and one form* of αAlFeSi is also cubic (Phragmen 1950).

The compound βAlMnSi has a range of homogeneity including the composition Mn_3SiAl_{10} i.e. $(Mn+Si)_2Al_5$, and its structure is similar to that of Co_2Al_5. According to Robinson (1952 b), the structure should

* According to Robinson and Black (1953) there may be four different compounds in the α region of this system, one of which is hexagonal with $a = 12{\cdot}3$, $c = 26{\cdot}2$ kx.

be regarded as derived from a hypothetical Mn_3SiAl_9 which may be considered structurally as being $(Mn_4–Mn)(Si, Al)_{10}$ and resembling Co_2Al_5 $(=Co_4Al_{10})$, with silicon replacing aluminium, and one manganese atom out of four dropping out of the structure. All the samples prepared had a higher aluminium content than corresponded to Mn_3SiAl_9, but the density and x-ray intensity measurements made it probable that the omission of manganese atoms is a real characteristic of the structure; fig. 31 shows the arrangement of aluminium atoms round one of the 'vacant sites' (i.e. the sites which, if occupied would make the structure analogous to Co_2Al_5). There is need for further work on the way in which variation of composition affects the occupation of positions in this structure. The methods of electron counting suggested that the aluminium atoms had fewer and the manganese atoms more electrons than expected for neutral atoms. The extent of the transfer was difficult to estimate but was probably not more than two electrons per manganese atom. This interpretation was not, however, unambiguous, and some of the data might indicate an absorption of electrons by the silicon atoms. It is to be noted that the compound βAlMnSi does not appear to resemble βAlFeSi.

Fig. 31

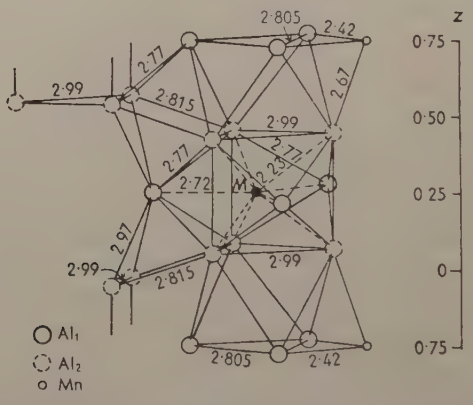

Perspective view of the group of aluminium atoms surrounding the vacant site *M* together with some of their contacts with other groups of atoms. Distances in Ångström units.

The ternary system Al–Cr–Si has also yielded results of great interest. There are two ternary compounds, of which βAlCrSi has a hexagonal structure with $a=4{\cdot}487$ kx, $c=6{\cdot}364$ kx, and 9 atoms per unit cell (Robinson 1953). The structure is similar to that of $CrSi_2$, and the phase may be a solid solution in the binary compound. The αAlCrSi has a range of composition (see fig. 30) which almost includes the simple ratio Al_3SiCr. The structure has been studied in detail by Robinson (1952 a), and is cubic, with $a=10{\cdot}895$ kx, and 84 atoms per unit cell, and the structural formula is $Cr_4Si_4Al_{13}$; as shown in fig. 30 the variation in composition is such as to maintain an approximately constant atomic

percentage of chromium. The crystal structure is of extreme interest. Each silicon atom has 4 close neighbours (one Si and three Al) arranged tetrahedrally. The aluminium atoms are divided into three classes, of which one has four silicon neighbours arranged tetrahedrally. This is one of the few examples of 4-coordinated aluminium, and the Al–Si distance equals 2·38 kx which is nearly the sum of the single bond radii (Al 1·26+Si 1·17=2·43 kx). The chromium atoms have 9 close neighbours. The electron counting methods suggest that there is no marked absorption of electrons by the chromium atoms, and for the low angle lines the observed intensities agreed well with those calculated on the assumption that no absorption took place.

For convenience the composition ranges of the aluminium-transition phases are summarized in fig. 30.

6.6. *Theoretical Discussion*

The theoretical interpretation of the alloys of aluminium with the transition metals is a matter of acute controversy. We have seen that in the Pauling hypothesis the distribution of the electrons between the atomic and bonding orbitals is assumed to be such that, in the crystals of the elements, the following numbers of vacancies exist in the supposed atomic 3d electron groups :

Cr	Mn	Fe	Co	Ni
4·66	3·66	2·66	1·66	0·66

It was suggested by Raynor (1949) that these vacancies could be regarded as definite characteristics of the elements concerned, and that in the aluminium-rich phases described above, the valency electrons from the aluminium atoms filled the vacancies, and that the remaining outer electrons of the transition atoms could be neglected, so that the transition metals exerted negative valencies equal to the above vacancy numbers. In this case the electron : atom ratio for $MnAl_6$ was $(18-3{\cdot}66)/7=2{\cdot}05$, and the compounds $CrAl_7$, $MnAl_6$, Co_2Al_9, and $NiAl_3$ gave approximately the same electron : atom ratios, although $FeAl_3$ fell out of sequence. This approach explained the isomorphism of $FeNiAl_9$ and Co_2Al_9 since the number of vacancies* in two cobalt atoms was equal to that in one nickel and one iron atom. The equilibrium diagrams of some of the ternary systems were discussed in detail from this viewpoint, and it was concluded that, in some cases, the composition limits of the phases occurred at electron : atom ratios which, on the above scheme, were constants.

Interest in this work was increased by the discovery that the x-ray diffraction patterns of $MnAl_6$, Co_2Al_9, $NiAl_3$, and β AlMnSi gave strong

* For simplicity we have assumed the Pauling values and the above formulae throughout this description. Some of the values differ slightly from those of Raynor who sometimes used the experimental value of 1·71 for the number of vacancies in cobalt, and also allowed for the slight differences from the ideal formulae.

reflexions indicating prominent Brillouin Zones which would accommodate from 1·6–2·2 electrons per atom in the above compounds. These zones were assumed to be the only ones concerned, and the negative valencies of the Raynor scheme were regarded as reducing the electron : atom ratios to the above relatively low values. Good agreement was found in some cases, although the treatment was not always consistent. Thus Robinson (1952 b) regarded the manganese atoms as dropping out from the structure of β AlMnSi in order to prevent the electron : atom ratio from falling below that at which the Fermi sphere touched the surface of the zone, whereas in their discussion of the solubility of iron in Co_2Al_9 Raynor and Waldron (1948) concluded that although "the effects of increasing the number of electrons per atom depend upon the Brillouin Zone characteristics, the behaviour on decreasing the number of electrons per atom probably depends on the details of the atomic arrangement in the structure itself".

The negative valency schemes have aroused much interest, and have provided a great stimulus to experimental work of the highest quality in the fields of crystal structure and alloy constitution. A critical examination suggests, however, that in spite of their apparent success they are physically improbable. In the case of cobalt, for example, the neutral atom contains 9 electrons outside the argon shell, and if it absorbs 1·66 electrons, there will be a total of 10·66 electrons, of which only 10 can be accommodated in 3d orbitals. There must, therefore, be at least 0·66 electrons per atom in 4s states (pure or as the s part of a hybrid). Whatever arguments may be advanced for excluding 3d electrons from Brillouin zones, it can hardly be suggested that 4s electrons, or the s parts of a hybrid, can be neglected in the way that the negative valency schemes require, and we must reluctantly conclude that the schemes based on the Pauling vacancies are impossible.

If negative valencies are postulated, the greatest possible values are 0, −1, −2, −3, −4 . . . for Ni, Co, Fe, Mn, Cr . . . Raynor and his collaborators have shown that with these negative valencies, some generalization of the facts is obtained, although not so satisfactorily as when the larger and non-integral valencies based on the Pauling vacancies are employed. For nickel and cobalt, negative valencies of 0 and −1 may be correct, although they are unproved, and as emphasized on p. 195 a mere preponderance of a donating atom does not necessarily lead to a completely filled d shell. For chromium and manganese, negative valencies of −4 and −3 seem improbable because of the size and instability of the $(3d)^{10}$ sub-group (see p. 219), and they are not confirmed by the electron counts. Fortunately this does not mean that all of the generalization must be discarded. Thus the isomorphism of Co_2Al_9 and $FeNiAl_9$ would agree with any valency scheme which placed cobalt midway between iron and nickel, whilst as explained on p. 215 constant electron : atom ratios for the ternary (FeCuAl), (CoCuAl) and (NiCuAl) phases result from any scheme in which the valencies in the

sequence $Fe \rightarrow Co \rightarrow Ni$ increase by unit steps. So far as constant electron : atom ratios are concerned, many generalizations of the negative valency schemes can be retained in terms of other and more probable valencies. The discarding of the large negative valencies mean an increase in the electron : atom ratios, but this is not necessarily in conflict with the Brillouin zone data. The crystal structure work shows clearly that for each of the compounds referred to above there is a Brillouin zone which contains from 1·6 to 2·2 electrons per atom, but there is no more reason for assuming this to be the only zone concerned than there is for assuming that in, say tantalum, the dodecahedral zone containing 2 electrons per atom (corresponding with the first very strong (110) reflection) is the only zone occupied. We suggest that the theory of these alloys has been misdirected by the apparently quite unjustified assumption that the first or lowest zones observed are the only ones concerned. Unfortunately with larger zones and larger numbers of electrons per atom, the simple assumptions of free electrons and spherical surfaces in k space are no longer justified, and little progress can be made in simple terms.

The following points may be noted in attempting to understand this class of alloy. In metallic copper, the $(3d)^{10}$ sub-group is complete, and the structure may be regarded as one in which the Cu^{+} ions are pulled ' into contact ' by the valency electrons, so that on the one hand the ions are held apart by the exchange forces arising from the ionic overlap, and on the other hand the van der Waals forces due to the mutual perturbation of the outermost electrons of the ions, add to the cohesion (see Mott 1953). The univalent ionic radius (table 2 (a)) of the Cu^{+} ion is 0·96 kx, whilst the atomic radius is 1·27 kx. In so far, therefore, as it is justifiable to regard a crystal of copper as consisting of ' ions in contact ', the effective ionic radius (E.I.R.) is about 0·3 kx larger than the univalent ionic radius. By extrapolation of the univalent ionic radii of the Ge^{4+}, Ga^{3+}, Zn^{2+}, and Cu^{+} ions, we may conclude that there is an increase of roughly 0·1 kx on passing back from $Cu^{-} \rightarrow Ni^{0} \rightarrow Co^{-}$, and for the (E.I.R.) values we have to a very rough approximation (in kx units) :

Ni^{0}	Co^{-}	Fe^{2-}	Mn^{3-}	Cr^{4-}
1·4	1·5	1·6	1·7	1·8

These values will tend to be too small for Mn^{3-} and Cr^{4-} because the electron clouds become rapidly more diffuse as the atomic numbers decrease.*

For aluminium the univalent ionic radius (Pauling 1945) is 0·7 kx, and the E.I.R. will be of the order 1·0 kx if we assume the same difference as in the case of copper. This assumption is unlikely to involve an error greater than 0·1 kx, and will not affect the following general argument. Table 6 gives the observed Al–X distances in the compounds concerned,

* See the tables and graphs of ionic radii in Pauling's *Nature of the Chemical Bond*.

and also the sum of E.I.R. values, and the figures show at once the improbability of the existence of large negative charges on the ions. Thus in the system Al–Mn, the sum of the E.I.R. values for Al^{3+} and Mn^{3-} is 2·7 kx whilst the Al–Mn closest distances of approach are 2·43 kx in $MnAl_6$ and 2·42 kx in Mn_3SiAl_9. The large Mn^{3-} ion would be unstable, and if opposite charges were to pull the atoms as closely together as the above values indicate, a breakdown to co-valent or metallic bonding would occur. The same objection applies *a fortiori* to a manganese atom with the negative charge of —3·66 e assumed in the Raynor-scheme, since here there is not only a $(3d)^{10}$ sub-group, but an additional 0·66 s electron not involved in the bonding.

Table 6

System	Sum of E.I.R. values	Al–X distance in compounds
Al–Ni	2·4	2·42
Al–Co	2·5	2·37 Co_2Al_9. 2·41 Co_2Al_5
Al–Fe	2·6	—
Al–Mn	2·7	2·43 in $MnAl_6$ 2·42 in Mn_3SiAl_9
Al–Cr	2·8	—

Both experiment (electron counting) and theoretical considerations suggest that large negative valencies are improbable. We may note next that the (supposedly) abnormal interatomic distances in the above compounds are roughly equal to those expected for normal single co-valent linkages. For aluminium, the Pauling single-bond radius of 1·26 kx is probably nearly correct, because (1) the valency of the element is certainly 3, and (2) the element is in Group III, i.e. next to Group IV on which the Pauling equation is based (see § 3, p. 169). For manganese Pauling (1940) estimates 1·24 kx for the d^2sp^3 radius of univalent manganese, which "should not be different from that of bi-valent manganese by more than 0·01 or 0·02 kx". The Pauling single-bond radius for mangenese is 1·17 kx, and would be less than this if a valency lower than 5·78 had been used in the Pauling equation. We see therefore that a normal Al–Mn co-valent bond would be of the order 2·4–2·5 kx which includes the observed values. For nickel, the empirical co-valent radii vary from 1·22 to 1·39 kx according to the valency state assumed, whilst the Pauling single bond radius is 1·15 kx, and a smaller value would again be obtained if a valency lower than 5·78 were assumed. A normal Al–Ni co-valent bond would thus be of the order 2·4–2·66 kx and this again includes the observed values, and for the Al–Co bond length the values are very similar. The observed interatomic distances can thus be reconciled with the presence of normal co-valent bonds, or with bonds of slightly lower bond-number, and the existence of large

negative valencies need not be postulated. It is also perhaps significant that in $CuAl_2$ the Cu–Cu distance (2·44 kx) is nearly that (2·36 kx) for univalent copper forming two collinear bonds (Wells 1950).

The electron counts suggest that slight electron transfer takes place from the aluminium to the transition metal atoms, and here two processes must be considered. First, the relatively electropositive nature of the aluminium will result in unsymmetrical bonds in which, quite regardless of any filling of the (3d) shell, the electrons are associated more with the transition than with the aluminium atoms. Apart from this, the (3d) shell may be filled as in the negative valency schemes. These two effects may not be distinguished in the ordinary electron counts, and the slight charge transference indicated need not involve a negative valency from the Brillouin zone point of view.

As explained previously (§ 3, p. 169) it is uncertain whether the building up of opposite charges will result in bond shortening although this has been generally assumed in the theory of alloys. We should expect the creation of opposite charges to increase the cohesion, and we shall here assume that slight bond-shortening also occurs. The melting points in fig. 19 suggest that the cohesion in the Al-rich aluminium–cobalt alloys is systematically higher than that in aluminium–nickel alloys of similar composition, although for the equi-atomic alloys the melting points are almost the same. This would agree with a somewhat greater absorption of electrons by cobalt than by nickel which is to be expected, since we know from the magnetic properties that there is a tendency to fill (3d) holes in both cases, and there are more available holes in cobalt. The melting point data for the Al-rich aluminium–iron compounds resemble those for cobalt, and thus suggest that some filling of the (3d) shell is still occurring, but not to a greater extent than in cobalt. For the equi-atomic alloys, the equilibrium diagrams suggest that there is much weaker cohesion in FeAl than in FeCo and FeAl, and we may conclude that there is less building up of opposite charges. Magnetic data for the Al–Ni, Al–Co, and Al–Ni phases would be of great interest particularly in view of the close resemblance between AlNi and AlCo. On passing to manganese, the melting points suggest that the cohesion becomes weaker for phases of similar composition, and then on going further back to chromium and titanium there is a striking increase in the melting points. In a general way we may therefore conclude that on passing from Ni → Co there is an increase in cohesion, which may perhaps be identified with the building up of opposite charges. There is no further increase on passing from Co → Fe, and then a decrease occurs on passing from Fe→Mn. After this a complete change takes place, and the Al–Cr and Al–Ti diagrams appear to follow some different principle.

For the transition elements of the later Groups, the (3d) electrons may give rise both to attractive and repulsive forces, and as regards the latter these are two opposing tendencies on going back from Ni → Co → Fe . . . On the one hand the decrease in the atomic number means a larger electron cloud, and this fact alone may account for the general tendency for an

increased aluminium content in the aluminium-rich compounds $CuAl_2$, $NiAl_3$, Co_2Al_9, ($FeAl_3$), $MnAl_6$, $CrAl_7$ (see p. 200), since the larger the ion to be accommodated, the more aluminium atoms will be required to take up the strain. The important thing here is that, although the atomic radii of the transition metals are smaller than that of aluminium, their ionic radii are much larger. If we are correct in saying that the (3d) sub-group is not filled in chromium, manganese and iron, the above effect will to some extent be counterbalanced by the increasingly thin nature of the electron cloud as the number of electrons diminishes. We may further expect manganese and iron to exhibit a dual behaviour, one in which they give rise to (spd) hybrid bonding, and the other in which the stable half-filled $(3d)^5$ group persists, and the bonding is of the sp^3 type.

For the present we must reluctantly conclude that there is no real understanding of the binary compounds of aluminium with the transition elements. In the ternary systems it must be remembered that the limits of phase-fields are determined by the relative free-energies of several phases. In cases where the general composition limits of a phase, or the general direction of a phase-boundary runs parallel to lines of constant electron concentration, or of constant size-factor ratios, we may reasonably conclude that the factor concerned is predominant in determining the compositions. It is much less justifiable to attempt to relate constant electron concentration with phases of different structures, or with arbitrary points on solubility curves.* In fig. 28 the whole tendency is for the curves referring to the solid solutions in Fe_3Al, $FeNiAl_9$, and Co_2Al_9 to run parallel to the side of the equilateral triangle so as to give a constant ratio of large (Al) to small (Ni, Co, Fe) atoms. The isomorphism of $FeNiAl_9$ and Co_2Al_9 agrees with many reasonable valency schemes for iron, cobalt, and nickel, but otherwise there is as yet nothing which suggests that electron concentration plays an important part in determining this diagram.

In the system Al–Cr–Mg, the shape of the AlCrMg phase field implies an almost constant ratio of small (Cr) to large (Al, Mg) atoms, and suggests that the size factor is predominant. The way in which the phase fields for αMnSi, βFeSi, and αCrSi extend up to the line representing equal proportions of Si : (Cr, Mn, or Fe) suggests that atomic packing is important in determining these limits. The approximation of compositions to the lines representing 2 : 1 and 1 : 2 atomic ratios also suggests that atomic packing is important.

In the ternary alloys with manganese, the TAlZnMn, TAlCuMn, and TAlNiMn phases of the same general structure all occur at compositions corresponding to a ratio of 4 large (Al) to 1 small (Zn, Mn, Cu, Ni) atom, and as pointed out by Raynor (1949), this constant proportion of aluminium atoms is undoubtedly one factor controlling the formation of this structure. From fig. 30 it will be seen that the compositions of

* See p. 223 below for an example of this.

these phases on the 80 atomic per cent aluminium line do not follow the sequence Zn → Cu → Ni required by the negative valency schemes, and the constancy of the electron : atom ratios proposed by Raynor and Wakeman was obtained only by comparing the manganese-rich limit of the TAlCuMn phase with the composition of the other phases on the 80 atomic per cent aluminium line. As pointed out on p. 214 the general slope of the TAl–Cu–Mn line in fig. 30 would be accounted for if manganese acted as a divalent element in agreement with the known stability of the $(3d)^5$ half-filled grouping. In fig. 30 the position of the points for TAlZnMn, TAlCuMn, and TAlNiMn on the 80 atomic per cent aluminium line can be reconciled with a valency of between 1 and 2 for nickel, which is reasonable. This concept of di-valent manganese might also account for the solubility of zinc in the binary aluminium–manganese phase referred to on p. 213.

§ 7. Physical Properties as a Source of Information on Electronic Structures

The present section will be concerned mainly with the discussion of those physical properties of transition metals and their alloys which provide some indication of the appropriateness of particular theoretical models, and of the evidence provided by the data at present available. A difficulty encountered at the outset is that the properties to be expected of a particular model are by no means unambiguously indicated. Thus we cannot yet use the ferromagnetic properties of these metals as a test of the validity of, say, the Heitler–London–Heisenberg model of a ferromagnetic, for the difficulties facing the calculation of the properties expected of this model have not been completely solved. In discussing experimental results it is therefore often helpful to use approximate and rather speculative pictures, but these should not be confused with the quantum-mechanical treatments which have been attempted. A second difficulty is presented by the paucity of data on the properties of metals and alloys whose electronic structures are, by comparison, well understood ; direct comparisons of the properties of simple and complex materials are not therefore possible.

7.1. *Properties of Interest*

From the general characteristics, considered in § 2 of the crystallography and strength of bonding of these materials it is not possible to make clear deductions of their electronic structures. Thus a high cohesive energy may indicate that a given number of electrons is accommodated at a very much lower energy in the solid than in the free atoms or that a larger number of electrons is accommodated at a slightly lower energy. It seems probable that the first effect predominates at the beginning of a transition group and the second effect near its end. There would appear to be some indication that the contribution to bonding of

the d-electrons is less in silver than in copper and gold, and this may be correlated with optical and x-ray absorption evidence that in silver the d-band lies further below the Fermi limit than in copper and gold.

The main points on which experimental evidence is sought are :—

(1) The energy range over which the outermost electrons are distributed (the band width).

(2) The form of the distribution of the electrons over this energy range (the density of states, or $N(E)$, curve).

(3) The relative numbers of electrons with positive and negative spins in ferromagnetics and antiferromagnetics.

(4) The signs, numbers, and mobilities of the charge carriers in electrical conduction.

(5) The source of the internal field in ferromagnetics.

(6) The type of wave-function to be ascribed to the electrons, especially whether in alloys electrons are to be regarded as occupying localized or non-localized states.

The experimental sources of information most likely to prove useful are :—

(*a*) x-ray emission spectroscopy.

(*b*) Electronic specific heat measurements.

(*c*) Saturation magnetic moment and paramagnetic susceptibility measurements.

(*d*) Electrical resistance and galvanomagnetic effect measurements.

(*e*) Neutron diffraction investigations.

Mention might be made at this point of the importance of investigating the change of such properties with concentration in alloys, especially in those where the only important variation with concentration is that of the extent to which the electronic energy bands are occupied.

7.2. *Band Widths and X-Ray Spectroscopy*

It has never been possible for spectroscopy to throw as much light on the electronic structures of solids as it can do on those of free atoms, largely because of the difficulties that arise in connection with transition probabilities. These difficulties have been discussed in various places (see Skinner 1940, and Wilson 1953) and a full discussion of the interpretation of her data on copper and nickel has recently been given by Cauchois (1953). In particular it must be concluded that, while general indications can be obtained of the energy band breadth corresponding to the outer electrons, one cannot derive the density of states curve from x-ray emission intensities in any simple manner. Furthermore, recent results by Gyorgy and Harvey (1952, 1954), Kingston (1952) and Kingston *et al.* (1952) suggest that much of the detail of emission bands has been obscured by very slight superficial contamination of specimen targets.

The main electronic transitions of importance in giving rise to the soft x-ray emission from the first transition group metals are those of

the form 3d → 2p and 4s → 2p which form part of the $L_{III, II}$ (or Lα and Lβ) spectrum, but some investigations of the $M_{III, II}$ spectrum (3d or 4s → 3p), and of part of the harder K spectrum have also been carried out. The interpretations to be applied to results on K emission are by no means clear, since transitions to the K shell are forbidden for 3d and 4s electrons, and it has been suggested that they reveal the 3d and 4s bands because these contain an admixture of p-functions.

The band widths found for elements of the first transition group are shown in table 7, together with the band breadths suggested by theoretical calculation (see § 4) and those expected for the indicated number of conduction electrons.

Table 7. X-Ray Emission Band Widths (Electron Volts)

Element	Emission Type					Calculated d-band width	Estimated s-band width
	M	M	L	L	L		
Ti	—	—	6	—	—	—	—
V	6	—	7·5	—	—	—	—
Cr	7	7·2	6·5	—	—	—	—
Mn	6·5	5·8	6	—	—	—	—
Fe	5	3·7	5·5	—	—	7·7	6·2 (0·8) 2·5 (0·2)
Co	6·5	—	6	—	—	—	5·7 (0·7)
Ni	5	5·8	5·5	6	5	2·7	5·2 (0·6)
Cu	7·5	7·1	—	7	<5	3·46	7·1 (1·0)
Reference	S	G and H	S	F	C	—	—

S=Skinner unpublished, quoted by Kingston (1952) ; G. and H=Gyorgy and Harvey (1952, 1954) ; F=Farineau (1938, 1939) ; C=Cauchois (1953).

The d-band calculations are those referred to in § 4 and the s-band values are those estimated on the assumption of a number of free electrons equal to that shown in brackets after the band width.

In the later elements where the d-band is expected to be narrow the width observed will be controlled mainly by the band width corresponding to s-band electrons ; and it can be seen that, with the exception of Cauchois' result for copper, the values for cobalt, nickel, and copper show good agreement with this suggestion. The value obtained from Manning and Greene's calculation on iron is appreciably larger than that observed but a more refined use of the cellular method may produce a narrowing of the band for iron as it did for copper.

X-ray absorption curves are normally difficult to interpret, but recent results of Cauchois (1952, 1953) for silver and copper show strong absorption effects which can be correlated with optical absorption data. These latter have been interpreted by Mott (1936 c) as originating from excitation of electrons from the d-band into empty states at the Fermi surface. The depths of the d-band below the Fermi surface indicated

by the x-ray data are about 2·3 ev for copper and 4 ev for silver ; these values are in good agreement with those obtained from the optical absorption curves, and the value of 3·7 ev given by Howarth's calculations for copper is in reasonable agreement with experiment. Some interesting results on the fine structure of K-excitation edges have recently been obtained by Nilsson (1953) for a number of metals of the first transition group, but a satisfactory theoretical discussion of them has yet to be given.

The only results available on the *soft* x-ray emission from alloys of transition metals are those of Farineau (1939) on nickel–copper alloys. In binary alloys there are two sets of emission bands, corresponding to transitions made by outer electrons to empty, low-lying states of the two types of atom. If the forms of the two bands are found to be very different for a given transition it suggests that there does not exist a 3d-band collective to both types of atom. Farineau's results show this type of effect for copper-rich alloys, whereas in the nickel-rich alloys the two bands are closely similar, and show the broadening with increasing copper concentration expected on collective electron treatments. In copper-rich alloys the nickel Lα emission is narrower in energy than in pure nickel and suggests that the localized wave-function picture of the d-electrons is appropriate here. This behaviour has been shown to be compatible with other properties of these alloys in a general survey by Coles (1952) (see § 5.4).

7.3. *The Density of States : Specific Heats and Paramagnetic Susceptibilities*

The form of the density of states curve for a metal, especially that in the neighbourhood of the Fermi surface, is one of its most important characteristics ; and an indication of the form of this curve is a very useful result of theoretical calculations of band structures. In the present state of theoretical work too much attention should not be paid to the fine structure of calculated curves, and there is no justification for assuming that a single band form can be appropriately used in the discussion of all the elements of a given transition group. The two quantities which control a large number of properties of a metal are the density of states at the Fermi limit ($N(E)_{\mathrm{F}}$) and the slope of the curve ($d\,N(E)/dE$) at the same point, but direct indications can only be obtained of the former.

Values of the linear term (γT) in the specific heat of a metal may be derived, in principle, from both high and low temperature measurements: this term is to be ascribed to the electrons in collective bands. At high temperatures the lattice specific heat tends to a constant value, and at low temperatures it tends to zero following a T^3 law. In practice low temperature measurements are probably more reliable, especially when, as is the case with the transition metals, the degeneracy temperature of the electrons is comparatively low. The value of γ is given by

$$\gamma T = \tfrac{2}{3}\pi^2 \boldsymbol{k}^2 N(E)_{\mathrm{F}} \,.\, T,$$

where $\boldsymbol{k}$ is Boltzmann's constant giving $C_e = 1{\cdot}1263 \times 10^{-3} N(E)_F \, . \, T$, where C_e is in cal per mole and $N(E)_F$ in states/atom/ev. This result is independent of the band shape, but unfortunately results are frequently quoted in terms of T/T_0, where T_0 is a degeneracy temperature (see fig. 9) a particular band shape being assumed. In the absence of exchange interaction effects the low temperature paramagnetic susceptibility of the collective band electrons is $\chi_e = 2\mu_B{}^2 \, . \, N(E)_F$ (where μ_B is the Bohr magneton), giving for their g-atomic contribution to the susceptibility

$$(\chi_A)_e = 6{\cdot}466 \times 10^{-5} N(E)_F.$$

It is well known (Mott and Jones 1936) that for palladium the agreement between values of $N(E)_F$ derived from the two types of measurement is poor, and this has been ascribed to the presence of exchange interaction of insufficient magnitude to produce ferromagnetism. Such effects have been discussed in detail by Stoner (1947) and Wohlfarth (1949 a).

In fig. 32 the values of $\gamma (= C_e/T)$ and χ_A are compared for each of the transition groups. The values of γ have been taken from the data assembled by Horowitz and Daunt (1953), the sources of the data for χ_A being shown. Some values have also been inserted for palladium-rich palladium–silver and palladium–rhodium alloys : these have been taken from the work of Hoare *et al.* (1952, 1953). Values of χ_A should be corrected for diamagnetic contributions, but it is not clear what these can be assumed to be. The values of γ for tungsten, iron and nickel can be compared with those obtained from the calculated bands discussed in § 4. Thus the latest experimental value for tungsten is about 2×10^{-4} and the theoretical value is $4{\cdot}8 \times 10^{-4}$; for iron the experimental and theoretical values are $12{\cdot}0 \times 10^{-4}$ and $4{\cdot}6 \times 10^{-4}$ respectively, and for nickel they are $17{\cdot}4 \times 10^{-4}$ and $16{\cdot}9 \times 10^{-4}$ respectively. In his calculation for nickel, Fletcher points out that this closeness of agreement is probably fortuitous.

Horowitz and Daunt discussed their results in terms of the various calculated band forms, suggesting that the general band form should alter little in passing, not only from titanium to copper, but also from one transition group to the next. That the latter part of this suggestion is invalid is shown clearly by the contrast between the similarities shown by iron, cobalt, and nickel, and the marked differences between palladium and rhodium or ruthenium. This contrast can be correlated with those, pointed out in § 2, which are shown in comparisons of other properties of these elements. That such differences between the first and second transition groups are not restricted to the properties of the pure metals is shown by the widely differing magnetic properties of salts of the elements (Cabrera 1940). With the exception of the anomalous peak shown by manganese, the data of fig. 32 tend to confirm the double-peaked structure suggested for the $N(E)$ curves by most of the theoretical work.*

* Recent work on Tc (Nelson 1953) indicates a maximum in χ_A at Group VII, greater at Tc than at Re, but smaller than at Mn.

Stoner (1954) has discussed the exchange interaction effects (which are positive in all cases) implied by the larger values of $N(E)_F$ calculated from the magnetic data, but quantitative estimates can only be made by assuming a particular band form.

Fig. 32

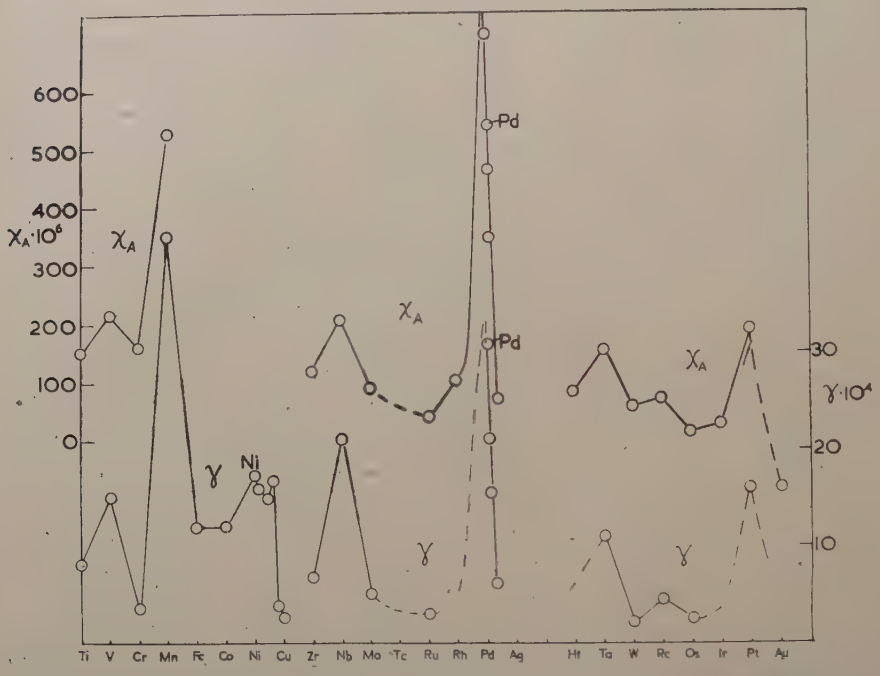

g-atomic susceptibilities (χ_A) and electronic specific heat coefficients (γ).

Origin of χ_A values :—

Ti, Zr	Squire and Kaufmann (1941)
V, Nb, W, Mo, Hf	Kriessman (1953)
Cr	McGuire and Kriessman (1952)
Ru, Os, Ir	Guthrie and Bourland (1931)
Ta, Rh, Pd, Pt	Hoare and Walling (1951)
Mn	Serres (1938)
Re	Perakis and Capatos (1935)
Pd–Ag, Pd–Rh	Hoare *et al.* (1952, 1953)

As suggested in § 5.4, it is probably justified to assume that one can, by γ and χ_A measurements on dilute alloys of a metal with its nearest neighbours in the Periodic Table, explore the density of states curve for the metal over small energy ranges above and below the normal Fermi surface ; that is, to assume that the band structure, as distinct from its degree of occupation, is unaffected by such alloying. This assumption has been made by Elcock, Rhodes, and Teviotdale (1954) in discussing the measurements on palladium–silver alloys referred to above. By comparisons of the experimental results and the predictions of collective electron theory for various idealized band forms, they show that a parabolic

d-band ($N(E)$=const. $(E_0-E)^{1/2}$) cannot be appropriate, although there are general theoretical grounds for expecting that this expression should hold when the number of holes in the band is very small. The results correspond more closely to a band of the form $N(E)=A+B\ (E_0-E)^3$, where both A and B are constants. The data on the palladium–rhodium alloys are incomplete, but those available suggest strongly that the Fermi limit in palladium lies only a small distance above a peak in the $N(E)$ curve.

That the reliability of the γ values is sometimes doubtful is shown by a comparison of the remarkably high value of 51×10^{-4} cals/degree/mole for tungsten resulting from an earlier investigation with the most recent value of 2×10^{-4}. In ferromagnetic metals and alloys interpretations of γ values are complicated by the removal of spin degeneracy* and Wohlfarth (1949 a) has shown how variations in the relative magnetization (ζ_0) may mask the signs of a falling $N(E)$ curve. He explains in terms of this effect the behaviour shown by the γ values of the nickel-rich nickel–copper alloys (Keesom and Kurrelmeyer 1940), which are included in fig. 32.

7.3.1. *Electrical Properties*

Another measurement which might, in principle, give information about the form of the $N(E)$ curve in alloys is the electrical resistance, for it is well known that for a given perturbation in the lattice the transition probability is proportional to the density of states at the Fermi surface ($N(E)_F$), and Mott (1936 a, b) has shown that a satisfactory account of the electrical properties of transition metals can be given on the assumption that the main resistance-producing transitions are of s-band electrons to unoccupied states in the d-band. Resistance values of alloys are complicated by the presence of two types of perturbation (thermal and 'impurity'), and are not always easy to interpret, but recent measurements over a range of temperatures on various palladium–silver alloys (Coles and Taylor, to be published) can be correlated with the band form implied by the results already discussed. Such measurements on alloys may prove increasingly useful when there are specific heat and susceptibility data available for comparison. Hall effect coefficients have been discussed in § 4.8: few data are yet available for alloys, but measurements on those of metals of the second transition group (where the coefficient changes sign between rhodium and palladium) should prove interesting. Quantitative deductions from such data are limited by the need to make some assumptions about the relative mobilities of holes and electrons.

7.4. *Ferromagnetic Moments and d-band Holes*

It was seen in § 4 that the most important data giving a quantitative aspect to early collective electron theories were those for the saturation magnetic moments (σ_0) of transition metals and their alloys; these also governed the assumptions made by Pauling in building up a resonating

* If all d-band holes are aligned by the internal field, only electrons in the unfilled half-band contribute to the specific heat.

valence-bond model for such materials. It has often been assumed that these saturation intensities, expressed in Bohr magnetons per atom (q_f), can be identified with the number of unoccupied states (n_d) in the d-band ; but it should be recognized that this identification implicitly assumes a state of maximum spin multiplicity for the d-band holes, and that the s-band electrons make no contribution to the measured moment. The limitations of the former assumption have long been recognized in the collective electron theories of ferromagnetism, where a relative magnetization parameter ($\zeta_0 = q_f/n_d$) is introduced to give the fraction of d-band holes aligned by the internal field at absolute zero. The permanent moment induced by this field in the s-band electrons has not yet been considered in the more orthodox theories of ferromagnetism, but has played a major part in the theory of Zener, considered in § 4.6.

The experimental data for the saturation moments of iron, cobalt, nickel, and many of their alloys have been surveyed in detail by Stoner (1947) (see fig. 33). It is well known that when non-transition metals are

Fig. 33

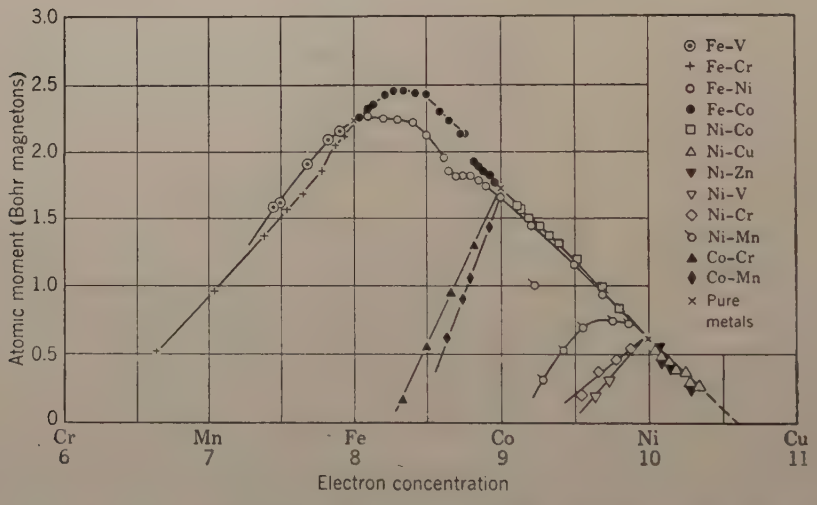

Average atomic moments of binary alloys of the elements in the iron group.

added to nickel the σ_0 values fall as if the valency electrons of the added metal entered the unoccupied d-states of the nickel atoms, the number of electrons in the s-band (n_s) remaining constant at 0·6 per atom ; that is, dq_f/dc is equal to v, where c is the atomic fraction of the added metal and v is its conventional valency. The concentration by which all holes have been filled is thus given by

$$0{\cdot}6\,(1-c)=(v-0{\cdot}6)\,c \quad \text{or} \quad c=0{\cdot}6/v.$$

The nickel–copper alloys provide a particularly simple example, and the ferro- and para-magnetic data for this system have been examined in

terms of a collective electron model by Wohlfarth (1949 a), who assumed bands common to both types of atom and an idealized parabolic form for the d-band. He concluded that there is a slight increase in n_s as copper is added, but that the slower fall in observed moment which would then seem to be required is counteracted by a fall in the magnitude of the exchange interaction and a corresponding decline from 1·0 of the value of ζ_0. In such a treatment the d-band holes are assumed to be associated with both types of atom, and it cannot easily be extended to systems like nickel–zinc and nickel–aluminium ; in the former this assumption seems improbable and in the latter impossible, although a common conduction band will, of course, exist. The fact that the simple relationship given above holds for these systems suggests that the d-band is a property of the nickel atoms only. Wohlfarth (1949 b) has applied a common collective band treatment to the nickel–cobalt alloys, and he concludes that the exchange interaction in this system is sufficiently large to maintain ζ_0 at unity over the whole composition range. It may be pointed out here that the d-band must move to slightly higher energies relative to the s-band on passing from nickel to cobalt ; the simple subtraction of one electron per atom from the band system of nickel would lead to values for n_s and n_d of a little less than 0·6 and a little less than 1·6 respectively, while values of 0·71 and 1·71 seem to be indicated by experiment.* Similar behaviour is shown by the nickel-rich nickel–iron alloys, and this is in accord with expectation, for the atomic d-levels move to lower energy relative to the atomic s-levels on passing along the series $\mathrm{Fe} \rightarrow \mathrm{Co} \rightarrow \mathrm{Ni} \rightarrow \mathrm{Cu}$.

The above considerations bear out the suggestion, made in § 5.4, that a band system common to both types of atom in an alloy can only be expected when the elements are close neighbours in the Periodic Table : and the saturation moment data for nickel–vanadium and nickel–chromium alloys are in agreement with this. On a common band system model σ_0 should increase with the concentration of vanadium or chromium, but the observed values fall, and in the vanadium alloys the value of dq_f/dc is about 5. All five of the outer electrons of vanadium might be able to behave like the two valence electrons of zinc or the three of aluminium, but an alternative explanation could be based on an L.W.F. model. If the outer electrons of the vanadium atoms were in localized d-states about their respective atoms a condition of maximum multiplicity would give them a moment of $5\mu_B$ and this might well be opposed to that of the surrounding nickel atoms. A model of this type has been suggested by Carr (1952), and corresponds to that suggested by Jones (see § 5.4) for dilute alloys of the transition metals in non-transition metals. An alloy system of particular interest is nickel–manganese, for it appears to show both the collective and the L.W.F. behaviour. At small manganese contents σ_0 increases with c, as in nickel–iron, but falls rapidly with more than about 10%

* Extrapolation of σ_0 values for the face-centred cubic alloys suggests values for face-centred cubic cobalt slightly larger again.

manganese, and is quite small at 25%. (If an alloy of the latter composition is annealed at low temperatures it takes up an ordered structure with σ_0 corresponding to about $4{\cdot}0\,\mu_B$ per Ni_3Mn group (Kaya and Nakayama 1940); but a detailed interpretation of this behaviour is scarcely justified, since both the configuration and the interactions of a manganese atom will probably depend strongly on its environment.)

In his survey of σ_0 data Stoner (*loc. cit.*) includes values for the alloys of cobalt, but the interpretation of these is complicated by the allotropy of this metal. If n_s is constant the concentration of an alloying element like zinc or aluminium at which all d-band holes are filled should be given by

$$1{\cdot}7\,(1-c)=(v-0{\cdot}7) \quad \text{or} \quad c=1{\cdot}7/(v+1),$$

so that dq_f/dc values of $v+1$ are to be expected; the observed values appear to be smaller than this. Meyer and Taglang (1950) report that copper additions have different effects in pure cobalt and in the equi-atomic nickel–iron alloy; in the former $dq_f\,dc$ is only about 1·4, whereas in the latter it has the value of 2·0 expected on a simple collective band model. Data on the alloys of cobalt with chromium, molybdenum, and tungsten seem to correspond with the type of behaviour suggested for the nickel–vanadium alloys; thus the $dq_f\,dc$ value of about 7·0 is just that to be expected if a chromium atom enters cobalt in the state $3d^5$, its one valency electron giving a dq_f/dc of 2·0 by entering the cobalt band structure, and its d-electrons providing an opposed spin of $5{\cdot}0\,\mu_B$.

It is well known that the magnetic properties of the alloys of iron are markedly different from those of nickel. A large number of elements, when present in solid solution in body-centred cubic iron, give rise to dq_f/dc values of 2·2; and since this is the value of q_f for pure iron the effect seems at first to be one of mere dilution. A more probable explanation (see Stoner 1951) however, is that the exchange interaction is of such magnitude that ζ_0 is less than unity, so that d-band holes of both spin directions are present. On the addition of, say, aluminium the electrons provided by the solute atoms would enter both halves of the band structure of iron, the number of *unpaired* d-electrons per iron atom remaining constant. The assumption that in iron the value of ζ_0 is less than one also makes possible a satisfactory discussion in terms of a collective electron model of the magnetic properties of the iron–cobalt alloys, and in particular of the appearance in the value of σ_0 in this system of a flat maximum (see fig. 33). (If ζ_0 were unity throughout the system this maximum would imply a reversal of the general trend of relative movement by the s- and d-bands referred to above.) On passing from cobalt to iron the energy breadth corresponding to d-band holes will increase, both because of the increase in their number and because of the general broadening of the band that is to be expected. If the exchange interaction energy remains constant on adding cobalt a point will be reached beyond which further holes will be created in pairs, the value of σ_0 remaining constant since this

is a measure of the number of unpaired holes ; in fact, the exchange energy is more likely to fall, at least relative to the band breadth corresponding to the d-band holes, and a maximum in σ_0 is thus to be expected. As mentioned in § 4.5, a detailed examination of the σ_0 data for this and other iron alloys suggests that the total number of holes in pure iron (n_d) is of the order of 2·9 per atom.

7.5. *Paramagnetic Measurements*

7.5.1. *Metals and Alloys of the Second and Third Transition Groups*

It might be expected that a discussion in terms of a comparatively small number of holes in a fairly narrow d-band would be as appropriate for palladium, rhodium, and ruthenium, and for platinum, iridium, and osmium, as it is for iron, cobalt, and nickel ; and some interest attaches to the numbers of such holes that seem to be implied by the properties of these elements. Reasonable estimates can only be made, however, for palladium and platinum, since a high density of states and a low degeneracy temperature do not seem to be indicated by the properties of the other elements (see § 7.3). Rhodium, ruthenium, iridium, and osmium have small paramagnetic susceptibilities with positive temperature coefficients, and in these respects resemble chromium, molybdenum and tungsten. For the three latter elements an antiferromagnetic structure has been suggested by Zener, but experimental evidence considered below seems to discount this suggestion. It appears more likely that the sign and magnitude of the temperature coefficient of susceptibility depends on the details of the band form. One expects, on general grounds, that a large susceptibility will be associated with a negative temperature coefficient, and this seems to hold for the elements of Group V(A) as well as for palladium and platinum. Wohlfarth (1948) has concluded, from a study of the magnetic properties of palladium, platinum, and their alloys, that these metals have 0·6 and 0·3 d-band holes per atom respectively ; the figure for palladium is probably more significant than that for platinum, and is especially supported by the effects of hydrogen absorption and of alloying with silver or gold on the susceptibility.

7.5.2. *Paramagnetic Moments in Dilute Alloys*

It has been pointed out (Coles 1953) that magnetic data on alloys containing small amounts of transition metals allow of a direct interpretation in terms of a localized d-state picture, of the type suggested by Jones (1953), for the dissolved atoms (see § 5.4.2). Where the temperature dependence of the paramagnetic susceptibility shows a Curie–Weiss behaviour, effective magneton numbers (p_{eff}), and from them total spin quantum numbers (S), can be derived. (The assumption is made that orbital contributions to the atom moments are quenched in such materials.) Results for various alloys are shown in table 8. It can be seen that in the γ phases (M_5Zn_{21}) the results bear out the original suggestion of Ekman (1931) that the transition metals should be regarded as zerovalent in such phases.

Table 8. Paramagnetic Data for Dilute Alloys

Alloy	p_{eff}	S	d-state	Valency
Ni in Cu	>0*	>0	$3d^9$?	>0
Ni_5Zn_{21}	0	0	$3d^{10}$	0
Zn, 7% Co	0	0	$3d^{10}$	−1
Co_5Zn_{21}	1·9	$\frac{1}{2}$	$3d^9$	0
Fe_5Zn_{21}	2·6	1	$3d^8$	0
Fe in Au	3·6	$1\frac{1}{2}$	$3d^7$	1
Mn in Cu	4·8	2	$3d^6$	1
Mn in Ag or Au	5·5	?	$3d^5$?	2 ?

* Although markedly paramagnetic these alloys do not show a Curie–Weiss behaviour, and in some cases χ increases with temperature at higher temperatures. Jones has pointed out that the $3d^8$ and $3d^9$ configurations lie very close to one another, and changes in the relative abundance of nickel atoms in the two configurations might take place with change of temperature.

Such measurements cannot always confirm the validity of an L.W.F. model. Thus it seems probable from the results already discussed (§ 5.4.1) that a common collective d-band is formed in palladium-rich palladium–silver alloys, but it is not possible to say, from magnetic data whether or not this picture breaks down for the silver-rich alloys as it does in copper-rich nickel–copper alloys. Were the L.W.F. model valid, palladium would probably enter silver in a $4d^{10}$ configuration, and the resultant diamagnetism would be indistinguishable from that expected on a common, collective d-band model.

7.6. *Atomic Moments from Neutron Diffraction*

Neutron diffraction measurements are able in principle to reveal the strengths and orientations of atomic moments in a scattering lattice, and they have therefore been used to test the validity of the suggestion of Zener (1951 a and b) that the elements of Groups V(A) and VI(A) are antiferromagnetic in character, the two simple cubic lattices which interpenetrate to form their body-centred cubic lattices having opposed spins of 4 and $5\mu_B$ per atom. Shull and his co-workers (1951, 1952, 1953) have now investigated a large number of transition metals and alloys by these methods. Some of their results are summarized in table 9, together with indications provided by susceptibility and specific heat data. (The temperature variations of susceptibility and specific heat expected of an antiferromagnetic material are fairly well understood.)

By measurements of diffuse neutron scattering it is possible to put an upper limit on the magnitudes of atom moments which are uncorrelated in orientation, and for the elements of Groups V(A) and VI(A) that have been examined this is not greater than about $0{\cdot}2\,\mu_B$. A small positive result is found for chromium in spite of the complete absence of any indication of antiferromagnetism in the susceptibility results; but

Lidiard (1953) has recently shown that this apparent disagreement can be explained on the basis of a collective electron treatment of antiferromagnetism. The result for manganese is of interest but the difficulties of choosing a suitable sub-lattice structure for the complicated structure of the α modification makes a detailed discussion of it impossible. Results of an examination of iron by these techniques have shown that atoms at cube corners and cube centres cannot have moments differing by more than about $0{\cdot}4\,\mu_B$, and that the mean moment indicated is close to the magnetically observed value of $2{\cdot}22\,\mu_B$.

Table 9. Neutron Diffraction and other Data on Elements of Groups V(A) and VI(A)

	V	Nb	Mo	Cr	Mn
Atomic moment (μ_B)	0	0	0	0·4	~0·3
Antiferromagnetic Curie temperature (°K)	—	—	—	470°	~100°
Temperature coefficient of susceptibility	−ve	−ve	−ve	+ve	—
Antiferromagnetic behaviour of susceptibility	No	No	No	No	—
Antiferromagnetic behaviour of specific heat	No	No	No	Not at 470°K	—

In general these data seem to discount the model put forward by Zener, and his suggestion that rapid, but synchronized oscillations of the array of moments would account for the small or zero values observed does not seem to be borne out by experiments with a wide range of neutron velocities (see § 4.6).

Some neutron diffraction experiments have also been carried out on ordered structures in ferromagnetic binary alloys of the transition metals. Thus it would appear that in the ordered body-centred-cubic FeCo structure the same atomic moment is associated with both types of atom (Shull, quoted by Van Vleck, 1951), but in the ordered face-centred-cubic alloys Ni_3Mn and Ni_3Fe (Shull, quoted by Goldman, 1953) the nickel atom moments are about $0{\cdot}3\,\mu_B$ and those of manganese and iron about 3·3 and $2{\cdot}4\,\mu_B$ respectively. It has already been remarked that a collective d-band common to both atomic species is hardly to be expected in Ni_3Mn, ordered or disordered, but in Ni_3Fe the departure from a common band may occur only on ordering.

7.7. *Ferromagnetic Alloys of Manganese*

In most theories of ferromagnetism inter-atomic distances are regarded as of importance, and the ability of manganese to show ferromagnetism in alloys has frequently been discussed in terms of such distances. There

can be no doubt, however, that the nature of the alloying elements and the type of crystal structure are also of importance. In table 10 are shown data for binary alloys given by Guillaud (1951), Willis and Rooksby (1954), and Foëx (1951), and for the ternary Heusler alloys given by Coles, Hume-Rothery and Myers (1949).

Table 10. Magnetic Properties and Interatomic Distances in Manganese Alloys

	MnAs	MnSb	MnBi	MnTe	Cu_2MnAl	Cu_2MnSn	Cu_2MnIn
σ_0 (μ_B per Mn atom)	3·4	3·53	3·52	*	4·04	4·0	4·14
Curie temperature °C	130	320	—	30*	330	340†	233
Mn–Mn distances (Å)	2·84	2·89	3·06	3·30	4·17	4·36	4·38
	3·71	4·12	4·30	4·56			

* MnTe is antiferromagnetic, and 30° is the temperature at which antiferromagnetic ordering breaks down.

† This value is taken from the recent work of Valentiner (1953).

The binary alloys all have the hexagonal NiAs structure in which each transition metal atom has two nearest neighbours (above and below it in the *c*-direction) and six near neighbours (in the same plane perpendicular to the *c*-direction) at the larger distances shown in table 10. Willis and Rooksby (*loc. cit.*) have recently examined in detail the variations of structure with temperature of the three ferromagnetic binary compounds, and have shown that discontinuous changes of lattice dimensions take place, in MnAs at 40°C, and in MnBi at 320°C; the latter phase decomposes at about 440°C without showing a second order magnetic transition. These results suggest strongly that the second nearest neighbour interactions are significant in the binary phases, and that ferromagnetism rapidly becomes less favourable at separations of more than about 4·36 Å.

APPENDIX A

Co-Valent Radii

In his paper on atomic radii and interatomic distances in metals, Pauling (1947) deduces the equation (see p. 168)

$$R(1)-R(n)=0{\cdot}300 \log n$$

to connect the single bond, $R(1)$, atomic radius, with the apparent radius $R(n)$ in a structure where v single bonds resonate among N positions, and $n=v/N$. The assumptions made in the derivation of this equation may be summarized as follows :—

(1) It is stated that "the available evidence indicates that the differences between single-bond, double-bond, and triple-bond radii are

very nearly the same for all atoms, and hence that an expression can be found for a term to be added to the single-bond co-valent radius for any atom to give approximately the bond radius corresponding to another bond type". The reference for this statement is Chapter V of *The Nature of the Chemical Bond*, and examination of this source shows that the following steps are involved. The single bond C—C, and double bond C=C interatomic distances were well established, and indicated a double bond factor of 0·87, i.e. the double bond distance is 0·87 times that for the single bond. This factor was assumed to be constant for the row and was used to obtain the double bond radii for all the first-row atoms. For the second-row elements, the P—P interatomic distance was known for the P_4 molecule, and for crystalline black phosphorus, and the triple bond P≡P distance was known from spectroscopic work on the P_2 and PN molecules, and these indicated a triple bond factor of 0·85 for phosphorus, which was assumed to be constant for the row and used to calculate triple bond radii of the second row elements. By comparison with first row factors, an interpolated value of 0·91 was assumed for the double bond factor of the second row elements. Using these calculated values, it was then noted that the differences between the single bond radii and double bond radii were the same for the first and second row elements, and this relation was assumed to hold for the elements of the later rows.‡

Table 11. Differences between Single, Double, and Triple-bond Radii

Element	C	O	S	Se	Te	N	P
Single-bond radius	0·77	0·74	1·04	1·17	1·37	0·74	1·10
Double-bond radius	0·67	0·60*	0·95*	1·08*	1·30*†		
Triple-bond radius						0·55*	0·95*
Differences	0·10	0·14	0·09	0·09	0·07	0·19	0·15

* From Herzberg, *Spectra of Diatomic Molecules.*
† Electron diffraction result.

The slender nature of the experimental evidence is apparent, and the position was further confused by the later discovery (see Wells 1950)§ that the single bond radii assumed for nitrogen, oxygen, and fluorine were incorrect. Using more recent data, we obtain the results shown in table 11 from which it is clear that the assumption of constant differences is incorrect. Thus the differences between single and double bond radii

‡ These details are from the 1939 edition of Pauling's book, *The Nature of the Chemical Bond* (pp. 158–9). In the 1940 edition details were given for some of the elements only, and it was stated that the other double-bond and triple-bond were "assigned reasonable values, in most cases less than the single-bond values by 0·10 and 0·17 Å, respectively" (p. 169). The radii in the two editions are almost the same.

§ The above single-bond radii are from this book.

vary from 0·07 for Te to 0·14 for O. The simplifying assumptions were of course entirely justifiable in order to produce a preliminary set of co-valent radii, but the extension of these assumptions to the elements as a whole is unsupported by any evidence, and we can only conclude that comparisons involving a degree of accuracy greater than 0·1A should not be undertaken unless the sources of the co-valent radii have been checked in full detail.

(2) After using the supposed constancy of the bond number effects to justify the derivation of a general equation, Pauling's method involves an approximation which is exact for $v=1$, but is inaccurate for the high valencies assumed for the transition metals. This affects only the resonance correction, but means that the figures in the third place of decimals are uncertain.

(3) The logarithmic form of eqn. (3) depends on the empirical fact that the C—C, C=C, and C≡C interatomic distances gave differences of 0·212 kx and 0·338 kx between the lengths of a single bond, and of double and triple bonds respectively. The ratio $0{\cdot}212/0{\cdot}338=0{\cdot}627$ is approximately equal to $\log 2/\log 3=0{\cdot}631$, but this relation is for carbon, and its extension to other elements is arbitrary.

(4) A further complication arose because when eqn. (3) was used to calculate the change from [12] → [8] co-ordination, the contraction (0·053 kx) was much larger than the obtained values for the change from b.c. cubic to f.c. cubic of c.p. hexagonal structures. This was quite reasonably attributed to some bonding taking place to the 6 second-closest neighbours in the b.c. cubic structure, and eqn. (3) was then used to distribute the bonds between the closest and second-closest neighbours in the b.c. cube. This procedure may be criticized, particularly for metals such as iron where the electron clouds of the atomic cores or ions are ' in contact '. Using these calculated bond-distributions, the contractions were calculated by eqn. (3) and the results were thought not to agree with the experimental data. For the b.c. cubic metals, Pauling corrected to C.N. 12 by means of an empirical curve based on supposed data for iron, titanium, thallium and zirconium. It was shown by Thewlis (1953) that the data used were in error owing to a failure to allow for thermal expansion when two allotropes were compared at widely different temperatures, and according to this author, eqn. (3) is in reasonable agreement with the facts, but unfortunately critical tests are difficult to make. The data for iron are uncertain, whilst those for the c.p. hexagonal metals involve the arbitrary definition of atomic radius (see p. 163). Recently Basinski (unpublished) has found a contraction of 0·034 kx in the radius for the transformation γ-Mn (f.c. cube) → δ-Mn (b.c. cube). This is slightly less than the 3% contraction (0·041 kx) of Goldschmidt, but in good agreement with the value (0·034 kx) obtained by applying the Pauling equation to the distribution of bonds within the b.c. cube, although as explained above this application is doubtful. Unfortunately transition metals are not very suitable for this kind of test, because the valencies and bond-types

may not be the same in the two forms. For the present it is not possible to choose between the Goldschmidt and Pauling factors, and since both are empirical, it seems better to use the factor of Goldschmidt because this is based on data for metals and alloys, and is much more simple than the method of Pauling which, considered fundamentally, is based on empirical relations for carbon bands.

(In this review the terms ' bond number ' and ' bond order ' are used synonymously, although the latter is sometimes given a more complicated meaning.)

APPENDIX B

In trimethylamine oxide $(H_3C)_3\,N^+—O^-$, Pauling predicted the normal value, 1·36 kx, for the N—O distance, but this involved the erroneous values of 0·70 and 0·66 for the single co-valent radii of nitrogen and oxygen. Using the now accepted values* we find as follows :—

Normal co-valent radii	C 0·77 N 0·74 O 0·74
Normal length of bonds	C–N 1·51 ; N–O 1·48
Bond length in trimethylamine oxide*	C–N $1·49 \pm 0·02$; N–O $1·36 \pm 0·02$

There is thus appreciable shortening of the N–O bond.

APPENDIX C

Bonding in Copper, Silver, and Gold

The physical properties in figs. 2–6 show that the cohesion in copper, silver and gold is greater than would be expected for normal univalent elements, and suggest clearly that the d-electrons of the ions are contributing to the cohesive forces. As explained elsewhere (Hume-Rothery 1952) we consider that the most likely explanation of this is that of Mott (1944), according to whom the outermost electrons of the ions are strongly perturbed and give rise to forces of a Van der Waal's type. This concept agrees with the fact that the bonding in silver is less strong than in copper or gold, because the $(5d)^{10}$ sub-group is more stable and hence less easily perturbed than the $(3d)^{10}$ or $(4d)^{10}$ sub-groups. The alternative explanation of Pauling (Pauling 1947) is that 4·44 of the 3d electrons of the copper atoms, together with the one 4s electron form hybrid spd bonds, with a total of 5·44 bonding electrons per atom. This concept was combined with the suggestion of a regular sequence of 5·44, 4·44 and 3·44 bonding electrons per atom in copper, zinc and gallium, but we suggest that this must be rejected in view of the very satisfactory theory of the zinc crystal in terms of the normal valency of 2, whilst many consider a valency of 5·44 as improbably high for copper. Although the details are in dispute, there is thus general agreement that the d-electrons of the ions contribute to the cohesion in solid copper, silver and gold, and that the contribution is least for silver.

---

* All values are from A. F. Well's *Structural Inorganic Chemistry*, 1950 edition, pp. 58, 461.

Acknowledgment

The authors acknowledge with gratitude the help received in many useful discussions with colleagues and with friends in other universities.

References

Andrews, K. W., 1952, *Metal Treatm.*, **19,** 425 and 489.
Betterton, J. O. B., and Hume-Rothery, W., 1951, *J. Inst. Met.*, **80,** 459.
Bradley, A. J., Goldschmidt, H. J., and Lipson, H., 1938, *J. Inst. Met.*, **63,** 149.
Bradley, A. J., and Jay, A. H., 1932, *Proc. Roy. Soc.* A, **136,** 210.
Bradley, A. J., and Rodgers, J. W., 1936, *Proc. Roy. Soc.* A, **144,** 340.
Bradley, A. J., and Taylor, A., 1937 a, *Proc. Roy. Soc.* A, **159,** 56 ; 1937 b, *Phil. Mag.*, **23,** 1049 ; 1938, *Proc. Roy. Soc.* A, **166,** 353.
Cabrera, B., 1940, *Le Magnétisme* (Paris : Institut Internationale de Coopération Intellectuelle, Vol. 3), p. 153.
Carr, W. J., 1952, *Phys. Rev.*, **85,** 590.
Cauchois, Y., 1952, *C.R. Acad. Sci., Paris,* **235,** 613 ; 1953, *Phil. Mag.*, **44,** 173.
Coles, B. R., 1950, *D.Phil. Thesis,* Oxford ; 1951, *J. Inst. Met.*, **80,** 702 ; 1952, *Proc. Phys. Soc.* B, **65,** 221 ; 1953, *Phil. Mag.*, **44,** 915.
Coles, B. R., and Hume-Rothery, W., 1951, *J. Inst. Met.*, **80,** 85.
Coles, B. R., Hume-Rothery, W., and Myers, H. P., 1949, *Proc. Roy. Soc.* A, **196,** 125.
Douglas, A. M. B., 1950, *Acta Cryst.*, **3,** 19.
Ekman, W., 1931, *Z. Phys. Chem.* B, **12,** 57.
Elcock, E. W., Rhodes, P., and Teviotdale, A., 1954, *Proc. Roy. Soc.* A, **221,** 53.
Farineau, J., 1938, *Ann. Phys., Paris,* **10,** 20 ; 1939, *J. Phys. Radium,* **10,** 327.
Fletcher, G. C., 1952, *Proc. Phys Soc.* A, **65,** 192.
Fletcher, G. C., and Wohlfarth, E. P., 1951, *Phil. Mag.*, **42,** 106.
Foëx, G., 1951, *J. Phys. Radium,* **12,** 153.
Friedel, J., 1952 a, *Phil. Mag.*, **43,** 153 ; 1952 b, *Proc. Phys. Soc.* B, **65,** 769.
Gehloff, P. O., and Justi, E., 1949, *Z. Naturf.* A, **4,** 561.
Guillaud, C., 1951, *J. Phys. Radium,* **12,** 223.
Guthrie, A. N., and Bourland, L. T., 1931, *Phys. Rev.*, **37,** 303.
Gyorgy, E. M., and Harvey, G. C., 1952, *Phys. Rev.*, **87,** 861 ; 1954, *Phys. Rev.*, **93,** 365.
Hartree, D. R., 1933, *Proc, Roy. Soc.* A, **141,** 282 ; 1934, *Proc. Roy. Soc.* A, **143,** 516.
Hartree, D. R., and Hartree, W., 1936, *Proc. Roy. Soc.* A, **157,** 490.
Heisenberg, W., 1928, *Z. Phys.*, **49,** 619.
Hoare, F. E., Matthews, J. C., and Walling, J. C., 1953, *Proc. Roy. Soc.* A, **216,** 502.
Hoare, F. E., Kouvelites, J. S., and Matthews, J. C., 1952, *Nature, Lond.*, **170,** 537.
Hoare, F. E., and Walling, J. C., 1951, *Proc. Phys. Soc.* B, **64,** 337.
Horowitz, M., and Daunt, J. G., 1953, *Phys. Rev.*, **91,** 1099.
Howarth, D. J., 1953, *Proc. Roy. Soc.* A, **220,** 513.
Hume-Rothery, W., 1948, *Phil. Mag.*, **39,** 89 ; 1949, *Rep. Progr. Chem.* **46,** 42 ; 1952, *Atomic Theory for Students of Metallurgy,* 2nd Edn. (London : Institute of Metals).
Hume-Rothery, W., Betterton, J. O., and Reynolds, J., 1951, *J. Inst. Met.*, **80,** 609.
Hume-Rothery, W., and Haworth, J. B., 1952, *Phil. Mag.*, **43,** 613.

HUME-ROTHERY, W., IRVING, H. M., and WILLIAMS, R. J. P., 1951, *Proc. Roy. Soc.* A, **208,** 431.
HUME-ROTHERY, W., MABBOTT, G. W., and CHANNELL-EVANS, K. E., 1934, *Phil. Trans.* A, **233,** 1.
HUME-ROTHERY, W., and RAYNOR, G. V., 1940, *Proc. Roy. Soc.* A, **177,** 27 ; 1954, *The Structure of Metals and Alloys* (London : The Institute of Metals).
JOHNSTON, H. L., *et al.*, 1950, *J. Amer. Chem. Soc.*, **72,** 4142 ; 1951, *Ibid.*, **73,** 172 and 4727 ; 1952, *Ibid.*, **74,** 1539 ; 1953, *Ibid.*, **75,** 2467.
JONES, H., 1937, *Proc. Phys. Soc.*, **49,** 250 ; 1949, *Physica*, **15,** 13 ; 1950, *Phil. Mag.*, **41,** 663 ; 1953, *Ibid.*, **44,** 907.
KAPLAN, H., 1952, *Phys. Rev.*, **85,** 1038.
KAUFMANN, A. R., PAN, S. T., and CLARK, J. R., 1945, *Rev. Mod. Phys.*, **17,** 87.
KAYA, S., and NAKAYAMA, N., 1940, *Proc. Phys.-Math. Soc. Japan*, **22,** 126.
KEESOM, W. H., and KURRELMEYER, B., 1940, *Physica*, **7,** 1003.
KELLEY, K. K , 1935, *U.S. Bureau of Mines*, Bull. No. 383 ; 1946, *Ibid.*, T.P. 686.
KINGSTON, R. H., 1952, *Phys. Rev.*, **84,** 944.
KINGSTON, R. H., HARVEY, G. C., PIORE, E. R., and GYORGY, E. H., 1952, *Rev. Sci. Instrum.*, **23,** 8.
KOSTER, W., and ZWICKER, U., 1951, *Heraeus-Festschrift*, 76.
KRIESSMAN, C. J., 1953, *Rev. Mod. Phys.*, **25,** 122.
KRÜTTER, H. M., 1935, *Phys. Rev.*, **48,** 664.
LIDIARD, A. B., 1953, *Proc. Phys. Soc.* A, **66,** 1188.
LIPSON, H., and TAYLOR, A., 1939, *Proc. Roy. Soc.* A, **173,** 232.
MANNING, M. F., 1943, *Phys. Rev.*, **63,** 190.
MANNING, M. F., and CEODOROW, M., 1939, *Phys. Rev.*, **55,** 675.
MANNING, M. F., and GREENE, J. B., 1943, *Phys. Rev.*, **63,** 203.
MANNING, M. F., and KRÜTTER, H. M., 1937, *Phys. Rev.*, **51,** 761.
MCGUIRE, T. R., and KRIESSMAN, C. J., 1952, *Phys. Rev.*, **85,** 452.
MCQUILLAN, A. D., 1951, *J. Inst. Met.*, **80,** 363.
MEYER, A. J.-P., and TAGLANG, P., 1950, *C.R. Acad. Sci., Paris*, **231,** 956.
MOTT, N. F., 1935, *Proc. Phys. Soc.*, **47,** 571 ; 1936 a, *Proc. Roy. Soc.* A, **153,** 699 ; 1936 b, *Proc. Roy. Soc.* A, **156,** 368 ; 1936 c, *Phil. Mag.*, **22,** 287 ; 1944, *J. Inst. Met.*, **70,** 270 ; 1949, *Proc. Phys. Soc.* A, **62,** 416 ; 1951, *Semi-Conducting Materials* (London : Butterworth), p. 5 ; 1952, *Progr. Metal Phys.*, **3,** 76 ; 1953, *Phil. Mag.*, **44,** 187.
MOTT, N. F., and JONES, H., 1936, *The Theory of the Properties of Metals and Alloys* (Oxford : University Press).
NELSON, C. M., 1953, *Phys. Rev.*, **92,** 507 (quoted by Daunt, J. G., and Cobble, J. W.).
NICOL, A. D. I., 1953, *Acta Cryst.*, **6,** 285.
NILSSON, A., 1953, *Ark. Fys.*, **6,** 513.
NOWOTNY, H., BAUER, E., and STEMPFL, A., 1950, *S.B. öst. Akad. Wiss.*, IIB, **149,** 679, 1164 ; 1951, *Mh. Chemie*, **82,** 1086.
NOWOTNY, H., BAUER, E., STEMPFL, A., and BITTNER, H., 1952, *Mh. Chemie*, **83,** 222.
NOWOTNY, H., STEMPFL, A., and BITTNER, H., 1951, *Mh. Chemie*, **82,** 949.
OWEN, E. A., and ROBERTS, E. W., 1937, *Z. Kristallogr.*, **96,** 497.
PAULING, L., 1932, *J. Amer. Chem. Soc.*, **54,** 3575 ; 1938, *Phys. Rev.*, **54,** 899 ; 1940, *The Nature of the Chemical Bond* (Ithaca : Cornell University Press) ; 1947, *J. Amer. Chem. Soc.*, **69,** 542 ; 1949, *Proc. Roy. Soc.* A, **196,** 343, 350 ; 1951, *Acta Cryst.*, **4,** 138 ; 1953, *Proc. Amer. Acad. Arts Sci.*, **39,** 551.
PEARSON, W. B., 1951, *D.Phil. Thesis*, Oxford.

Pearson, W. B., and Hume-Rothery, W., 1951, *J. Inst. Met.*, **80,** 641.
Perakis, N., and Capatos, L., 1935, *J. Phys. Radium*, **6,** 642.
Phragmen, G., 1950, *J. Inst. Met.*, **77,** 489.
Pratt, J. N., and Raynor, G. V., 1951, *Proc. Roy. Soc.* A, **205,** 103.
Pugh, E. M., and Foner, S., 1953, *Phys. Rev.*, **91,** 20.
Pugh, E. M., and Schindler, I., 1953, *Phys. Rev.*, **89,** 295.
Pugh, E. M., and Rostoker, N., 1953, *Rev. Mod. Phys.*, **25,** 151.
Raynor, G. V., 1944, *J. Inst. Met.*, **70,** 507, 531 ; 1949, *Progr. Metal Phys.*, **1,** 1.
Raynor, G. V., and Little, K., 1945, *J. Inst. Met.*, **71,** 493.
Raynor, G. V., and Pfeil, P. C. L., 1946, *J. Inst. Met.*, **73,** 387, 609.
Raynor, G. V., and Wakeman, D. W., 1947, *Proc. Roy. Soc.* A, **190,** 83.
Raynor, G. V., and Waldron, M. B., 1948, *Proc. Roy. Soc.* A, **194,** 362.
Robinson, K., 1952 a, *Ph.D. Thesis*, Cambridge ; 1952 b, *Acta Cryst.*, **5,** 397 ; 1952 c, *Phil. Mag.*, **43,** 775 ; 1953, *Acta Cryst.*, **6,** 667.
Robinson, K., and Black, P. J., 1953, *Phil. Mag.*, **44,** 1392.
Schomaker, V., and Stevenson, D. P., 1941, *J. Amer. Chem. Soc.*, **63,** 37.
Schramm, J., 1938, *Z. Metallk.*, **30,** 327.
Seitz, F., 1940, *Modern Theory of Solids* (New York : McGraw-Hill), p. 488.
Serres, A., 1938, *J. Phys. Radium*, **9,** 377.
Shull, C. G., 1951, *J. Phys. Radium*, **12,** 269 (quoted by Van Vleck, J. H.) ; 1953, *Rev. Mod. Phys.*, **25,** 108 (quoted by Goldman, J. E.).
Shull, C. G., Strauser, W. A., and Wollan, E. O., 1951, *Phys. Rev.*, **83,** 333.
Shull, C. G., and Wilkinson, M. K., 1953, *Rev. Mod. Phys.*, **25,** 100.
Skinner, G. R., and Johnston, H. L., 1953, *J. Chem. Phys.*, **21,** 1383.
Skinner, H. W. B., 1940, *Phil. Trans.* A, **239,** 95.
Slater, J. C., 1936, *Phys. Rev.*, **49,** 537, 931 ; 1953, *Rev. Mod. Phys.*, **25,** 199.
Sondheimer, E. H., 1948, *Proc. Roy. Soc.* A, **193,** 484.
Sondheimer, E. H., and Wilson, A. H., 1947, *Proc. Roy. Soc.* A, **190,** 435.
Squire, C. F., and Kaufmann, A. R., 1941, *J. Chem. Phys.*, **9,** 673.
Stoner, E. C., 1933, *Phil. Mag.*, **15,** 1018 ; 1938, *Proc. Roy. Soc.* A, **165,** 372 ; 1939, *Ibid.*, **169,** 339 ; 1947, *Rep. Progr. Phys.*, **11,** 43 ; 1951, *J. Phys. Radium*, **12,** 372 ; 1954, *Acta Metall.*, to be published.
Sully, A. H., 1951, *J. Inst. Met.*, **80,** 173 ; 1954, *Chromium* (London : Butterworth).
Sully, A. H., and Heal, J. J., 1948, *Research, Lond.*, **1,** 288.
Thewlis, J., 1953, *J. Amer. Chem. Soc.*, **75,** 2279.
Valentiner, S., 1953, *Z. Metallk.*, **44,** 59.
Van Vleck, J. H., 1953, *Rev. Mod. Phys.*, **25,** 220.
Wallbaum, H. J., 1935, *Z. Metallk.*, **14,** 218.
Wells, A. F., 1950, *Structural Inorganic Chemistry* (Oxford : University Press).
Willis, B. T. M., and Rooksby, H. P., 1954, *Proc. Phys. Soc.*, to be published.
Wilson, A. H., 1953, *The Theory of Metals*, 2nd Edn. (Cambridge : University Press).
Wohlfarth, E. P., 1948, *Proc. Leeds Phil. Lit. Soc.*, **5,** 89 ; 1949 a, *Proc. Roy. Soc.* A, **195,** 434 ; 1949 b, *Phil. Mag.*, **40,** 1095 ; 1949 c, *Nature, Lond.*, **163,** 57 ; 1949 d, *Phil. Mag.*, **40,** 703 ; 1951, *Ibid.*, **42,** 374 ; 1953, *Rev. Mod. Phys.*, **25,** 211.
Zener, C., 1951 a, *Phys. Rev.*, **81,** 440 ; 1951 b, *Ibid.*, **82,** 403 ; 1951 c, *Ibid.*, **83,** 299 ; 1952, *Ibid.*, **85,** 324.

We beg to acknowledge the source of the following text-figures :—

Figure 5 from HUME-ROTHERY, W., and RAYNOR, G. V., *The Structure of Metals and Alloys* (Institute of Metals).
Figure 10 from FLETCHER, G. C., 1952, *Proc. Phys. Soc.* A, **65**, 200 (fig. 3).
Figures 11 *a*, *b* from HUME-ROTHERY, W., 1953, *Atomic Theory for Students of Metallurgy* (Institute of Metals) (figs. 125, 126, pp. 305, 306), and *Physical Review*.
Figures 12 *a*, *b*, *c* from PEARSON, W. B., *D. Phil. Thesis*, Oxford (figs. 144, 142, 143).
Figure 13 from PEARSON, W. B., and HUME-ROTHERY, W., 1951, *J. Inst. Metals*, **80**, 651 (fig. 11).
Figure 14 from PEARSON, W. B., and HUME-ROTHERY, W., 1951, *J. Inst. Metals*, **80**, 649 (fig. 8).
Figure 15 from PEARSON, W. B., and HUME-ROTHERY, W., 1951, *J. Inst. Metals*, **80**, 643 (fig. 1).
Figure 16 from PEARSON, W. B., and HUME-ROTHERY, W., 1951, *J. Inst. Metals*, **80**, 650 (fig. 10).
Figure 20 from EWALD, P. P., and HERMANN, C., 1931, *Zeit. Kristallographie* (*Strukturberichte*) **1**, 491 (figs. 204, 205).
Figure 22 from DOUGLAS, A. M. B., *Ph. D. Thesis*, Cambridge.
Figures 24 and 25 from NICOL, A. D. I., 1953, *Acta Crystallographica*, **6**, 289 (figs. 5 and 4).
Figures 28 *a*, *b* from RAYNOR, G. V., and WALDRON, M. B., 1948, *Proc. Roy. Soc.* A, **194**, 373 (figs. 14, 15).
Figure 29 from RAYNOR, G. V., and LITTLE, K., 1945, *J. Inst. Metals*, **71**, 512 (fig. 10).
Figure 31 from ROBINSON, K., 1952, *Acta Crystallographica*, **5**, 400 (fig. 5).
Figure 33 from KITTEL, C., 1953, *Introduction to Solid State Physics*, p. 197 (fig. 10.26) (London : Chapman and Hall ; New York : John Wiley and Sons).

Annals of Science

A QUARTERLY REVIEW OF THE HISTORY OF SCIENCE SINCE THE RENAISSANCE

EDITORS

D. McKIE, D.Sc., Ph.D.,
University College, London.

HARCOURT BROWN, M.A., Ph.D.,
Brown University, Providence, R.I., U.S.A.

H. W. ROBINSON,
Former Librarian,
Royal Society of London.

N. H. de V. HEATHCOTE, B.Sc., Ph.D.,
University College, London.

ANNUAL SUBSCRIPTION

£3 3s. 0d.

OR

18s. 0d.
PER PART
POST FREE

Contents of Vol. 10, No. 1, March 1954

THE EARLY PROGRESS OF BRITISH GEOLOGY.—II. From Strachey to Michell, 1719–1788. By J. CHALLINOR, M.A.

ON THE HISTORY OF NATURAL LENGTHS. By L. L. WHYTE, M.A.

ON THE FIRST ECHO-SOUNDING EXPERIMENT. By H. DRUBBA, Dip.-Phys., and H. H. RUST, Dr. Phil. (Plate I.)

THE BIRDS OF DANTE. By M. F. M. MEIKLEJOHN, M.A.

GALILEO'S THEORY OF THE TIDES. By E. J. AITON, M.Sc.

A LETTER FROM BERTHOLLET TO BLAGDEN RELATING TO THE EXPERIMENTS FOR A LARGE-SCALE SYNTHESIS OF WATER CARRIED OUT BY LAVOISIER AND MEUSNIER IN 1785. By DENIS I. DUVEEN, F.R.I.C., and HERBERT S. KLICKSTEIN, M.D.

ANTOINE LAURENT LAVOISIER (1743–1794) AND CHRISTOPHER COLUMBUS (1446 ?–1506). By DENIS I. DUVEEN, F.R.I.C., and HERBERT S. KLICKSTEIN, M.D.

THOMAS LOVE PEACOCK: CRITIC OF SCIENTIFIC PROGRESS. By ERIC ROBINSON, M.A. (Plate II.)

REVIEWS

TAYLOR & FRANCIS, LTD., Red Lion Court, Fleet Street, LONDON, E.C.4